FUNCTIONS OF PLASTOGLOBULES AND THEIR ABC1K ATYPICAL KINASES IN CHLOROPLAST METABOLISM AND STRESS RESPONSE

A Dissertation

Presented to the Faculty of the Graduate School

Of Cornell University

In Partial Fulfillment of the Requirements for the Degree of

Doctor of Philosophy

by

Peter Knut Lundquist

May 2012

FUNCTIONS OF PLASTOGLOBULES AND THEIR ABC1K ATYPICAL KINASES IN CHLOROPLAST METABOLISM AND STRESS RESPONSE

Peter Knut Lundquist, Ph.D.

Cornell University 2012

The plastoglobule (PG) is an enigmatic lipoprotein particle in photosynthetic and non-photosynthetic plastids in plants. In chloroplasts, PGs are attached to the thylakoid membrane, providing a dynamic reservoir for prenyl- and neutral-lipids and a small set of proteins. Identification of the PG proteome suggests an active role for PGs in chloroplast metabolic processes. However, the majority of the proteins of the PG have not been characterized, making a comprehensive understanding of PG function difficult. The objective of this dissertation was therefore to clarify the functional role of the PG in chloroplasts. The PG proteome from *Arabidopsis thaliana* leaf chloroplasts was determined by mass spectrometry of isolated PGs and quantitative comparison with the proteomes of unfractionated leaves, thylakoids and stroma. This refined PG proteome consisted of 30 proteins, including 6 ABC1K atypical kinases and 7 fibrillins together comprising more than 70% of the PG protein mass. Compared to previous PG proteome analyses, several proteins were excluded and six new PG proteins were identified, including an M48 metallopeptidase and two additional ABC1K atypical kinases, confirmed by immunoblotting. A genome-wide co-expression network for the PG genes was constructed from mRNA expression data revealing a network with four distinct modules that each contain at least one ABC1K and/or fibrillin gene. Each module showed clear enrichment in specific functions, including chlorophyll degradation/senescence, isoprenoid biosynthesis, plastid proteolysis and

plastid redox and kinase regulators of electron flow. A new testable model for the PGs is presented, in which sets of genes are associated with specific PG functions. The PG is proposed to serve as a thylakoid membrane microdomain, recruiting low-abundant proteins into physical proximity facilitating specific metabolic reactions and physiological responses, comparable to lipid rafts of plasma membranes. Extensive phylogenetic evidence for the ABC1K family showed their ancient origin prior to the archaea-bacteria split and organization into three primary clades characterized by evolutionary origin and sub-cellular localization; ABC1Ks appear to have been introduced into photosynthetic eukaryote genomes through both plastid and mitochondrial endosymbiosis. Hypothesized functions of the PG-localized ABC1K1 and ABC1K3 as regulators of chloroplast prenyl-lipid metabolism are investigated. It was found that *A. thaliana* T-DNA insertion single (a*bc1k1* and *abc1k3)* and double (*k1k3*) mutants have a dose dependent, conditional light stress phenotype manifested as leaf degreening and necrosis; the minimal threshold for the visible phenotype is lower in the double mutant than either single mutant, suggesting additive or synergistic roles for each gene in the adaptation to excess excitation energy. Light stress treatments of *k1k3* also resulted in granal hyperstacking and the altered size, number and morphology of PGs as compared to the wild-type indicates an increased ratio of prenyl- to neutral-lipid in PGs. Comparison of metabolite and protein compositions in wild-type and *k1k3* leaves revealed reduced accumulation of PG-localized carotenoid cleavage dioxygenase 4 and altered levels of various prenyl-lipids in *k1k3*, supporting a regulatory role for ABC1K1 and ABC1K3 in prenyl-lipid metabolism as an adaptation to excess excitation energy. Finally, based on the coexpression, phylogenetic and phenotypic mutant analyses, targets of ABC1K1 and ABC1K3 are hypothesized.

BIOGRAPHICAL SKETCH

Born in Davis, California, and raised in Minnetonka, Minnesota, Peter Lundquist graduated from Minnetonka High School in 2001. He completed his Bachelor of Science degrees in Agronomy and Biochemistry at Kansas State University in 2006. As an undergraduate, he carried out an Honors project under the supervision of Dr. Subbaratnam Muthukrishnan in the Department of Biochemistry, studying the effect of the ecdysone hormone on chitin synthase expression. In 2006, Peter entered the graduate program in Plant Biology at Cornell University, where he has worked in the laboratory of Dr. Klass van Wijk. Outside of the laboratory, Peter is involved in the Cornell International Christian Fellowship and enjoys skiing and playing softball and enjoying the natural beauty of the Finger Lakes.

I dedicate this work to my Lord and Savior, Jesus Christ. For His glory!

"For I can do everything through Christ, who gives me strength."
Phillipians 4:13 NLT

"For apart from Me you can do nothing"
John 15: 5b NLT

ACKNOWLEDGEMENTS

Many thanks are owed for this work.

I thank my advisor Dr. Klaas van Wijk, for his mentorship, support and guidance. I am grateful for the many hours he has invested in my education. It has been a great pleasure working under him. And I thank my committee members, Drs. Olena Vatamaniuk and Susheng Gan for their invaluable support and contributions.

Thanks to the van Wijk lab members over the years, who have provided instruction and an enjoyable, pleasant lab environment. Thanks especially to Lisa Giacomelli for initiating this project, to Jitae Kim for all the advice and instruction and isolating the *k1k3* double mutant, to Yuka Asakura for her instruction and help with the antibody production, Giulia Friso, Boris Zybailov, and Anton Poliakov for their expertise with in-gel digestion and mass-spectrometry analysis, to Greg Buda for his help with imaging the tissue stains and to the undergraduate students who have worked with me studying plastoglobules, Mason Appel, Kevin Murphy, and Zheng Ser.

Thanks to Dr. Jerry Davis for his patient instruction in phylogenetic analysis and contribution to the ABC1K studies, to Carole Daugherty for carrying out the scanning electron microscopy work, Dr. Dean DellaPenna for providing the VTE1 antisera, Ry Forseth for his instruction with the HPLC-MS/MS in the Schroeder laboratory, and Stuart Krasnoff for his invaluable contribution to the HPLC-MS identification of prenyl-lipid metaoblites.

I am exceedingly grateful for the friendship and prayers of my many, many friends who I have known through CICF! You have all made my time at Cornell more enriching and valuable than I

can fully appreciate or express. I wish I could list each one of you, but that would take up this entire dissertation! Thank you from the bottom of my heart.

I wish to offer special thanks to my dear friend Tiju Thomas for his constant companionship, his support and prayers; no one could have a greater friend than you Tiju. And to my best buddy, Francis Ngure for the laughter and prayers that we have shared.

Financial support was provided by the Hudson H Lyon memorial fund, Cornell TAships, and the Chemistry-Biology training grant through the National Institutes of Health (Grant # 5T32GM008500).

TABLE OF CONTENTS

LIST OF FIGURES

Page #

CHAPTER ONE

CHAPTER TWO

CHAPTER THREE

CHAPTER FOUR

LIST OF TABLES

Page #

CHAPTER ONE

INTRODUCTION

1.1 THE PLASTID ORGANELLE

1.1.1. Plastid characteristics and sub-types Plastids are the unique organelle of photosynthetic eukaryotes, believed to be derived from an ancient endosymbiotic event of a eukaryote host and prokaryotic cyanobacterial ancestor estimated to have occurred about 1500 million years ago [1-3]. Plastids are enclosed by a double membrane system, referred to as the inner and outer envelope membranes, which delineates the plastid from the surrounding cytosol and controls passage of proteins and other molecules between these two compartments. Plastids are self-replicating and harbor their own minimal set of genetic material on a single chromosome of several hundred kilobases, encapsulated by protein, RNA and ribosomes, creating a complex of nucleic acid and protein known as the plastid nucleoid [4]. This minimal genome encodes for 88 proteins in *Arabidopsis thaliana* and primarily includes various components of the electron transport chain of photosynthesis and gene expression and translation machinery, such as an RNA polymerase (plastid-encoded RNA polymerase, PEP), and ribosomal subunits [5].

It is estimated that the full plastid proteome complement is comprised of ca. 3000 proteins, based on plastid proteome analyses and various plastid targeting predictor algorithms [6]. Thus, a clear majority of proteins required for the function and homeostasis of the plastid are encoded by the nuclear genome. These transcripts are translated at the cytosolic ribosome, and typically (there are <10% other signals) targeted to the plastid by a degenerate N-terminal

localization signal, known as the chloroplast transit peptide (cTP). Import of these nuclear-encoded plastid proteins requires the TOC (translocon of the outer chloroplast envelope) and TIC (translocon of the inner chloroplast envelope) complex spanning the outer and inner plastid envelope, an elaborate protein complex capable of recognizing plastid-targeted proteins and transporting them from the cytosol into the plastid [7-9].

An uncharacterized system of signaling between the nucleus and plastid permits the careful control of synthesis and accumulation of the amalgam of plastid- and nuclear-encoded plastid proteins. This bidirectional signaling from nucleus to plastid and plastid to nucleus, known as anterograde and retrograde signaling, respectively, is critical to balance the dynamic needs of the plastid with accumulation of nuclear-encoded plastid proteins [10]. As the site of light harvesting, the chloroplast serves as an invaluable sensor of environmental conditions and stresses, which are signaled back to the nucleus via (thus far, largely unknown) retrograde signaling pathways [11, 12].

Some components of retrograde signaling pathways have been elucidated. A genetic screen revealed five mutants impaired in retrograde signaling, dubbed genome uncoupled (*gun*) mutants, four of which (*gun 2, 3, 4, and 5*) were mutants in tetrapyrrole biosynthesis, implicating chlorophyll intermediates as potential signaling molecules [13-16]. The thylakoid-localized EXECUTER 1 and 2 proteins are necessary for transduction of a singlet oxygen-derived signal produced from the photosensitizer, protochlorophyllide [17, 18]. Remarkably, a transcription factor involved in retrograde signaling was demonstrated to localize to the outer-envelope membrane of the plastid and undergo selective proteolytic cleavage under the control of multiple retrograde signals, causing its release from the plastid and re-targeting to the nucleus [19]. 3'-phosphoadenosine 5'-phosphate (PAP) was recently demonstrated to serve as a mobile,

molecular signal between the plastid and nucleus in response to drought and high light [20]. The PAP signaling molecule is proposed to act through inhibition of 5' to 3' exoribonucleases in the nucleus.

Non-photosynthetic proplastids of meristematic tissue can differentiate to take on specialized forms, displaying unique morphological and biochemical characteristics. Plastid sub-types are specialized for particular functions such as photosynthesis (chloroplasts), gravity sensing and starch accumulation (amyloplasts), storage of oils (elaioplasts), or carotenoid pigments (chromoplasts) or salvage of nitrogen and carbon during senescence (gerontoplasts). Chloroplasts, the photosynthetic plastids of leaf and stem tissue, are the main subject of research in the van Wijk laboratory and the focus of plastoglobule research for this dissertation. Thus chloroplasts and their plastoglobules will now be described in greater detail.

1.1.2 Substructures of chloroplasts Chloroplasts are plastids specialized for the capture of light energy and assimilation of atmospheric carbon via photosynthesis. They are comprised of four primary substructures: the envelope, stroma, thylakoid membrane, and plastoglobules (Figure 1A).

The water-soluble supernatant of the chloroplast, known as the stroma, is the site of CO_2 assimilation via ribulose-1,5-bisphosphate carboxylase/oxygenase (RuBisCo) and the Calvin cycle. The apparatus for harvesting of light energy is housed in the thylakoid membrane, an extensive membrane system in the interior of the chloroplast, which encloses a small aqueous compartment called the lumen. Lipid-protein particles of plastids are known as plastoglobules (PGs). PGs of chloroplasts are derived from the thylakoid membrane by blebbing of the outer lipid leaflet of the membrane bilayer and remain attached to the thylakoid membrane throughout

their lifetime (Fig 1B) [21]. The structure of the plastoglobule implies a hydrophobic interior for lipid accumulation with a thin hydrophilic perimeter allowing deposition of amphiphilic metabolites such as prenyl lipids and free fatty acids and a small protein population.

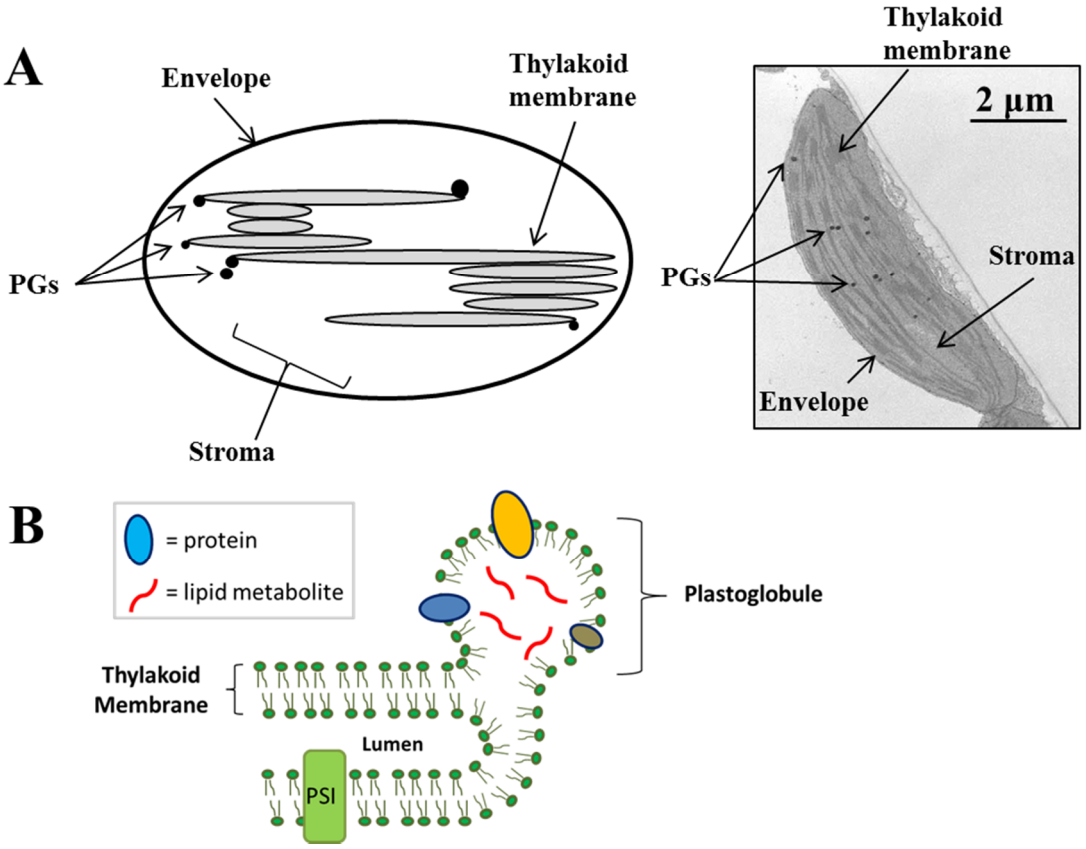

Figure 1. Chloroplast and plastoglobule ultrastructure. A, Cartoon illustration of the four main compartments of the chloroplast alongside a transmission electron micrograph of a healthy *A. thaliana* leaf chloroplast. B, Cartoon illustration of the plastoglobule ultrastructure. Note the blistering of the outer leaflet of the thylakoid membrane, creating a hydrophobic interior for the deposition of non-polar metabolites. Plastoglobule-localized proteins associate peripherally with the plastoglobule structure.

1.1.2.1 The Plastoglobule – PGs can be seen sharply in transmission electron microscopy (TEM) where they stain darkly in the presence of the lipophilic fixative osmium tetroxide. TEM has demonstrated a highly dynamic and reversible nature of PGs, involving changes in size, number and staining properties in response to various (a)biotic stresses and developmental states (Figure

2) [22]. Furthermore, PGs are thought to be the progenitors of carotenoid-rich fibrils of chromoplasts and eyespot pigment granules of phototactic algae [23, 24].

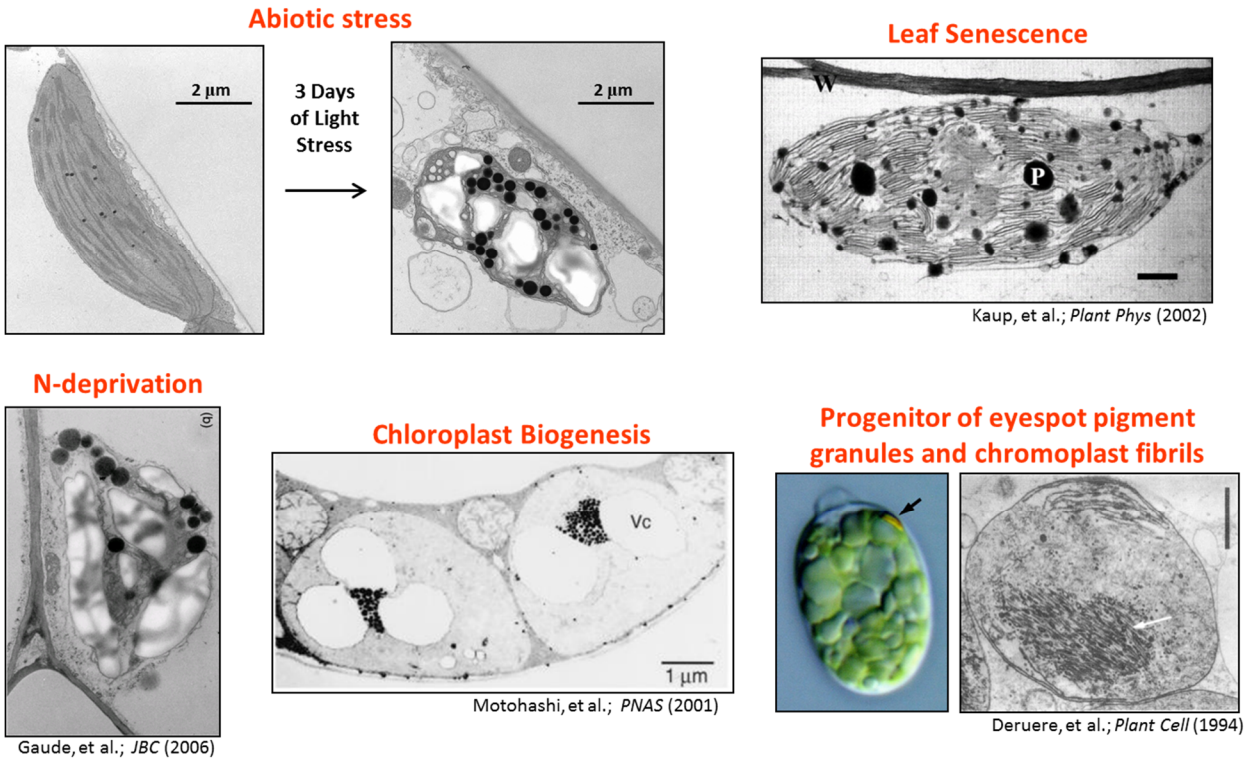

Figure 2. Plastoglobules are implicated in stress response and development. The dynamic nature of plastoglobules is illustrated in transmission electron micrographs of plastids under various (a)biotic stresses and developmental states. The abiotic stress images are the unpublished work of the author. The leaf senescence image is courtesy of [25], the N-deprivation image is courtesy of [26]. The chloroplast biogenesis image is taken from [27] and the chromoplast fibril image is courtesy of [24].

The very high lipid:protein ratio of PGs facilitates their purification using density flotation centrifugation. Analyses of purified PGs from *Pisum sativum* and *A. thaliana* chloroplasts revealed a metabolite population enriched in triacylglycerols, fatty acid phytyl esters, β-sitosterol, and a number of prenyl-lipids, especially plastoquinone (PQ) and α-tocopherol (Table 1) [22, 26, 28-34]. Surprisingly, independent in-depth proteome analyses

identified a small proteome of about 35 proteins in the PG including a number of enzymes [35, 36]. The majority of these proteins are uncharacterized; only tocopherol cyclase (VTE1), allene oxide synthase (AOS), and NAD(P)H dehydrogenase C1 (NDC1) have characterized functions in tocopherol synthesis, jasmonic acid (JA) synthesis and plastoquinone redox cycling, respectively (Table 1) [37-39]. Those uncharacterized proteins of the PG include four proteins of the ABC1K atypical kinase family, eight fibrillin proteins with a putative structural role in the particle, and various proteins with predicted oxido-reductase, methyl-transferase, or acyltransferase activity. The long-held hypothesis that PGs served solely as deposition sites for lipid compounds, a sort of trash can for the plastid, was discredited by the discovery of enzymes known or hypothesized to function in diverse metabolic pathways and physiological processes of the plastid.

Our current state of knowledge paints the picture of the PG as a crossroad of metabolic and developmental activity in the plastid, critical for proper response to fluctuating environmental conditions (Figure 3). Numerous prenyl-lipids, and several enzymes involved in their metabolism, are found to accumulate in the PG. For instance, VTE1 and NDC1 contribute to the synthesis of tocopherols and PQ [38, 39], important reactive oxygen scavengers in the chloroplast [40-42]. In addition, the phytol salvage pathway of chlorophyll degradation uses the PG for deposition of esterified phytol, which can then be recycled for tocopherol synthesis [26, 43]. PG-localized allene oxide synthase serves as a regulation point in biosynthesis of the phytohormone, JA which can be derived from peroxidized fatty acids deposited in the PG [44]. A carotenoid cleavage dioxygenase (CCD4) may serve to degrade carotenoid released from photosynthetic complexes or in the synthesis of an unknown apocarotenoid-derived phytohormone [45-47].

Table 1. Proteins and metabolites of the plastoglobule

Proteins[a]	Metabolites	Reference
Fibrillin 1a	α-tocopherol	[32, 36]
Fibrillin 1b	Plastochromanol	[32]
Fibrillin 2	Plastoquinone	[31, 32, 36]
Fibrillin 3a	Phylloquinone	[30, 48]
Fibrillin 4	Phytoene	[29]
Fibrillin 7a	Fatty acid phytyl esters	[26]
Fibrillin 7b	Triacylglycerols	[48]
Fibrillin 8	β-sitosterol	[33, 34]
Fructose-bisphosphate aldolase 1		
Fructose-bisphosphate aldolase 2		
Fructose-bisphosphate aldolase 3		
Allene oxide synthase		
Carotenoid cleavage dioxygenase 4		
Tocopherol cyclase		
NAD(P)H dehydrogenase C1		
Aldo/keto reductase-like		
SOUL heme-binding protein-like		
UbiE methyltransferase-like 1		
UbiE methyltransferase-like 2		
Diacylglycerol acyltransferase-like 1		
Diacylglycerol acyltransferase-like 2		
Flavin-reductase-like 1		
Flavin-reductase-like 2		
ABC1K1[b]		
ABC1K3[b]		
ABC1K5[b]		
ABC1K9[b]		
RAP38		
RAP41		
Unknown 1		
Unknown 2		

(a) Reference [22].

(b) For nomenclature see Chapter 3.

A number of important key questions about PGs can be raised in light of their dynamic nature, ultrastructure and metabolite and protein compositions. First, what is controlling the formation of the PGs? It is not apparent what induces the blebbing of the thylakoid resulting in PGs, but initiators of their formation include two possible sources, i) deposition of lipids or, ii) recruitment of structural proteins such as fibrillins. Similarly, what is controlling the size of the PGs and how is their dynamic, responsive nature achieved? Second, how is the metabolite and protein composition controlled? Proteome and metabolome analyses of purified PGs have clearly demonstrated a population of compounds in these structures that is distinct from that of the associated thylakoid [35, 36, 48]. Maintenance of this distinct population requires some level of control over passage of proteins and metabolites at the PG-Thylakoid interface. It is not known

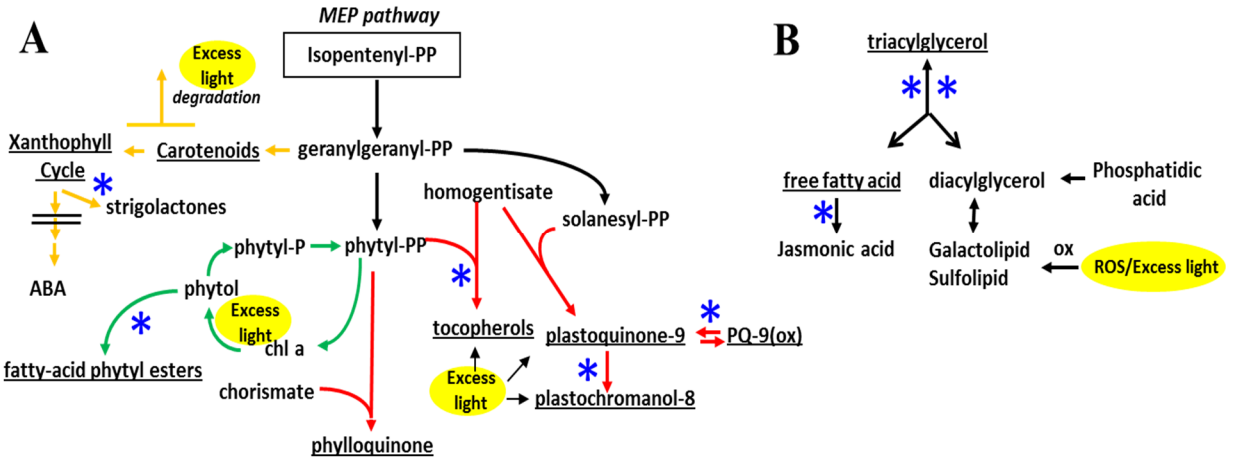

Figure 3. The plastoglobule as a metabolic crossroad in the plastid. Lipid metabolic pathways of the plastid including carotenoid, quinone, tocopherol, and galactolipid metabolism are illustrated. A, Prenyl-lipid pathways synthesizing important antioxidants and photochemical quenchers cross the plastoglobule at multiple points. B, Oxidative stresses or senescence induce degradation of thylakoid lipids. Enzymes and metabolites involved in turnover of these lipids and conversion to storage compounds (TAG) or phytohormone (JA) intersect the plastoglobule. Metabolic reactions catalyzed by a plastoglobule-localized enzyme are marked with a blue asterisk. Metabolites found to accumulate in the plastoglobule are underlined.

if this is controlled enzymatically or by physico-chemical properties of the thylakoid/PG structures and the proteins and metabolites. And third, why do plastids need a special site for sequestering certain metabolites and proteins? Indeed, the evidence thus far indicates that PGs are necessary in that they have been identified in all investigated photosynthetic organisms from cyanobacteria and algae, to moss and diverse angiosperms [22] and are present in all plastid types. What integral role(s) does the PG play in plastid function?

1.2 PHOTOSYNTHESIS

Oxygenic photosynthesis found in plants occurs in two phases: 1) the light-dependent oxidation of water and reduction of $NADP^+$ with concomitant pumping of protons across the thylakoid membrane to drive ATP synthesis, and 2) the light-independent assimilation of atmospheric CO_2 by the Calvin cycle using ATP and NADPH produced from the steps in phase 1.

1.2.1 The light reaction Light energy is captured, or absorbed, by chlorophyll and carotenoid pigments through excitation of electrons. Excited electrons are liberated from the chlorophyll molecule (an event known as charge-separation) and transferred via step-wise exergonic redox reactions through a linear chain of three protein complexes, the small molecules, plastoquinone, and ferredoxin, and the soluble protein plastocyanin (Figure 4). This linear electron transport chain (ETC) is located within the thylakoid membrane and the step wise losses of energy through the ETC are coupled to the 'pumping' of protons from the stroma to the thylakoid lumen, against a concentration gradient. Release of the proton concentration gradient by passage through ATP synthase drives synthesis of ATP from ADP and P_i.

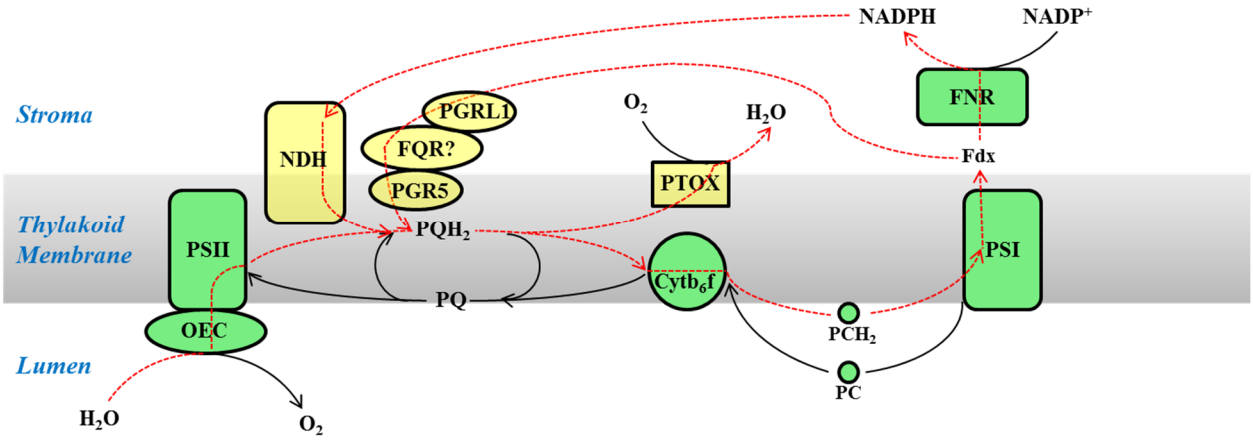

Figure 4. Diagram of the photosynthetic electron transport chain and alternative electron flows. Linear electron transport derives electrons from water molecules by the oxygen evolving complex (OEC) which are subsequently driven through the photosystem complexes (PSI and PSII) and the cytochrome b_6f complex (cyt b_6f) using lipophilic plastoquinone (PQ) and soluble plastocyanin protein (PC) as intermediaries, to ultimately reduce $NADP^+$. Alternative electron flows include the cyclic transport chains mediated by the NAD(P)H dehydrogenase complex (NDH) and the hypothesized ferredoxin:quinone oxidoreductase (FQR) regulated by PGR5 and PGRL1. Chlororespiration is mediated by the plastid terminal oxidase (PTOX). The paths of electrons in linear and cyclic flow are illustrated with red, dashed lines. Protein complexes of the linear electron transport chain are colored in green, protein complexes involved in alternative electron flows are colored in yellow.

Capture of light energy is accomplished by elaborate complexes of protein and pigment: the reaction centers of photosystem I and II (PSI and PSII) and their accessory light-harvesting complexes (LHCI and LHCII). The reaction centers are comprised of several protein subunits and are the site of the charge-separation event, involving transfer of an excited state electron from chlorophyll a to pheophytin (Phein). Peripheral LHC protein complexes contain chlorophyll a and b as well as several carotenoid compounds. The LHCs serve as antennae to capture light energy and funnel it to the reaction center and the ETC. The presence of multiple carotenoid and chlorophyll compounds in the LHCs permits capture of a wider cross-section of available light energy.

Electrons used in the ETC are derived from splitting of H_2O molecules by the oxygen evolving complex (OEC) in association with the PSII reaction center. Water-splitting results in extraction of four electrons and an O_2 molecule from every pair of H_2O molecules. At the end of the ETC a ferredoxin:NADPH reductase complex (FNR) catalyzes the reduction of $NADP^+$ via ferredoxin [49].

1.2.2 The light-independent reaction The second phase, or dark phase, of photosynthesis concerns the reduction of CO_2 through the Calvin cycle in the chloroplast stroma and does not directly involve light (though some enzymes are regulated by light) but requires ATP and NADPH, produced from the light reaction of phase 1. The Calvin cycle consists of carboxylation, reduction, and regeneration phases. The entry point of CO_2 into the Calvin cycle is RuBisCo, catalyzing the carboxylation of ribulose 1,5-bisphosphate (RuBP). For every three RuBP molecules, three CO_2 molecules are carboxylated, resulting in six 3-phosphoglycerate (PGA) molecules. Subsequent phosphorylation and reduction of the PGA molecules produces six molecules of glyceraldehyde 3-phosphate (GAP), one of which can be used for cellular metabolism while the other five are regenerated into five molecules of RuBP to complete the Calvin cycle. The reduction phase of the Calvin cycle uses ATP and NADPH, resulting in ADP and $NADP^+$ to be re-used in the light reaction of photosynthesis.

Regulation of the Calvin cycle proceeds by adjustment of stromal pH and Mg^{2+} concentration as well as post-translational modifications of enzymes by the ferredoxin-thioredoxin system [50-52]. A mechanism of Calvin cycle inhibition is imperative because several enzymes in the cycle additionally serve in the glycolytic pathway (in the dark). To prevent futile cycling, activity of the anabolic portion of the Calvin cycle must be turned off in

the dark. The ferredoxin-thioredoxin redox system provides a convenient mechanism to couple photosynthetic activity with activation of the Calvin cycle. As ferredoxin is reduced by the linear ETC under light, the reductive potential can be transferred to various plastid-localized classes of thioredoxins (f, m, x and y) via the ferredoxin-thioredoxin reductase (FTR). Reduced thioredoxin subsequently introduces one or more disulfide bridges into the target enzyme, resulting in light activation of the enzyme and the Calvin cycle [50].

1.2.3 Photoprotection mechanisms – Dealing with excess excitation energy Highly fluctuating environmental conditions experienced by plants create a need for a delicate balance of photosynthetic requirements and light harvesting. Environmental stresses such as high light, drought, salinity, etc. can reduce a plant's demand for photosynthetic products and the fixation of CO_2, leading to harvesting of more light energy than can be used for photosynthesis. This situation can result in light-induced damage in plant cells and even whole plant death. This light-induced damage results primarily from uncontrolled production of various reactive oxygen species (ROS) such as $^1O_2$, H_2O_2 and O_2^- [53]. Many molecular mechanisms have arisen in plants to prevent light-induced damage and ameliorate such damage when it occurs [53-55]; some of these mechanisms are briefly described below (*sections 1.2.3.1 – 1.2.3.6*).

1.2.3.1 State transitions – Under conditions of over-reduction of the photosynthetic ETC, redox signals such as reduced PQ, trigger the migration of LHCII proteins associated with PSII to PSI, a process known as a state transition [56]. This migration of LHCII alters the antennae size around each photosystem, increasing the excitation energy of PSI relative to PSII [56-58]. State transitions are a short-term and reversible process, regulated by

phosphorylation/dephosphorylation of LHCII subunits by state transition kinase 7 (STN7) and thylakoid-associated phosphatase 38 (TAP38), respectively [57, 59, 60]. Although control of relative light harvesting capacity of the two photosystems could provide a mechanism for relief from excess excitation energy and facilitate cyclic electron flow, inhibition of STN7 by the thioredoxin-ferredoxin system suggests it is primarily a low light phenomenon [61].

1.2.3.2 Regulation of gene expression – In conjunction with the state transition response there is a long-term adaptive response mediating precise control of photosystems I and II stoichiometry. Control of photosystem stoichiometry is regulated by the redox state of PQ, as in the state transition response, and provides reduction of light harvesting capacity in the presence of light stress [61-63]. A two-component sensor kinase (named chloroplast sensor kinase, CSK) has been identified as a mediator of PQ regulation of photosynthetic gene expression [64]. Physical interaction between CSK and plastid transcription kinase (PTK) and the RNA polymerase, Sigma factor 1 (SIG-1), was demonstrated, leading to the suggestion that CSK regulates photosynthetic gene expression through direct phosphorylation of PTK and SIG-1 [65].

1.2.3.3 Thermal dissipation – The cycling of zeaxanthin and violaxanthin, known as the violaxanthin cycle (V cycle) [66, 67], provides rapid regulation of light harvesting at the LHCs. Molecular characteristics of violaxanthin and zeaxanthin give rise to redox potentials above and below that of the chlorophylls, respectively [68]. Thus, violaxanthin serves as an effective light harvesting pigment through donation of excitation energy to chlorophyll, whereas zeaxanthin accepts excitation energy from chlorophyll which is then harmlessly released by thermal dissipation. Accumulation of zeaxanthin at the expense of violaxanthin, serves as a mechanism

of photoprotection by limiting additional light harvesting while simultaneously dissipating excess light in the photosystems. This conversion is rapidly induced – on a time scale of several minutes – and is regulated in part by the acidity of the lumen, which increases under high activity of the ETC [69].

1.2.3.4 Chlororespiration – The chlororespiratory pathway in chloroplasts can serve as an additional mechanism of energy dissipation from the ETC. Chlororespiration is an alternative nonphotochemical ETC which uses molecular oxygen as a sink for electrons of the thylakoid plastoquinone pool (Figure 4), thus diverting them from photosynthesis [70, 71] and preventing over-reduction at PSII. The *immutans* mutant in *A. thaliana* has been identified as a quinol oxidase, homologous to the alternative oxidase of mitochondria, and has been demonstrated to catalyze the plastoquinone:O_2 oxidoreductase reaction of the chlororespiratory pathway [72, 73]. Because desaturation reactions of carotenoid biosynthesis require oxidized PQ as acceptors of electrons, chlororespiration is also linked to carotenoid biosynthesis.

1.2.3.5 Photorespiration – The potentially wasteful by-reaction of the RuBisCo enzyme - oxygenation of RuBP - leads to photorespiratory metabolism, which serves as an effective sink for excess energy under light stress. This oxygenation reaction results in one molecule of PGA and one molecule of the toxic 2-phosphoglycolate (2-PG). The fixed carbon lost to 2-PG is salvaged by reactions distributed throughout the plastid, mitochondria, and peroxisome. These reactions, collectively known as photorespiration, consumes ATP and NADPH thereby removing some excess pressure on the photosynthetic ETC.

1.2.3.6 The water-water cycle – So named because the pathway for electrons begins and ends with the water molecule, the water-water cycle creates another sink for excess electrons in the ETC. This cycle is in effect a scavenger of O_2^-, produced as a harmful ROS byproduct from PSI photochemical reduction of O_2. This O_2^- is subsequently disproportionated to H_2O_2 by superoxide dismutase (SOD). Although SOD is a soluble protein complex localized in the chloroplast stroma, evidence indicates a significant pool of SOD is tethered to the thylakoid membrane, creating a local concentration around the source of O_2^- production [74]. Resulting H_2O_2 is then reduced to water by ascorbate peroxidase (APX). Ascorbate serves as the electron donor which is recycled by reduced ferredoxin of the ETC [75].

1.3 PRENYL-LIPID METABOLIC PATHWAYS

1.3.1 MEP vs. MVA pathways All isoprenoids (i.e. terpenoids) are derived from condensation reactions of the 5 carbon precursor, isopentenyl diphosphate (IPP). IPP is synthesized by two independent pathways localized in separate cellular compartments, the mevalonate (MVA) pathway in the cytosol and the methyl-erythritol-4-phosphate (MEP) pathway in the plastid [76, 77]. The two pathways produce IPP from different precursors, acetyl-CoA in the MVA pathway and pyruvate and glyceraldehyde 3-phosphate in the MEP pathway. Evidence of IPP exchange between the plastid and cytosol has been documented [78, 79], but generally it is believed that exchange is very limited.

Isoprenoids can be synthesized by serial condensation reactions into C15 (sesquiterpene), C20 (diterpene), C30 (triterpene) and C40 (tetraterpene) compounds by the activity of isoprenoid synthase enzymes [80-82]. Because of compartmentation of enzymes, C15 and C30 isoprenoids,

such as sterols, are synthesized specifically in the cell cytosol and endoplasmic reticulum, while synthesis of C10, C20 and C40 compounds, such as carotenoids, are specific to the plastid [82].

1.3.2 Plastid prenyl-lipid metabolism In plastids, the C20 diterpene, geranylgeranyl diphosphate (GGPP), is produced from condensation of two monoterpene geranyl diphosphate molecules which can subsequently be directed into multiple prenyl-lipid pathways, including that of carotenoids, chlorophylls, tocochromanols, and gibberellic acid [83].

1.3.2.1 Carotenoids – Carotenoids are 40-carbon tetraterpenoid pigments derived from condensation of two GGPP molecules by phytoene synthase. They are characterized by the presence of a series of conjugated double bonds, conveying resonance to the molecular structure and, thus, the characteristic absorption spectrum absorbing in the 400 nm range. Carotenoids play a number of important roles in the chloroplast and serve as substrates for synthesis of various phytohormones.

The committed step of carotenoid synthesis is the condensation of two GGPP molecules catalyzed by phytoene synthase (PSY), producing the C40 compound, 15-cis-phytoene. As the committed step in carotenoid biosynthesis, PSY forms the rate-limiting step and is under tight transcriptional regulation by environmental conditions such as ABA, high light, salt, drought, temperature, photoperiod, and developmental state [84]. Attempts to increase carotenoid accumulation in plant tissue, particularly tomato fruit, have focused to a large extent on over-expression of PSY [85-89].

In higher plants, successive desaturation reactions by phytoene desaturase (PDS) and ζ-carotene desaturase (ZDS), introduce double bonds at the 7,7',9 and 9' carbons, completing a 22-

carbon conjugated double bond system [84, 90]. The desaturation reactions use oxidized plastoquinone as electron acceptor, creating a link between carotenoid metabolism and photosynthesis [91]. Because the desaturases introduce double bonds in the *cis* configuration, isomerase activity is necessary to produce the all-*trans* lycopene required for subsequent steps in carotenoid biosynthesis. These isomerization reactions are catalyzed by carotenoid isomerase (CRTISO) and ζ-carotene isomerase (Z-ISO), though the isomerization can also be catalyzed with lower efficiency by light [92-94]. Linear all-*trans* lycopene is subsequently cyclized at each end by activity of lycopene β- or ε-cyclase [95]. The cyclization introduces a branch point in the pathway, leading either to β-carotene with two β-rings or α-carotene with a β- and an ε-ring. The rings of β-carotene and α-carotene are then hydroxylated by β- or ε-hydroxylase, resulting in the xanthophyll pigments, zeaxanthin and lutein, respectively [96]. Subsequent epoxidation of zeaxanthin is catalyzed by the well-known enzyme, zeaxanthin epoxidase (ZEP) forming the back reaction of the V cycle [69]. The forward reaction of the V cycle, catalyzed by violaxanthin deepoxidase (VDE) in the thylakoid lumen, is induced under conditions of excess excitation energy altering the lumenal pH. Evidence for post-translational control of ZEP activity has been presented, possibly including phosphorylation [97, 98]. An auxiliary xanthophyll cycle, the lutein-epoxide cycle (Lx cycle) involving epoxidation of lutein, has been demonstrated in certain plant species such as tomato [99], and parasitic plants [100, 101]. Deepoxidation of lutein is catalyzed by VDE of the V cycle and it has been suggested that epoxidation may also be catalyzed by ZEP [102, 103]. The Lx cycle is regulated similar to the V cycle, although activation/deactivation proceeds slower [100, 104].

The primary function of carotenoids is in harvesting of light energy for photosynthesis. The absorption spectra of carotenoids expand a plant's cross-section of photosynthetically active

radiation (PAR). Carotenoids serve as essential structural components of reaction centers and light-harvesting complexes, bound non-covalently in specific binding pockets. The two classes of carotenoids, the carotenes and xanthophylls appear to be segregated between reaction centers and LHCs. In higher plants, β-carotene binds to the reaction centers of both PSI and PSII, whereas xanthophylls are found in LHCs, in particular lutein, neoxanthin and violaxanthin [105, 106]. Upon induction of the V cycle, violaxanthin can be replaced by zeaxanthin in the LHCs [107]. Together, β-carotene and xanthophylls serve as structural components of PSI and II, and light harvesting chromophores, and as ROS scavengers [108-111].

Carotenoids also serve as substrates for the phytohormones, abscisic acid and stigolactone. Oxidative cleavage of double bonds in C40 carotenoids proceeds by a class of enzymes known as carotenoid cleavage dioxygenases (CCDs). Cleavage activity results in biologically active apocarotenoids, serving as phytohormones and volatiles. Two classes of CCDs have been identified in plants, based on the presence or absence of activity upon 9-cis-violaxanthin and 9-cis-neoxanthin. The NCED-catalyzed double-bond cleavage has been demonstrated to be the rate-limiting step in ABA biosynthesis [112, 113]. The 9-cis-epoxycarotenoid dioxygenases (NCEDs) specifically cleave the 11,12 double bond of these two substrates, leading to synthesis of ABA. The CCDs on the other hand hold cleavage activity towards a number of other (apo)carotenoid substrate compounds. CCD7 of the strigolactone biosynthesis pathway, for example, specifically cleaves the 9'-10' double bond of the 9-cis form of β-carotene [114].

A long standing question in apocarotenoid formation is the origin of the 9-cis isomerization required for the NCED and CCD7 enzymes, since only all-*trans* lycopene is used as substrate by the carotenoid cyclase and hydroxylase enzymes. Thermal or photo isomerization

has been proposed to produce the 9-cis kink in these carotenoids, however, enzyme-mediated isomerization of trans-β-carotene has recently been demonstrated in the D27 enzyme, which is necessary for accumulation of strigolactone hormone [114]. A similar enzyme-mediated isomerization may be responsible for the 9-cis form of neoxanthin and violaxanthin necessary for ABA biosynthesis, though no corresponding gene has been proposed.

1.3.2.2 Quinones and Tocopherols – Quinone and tocopherol prenyl lipids (collectively known as prenyl-quinones) function in higher plant photosynthesis as electron carriers in the ETC and as lipid antioxidants, through their inherent redox activity. Prenyl quinones are amphiphilic compounds comprised of an isoprenoid-derived hydrophobic tail of variable length and saturation and a polar aromatic head group. Redox activity of the prenyl quinones derives from the carbonyl group(s) of the head which can be reduced or oxidized between the quinol and quinone forms, respectively.

Phylloquinone (vitamin K_1, PhyQ) is bound within the PSI reaction center where it functions as an electron carrier of the ETC. PhyQ is synthesized from the condensation of naphthoate and phytyl-PP, followed by a single methylation step. The napthoate head group, common to menaquinone and phylloquinone, is derived from chorismate through a series of six enzymatic steps [115, 116]. Remarkably, four of these enzymatic steps, which are encoded as individual genes in bacterial species, have been fused into the phyllo gene in higher plants [115]. The phytyl-PP tail is formed from GGPP by the geranylgeranyl reductase enzyme. Loss of the final step in PhyQ biosynthesis, methylation by menG, leads to accumulation of the demethylated substrate in the PG and reduced PSI stability [30].

Despite reduced stability of PSI, limited photosynthetic activity has been detected in PhyQ-deficient mutants (5-15% of wild-type), indicating some functional replacement of PhyQ with another quinone, as has been shown in PhyQ-deficient *Synechocystis sp. PCC 6803*. [117]. The presence of substantial pools of PhyQ not associated with PSI, particularly in PGs, suggests additional roles for PhyQ apart from PSI activity [30, 118, 119]. In fact, enzymatic modulation of the PhyQ redox state has been demonstrated in a bimodular protein, containing PhyQ-specific reductase activity and a functional thioredoxin domain, likely to use thioredoxin as a source of electrons for PhyQ reduction [118]. It has been suggested, based on the redox potential of the thioredoxin domain, that this enzyme may also act as a protein disulfide isomerase of stromal proteins [118].

Plastoquinone (PQ) in higher plants contains a C45 nonpolar tail derived from solanesyl-PP. Solanesyl-PP is synthesized by solanesyl diphosphate synthase (SPS), of which there are two isoforms in *A. thaliana*, SPS1 in the cytosol and SPS2 in the plastid. The head group of PQ in higher plants is derived from homogentisate. Prenylation by homogentisate solanesyl transferase (HST) followed by a single methylation step catalyzed by VTE3, results in PQ. The biosynthetic pathway of PQ differs in cyanobacteria, where the head group is derived from 4-hydroxybenzoate similar to bacterial synthesis of ubiquinone [120].

PQ is a structural component of PSII and an electron carrier of the ETC, where it shuttles electrons between PSII and cytochrome b_6f complexes (Figure 4). As such it serves as an important sensor of photosynthetic activity and imbalance between PSII and PSI activity [121, 122]. As indicated in *section 1.2.3* above, the redox state of PQ is implicated in regulation of multiple plastid processes, including regulation of plastid gene expression, state transitions, and carotenoid biosynthesis.

Consistent with the importance of PQ as an important sensor of photosynthetic rates, multiple points of control of PQ redox state have also been identified or proposed. The NAD(P)H dehydrogenase (NDH) complex was identified in plants by sequence homology to the well-known NDH complex of mitochondria [123, 124]. The NDH complex functions in cyclic electron flow and directs electrons from NAD(P)H into PQ. An alternative pathway of cyclic electron flow using a hypothesized ferredoxin;quinone reductase (FQR) has been proposed which reduces thylakoid PQ using electrons from ferredoxin [71, 125]. Recently, the PG-localized NAD(P)H dehydrogenase C1 (NDC1) protein has been demonstrated to provide NAD(P)H:quinone reductase activity at the plastoglobule, likely targeting the abundant plastoquinone PG pool for reduction using stromal NADPH [39]. Furthermore, the PTOX complex couples oxidation of thylakoid PQ to reduction of molecular oxygen in the chloroplast [72, 73].

PQ also serves as an important nonpolar antioxidant compound in the plastid membrane systems. It is demonstrated to contain strong antioxidant properties towards $^1O_2$ and O_2^- and serve as a capable inhibitor of membrane lipid peroxidation [40-42, 126, 127]. Heightened accumulation of reduced PQ in light stressed plants, especially in PGs, is consistent with its likely ROS scavenging role [31, 116].

Tocochromanols are prenyl lipids containing a double-ring chromanol head group. Tocochromanols include tocopherols and tocotrienols, containing prenyl tails derived from phytyl-PP or GGPP, respectively. The chromanol head group can be formed from a quinone by cyclization reaction involving the isoprenoid tail and one of the hydroxyl groups of the quinone. Tocopherol cyclase (VTE1) has been demonstrated to use PQ as substrate to synthesize plastochromanol (PC), a tocochromanol with a C40 prenyl lipid tail. VTE1 is also responsible for

the cyclization reactions of benzoquinone substrate leading to tocotrienols and tocopherols [38]. The benzoquinone substrates of VTE1 are derived from a homogentisate head group, as in PQ of higher plants.

Tocochromanols provide additional antioxidant capacity to plant cells. The importance of tocochromanols in the inhibition of non-enzymatic lipid peroxidation in seed tissue has been demonstrated by the significantly shortened seed longevity in tocopherol-deficient seed and massive accumulation of lipid peroxides in tocopherol-deficient seedlings [128, 129]. Surprisingly, tocochromanols also hold a significant role in low-temperature adaptation and phloem loading. Tocopherol mutants in *A. thaliana* and maize have impaired ability to export carbohydrates from cells [130, 131]. This may be related to tocopherol regulation of polyunsaturated fatty acid metabolism at low temperature through an unknown mechanism [132]. Although, ROS scavenging and antioxidant ability in tocochromanols has been well established, see e.g. [133-136], the tolerance of tocochromanol-deficient mutants to light stress indicates they play only a limited role in photoprotection [130]. One possibility is that carotenoids sufficiently fulfill the photoprotection role in the absence of tocopherol, as indicated by overlapping photoprotective ability demonstrated in *Chlamydomonas reinhardtii* [137]. Interestingly, a study of *in vitro* and *in vivo* tocopherol oxidation under high light stress revealed that while *in vitro* treatment of tocopherols with the oxidant 2,2'-azodi-2,4'-dimethylvaleronitrile resulted in 23 distinct oxidation products, analysis of oxidation products from light stressed *A. thaliana* leaf tissue could detect only two, α-tocopherolquinol and γ-tocopherolquinol, which were minor oxidation products in the *in vitro* assay [138]. This apparent specificity indicates oxidation of tocopherol *in vivo* occurs by an enzyme-mediated pathway in tocopherol oxidation and recycling under light stress.

1.3.2.3 – Chlorophyll Chlorophylls (chls) are the green pigments of photosynthesis, characterized by a polar tetrapyrrole head group chelating a Mg^{2+} atom, and a non-polar phytyl tail. Several forms of chlorophyll are found in nature. Higher plants synthesize just two forms of chl called chl a and b, which differ only in the methyl group on one of the pyrrole rings (Figure 5A). Initial steps in the biosynthetic pathway of chlorophyll are shared with heme biosynthesis and are localized in the plastid stroma. The committed step of tetrapyrrole synthesis is synthesis of δ-aminolevulinic acid (ALA) derived from glutamate. Six subsequent steps result in the protoporphyrin IX intermediate, the branch point of heme and chlorophyll synthesis. Activity of magnesium chelatase inserts Mg into the protoporphyrin ring, directing the tetrapyrrole intermediate into chlorophyll synthesis. Subsequent reactions convert the Mg-protoporphyrin into protochlorophyllide which is reduced to chlorophyllide (Chlide) by protochlorophyllide oxidoreductase (POR). Phytol esterification, the final step in chlorophyll synthesis, is then catalyzed by chlorophyll synthetase producing chl a. Interconversion of chl a and chl b requires a single oxidation step, catalyzed by chl a oxygenase (CAO) [139].

The photosensitivity of chl intermediates in free form can lead to formation of $^1O_2$, and thus chl synthesis demands tight control to prevent excess accumulation of unbound intermediates. A feedback mechanism has been identified in plants designed to shut down chl biosynthesis in the absence of light. POR activity is encoded in three isozymes in higher plants (POR-A, -B, -C), all of which are light-dependent for their activity. Thus, in the absence of light the substrate protochlorophyllide will accumulate and result in negative feedback on ALA synthesis [140]. Heme similarly displays feedback inhibition on ALA synthesis, as demonstrated

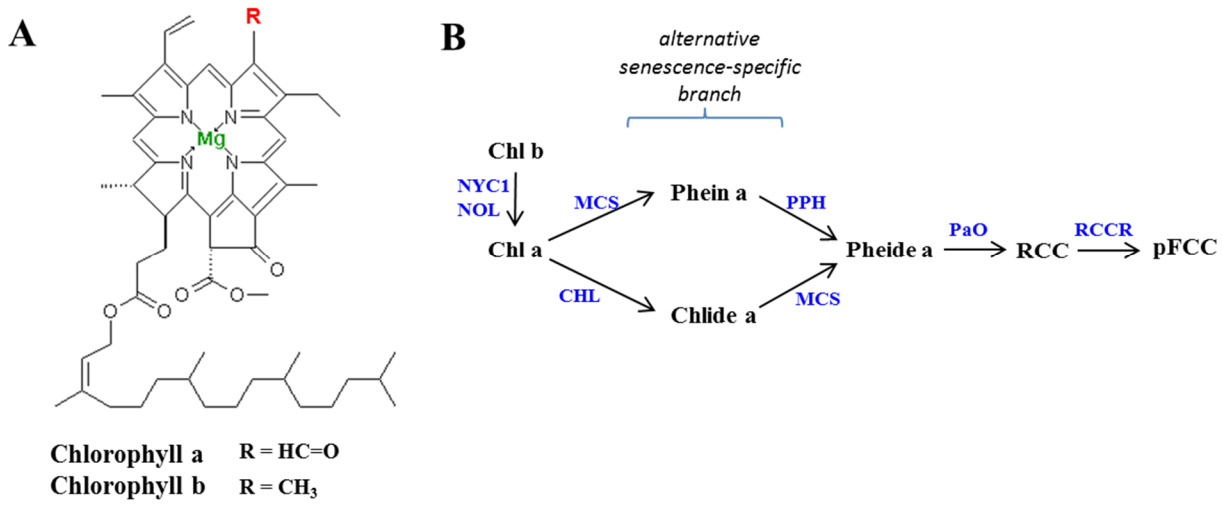

Figure 5. Plant chlorophylls and the chlorophyll degradation pathway. A, The molecular structure of plant chlorophylls a and b are shown. B, Plastid-localized chlorophyll degradation can follow two pathways, differing in the sequence of metal dechelation and dephytylation. Metabolites are in black and enzymes are in blue. See text for the explanation of abbreviations.

by abrogation of heme oxygenase activity leading to significantly reduced levels of ALA and protochlorophyllide [141, 142]. This protochlorophyllide-mediated inhibition is dependent on the flu gene, which targets glutamyl-tRNA synthase for inhibition by an unknown mechanism [143]. The *flu* mutant accumulates harmful $^1O_2$ causing cell death, but only upon transition from dark-to-light, because the photosensitizer protochlorophyllide accumulates uncontrollably in the dark in the absence of the FLU protein [143]. Recently, FLU was identified in a protein complex with the final 4 steps of chl biosynthesis [144].

POR-C has been found to be the primary form of POR in developed chloroplasts. POR-A and POR-B are the primary isoforms found in prolamellar bodies of developing chloroplasts, and demonstrate strict tissue- and organ-specific plastid import [145]. Interestingly, non-angiosperm plant species (e.g. algae, moss, lycopod, gymnosperms) contain an additional light-independent

form of POR (DPOR), and anoxygenic photosynthetic bacteria only contain the DPOR isoform [140].

Chl degradation into nonfluorescent chl catabolites (NCCs) occurs during developmental conditions such as senescence and fruit development and also appear to occur continuously on a smaller scale in photosynthetically-active leaf tissue as part of normal PS turnover [146]. As in chl synthesis, degradation requires delicate control to prevent accumulation of phototoxic intermediates. Degradation appears to proceed through chl a, and thus chl b must first be converted to chl a by chl b reductase (NYC1 and NOL) [147]. Initial steps of chl a degradation can proceed through two different pathways that might be determined by developmental cues (Figure 5B). In the first pathway, chl a is initially dephytylated by chlorophyllases (CHL1 and CHL2) leading to chlide a, which is subsequently dechelated by an unknown metal chelating substance (MCS), producing pheophorbide a (pheide a). The second pathway reverses the sequence of dephytylation and Mg dechelation. Chl a is first dechelated by MCS and subsequently dephytylated by phein pheide hydrolase (pheophytinase, PPH). Evidence indicates that the PPH-dependent pathway is favored specifically under leaf senescence [148, 149].

Regardless of the pathway, pheide a is subsequently oxidized to red chlorophyll catabolite (RCC) by pheide a oxygenase (PaO) and then reduced by red chlorophyll catabolite reductase (RCCR) to the primary fluorescent chlorophyll catabolite (pFCC). pFCC is then exported from the plastid by an unknown transporter where it is further catabolized in the cytosol and stored in the vacuole as NCCs [149].

The care taken by plants to prevent accumulation of chl intermediates is evident in the metabolic channeling identified at the LHCII. Recent evidence shows that STAY-GREEN (SGR) along with NYC1 and NOL (responsible for converting chl a to chl b), PPH, PaO, and RCCR all

bind as a complex to LHCII facilitating efficient breakdown of chl from LHCII [150]. SGR is necessary for chl degradation and it was suggested that SGR is responsible for binding to LHCII and initiating formation of the complex by recruiting the catabolic enzymes [150].

Free phytol released during chlorophyll degradation is harmful to lipid membranes and must be rapidly metabolized. A salvage pathway for phytol has been identified in higher plants [43] involving two successive phosphorylation steps catalyzed by distinct kinases, producing phytyl-PP which can re-enter prenyl lipid metabolism. The first of the two kinases has been identified as VTE5 and is critical for synthesis of tocopherols, indicating substantial flux of recycled phytol into tocopherol, consist with the dramatic increase in tocopherol accumulation during leaf senescence [151]. No candidate gene for the second kinase has been identified. An alternative fate of free phytol is to be esterified to free fatty acids, resulting in fatty acid phytyl esters deposited in PGs [26].

1.4 THYLAKOID GALACTOLIPID DEGRADATION AND JA SYNTHESIS

1.4.1 Galactolipid degradation As with other lipid compounds, galactolipids undergo continuous metabolic turnover. Degradation of galactolipids is enhanced under certain developmental programs such as senescence and in response to various stresses, such as cold stress, P_i- or N-limitation and wounding. In fact, evidence suggests that plastid membrane disassembly by lipases is a key initial step in triggering the senescence cascade [152, 153]. Nitrogen deprivation has been shown to result in disassembly of the thylakoid membrane system and deposition of lipophilic catabolites in the PG [26].

Galactolipid degradation occurs by the concerted action of galactolipases and galactosidases, leading to the release of galactose, glycerol, and free fatty acids. Little is known about the regulation of these catalytic steps and few of the genes have been identified. All seven class I acylhydrolases in *A. thaliana* were demonstrated to localize to the plastid, six of which demonstrated galactolipase activity in *in vitro* assays [154]. However, physiologically relevant activity has been demonstrated for only two of these, Defective in Anther Dehiscence 1 (DAD1) and Dongle (DGL) [155]. Both galactolipases were shown to be necessary for fatty acid supply of the JA biosynthetic pathway but under distinct conditions. DGL is highly expressed in leaf tissue and is required for maintenance of basal JA levels regulating vegetative growth. DAD1 and DGL together are involved in JA synthesis in response to wounding, though they demonstrate different induction kinetics [155].

1.4.2 Jasmonic acid synthesis JA is an important endogenous regulator of plant defense responses to pathogen attack and wounding, and developmental programs including vegetative growth, senescence, and stamen development [156-158]. The current understanding of galactolipase function highlights the connection between galactolipid degradation and JA biosynthesis. JA is an oxylipin derived from α–linolenic acid (18:3). Most or all of the 18:3 originates from galactolipid acyl groups, though there is some question whether initial steps in biosynthesis require free fatty acid substrate or modifications are introduced while still esterified to the glycerol group [44]. Synthesis of JA occurs across three cellular compartments: the plastid, peroxisome and cytosol. The initial step is the enzymatically-mediated peroxidation of 18:3 at carbon 13, catalyzed by 13-lipoxygenase (13-LOX). In *A. thaliana* LOX2, 3, 4, and 6 have demonstrated 13-LOX activity, while LOX1, and LOX5 have 9-LOX activity not involved in JA

synthesis [159]. The 13-LOX isoforms likely show tissue- or subcellular specificity. Indeed, AtLOX2 does not appear to be involved in the JA synthesis of developing pollen grains, in contrast to AtLOX3 and AtLOX4 and *Zea mays* TASSELSEED 1 [158, 160].

The resulting oxylipin (13(S)-hydroperoxy octadecatrienoic acid) serves as substrate for allene oxide synthase (CYP74A, AOS) localized at the PG and thylakoid, which synthesizes the highly reactive intermediate allene oxide [37, 161]. Allene oxide is rapidly cyclized by allene oxide cyclase producing the cyclopentenone, 12-oxophytodienoic acid (OPDA) [162]. OPDA is subsequently exported (through an unidentified transporter) from the plastid to the peroxisome, where it undergoes reduction by OPDA reductase, followed by three successive β-oxidations to form JA. The active form of JA is the isoleucine conjugated form [163], synthesized in the cytosol.

Little is known about the regulation of the JA biosynthesis pathway. JA can be detected in leaves distant to a wound site within just three minutes. Interestingly, *A. thaliana* microRNA319a (miR319a) is an inhibitor of the JA pathway, by targeting certain members of the TCP family of transcription factors, responsible for expression of several JA biosynthetic genes.

1.5 MOTIVATION AND SUBJECT OF THE DISSERTATION

The PG is an enigmatic lipid-protein particle of plastids. Its size and abundance is highly dynamic and responsive to disturbances in plastid homeostasis caused by developmental transitions and (a)biotic stresses. The PG is a very prominent component of the plastid under these conditions. Yet, the significance of the PG is almost wholly unexplored.

The PG proteome, along with the known metabolites of the PG, has provided some clues to PG function in the plastid. A picture has begun to emerge of the PG serving as a crossroad of numerous metabolic pathways of the plastid, as well as a site for regulatory control of certain pathways and the general response of photoacclimation. PG-localized atypical ABC1 kinases are likely central in the regulatory network of PG activity.

The objective of this dissertation is to investigate the role of the PG in plastid metabolism and the light stress response. Systems biology analyses of the PG, as well as phenotypic analyses of PG-localized *abc1k* mutants are used to confront this objective.

C*hapter 2* reports on an extensive proteomics analysis of the PG to dig deeper into the PG proteome to provide a quantitative picture and identify lower abundant members. A novel strategy is applied to compare protein abundance in proteomics experiments of various cellular compartments which successfully identified several new proteins highly enriched in the PG, including a metallopeptidase. A genome-wide co-expression analysis of the PG genes was then performed and used to construct a comprehensive model of PG function.

Chapter 3 reconstructs the evolutionary history of the ABC1K family and a systematic nomenclature is proposed for the family. A functional domain analysis is then carried out for the ABC1K domain and conserved motifs are compared with those of the well characterized eukaryotic protein kinase domain. Finally, functions of the ABC1K proteins in higher plants are proposed.

In *Chapter 4* a phenotypic analysis of *A. thaliana* defective in *ABC1K1* and *ABC1K3* is presented. A conditional light stress phenotype is found in both single mutants and the double mutant at the whole plant level. Molecular analyses of the double mutant, including transmission

electron microscopy, metabolite profiling and proteomics, are presented. The results are consistent with impaired metabolism in multiple prenyl-lipid pathways.

Chapter 5 outlines the ongoing yeast 2-hybrid analysis focused on identification of direct and indirect targets of the ABC1K family in PGs. Working hypotheses for ABC1K1 and ABC1K3 targets are presented. The current state of experimentation is described.

1.6 LITERATURE CITED

1. Price, D.C., et al., *Cyanophora paradoxa Genome Elucidates Origin of Photosynthesis in Algae and Plants.* Science, 2012. **335**(6070): p. 843-847.

2. Green, B.R., *Chloroplast genomes of photosynthetic eukaryotes.* The Plant Journal, 2011. **66**(1): p. 34-44.

3. Chan, C.X., et al., *Plastid Origin and Evolution: New Models Provide Insights into Old Problems.* Plant Physiology, 2011. **155**(4): p. 1552-1560.

4. Majeran, W., et al., *Nucleoid-Enriched Proteomes in Developing Plastids and Chloroplasts from Maize Leaves: A New Conceptual Framework for Nucleoid Functions.* Plant Physiology, 2012. **158**(1): p. 156-189.

5. Sato, S., et al., *Complete Structure of the Chloroplast Genome of Arabidopsis thaliana.* DNA Research, 1999. **6**(5): p. 283-290.

6. van Wijk, K.J. and S. Baginsky, *Plastid Proteomics in Higher Plants: Current State and Future Goals.* Plant Physiology, 2011. **155**(4): p. 1578-1588.

7. Strittmatter, P., J. Soll, and B. Bolter, *The Chloroplast Protein Import Machinery: A Review*, in *Protein Secretion: Methods and Protocols*, A. Economou, Editor. 2010, Humana Press: New York. p. 307-321.

8. Andrès, C., B. Agne, and F. Kessler, *The TOC complex: Preprotein gateway to the chloroplast.* Biochimica et Biophysica Acta (BBA) - Molecular Cell Research, 2010. **1803**(6): p. 715-723.

9. Agne, B. and F. Kessler, *Protein transport in organelles: The Toc complex way of preprotein import.* FEBS Journal, 2009.

10. Nott, A., et al., *Plastid-to-Nucleus Retrograde Signaling.* Annual Review of Plant Biology, 2006. **57**(1): p. 739-759.

11. Fernández, A.P. and Å. Strand, *Retrograde signaling and plant stress: plastid signals initiate cellular stress responses.* Current Opinion in Plant Biology, 2008. **11**(5): p. 509-513.

12. Chan, K.X., et al., *Chloroplast-to-nucleus communication: Current knowledge, experimental strategies and relationship to drought stress signaling.* Plant Signaling and Behavior, 2010. **5**(12): p. 1575 - 1582.

13. Larkin, R.M., et al., *GUN4, a Regulator of Chlorophyll Synthesis and Intracellular Signaling.* Science, 2003. **299**(5608): p. 902-906.

14. Susek, R.E., F.M. Ausubel, and J. Chory, *Signal transduction mutants of arabidopsis uncouple nuclear CAB and RBCS gene expression from chloroplast development.* Cell, 1993. **74**(5): p. 787-799.

15. Mochizuki, N., et al., *Arabidopsis genomes uncoupled 5 (GUN5) mutant reveals the involvement of Mg-chelatase H subunit in plastid-to-nucleus signal transduction.* Proceedings of the National Academy of Sciences, 2001. **98**(4): p. 2053-2058.

16. Strand, A., et al., *Chloroplast to nucleus communication triggered by accumulation of Mg-protoporphyrin IX.* 2003. **421**(6918): p. 79-83.

17. Wagner, D., et al., *The Genetic Basis of Singlet Oxygen-Induced Stress Responses of Arabidopsis thaliana.* Science, 2004. **306**(5699): p. 1183-1185.

18. Lee, K.P., et al., *EXECUTER1- and EXECUTER2-dependent transfer of stress-related signals from the plastid to the nucleus of Arabidopsis thaliana.* Proceedings of the National Academy of Sciences, 2007. **104**(24): p. 10270-10275.

19. Sun, X., et al., *A chloroplast envelope-bound PHD transcription factor mediates chloroplast signals to the nucleus.* Nature Communications, 2011. **2**: p. 477.

20. Estavillo, G.M., et al., *Evidence for a SAL1-PAP Chloroplast Retrograde Pathway That Functions in Drought and High Light Signaling in Arabidopsis.* The Plant Cell, 2011. **23**(11): p. 3992-4012.

21. Austin, J.R., 2nd, et al., *Plastoglobules are lipoprotein subcompartments of the chloroplast that are permanently coupled to thylakoid membranes and contain biosynthetic enzymes.* Plant Cell, 2006. **18**(7): p. 1693-703.

22. Brehelin, C., F. Kessler, and K.J. van Wijk, *Plastoglobules: versatile lipoprotein particles in plastids.* Trends in Plant Science, 2007. **12**(6): p. 260-6.

23. Kreimer, G., *The green algal eyespot apparatus: a primordial visual system and more?*, in *Current Genetics*. 2009, Springer Berlin / Heidelberg. p. 19-43.

24. Deruere, J., et al., *Fibril Assembly and Carotenoid Overaccumulation in Chromoplasts: A Model for Supramolecular Lipoprotein Structures.* Plant Cell, 1994. **6**(1): p. 119-133.

25. Kaup, M.T., C.D. Froese, and J.E. Thompson, *A Role for Diacylglycerol Acyltransferase during Leaf Senescence.* Plant Physiol., 2002. **129**(4): p. 1616-1626.

26. Gaude, N., et al., *Nitrogen deficiency in Arabidopsis affects galactolipid composition and gene expression and results in accumulation of fatty acid phytyl esters.* The Plant Journal, 2007. **49**(4): p. 729-739.

27. Motohashi, R., et al., *An essential role of a TatC homologue of a ΔpH- dependent protein transporter in thylakoid membrane formation during chloroplast development in Arabidopsis thaliana.* Proceedings of the National Academy of Sciences, 2001. **98**(18): p. 10499-10504.

28. Eugeni Piller, L., et al., *Plastid lipid droplets at the crossroads of prenylquinone metabolism.* Journal of Experimental Botany, 2012. **63**(4): p. 1609-1618.

29. Dahlin, C. and H. Ryberg, *Accumulation of phytoene in plastoglobuli of SAN-9789 (Norflurazon)-treated dark-grown wheat.* Physiologia Plantarum, 1986. **68**(1): p. 39-45.

30. Lohmann, A., et al., *Deficiency in Phylloquinone (Vitamin K1) Methylation Affects Prenyl Quinone Distribution, Photosystem I Abundance, and Anthocyanin Accumulation in the Arabidopsis AtmenG Mutant.* J. Biol. Chem., 2006. **281**(52): p. 40461-40472.

31. Szymanska, R. and J. Kruk, *Plastoquinol is the Main Prenyllipid Synthesized During Acclimation to High Light Conditions in Arabidopsis and is Converted to Plastochromanol by Tocopherol Cyclase.* Plant Cell Physiol., 2010. **51**(4): p. 537-545.

32. Zbierzak, A.M., et al., *Intersection of the tocopherol and plastoquinol metabolic pathways at the plastoglobule.* Biochemical Journal, 2009. **425**(2): p. 389-399.

33. Greenwood, A.D., R.M. Leech, and J.P. Williams, *The osmiophilic globules of chloroplasts: I. Osmiophilic globules as a normal component of chloroplasts and their isolation and composition in Vicia faba L.* Biochimica et Biophysica Acta, 1963. **78**(1): p. 148-162.

34. Bailey, J.L. and A.G. Whyborn, *The osmiophilic globules of chloroplasts II. Globules of the spinach-beet chloroplast.* Biochimica et Biophysica Acta, 1963. **78**(1): p. 163-174.

35. Ytterberg, A.J., J.B. Peltier, and K.J. van Wijk, *Protein profiling of plastoglobules in chloroplasts and chromoplasts. A surprising site for differential accumulation of metabolic enzymes.* Plant Physiology, 2006. **140**(3): p. 984-97.

36. Vidi, P.A., et al., *Tocopherol cyclase (VTE1) localization and vitamin E accumulation in chloroplast plastoglobule lipoprotein particles.* J Biol Chem, 2006. **281**(16): p. 11225-34.

37. Song, W.C., C.D. Funk, and A.R. Brash, *Molecular cloning of an allene oxide synthase: a cytochrome P450 specialized for the metabolism of fatty acid hydroperoxides.* Proceedings of the National Academy of Sciences, 1993. **90**(18): p. 8519-8523.

38. Porfirova, S., et al., *Isolation of an Arabidopsis mutant lacking vitamin E and identification of a cyclase essential for all tocopherol biosynthesis.* Proceedings of the National Academy of Sciences, 2002. **99**(19): p. 12495-12500.

39. Eugeni Piller, L., et al., *Chloroplast lipid droplet type II NAD(P)H quinone oxidoreductase is essential for prenylquinone metabolism and vitamin K1 accumulation.* Proceedings of the National Academy of Sciences, 2011. **108**(34): p. 14354-14359.

40. Kruk, J., G.H. Schmid, and K. Strzalka, *Antioxidant properties of plastoquinol and other biological prenylquinols in liposomes and solution.* Free Radical Research, 1994. **21**(6): p. 409-16.

41. Kruk, J., et al., *Scavenging of Superoxide Generated in Photosystem I by Plastoquinol and Other Prenyllipids in Thylakoid Membranes.* Biochemistry, 2003. **42**(28): p. 8501-8505.

42. Kruk, J. and A. Trebst, *Plastoquinol as a singlet oxygen scavenger in photosystem II.* Biochimica et Biophysica Acta (BBA) - Bioenergetics, 2008. **1777**(2): p. 154-162.

43. Ischebeck, T., et al., *A salvage pathway for phytol metabolism in Arabidopsis.* Journal of Biological Chemistry, 2006. **281**(5): p. 2470-2477.

44. Gfeller, A., et al., *Jasmonate Biochemical Pathway.* Science Signaling, 2010. **3**(109): p. cm3.

45. Auldridge, M.E., D.R. McCarty, and H.J. Klee, *Plant carotenoid cleavage oxygenases and their apocarotenoid products.* Current Opinion in Plant Biology, 2006. **9**(3): p. 315-321.

46. Walter, M., D. Floss, and D. Strack, *Apocarotenoids: hormones, mycorrhizal metabolites and aroma volatiles.* Planta, 2010. **232**(1): p. 1-17.

47. Giuliano, G., S. Al-Babili, and J. von Lintig, *Carotenoid oxygenases: cleave it or leave it.* Trends in Plant Science, 2003. **8**(4): p. 145-149.

48. Steinmuller, D. and M. Tevini, *Composition and Function of Plastoglobuli .1. Isolation and Purification from Chloroplasts and Chromoplasts.* Planta, 1985. **163**(2): p. 201-207.

49. Lintala, M., et al., *Structural and functional characterization of ferredoxin-NADP+-oxidoreductase using knock-out mutants of Arabidopsis.* The Plant Journal, 2007. **49**(6): p. 1041-1052.

50. Lemaire, S., et al., *Thioredoxins in chloroplasts.* Current Genetics, 2007. **51**(6): p. 343-365.

51. Schurmann, P. and B.B. Buchanan, *The Ferredoxin/Thioredoxin System of Oxygenic Photosynthesis.* Antioxidants & Redox Signaling, 2008. **10**(7): p. 1235-1274.

52. Foyer, C.H. and G. Noctor, *Redox Regulation in Photosynthetic Organisms: Signaling, Acclimation, and Practical Implications.* Antioxidants & Redox Signaling, 2009. **11**(4): p. 861-905.

53. Li, Z., et al., *Sensing and Responding to Excess Light.* Annual Review of Plant Biology, 2009. **60**(1): p. 239-260.

54. Niyogi, K.K., *Safety valves for photosynthesis.* Current Opinion in Plant Biology, 2000. **3**(6): p. 455-460.

55. Niyogi, K.K., *Photoprotection Revisited: Genetic and Molecular Approaches.* Annual Review of Plant Physiology and Plant Molecular Biology, 1999. **50**(1): p. 333-359.

56. Allen, J.F., et al., *Chloroplast protein phosphorylation couples plastoquinone redox state to distribution of excitation energy between photosystems.* Nature, 1981. **291**(5810): p. 25-29.

57. Bellafiore, S., et al., *State transitions and light adaptation require chloroplast thylakoid protein kinase STN7.* Nature, 2005. **433**(7028): p. 892-895.

58. Rochaix, J.-D., *Role of thylakoid protein kinases in photosynthetic acclimation.* FEBS Letters, 2007. **581**(15): p. 2768-2775.

59. Pribil, M., et al., *Role of plastid protein phosphatase TAP38 in LHCII dephosphorylation and thylakoid electron flow.* PLoS Biol, 2010. **8**(1): p. e1000288.

60. Shapiguzov, A., et al., *The PPH1 phosphatase is specifically involved in LHCII dephosphorylation and state transitions in Arabidopsis.* Proceedings of the National Academy of Sciences, 2010. **107**(10): p. 4782-4787.

61. Puthiyaveetil, S., I.M. Ibrahim, and J.F. Allen, *Oxidation-reduction signalling components in regulatory pathways of state transitions and photosystem stoichiometry adjustment in chloroplasts.* Plant, Cell & Environment, 2012. **35**(2): p. 347-359.

62. Puthiyaveetil, S., I.M. Ibrahim, and J.F. Allen, *Redox signalling components and regulatory pathways of state transitions and photosystem stoichiometry adjustment in chloroplasts.* Plant, Cell & Environment, 2011. **35**(2): p. 347-359.

63. Allen, J.F., et al., *Discrete redox signaling pathways regulate photosynthetic light-harvesting and chloroplast gene transcription.* PLoS One, 2011. **6**(10): p. e26372.

64. Puthiyaveetil, S., et al., *The ancestral symbiont sensor kinase CSK links photosynthesis with gene expression in chloroplasts.* Proceedings of the National Academy of Sciences, 2008. **105**(29): p. 10061-10066.

65. Puthiyaveetil, S., et al., *Transcriptional control of photosynthesis genes: the evolutionarily conserved regulatory mechanism in plastid genome function.* Genome Biol Evol, 2010. **2**: p. 888-96.

66. Yamamoto, H.Y., T.O.M. Nakayama, and C.O. Chichester, *Studies on the light and dark interconversions of leaf xanthophylls.* Archives of Biochemistry and Biophysics, 1962. **97**(1): p. 168-173.

67. Havaux, M. and K.K. Niyogi, *The violaxanthin cycle protects plants from photooxidative damage by more than one mechanism.* Proceedings of the National Academy of Sciences, 1999. **96**(15): p. 8762-8767.

68. Frank, H., et al., *Photophysics of the carotenoids associated with the xanthophyll cycle in photosynthesis*, in *Photosynthesis Research*. 1994, Springer Netherlands. p. 389-395.

69. Niyogi, K.K., A.R. Grossman, and O. Bjorkman, *Arabidopsis Mutants Define a Central Role for the Xanthophyll Cycle in the Regulation of Photosynthetic Energy Conversion.* Plant Cell, 1998. **10**(7): p. 1121-1134.

70. Peltier, G. and L. Cournac, *Chlororespiration.* Annual Review of Plant Biology, 2002. **53**(1): p. 523-550.

71. Rumeau, D., G. Peltier, and L. Cournac, *Chlororespiration and cyclic electron flow around PSI during photosynthesis and plant stress response.* Plant, Cell & Environment, 2007. **30**(9): p. 1041-1051.

72. Carol, P., et al., *Mutations in the Arabidopsis Gene IMMUTANS Cause a Variegated Phenotype by Inactivating a Chloroplast Terminal Oxidase Associated with Phytoene Desaturation.* The Plant Cell, 1999. **11**(1): p. 57-68.

73. Wu, D., et al., *The IMMUTANS Variegation Locus of Arabidopsis Defines a Mitochondrial Alternative Oxidase Homolog That Functions during Early Chloroplast Biogenesis.* The Plant Cell, 1999. **11**(1): p. 43-56.

74. Ogawa, K.i., et al., *Attachment of CuZn-Superoxide Dismutase to Thylakoid Membranes at the Site of Superoxide Generation (PSI) in Spinach Chloroplasts: Detection by Immuno-Gold Labeling After Rapid Freezing and Substitution Method* Plant and Cell Physiology 1995 **36** (4): p. 565-573

75. Asada, K., *The Water-Water Cycle in Chloroplasts: Scavenging of Active Oxygens and Dissipation of Excess Photons.* Annual Review of Plant Physiology and Plant Molecular Biology, 1999. **50**(1): p. 601-639.

76. Dubey, V.S., R. Bhalla, and R. Luthra, *An overview of the non-mevalonate pathway for terpenoid biosynthesis in plants.* Journal of Biosciences, 2003. **28**(5): p. 637-646.

77. Phillips, M.A., et al., *The plastidial MEP pathway: unified nomenclature and resources.* Trends in plant science, 2008. **13**(12): p. 619-623.

78. Hemmerlin, A., et al., *Cross-talk between the Cytosolic Mevalonate and the Plastidial Methylerythritol Phosphate Pathways in Tobacco Bright Yellow-2 Cells.* Journal of Biological Chemistry, 2003. **278**(29): p. 26666-26676.

79. Dudareva, N., et al., *The nonmevalonate pathway supports both monoterpene and sesquiterpene formation in snapdragon flowers.* Proceedings of the National Academy of Sciences, 2005. **102**(3): p. 933-938.

80. Camara, B., *Terpenoid Metabolism in Plastids.* Plant Physiology, 1984. **74**(1): p. 112-116.

81. Chappell, J., *The genetics and molecular genetics of terpene and sterol origami.* Current Opinion in Plant Biology, 2002. **5**(2): p. 151-157.

82. McGarvey, D.J. and R. Croteau, *Terpenoid Metabolism.* The Plant Cell, 1995. **7**(7): p. 1015-1026.

83. Vranova, E., D. Coman, and W. Gruissem, *Structure and Dynamics of the Isoprenoid Pathway Network.* Molecular Plant, 2012. **5**(2): p. 318-333.

84. Cazzonelli, C.I. and B.J. Pogson, *Source to sink: regulation of carotenoid biosynthesis in plants.* Trends in Plant Science, 2010. **15**(5): p. 266-274.

85. Fraser, P.D., et al., *Manipulation of Phytoene Levels in Tomato Fruit: Effects on Isoprenoids, Plastids, and Intermediary Metabolism.* Plant Cell, 2007. **19**(10): p. 3194-3211.

86. Burkhardt, P.K., et al., *Transgenic rice (Oryza sativa) endosperm expressing daffodil (Narcissus pseudonarcissus) phytoene synthase accumulates phytoene, a key intermediate of provitamin A biosynthesis.* The Plant Journal, 1997. **11**(5): p. 1071-1078.

87. Fraser, P.D., et al., *Evaluation of transgenic tomato plants expressing an additional phytoene synthase in a fruit-specific manner.* Proceedings of the National Academy of Sciences, 2002. **99**(2): p. 1092-1097.

88. Fray, R.G., et al., *Constitutive expression of a fruit phytoene synthase gene in transgenic tomatoes causes dwarfism by redirecting metabolites from the gibberellin pathway.* The Plant Journal, 1995. **8**(5): p. 693-701.

89. Shewmaker, C.K., et al., *Seed-specific overexpression of phytoene synthase: increase in carotenoids and other metabolic effects.* The Plant Journal, 1999. **20**(4): p. 401-412.

90. Hirschberg, J., *Carotenoid biosynthesis in flowering plants.* Current Opinion in Plant Biology, 2001. **4**(3): p. 210-218.

91. Norris, S.R., T.R. Barrette, and D. DellaPenna, *Genetic Dissection of Carotenoid Synthesis in Arabidopsis Defines Plastoquinone as an Essential Component of Phytoene Desaturation.* Plant Cell, 1995. **7**(12): p. 2139-2149.

92. Chen, Y., F. Li, and E.T. Wurtzel, *Isolation and characterization of the Z-ISO gene encoding a missing component of carotenoid biosynthesis in plants.* Plant Physiology, 2010. **153**(1): p. 66-79.

93. Park, H., et al., *Identification of the Carotenoid Isomerase Provides Insight into Carotenoid Biosynthesis, Prolamellar Body Formation, and Photomorphogenesis.* Plant Cell, 2002. **14**(2): p. 321-332.

94. Isaacson, T., et al., *Cloning of tangerine from Tomato Reveals a Carotenoid Isomerase Essential for the Production of β-Carotene and Xanthophylls in Plants.* The Plant Cell Online, 2002. **14**(2): p. 333-342.

95. Mialoundama, A.S., et al., *Characterization of Plant Carotenoid Cyclases as Members of the Flavoprotein Family Functioning with No Net Redox Change.* Plant Physiology, 2010. **153**(3): p. 970-979.

96. Kim, J., et al., *The evolution and function of carotenoid hydroxylases in Arabidopsis.* Plant Cell Physiol., 2009: p. pcp005.

97. Jahns, P., D. Latowski, and K. Strzalka, *Mechanism and regulation of the violaxanthin cycle: The role of antenna proteins and membrane lipids.* Biochimica et Biophysica Acta (BBA) - Bioenergetics, 2009. **1787**(1): p. 3-14.

98. Xu, C.C., et al., *Suppression of zeaxanthin epoxidation by chloroplast phosphatase inhibitors in rice leaves.* Plant Science, 1999. **146**(1): p. 27-34.

99. Rabinowitch, H.D., P. Budowski, and N. Kedar, *Carotenoids and epoxide cycles in mature-green tomatoes*, in *Planta*. 1975, Springer Berlin / Heidelberg. p. 91-97.

100. Matsubara, S., A.M. Gilmore, and C.B. Osmond, *Diurnal and acclimatory responses of violaxanthin and lutein epoxide in the Australian mistletoe Amyema miquelii.* Functional Plant Biology, 2001. **28**(8): p. 793-800.

101. Bungard, R.A., et al., *Unusual carotenoid composition and a new type of xanthophyll cycle in plants.* Proceedings of the National Academy of Sciences, 1999. **96**(3): p. 1135-1139.

102. Ladygin, V., *Lutein-5,6-epoxide cycle: A new xanthophyll cycle in higher plant chloroplasts*, in *Biochemistry (Moscow) Supplemental Series A: Membrane and Cell Biology*. 2008, Springer Science. p. 110-118.

103. Esteban, R., J.M.a. Becerril, and J.I. GarcÃ-a-Plazaola, *Lutein epoxide cycle, more than just a forest tale.* psb, 2009. **4**(1559-2316): p. 342-344.

104. Garcia-Plazaola, J., et al., *The operation of the lutein epoxide cycle correlates with energy dissipation.* Functional Plant Biology, 2003. **30**(3): p. 319-324.

105. Standfuss, J., et al., *Mechanisms of photoprotection and nonphotochemical quenching in pea light-harvesting complex at 2.5 A resolution.* 2005. **24**(5): p. 919-928.

106. Klimmek, F., et al., *Structure of the Higher Plant Light Harvesting Complex I: In Vivo Characterization and Structural Interdependence of the Lhca Proteins.* Biochemistry, 2005. **44**(8): p. 3065-3073.

107. Ruban, A.V., M.P. Johnson, and C.D.P. Duffy, *The photoprotective molecular switch in the photosystem II antenna.* Biochimica et Biophysica Acta (BBA) - Bioenergetics, 2012. **1817**(1): p. 167-181.

108. Jahns, P. and A.R. Holzwarth, *The role of the xanthophyll cycle and of lutein in photoprotection of photosystem II.* Biochimica et Biophysica Acta (BBA) - Bioenergetics, 2012. **1817**(1): p. 182-193.

109. Dall'Osto, L., et al., *Different Roles of α- and β-Branch Xanthophylls in Photosystem Assembly and Photoprotection.* Journal of Biological Chemistry, 2007. **282**(48): p. 35056-35068.

110. Havaux, M., L. Dall'Osto, and R. Bassi, *Zeaxanthin Has Enhanced Antioxidant Capacity with Respect to All Other Xanthophylls in Arabidopsis Leaves and Functions Independent of Binding to PSII Antennae.* Plant Physiol., 2007. **145**(4): p. 1506-1520.

111. Tracewell, C.A., et al., *Carotenoid Photooxidation in Photosystem II.* Archives of Biochemistry and Biophysics, 2001. **385**(1): p. 61-69.

112. Schwartz, S.H., et al., *Specific oxidative cleavage of carotenoids by VP14 of maize.* Science, 1997. **276**(5320): p. 1872-4.

113. Qin, X. and J.A.D. Zeevaart, *The 9-cis-epoxycarotenoid cleavage reaction is the key regulatory step of abscisic acid biosynthesis in water-stressed bean.* Proceedings of the National Academy of Sciences, 1999. **96**(26): p. 15354-15361.

114. Alder, A., et al., *The Path from β-Carotene to Carlactone, a Strigolactone-Like Plant Hormone.* Science, 2012. **335**(6074): p. 1348-1351.

115. Gross, J., et al., *A Plant Locus Essential for Phylloquinone (Vitamin K1) Biosynthesis Originated from a Fusion of Four Eubacterial Genes.* Journal of Biological Chemistry, 2006. **281**(25): p. 17189-17196.

116. Nowicka, B. and J. Kruk, *Occurrence, biosynthesis and function of isoprenoid quinones.* Biochimica et Biophysica Acta (BBA) - Bioenergetics, 2010. **1797**(9): p. 1587-1605.

117. Johnson, T.W., et al., *Recruitment of a Foreign Quinone into the A1 Site of Photosystem I. Genetic and Physiological Characterization of Phylloquinone Biosynthetic Pathways Mutants in Synechocystis sp. PCC 6803.* Journal of Biological Chemistry, 2000. **275**(12): p. 8523-8530.

118. Furt, F., et al., *A bimodular oxidoreductase mediates the specific reduction of phylloquinone (vitamin K1) in chloroplasts.* The Plant Journal, 2010. **64**(1): p. 38-46.

119. Lochner, K., O. Doring, and M. Bottger, *Phylloquinone, what can we learn from plants?* BioFactors, 2003. **18**(1-4): p. 73-78.

120. Sadre, R., J. Gruber, and M. Frentzen, *Characterization of homogentisate prenyltransferases involved in plastoquinone-9 and tocochromanol biosynthesis.* FEBS Letters, 2006. **580**(22): p. 5357-5362.

121. Gechev, T.S. and J.M.S. Frank Van Breusegem, Iliya Denev, Christophe Laloi,, *Reactive oxygen species as signals that modulate plant stress responses and programmed cell death.* BioEssays, 2006. **28**(11): p. 1091-1101.

122. Allen, J.F., *Photosynthesis: The Processing of Redox Signals in Chloroplasts.* Current Biology, 2005. **15**(22): p. R929-R932.

123. Shikanai, T., et al., *Directed disruption of the tobacco ndhB gene impairs cyclic electron flow around photosystem I* Proceedings of the National Academy of Sciences 1998 **95** (16): p. 9705-9709

124. Ifuku, K., et al., *Structure of the Chloroplast NADH Dehydrogenase-Like Complex: Nomenclature for Nuclear-Encoded Subunits.* Plant and Cell Physiology, 2011. **52**(9): p. 1560-1568.

125. Rochaix, J.-D., *Regulation of photosynthetic electron transport.* Biochimica et Biophysica Acta (BBA) - Bioenergetics, 2011. **1807**(3): p. 375-383.

126. Kruk, J., M. Jemiola-Rzeminska, and K. Strzalka, *Plastoquinol and α-tocopherol quinol are more active than ubiquinol and α-tocopherol in inhibition of lipid peroxidation.* Chemistry and Physics of Lipids, 1997. **87**(1): p. 73-80.

127. Gruszka, J., A. Pawlak, and J. Kruk, *Tocochromanols, plastoquinol, and other biological prenyllipids as singlet oxygen quenchers--determination of singlet oxygen quenching rate constants and oxidation products.* Free Radical Biology and Medicine, 2008. **45**(6): p. 920-928.

128. Mene-Saffrane, L., A.D. Jones, and D. DellaPenna, *Plastochromanol-8 and tocopherols are essential lipid-soluble antioxidants during seed desiccation and quiescence in Arabidopsis.* Proceedings of the National Academy of Sciences, 2010. **107**(41): p. 17815-17820.

129. Sattler, S.E., et al., *Nonenzymatic Lipid Peroxidation Reprograms Gene Expression and Activates Defense Markers in Arabidopsis Tocopherol-Deficient Mutants.* Plant Cell, 2006. **18**(12): p. 3706-3720.

130. Maeda, H., et al., *Tocopherols Play a Crucial Role in Low-Temperature Adaptation and Phloem Loading in Arabidopsis.* Plant Cell, 2006. **18**(10): p. 2710-2732.

131. Sattler, S.E., et al., *Characterization of Tocopherol Cyclases from Higher Plants and Cyanobacteria. Evolutionary Implications for Tocopherol Synthesis and Function.* Plant Physiology, 2003. **132**(4): p. 2184-2195.

132. Maeda, H., et al., *Tocopherols Modulate Extraplastidic Polyunsaturated Fatty Acid Metabolism in Arabidopsis at Low Temperature.* Plant Cell, 2008. **20**(2): p. 452-470.

133. Abbasi, A.-R., et al., *Specific Roles of α- and γ-Tocopherol in Abiotic Stress Responses of Transgenic Tobacco.* Plant Physiology, 2007. **143**(4): p. 1720-1738.

134. Matringe, M., et al., *Tocotrienols, the Unsaturated Forms of Vitamin E, Can Function as Antioxidants and Lipid Protectors in Tobacco Leaves.* Plant Physiol., 2008. **147**(2): p. 764-778.

135. Maeda, H., et al., *Tocopherols Protect Synechocystis sp. Strain PCC 6803 from Lipid Peroxidation.* Plant Physiol., 2005. **138**(3): p. 1422-1435.

136. Havaux, M., et al., *Vitamin E Protects against Photoinhibition and Photooxidative Stress in Arabidopsis thaliana.* Plant Cell, 2005. **17**(12): p. 3451-3469.

137. Li, Z., J.D. Keasling, and K.K. Niyogi, *Overlapping photoprotective function of vitamin E and carotenoids in Chlamydomonas.* Plant Physiology, 2011.

138. Kobayashi, N.D.D., *Tocopherol metabolism, oxidation and recycling under high light stress in Arabidopsis.* The Plant Journal, 2008. **55**(4): p. 607-618.

139. Tanaka, A., et al., *Chlorophyll a oxygenase (CAO) is involved in chlorophyll b formation from chlorophyll a.* Proceedings of the National Academy of Sciences, 1998. **95**(21): p. 12719-12723.

140. Reinbothe, C., et al., *Chlorophyll biosynthesis: spotlight on protochlorophyllide reduction.* Trends in Plant Science, 2010. **15**(11): p. 614-624.

141. Davis, S.J., J. Kurepa, and R.D. Vierstra, *The Arabidopsis thaliana HY1 locus, required for phytochrome-chromophore biosynthesis, encodes a protein related to heme oxygenases.* Proceedings of the National Academy of Sciences, 1999. **96**(11): p. 6541-6546.

142. Muramoto, T., et al., *The Arabidopsis Photomorphogenic Mutant hy1 Is Deficient in Phytochrome Chromophore Biosynthesis as a Result of a Mutation in a Plastid Heme Oxygenase.* The Plant Cell, 1999. **11**(3): p. 335-348.

143. Meskauskiene, R., et al., *FLU: A negative regulator of chlorophyll biosynthesis in Arabidopsisthaliana.* Proceedings of the National Academy of Sciences, 2001. **98**(22): p. 12826-12831.

144. Kauss, D., et al., *FLU, a negative feedback regulator of tetrapyrrole biosynthesis, is physically linked to the final steps of the Mg++-branch of this pathway.* FEBS letters, 2012. **586**(3): p. 211-216.

145. Kim, C. and K. Apel, *Substrate-Dependent and Organ-Specific Chloroplast Protein Import in Planta.* Plant Cell, 2004. **16**(1): p. 88-98.

146. Beisel, K.G., et al., *Continuous Turnover of Carotenes and Chlorophyll a in Mature Leaves of Arabidopsis Revealed by 14CO_2 Pulse-Chase Labeling.* Plant Physiology, 2010. **152**(4): p. 2188-2199.

147. Horie, Y., et al., *Participation of Chlorophyll b Reductase in the Initial Step of the Degradation of Light-harvesting Chlorophyll a/b-Protein Complexes in Arabidopsis.* Journal of Biological Chemistry, 2009. **284**(26): p. 17449-17456.

148. Schelbert, S., et al., *Pheophytin Pheophorbide Hydrolase (Pheophytinase) Is Involved in Chlorophyll Breakdown during Leaf Senescence in Arabidopsis.* Plant Cell, 2009. **21**(3): p. 767-785.

149. Hortensteiner, S. and B. Krautler, *Chlorophyll breakdown in higher plants.* Biochimica et Biophysica Acta (BBA) - Bioenergetics, 2011. **1807**(8): p. 977-988.

150. Sakuraba, Y., et al., *STAY-GREEN and Chlorophyll Catabolic Enzymes Interact at Light-Harvesting Complex II for Chlorophyll Detoxification during Leaf Senescence in Arabidopsis.* The Plant Cell Online, 2012.

151. Valentin, H.E., et al., *The Arabidopsis vitamin E pathway gene5-1 Mutant Reveals a Critical Role for Phytol Kinase in Seed Tocopherol Biosynthesis.* Plant Cell, 2006. **18**(1): p. 212-224.

152. Hopkins, M., et al., *Regulation and execution of molecular disassembly and catabolism during senescence.* New Phytologist, 2007. **175**(2): p. 201-214.

153. Williams, B. and M. Dickman, *Plant programmed cell death: can't live with it; can't live without it.* Molecular Plant Pathology, 2008. **9**(4): p. 531-544.

154. Seo, Y.S., et al., *Enzymatic characterization of class I DAD1-like acylhydrolase members targeted to chloroplast in Arabidopsis.* FEBS Letters, 2009. **583**(13): p. 2301-2307.

155. Hyun, Y., et al., *Cooperation and Functional Diversification of Two Closely Related Galactolipase Genes for Jasmonate Biosynthesis.* Developmental cell, 2008. **14**(2): p. 183-192.

156. Reinbothe, C., et al., *Plant oxylipins: role of jasmonic acid during programmed cell death, defence and leaf senescence.* FEBS Journal, 2009. **276**(17): p. 4666-4681.

157. He, Y., et al., *Evidence Supporting a Role of Jasmonic Acid in Arabidopsis Leaf Senescence.* Plant Physiology, 2002. **128**(3): p. 876-884.

158. Caldelari, D., et al., *Arabidopsis lox3 lox4 double mutants are male sterile and defective in global proliferative arrest*, in *Plant Molecular Biology*. 2011, Springer Netherlands. p. 25-33.

159. Bannenberg, G., et al., *Diversity of the Enzymatic Activity in the Lipoxygenase Gene Family of Arabidopsis thaliana*, in *Lipids*. 2009, Springer Berlin / Heidelberg. p. 85-95.

160. Acosta, I.F., et al., *tasselseed1 Is a Lipoxygenase Affecting Jasmonic Acid Signaling in Sex Determination of Maize.* Science, 2009. **323**(5911): p. 262-265.

161. Li, L., et al., *Modes of heme binding and substrate access for cytochrome P450 CYP74A revealed by crystal structures of allene oxide synthase.* Proceedings of the National Academy of Sciences, 2008. **105**(37): p. 13883-13888.

162. Schaller, F. and S.R. Philipp Zerbe, Christiane Reinbothe, Eckhard Hofmann, Stephan Pollmann,, *The allene oxide cyclase family of Arabidopsis thaliana, localization and cyclization.* FEBS Journal, 2008. **275**(10): p. 2428-2441.

163. Fonseca, S., et al., *(+)-7-iso-Jasmonoyl-L-isoleucine is the endogenous bioactive jasmonate.* Nature Chemical Biology, 2009. **5**(5): p. 344-350.

CHAPTER TWO

THE FUNCTIONAL NETWORK OF THE ARABIDOPSIS PLASTOGLOBULE PROTEOME BASED ON QUANTITATIVE PROTEOMICS AND GENOME-WIDE CO-EXPRESSION ANALYSIS [1,2]

2.1 ABSTRACT

Here the PG proteome is more carefully defined and a conceptual framework for further studies is provided. The PG proteome from Arabidopsis leaf chloroplasts was determined by mass spectrometry of isolated PGs and quantitative comparison with the proteomes of unfractionated leaves, thylakoids and stroma. Scanning electron microscopy showed the purity and size distribution of the isolated PGs. Compared to previous PG proteome analyses, we excluded several proteins and identified six new PG proteins, including an M48 metallopeptidase and two ABC1 atypical kinases, confirmed by immunoblotting. This refined PG proteome consisted of 30 proteins, including 6 ABC1 kinases and 7 fibrillins together comprising more than 70% of the PG protein mass. Other fibrillins located predominantly in the stroma or thylakoid and not PG; we discovered that this partitioning can be predicted by their isoelectric point and hydrophobicity. A genome-wide co-expression network for the PG genes was then constructed from mRNA expression data. This revealed a modular network with four distinct modules that each contained at least one ABC1K and/or fibrillin gene. Each module showed clear enrichment

[1] Previously published in Lundquist, et al, Plant Physiology 2012 158 (3) 1172-1192. Copyright owned by the American Society of Plant Biologists (ASPB).

[2] M48 antibody was constructed by Dr. Nazmul Bhuiyan. In-gel digestions and mass-spectrometry operation was performed by Drs. Anton Poliakov and Boris Zybailov.

in specific functions, including chlorophyll degradation/senescence, isoprenoid biosynthesis, plastid proteolysis and plastid redox and kinase regulators of electron flow (e.g. thioredoxins, STN7, RAP38). We propose a new testable model for the PGs, in which sets of genes are associated with specific PG functions.

2.2 INTRODUCTION

Plastoglobules (PGs) are lipoprotein particles localized in the various types of photosynthetic and non-photosynthetic plastids of photosynthetic organisms. In chloroplasts, PGs are contiguous with the thylakoid membrane – reviewed in [1-3]. PGs can be released from the thylakoid membrane by sonication, and purification based on their low density has facilitated analysis of their metabolites [4-7] and protein composition [4, 8]. This has shown that PGs contain various prenyl lipids and neutral lipids, including plastoquinone, phylloquinone, α-tocopherol, fatty acid phytyl esters, and triacylglycerol. For many years it was believed that PGs solely represented a passive lipid deposition site for the plastid. Thus, the discovery of several dozen PG-localized proteins, mostly with unknown functions, was highly surprising [4, 8]. The PG proteome contains a number of proteins of which only a few, such as tocopherol cyclase (VTE1) and allene oxide synthase (AOS), have an established function. In addition to these various (putative) enzymes, the PG proteome contains a number of proteins of the fibrillin (FBN) family, initially believed to play more structural functions. However, based on the presence of lipocalin domains in some of these FBNs, it has recently been suggested that they may also play a role in metabolite transport [2]. Finally, the PG proteome also contains a number of ABC1K proteins; these are putative atypical kinases with homology to an ABC1K in yeast and *E. coli,* where they regulate ubiquinone synthesis [9-11]. The presence of several of the ABC1K proteins in PGs is

puzzling and we earlier suggested that they play a central role in regulation of PG metabolism [1, 8].

PGs appear to play a role in chloroplast development, senescence, and stress defense. Their shrinking and swelling in response to (a)biotic stresses and during developmental transitions, as well as in plastid biogenesis mutants is well documented [6, 12-14]. Recent results suggest that PGs are involved in active channeling of hydrophobic metabolites between the thylakoid and PG, permitted by the contiguous association of the two structures [6, 15]. In particular during various abiotic stresses (e.g. N-starvation, drought or light stress), but also during senescence, components of thylakoid degradation, such as fatty acids and phytol tails from chlorophyll, are channeled into the PGs, likely accounting for the massive swelling. Within the PG, several of the observed proteins likely play a role in the recycling of such thylakoid catabolites, in addition to a role in synthesis of isoprenyl lipids such as tocopherol and plastoquinone [4, 8].

Despite the recent progress on PG analysis, it remains unclear how the PGs fit into plastid metabolism and chloroplast homeostasis, mostly because functions for many PG-localized proteins are unknown. Key questions about PGs are: i) what determines and controls their size, shape and content, ii) how are proteins recruited to the PG proteome and how does the PG proteome change in response to changes in developmental state or (a)biotic conditions, iii) what are the functions of the PG proteins and how are they related to each other? The current study aims to provide a better framework to help answer these questions by defining a functional network.

We first examined the quantitative protein composition of PGs isolated from leaves subjected to 5 days of increased light intensity (500 μmol photons.m^2.s^{-1}) and compared this

quantitatively against proteomics datasets of leaf, thylakoid, and stroma preparations to identify proteins specifically enriched in the PG. Because we used a far more sensitive mass spectrometer than used in previous PG proteome analyses [4, 8], combined with both in-gel and in-solution digestions, we expected to discover more low abundant members of the PG proteome. Indeed, we identified a number of new PG proteins, including an M48 metallopeptidase (M48), two additional ABC1K proteins and a senescence-associated gene (SAG) protein. The surprising localization of M48, as well as two ABC1K proteins, to PGs was confirmed by immunoblotting.

Transcripts or proteins involved in related biological pathways or complexes often accumulate simultaneously. Therefore, co-expression often implies the presence of functional or physical linkages between genes or proteins, allowing for identification of new components of processes or protein complexes. Indeed, co-expression analysis has been used extensively in plant biology to identify putative protein functions and determine physical or functional connections between proteins [16-26].

Here we employed such a transcriptional genome-wide co-expression analysis, using the core PG proteome as input, to provide a better framework for PG functions and to associate PG proteins to functional activities. This identified a co-expression network with 4 modules, each with a specific set of enriched functions, including plastid proteases, redox regulators, cyclic electron flow components and genes encoding for a specific subset of proteins involved in plastid prenyl-lipid metabolism. Specific ABC1K proteins and FBNs were centrally positioned in different modules within the network. This study better defines the core PG proteome and its functions in leaves. We propose a new conceptual model for the PGs, suggest a parallel to lipid rafts, and provide an intellectual and practical framework for further analysis.

2.3 RESULTS

2.3.1 Size distribution, extractability, coalescence, and purity of isolated PGs from light-shifted Arabidopsis leaves As starting material for our study, we grew *Arabidopsis* plants on soil for 2.5 weeks at 120 µmol photons.m^{-2}.s^{-1} and transferred them to 520 µmol.m^{-2}.s^{-1} for 5 days. The higher light intensity increased PG volume and yield and made them more amenable for experimental analysis [8]. The mild light stress treatment accelerated vegetative growth, increased anthocyanin accumulation in the leaves, and resulted in only minor visible damage at the edges of the oldest leaves, but no damage to younger leaves.

Isolation of PGs from the Arabidopsis leaf rosettes was performed by sonication of isolated thylakoid membranes followed by flotation density centrifugation, as in [8]. The enrichment of PGs was confirmed by immunodetection of the VTE1 protein (Figure 1A), known to be uniquely localized in the PG as determined by YFP localization and immunogold labeling [4], immunoelectron tomography [15] and proteomics [4, 8].

Densitometric analysis of the immunoblots indicated a more than 400-fold enrichment of VTE1 in the PG preparations compared to the original thylakoid membranes (the starting material). We also measured a ~4-fold depletion of VTE1 in thylakoids following sonication, indicating that ~75% of the PG material is extracted from the thylakoids by sonication (Figure 1B). Hence, our results demonstrate that the isolated PGs were highly enriched for PG particles and that the majority of the PGs were successfully extracted from the thylakoid membrane.

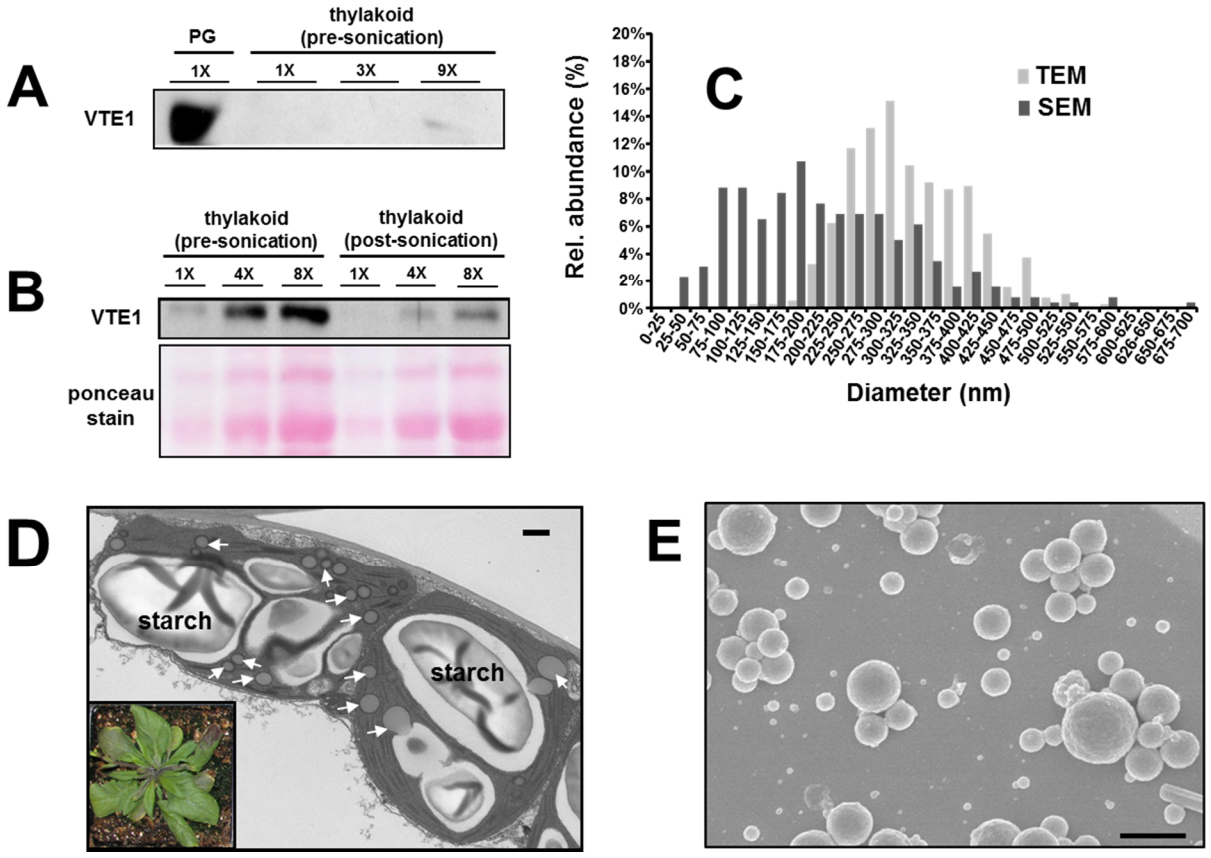

Figure 1. PG extraction and purification efficiency. A, Immunoblot of a thylakoid sample prior to sonication and purified PG fractions. Proteins were separated by 1D SDS-PAGE and probed with antibody against PG marker protein, VTE1. 1x corresponds to 2.2 µg protein. B, Immunoblot of thylakoid samples prior to sonication and after sonication for removal of PGs. A Ponceau stain of protein is included as a loading control. 1x corresponds to 10 µg protein. C, Histogram illustrating the distribution of PG diameters from transmission electron micrographs (TEM) of chloroplasts in mature light stressed leaf tissue and scanning electron micrographs (SEM) of purified PG preparations, $n \geq 263$ measurements. D, Transmission electron micrograph (TEM) of 5-day light stressed leaf chloroplast of *A. thaliana* (Col-0), representative of the time point PG preparations were made. An image of a typical light stressed Arabidopsis rosette plant is shown. PGs in the TEM, marked by white arrows, appear as gray circles with black periphery or, less frequently as solid black circles. E, SEM of *A. thaliana* (Col-0) purified PGs, demonstrating efficient isolation of PGs with varying diameters. Scale bars in (D) and (E) = 500 nm.

Transmission electron micrographs (TEM) of PGs *in vivo* have demonstrated a broad size distribution, even within the same chloroplast [15], however the relationship between PG size

and PG proteome is not known. For a correct and meaningful quantitative and qualitative analysis of the PG proteome, it was therefore critical to extract PGs representing the entire *in vivo* population, without bias for size or other (unknown) properties, while keeping contamination from thylakoids and other compartments to a minimum. Therefore we compared the size distribution of the extracted PG particles to the *in vivo* size distribution. TEM of the leaf tissue showed a broad distribution of PG sizes, with diameters ranging from ~175 nm to ~600 nm, and peaking between 250-350 nm (Figures 1C and D). PG preparations were analyzed by scanning electron microscopy (SEM) and also showed a broad size distribution from ~50 to ~600 nm, peaking between 100-250 nm (Figure 1C and E). This demonstrated that PGs of all physiologically relevant sizes were extracted efficiently, with a small bias to smaller particles. Interestingly, the micrographs of PG preparations sometimes showed PGs in grape-like clusters, similar to those described in TEM micrographs of leaves [5, 12, 15, 27] (Figure 2A and B). Despite the clustering found in the preparations, each PG clearly maintained its individual structure and they did not coalesce. Apparently, component(s) at the PG-solution interface act to maintain PG structural integrity and are extractable with the PGs, likely a FBN coat surrounding the PG periphery. Evidence of minor amounts of thylakoid membrane fragments was also found in the micrographs. While the isolated PGs demonstrated remarkably smooth surfaces, the SEM also showed infrequent amorphous structures scattered generally attached to PGs (Figure 2C). The size of these structures, the presence of attached PGs, and their amorphous shape suggested that they are thylakoid membrane fragments. Importantly, these amorphous structures were far less abundant than the PGs, indicating high PG purity, which was further confirmed by the proteomics experiments (see next section). Summarizing, our results demonstrate that more than

~75% of the PGs, from all physiologically relevant sizes, were successfully extracted from the thylakoid membrane into highly enriched PG preparations.

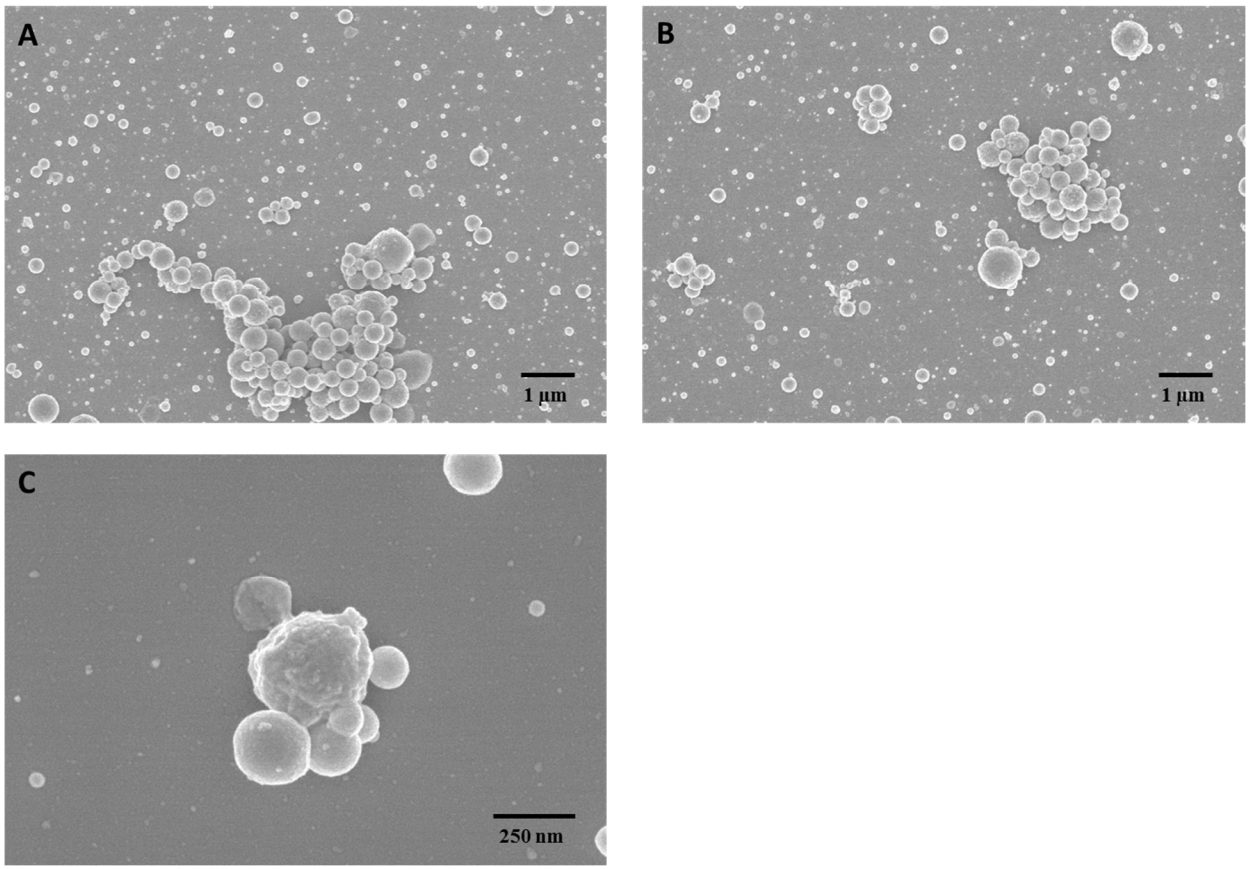

Figure 2. Scanning electron micrographs of PG preparations. A and B, Representative images demonstrating PG clustering. C, Representative amorphous globule, likely representing stromal lamellae thylakoid attached to PGs.

2.3.2 Improved coverage and quantification of the PG proteome The first comprehensive PG proteome analyses were carried out using a Q-TOF mass spectrometer [8] or a LCQ Deca XP ion trap mass spectrometer [4]. Recent improvements in sensitivity, mass accuracy, and speed of mass spectrometers have enabled detection of lower abundant proteins in complex mixtures and also facilitate mass spectrometry-based label-free proteome quantifications using spectral

counting [28-30]. Thus a much more sensitive and quantitative analysis of the PG proteome should now be possible. The spectral counting technique is based on the observation that the number of successful MS/MS acquisitions of peptides coming from a protein shows a positive and linear correlation to the relative concentration of this protein in the studied sample [31-34]. Spectral counting is particularly effective to detect large quantitative differences, as expected in our study where we compare (sub)cellular or suborganellar fractions that are very different in function and composition. We previously optimized the SPC workflow and tested it for *Arabidopsis* and maize organelles, cell-types and complexes, e.g. [35-38]. The relative normalized abundance (relative mass contribution) of each protein within each sample, NadjSPC, was calculated from the number of adjusted matched MS/MS spectra (adjSPC), normalized to the total adjSPC per sample, as defined previously [36]. Thus a protein with a NadjSPC= 0.01 contributes ~1% of the protein mass of the analyzed sample. As a general rule, the accuracy of quantification improves with the number of adjSPC per protein.

Here we employed a LTQ-Orbitrap mass spectrometer [39] coupled to a nanoLC system, to search for additional, more low-abundant proteins located in the PG. Moreover, we re-evaluated previous assignments of proteins to the PG [4, 8] based on quantitative comparative proteome information. Using three independent PG preparations, the PG proteome was analyzed in two different ways: i) PG proteins were separated by SDS-PAGE, each lane cut in 5 slices, and in-gel digested with trypsin, and ii) unfractionated PGs were delipidized and digested in-solution with trypsin. These protein digests were then analyzed by MS/MS in the LTQ-Orbitrap (Figure 3A). The rationale for using these two different protein extraction/separation methods was to: i) maximize detection of low abundant proteins, ii) increase the robustness of protein

quantification, and iii) improve protein sequence coverage. Proteins identified by only a single peptide sequence, irrespective of post-translational modification or charge state, were discarded

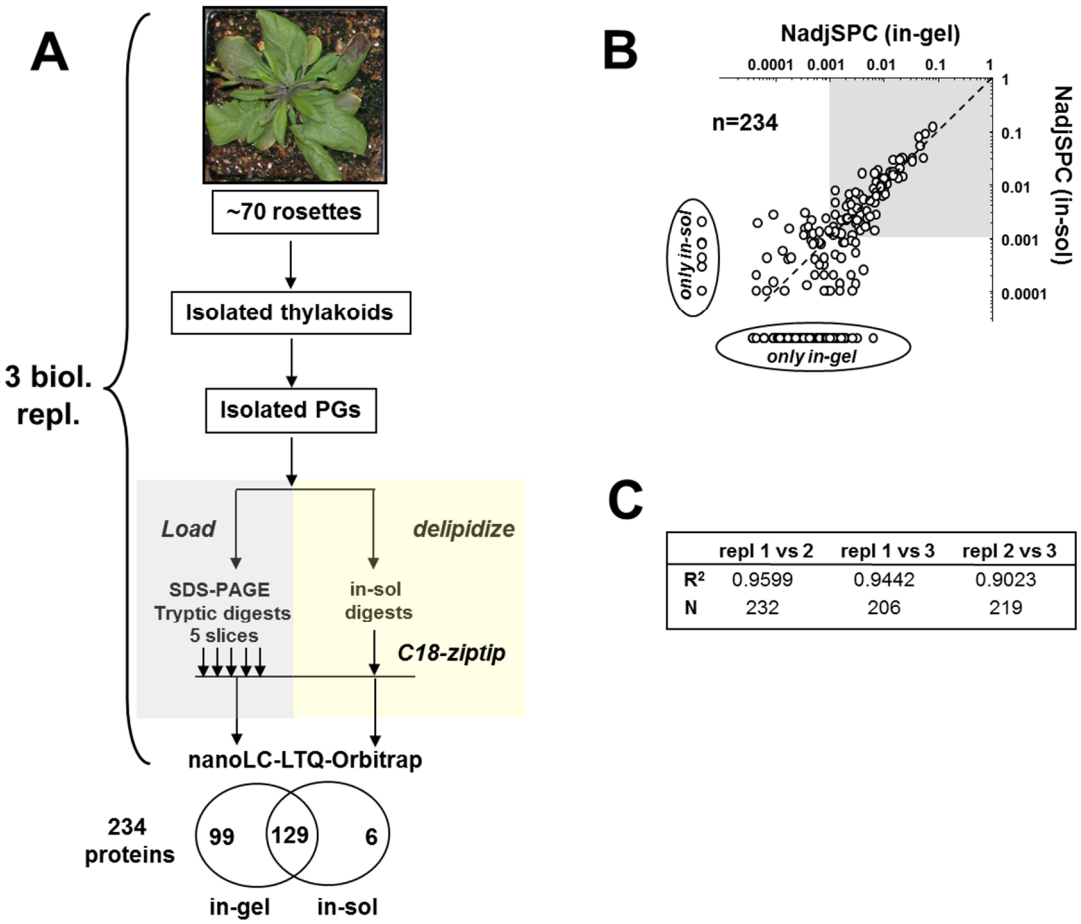

Figure 3. Identification of the PG proteome by in-gel and in-solution methods. A, Three independent preparations of PGs were made from 5-day light stressed *A. thaliana*. Thylakoids were isolated from total leaf tissue and sonicated to release PGs. Aliquots of each PG preparation were then separated by SDS-PAGE and in-gel digested or delipidized, in-solution digested, and zip-tipped. In-solution and in-gel digested peptides were analyzed with a nanoLC-LTQ-Orbitrap mass spectrometer. 234 unique proteins were identified in total, 129 of which were identified by both experimental methods. B, Comparison of NadjSPC between each of the 234 proteins between the in-gel and in-solution methods demonstrates consistent quantification of proteins above 0.001 NadjSPCs, marked in grey. C, Comparison of protein abundance (measured as NadjSPC) between each of the three biological replicates (repl). R2, Pearson Correlation Coefficient. N, number of proteins. Proteins only present in one of each pair were included in the correlation analysis and were represented by a zero value when absent.

to increase the robustness of the analysis and avoid any false-positive protein identification; these proteins represented <1% of the protein mass in PGs.

2.3.3 Defining the core PG proteome The combined proteome analysis identified 234 proteins, with 129 identified by both in-solution and in-gel workflows and respectively 6 and 99 proteins identified in only the in-solution or in-gel digestions (Figure 3A). The 129 proteins identified by both methods represented ~99% of the PG protein mass, showing that only the least abundant proteins were not identified by both methods. The in-solution and in-gel methods showed a good correlation for the relative protein abundance for proteins with abundance >0.001, i.e. proteins that each represent >0.1% of the protein mass of the PGs (Figure 3B - grey area). Protein sequence coverage was on average 26% for the in-gel method and 16% for the in-solution method; this increased to 37% and 27% respectively if we only considered the 129 proteins identified by both methods. The correlation of the average NadjSPC values (combining both in-gel and in-solution data) between the three biological replicates was excellent, with pair-wise correlation coefficients between 0.902 and 0.960 (Figure 3C).

We then determined those proteins highly-enriched in the PGs, hereafter named the 'core' PG proteome, using the workflow as depicted in figure 4A. The core PG proteins were distinguished from non-plastid contaminants or proteins localized primarily elsewhere in the chloroplast by comparing the abundance in PGs to their average abundance in total leaf extracts (5 biological replicates with 2 replicates from [40] and 3 from this study), and isolated thylakoid and stromal fractions [35]. Furthermore, core PG proteins were required to have a minimal abundance (NadjSPC >0.001) and be observed in the PGs by both in-gel and in-solution methods (Figure 4A).

For selection of core PG proteins, we first discarded those proteins with a PG/leaf abundance ratio below 10; only 52 proteins out of the 234 proteins passed this first filter. We emphasize that this was a relatively 'relaxed' minimal threshold considering that the PG

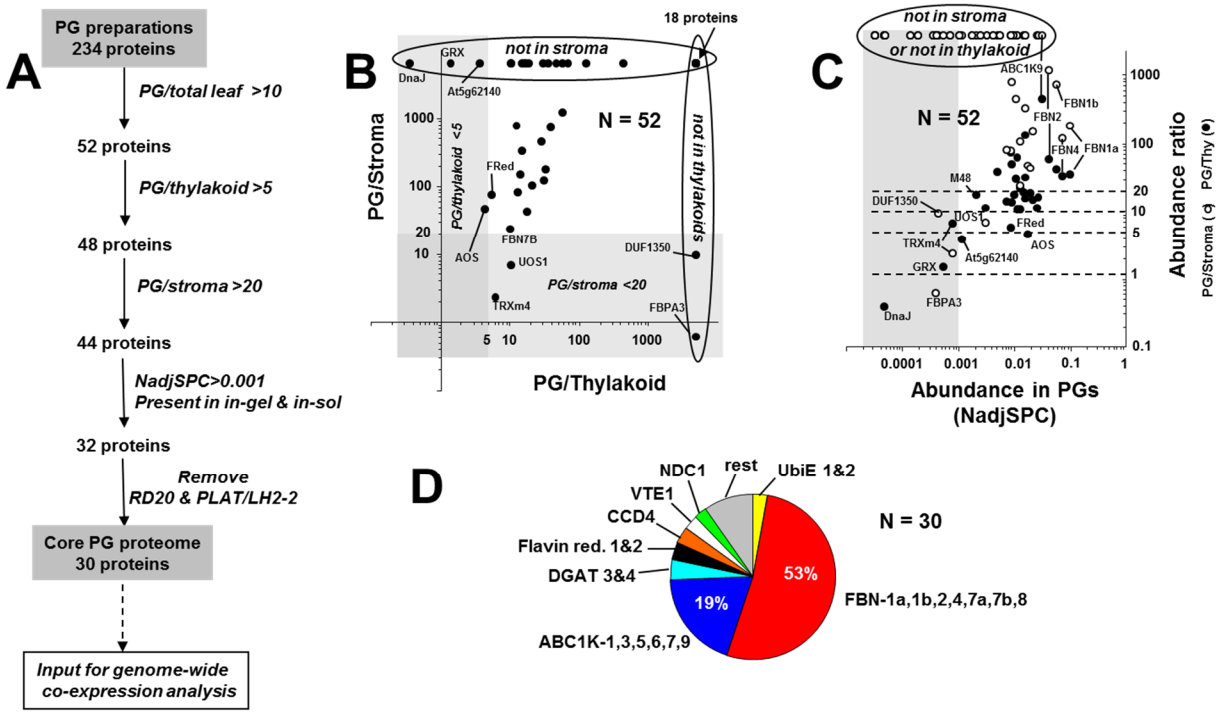

Figure 4. Determination of the PG core proteome. A, The PG proteome flow diagram. 234 unique proteins were identified and quantified from the in-solution and in-gel experiments of 5-day light-stressed *A. thaliana* (Col-0) PGs. These 234 proteins were passed through 4 sequential filters, first by comparing the protein abundance between the PG and representative preparations of total leaf, thylakoid and stroma (measured as average NadjSPC) and then discarding proteins with abundances less than 0.001 NadjSPC in PG preparations and not found in both methods. 32 proteins passed all 4 filters. Manual curation then found the caleosin, RD20, and PLAT/LH2-2, to be ER-localized (Aubert et al., 2010) (http://gfp.stanford.edu/index.html) and were manually removed, resulting in a core PG proteome comprised of 30 proteins. This core proteome then served as the input for a genome-wide co-expression analysis. B and C, Sub-organellar distribution (B) and abundance (C) of the 52 proteins passing the total leaf filter (enriched > 10-fold in PGs) were plotted. Proteins with PG/stroma < 20 or PG/thylakoid < 5 are gray and were eliminated from the core proteome by the filter series. D, Relative mass contributions of the 30 PG core proteins to the total PG core proteome.

proteome represents less than 10% of the leaf proteome – however, this was already very effective to remove non-plastid contaminants, as well as the abundant proteins of the photosynthetic apparatus, and other proteins not truly enriched in PGs. Importantly, it also removed several proteins that were earlier assigned to the PG, including fructose bisphosphate aldolase 1 and 2 (FBPA-1 and -2) [4, 8]. Furthermore, FBN3a and FBN10 were also eliminated, because they showed PG/leaf abundance ratios of only 0.9 and 4.7 respectively (Table 1). The relative abundance and distribution of the remaining 52 proteins between PGs, thylakoids and stroma is displayed in Figures 4B,C.

Table 1. Subplastid localization of fibrlllin proteins and their variants

accession #	name	PG/stroma	PG/thylakoid	PG core	thylakoid / stroma
AT1G51110.1	FBN10	not in stroma	1.8	no	not in stroma
AT4G04020.1	FBN1a	176.2	34.0	yes	5.2
AT4G22240.1	FBN1b	712.8	39.9	yes	17.9
AT2G35490.1	FBN2	1187.7	59.0	yes	20.1
AT3G26070.1	FBN3a	not in stroma	0.1	no	only thylakoid
AT3G26080.1	FBN3b	not in stroma	not in PG	no	only thylakoid
AT3G23400.1	FBN4	121.2	32.0	yes	3.8
AT5G09820.1	FBN5.1	not in PG	—	no	only stroma
AT5G19940.1	FBN6	not in PG	not in PG	no	15.0
AT3G58010.1	FBN7a	145.6	14.8	yes	9.9
AT2G42130.4	FBN7b	23.5	10.6	yes	2.2
AT2G46910.1	FBN8	434.1	29.4	yes	14.8
AT4G00030.1	FBN9	—	—	no	not observed
AT1G18060.1	FBN-like	not in PG	not in PG	no	22.7
variant (a)	FBN7a (1-290)		stroma		
variant (a)	FBN7a (1-133)		thylakoid		

(a) from Ref. [46]

As a next step, we removed proteins that failed to show at least a 5-fold enrichment in the isolated PGs compared to the thylakoid (Figure 4A). This resulted in removal of 4 proteins – a DnaJ domain protein, a glutaredoxin (GRX), a protein with an unknown function (At5g62140)

and allene oxide synthase (AOS) (Figure 4B). Finally, 4 proteins with a PG/stroma abundance ratio below 20 were discarded – these were thioredoxin m4 (TRXm4), UV-B/Ozone similarly-regulated protein (UOS1), an unknown protein with DUF1350 domain and fructose-bisphosphate aldolase-3 (FBPA-3) (Figure 4B).

The remaining 44 proteins were then evaluated for abundance and frequency of identification in the PG proteome analysis (Figure 4C). 12 proteins with a relative abundance below NadjSPC of 0.001 (corresponding to ≤0.1% of the protein mass) (Figure 4C), or only identified by one of the methods, were discarded (We note that none of these proteins were co-expressors of the PG core genes – see further below). Finally, we manually evaluated the remaining 32 proteins for known subcellular localization and/or function. Two proteins were discarded from the core proteome based on literature evidence. The extra-plastidic caleosin protein RD20 (at2g33380) has been shown to be localized in cytosolic lipoprotein particles [41], while a PLAT/LH2 domain protein (at2g22170) is likely ER-localized based on GFP-tagging (http://gfp.stanford.edu/index.html). Thus, these proteins were removed from the final list.

Because the PGs were isolated from plants shifted for 5 days to higher light intensities (500 μmol photons.s^{-1}.s^{-1}), we also determined and quantified the total leaf proteome of these plants (three independent replicates). However, using these quantitative total leaf proteome data in the workflow (Figure 4A) did not affect the final selection of core PG proteins.

2.3.4 The core PG proteome Table 2 summarizes the core PG proteome with their relative abundance (including the coefficient of variation - CV) and enrichment as compared to other plastid compartments. The CV of protein abundance across the 3 biological replicates was 24%, indicating an excellent reproducibility. Twenty-three of the 30 core proteins were previously

assigned to the PG in [4] or [8], with 18 identified in both studies (Table 2). VTE1 showed a PG/thylakoid ratio of 131, consistent with the high ratio determined by the immunoblot analysis (Figure 1A), and was not detected in chloroplast stroma.

Another seven proteins were newly identified as plastoglobular, namely two ABC1 kinases (ABC1K6 and K7), a PLAT/LH2-domain protein (PLAT/LH2-1), an esterase-domain protein (Esterase 1), two proteins of unknown function (Unknown-2 with DUF1350 and Unknown Senescence-Associated Gene - SAG), and a metallopeptidase M48-domain protein. Six of these seven proteins are the lowest abundant proteins of the core PG proteome (Table 2), explaining their previous lack of detection. Thirteen proteins previously assigned to the PG did not pass our filters (Table 2); these were AOS, FBPA-1,2,3, FBN3a, two RNA-associated proteins (Rap38&41), an ATPase, WAVE3, peroxiredoxin Q, and three proteins of unknown function (see Discussion).

Table 2. The plastoglobule core proteome

Accession #	Protein Name	NadjSPC[a]	CV [b]	Percentage Mass PG core	PG/Thylakoid	PG/Stroma	Reference[c]			
							1	2	3	
AT4G04020	Fibrillin 1a (FBN1a)	0.100	15	16.1	34	176	x	x	x	previously identified
AT3G23400	Fibrillin 4 (FBN4)	0.074	30	11.9	32	121	x	x	x	
AT4G22240	Fibrillin 1b (FBN1b)	0.059	12	9.6	40	713	x	x	x	
AT2G35490	Fibrillin 2 (FBN2)	0.044	4	7.1	59	1188	x	x	x	
AT5G05200	ABC1K9	0.032	8	5.2	440	-	x	x	x	
AT4G31390	ABC1K1	0.028	8	4.5	16	-		x	x	
AT1G79600	ABC1K3	0.027	23	4.3	11	-	x	x	x	
AT3G58010	Fibrillin 7a (FBN7a)	0.022	44	3.5	15	146	x	x	x	
AT4G19170	Carotenoid dioxygenase 4 (CCD4)	0.021	25	3.3	18	42	x	x	x	
AT4G32770	Tocopherol cyclase (VTE1)	0.016	5	2.6	131	-	x	x	x	
AT1G54570	Diacylglycerol acyltransferase 3 (DGAT3)	0.016	12	2.6	31	-	x	x	x	
AT5G08740	NAD(P)H dehydrogenase C1 (NDC1)	0.015	8	2.5	19	-	x	x	x	
AT2G42130	Fibrillin 7b (FBN7b)	0.013	45	2.1	11	23	x		x	
AT1G32220	Flavin reductase-related 1	0.013	23	2.1	22	102	x	x	x	
AT4G13200	Unknown 1	0.012	17	1.9	11	-	x	x	x	
AT3G10130	SOUL domain protein	0.011	10	1.8	61	-	x	x	x	
AT2G46910	Fibrillin 8 (FBN8)	0.011	12	1.8	29	434		x	x	
AT1G71810	ABC1K5	0.011	12	1.7	17	-		x	x	
AT1G78140	UbiE methyltransferase related 1	0.009	43	1.5	48	-	x	x	x	
AT1G06690	Aldo/keto reductase	0.009	35	1.5	13	765	x		x	
AT2G34460	Flavin reductase-related 2	0.009	26	1.5	6	75	x	x	x	
AT2G41040	UbiE methyltransferase related 2	0.009	17	1.5	72	-	x	x	x	
AT3G26840	Diacylglycerol acyltransferase 4 (DGAT 4)	0.009	14	1.4	-	-	x	x	x	
AT3G24190	ABC1K6	0.016	14	2.6	15	322			x	Newly-identified
AT4G39730	PLAT/LH2-1	0.010	29	1.6	-	-			x	
AT3G43540	Unknown 2 (DUF1350)	0.008	42	1.3	14	80			x	
AT3G07700	ABC1K7	0.005	27	0.8	37	-			x	
AT1G73750	Unknown SAG	0.002	80	0.4	-	-			x	
AT3G27110	M48 protease	0.002	42	0.3	17	-			x	
AT5G41120	Esterase 1	0.002	30	0.3	-	-			x	
AT5G42650	AOS							x		Removed
AT1G09340	Rap38/CSP41B							x		
AT1G26090	Anion-transporting ATPase							x		
AT1G28150	Unknown							x		
AT4G01150	Unknown							x		
AT3G63140	Rap41/CSP41A							x		
AT5G01730	WAVE3							x		
AT2G21330	FBPA-1						x	x		
AT4G38970	FBPA-2						x	x		
AT2G01140	FBPA-3						x	x		
AT3G26060	Peroxiredoxin Q (Prx Q)						x			
AT1G52590	Unknown (DUF39)						x			
AT3G26070	Fibrillin (FBN3a)						x			

(a) Abundance of each PG core protein.
(b) Coefficient of variation of the average NadjSPC across the three biological replicates.
(c) 1, Ref. [4]; 2, Ref. [8]; 3, current analysis.

The four most abundant proteins were all FBN proteins (FBN1a, 1b, 2, and 4) and were also found previously to be the homologues of the FBNs in red pepper chromoplast plastoglobules [8], suggesting they may hold a general function in maintenance of plastid lipid body structure. The six FBN core proteins constituted 53% of the PG proteome mass (Figure 4D). The second most abundant class of core proteins consisted of six ABC1 kinases, together constituting 19% of the core PG proteome mass. The original ABC1K proteins, identified in *Saccharomyces cerevisiae* (Abc1p/Coq8p) and *Escherichia coli* (UbiB), are implicated in regulation of ubiquinone metabolism [9, 42]. In particular, phosphorylation of several members of the ubiquinone biosynthetic complex is dependent on Abc1p/Coq8p [10]. However, the role and possible targets of the PG-localized ABC1K proteins are unknown. Carotenoid cleavage dioxygenase 4 (CCD4), with specificity for 8'-apo-β-caroten-8'-al in *Arabidopsis* [43], was 3.3% of the proteome mass. The VTE1 protein, involved in tocopherol biosynthesis [44], was 2.6% of the proteome mass and the NAD(P)H dehydrogenase C1 (NDC1), which reduces plastoquinone to plastoquinol and is necessary for phylloquinone synthesis [45] was 2.5% of the proteome mass. The M48 protein was only 0.3% of the proteome mass (Table 2).

2.3.5 Confirmation of PG localization of ABC1K2, ABC1K3 and Peptidase M48 by immunoblotting To further validate our quantitative proteomics analysis, we generated specific antisera against three PG core proteins, ABC1K2, ABC1K3 and the low abundant M48 protease because of its novelty as a potential PG-localized protease. Specific, polyclonal antisera were raised against affinity purified *E. coli* overexpressed domains of each of the three proteins. After confirming the specificity of the sera, we compared isolated thylakoid fractions and isolated PGs for protein abundance of M48, ABC1K2 and ABC1K3 using immunoblots. Figure 5 shows that

ABC1K2, ABC1K3 and M48 were ~10, 20 and >50-fold enriched in isolated PGs compared to (untreated) thylakoids, in agreement with the PG/thylakoid abundance ratios of respectively 11, 16 and 17 measured by mass spectrometry (Table 2). This provides independent evidence that metallopeptidase M48 and the two ABC1K proteins are highly enriched in the PG, and indicate that our mass spectrometry–based quantitative analysis does provide reliable information about the core PG proteome.

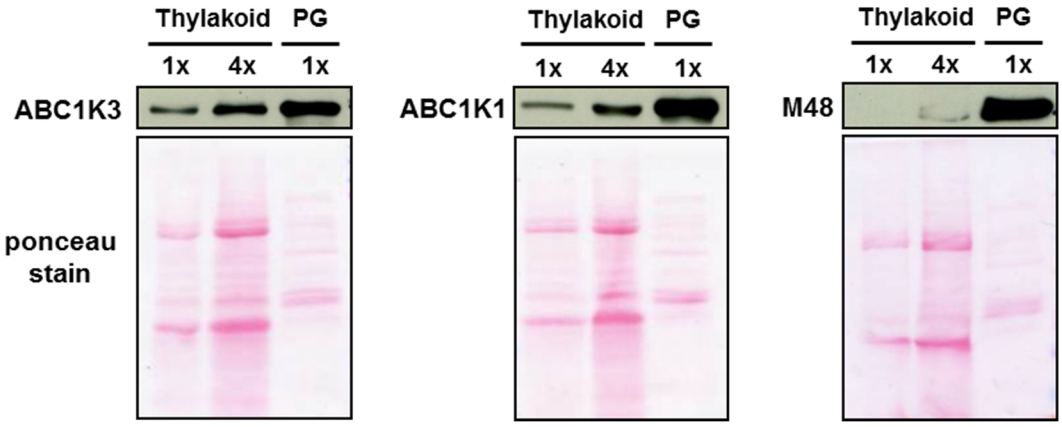

Figure 5. M48 protease, ABC1K2 and ABC1K3 are enriched in the PG preparations. Immunoblots of a thylakoid sample (prior to sonication) and the PGs (subsequently extracted by sonication), illustrate enrichment levels comparable to those determined by mass spectrometry. The Poinceau stain is included for each blot as a loading control. 1x = 10µg.

2.3.6 Partitioning of the FBN proteins between PGs and the thylakoid or stroma We identified all 12 known FBNs, as well as a FBN-like protein (AT1G18060), in our collective proteome data sets of leaves, chloroplast stroma, thylakoids and PGs (Table 1). However, we assigned only 7 FBNs to the PG core proteome, based on our quantitative analysis (Figure 4A), because the other FBNs did not preferentially locate to PGs. Therefore, we searched for physical-chemical properties of the FBN protein family that correlated with subplastid localization. We also included two truncation products of FBN7a, FBN7a (1-133) and FBN7a (1-290), which

localizations were determined by YFP-tagging as localized to stroma and PG, respectively [46]. The combination of isoelectric point (pI) and hydrophobicity (calculated as the GRAVY index) for each of the FBN correlated surprisingly well with their relative distribution between stroma, thylakoids and PG (Figure 6; Table 1). The FBN proteins could be placed in one of four groups: i) strongly enriched in the PG (at least 10-fold), ii) equal enrichment between the PG and thylakoid (PG/Thy ≈ 1), iii) strongly enriched in the thylakoid as compared to PG (>10-fold), and iv) stroma-localized, not identified in PG or Thy. All 7 PG-localized FBNs, as well as the truncated FBN7a (1-290), were found to display low pIs and (on average) higher hydrophobicity indices. Conversely, all 6 FBNs strongly enriched in the thylakoid membrane fraction displayed higher pIs and lower hydrophobicity indices. Importantly, FBN10, the only FBN with approximately equal ratio between PG and thylakoid (PG/thylakoid = 1.8) showed an intermediate pI and hydrophobicity index. Finally, the stroma-localized FBN5 and FBN7a (1-133) demonstrated a low pI and the lowest hydrophobicity indeces of the 16 proteins products. The pI and GRAVY index however did not predict subplastid localization of other members of the core PG proteome, likely because they have very diverse secondary structures.

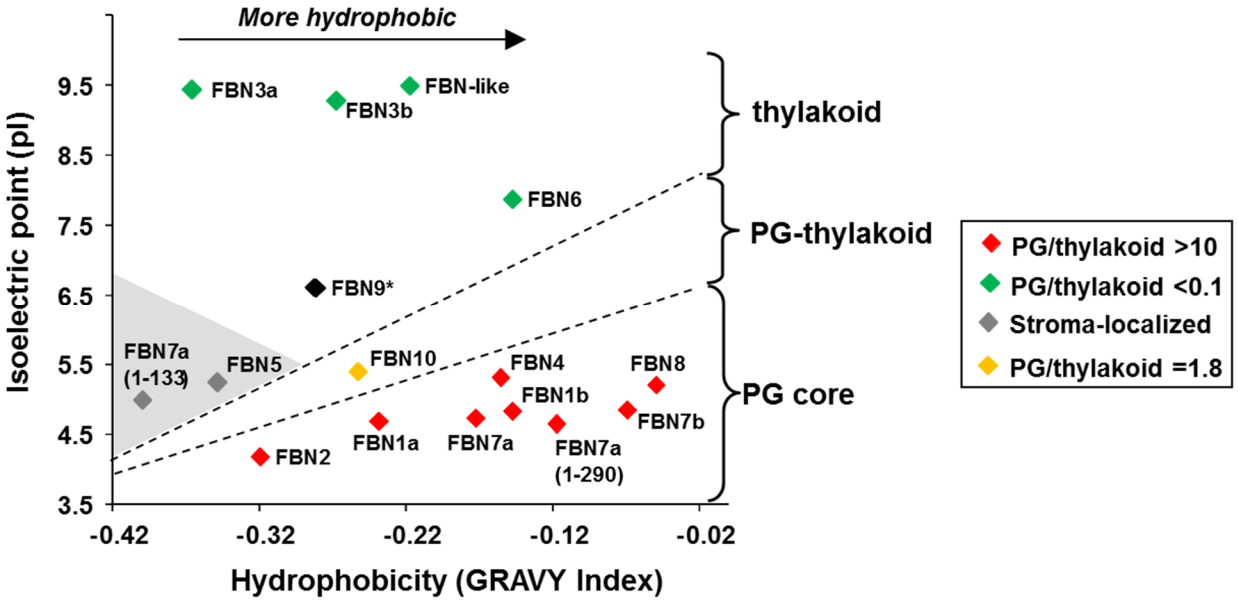

Figure 6. Fibrillin localization is determined by isoelectric point and hydrophobicity. The isoelectric point and hydrophobicity (GRAVY index) were measured for 16 FBN protein products (-cTP) using the ProtParam tool at the ExPasy website (http://expasy.org/). FBN7a(1-290) and FBN7a(1-133) indicate the two truncation products of FBN7a, analyzed for localization in (Vidi et al., 2006). The 16 proteins were grouped by sub-cellular localization and plotted by hydrophobicity (GRAVY index) and isoelectric point (pI). *FBN9 was only observed with low MOWSE scores in total leaf extracts.

2.3.7 A PG co-expression network shows strong, specific enrichment for genes of four plastid functions Because the functions of most PG proteins are unknown and hard to predict, we employed a genome-wide transcript co-expression analysis to identify putative functions for the PG core proteins, identify potential targets for the ABC1K proteins, generate testable hypotheses and provide a better framework for further studies. Several co-expression analysis tools have been developed and employed in plant co-expression analysis, each offering their own suite of functions and set of normalized microarray experiments, e.g. see [47-49]. We tested and compared three different publicly available co-expression tools – MetaOmGraph [50], BAR [51] and ACT [52] - for their ability to identify co-expression relationships among functionally and

physically associated gene products. Using the well-studied gene family encoding for the ClpPR protease complex in plastids and mitochondria [38] and 10 genes encoding for enzymes involved in tetrapyrrole biosynthesis, we first demonstrated that although the three software programs, MetaOmGraph, BAR and ACT, show quantitative differences in co-expression rankings, true co-expressers were consistently found (Figure 7). We also tested to see if PG core genes preferentially expressed with other PG core genes, rather than genes encoding for plastid proteins in general or with genes encoding for extra-plastidic proteins. This showed that PG core genes generally preferentially co-express with other PG genes at higher Pearson correlation coefficients (PCC) (Figure 8). Importantly, these tests also showed that genes encoding for plastid proteins are clearly not co-expressed as a single group, and thus that we should be able to find specific co-expression patterns for PG core proteins.

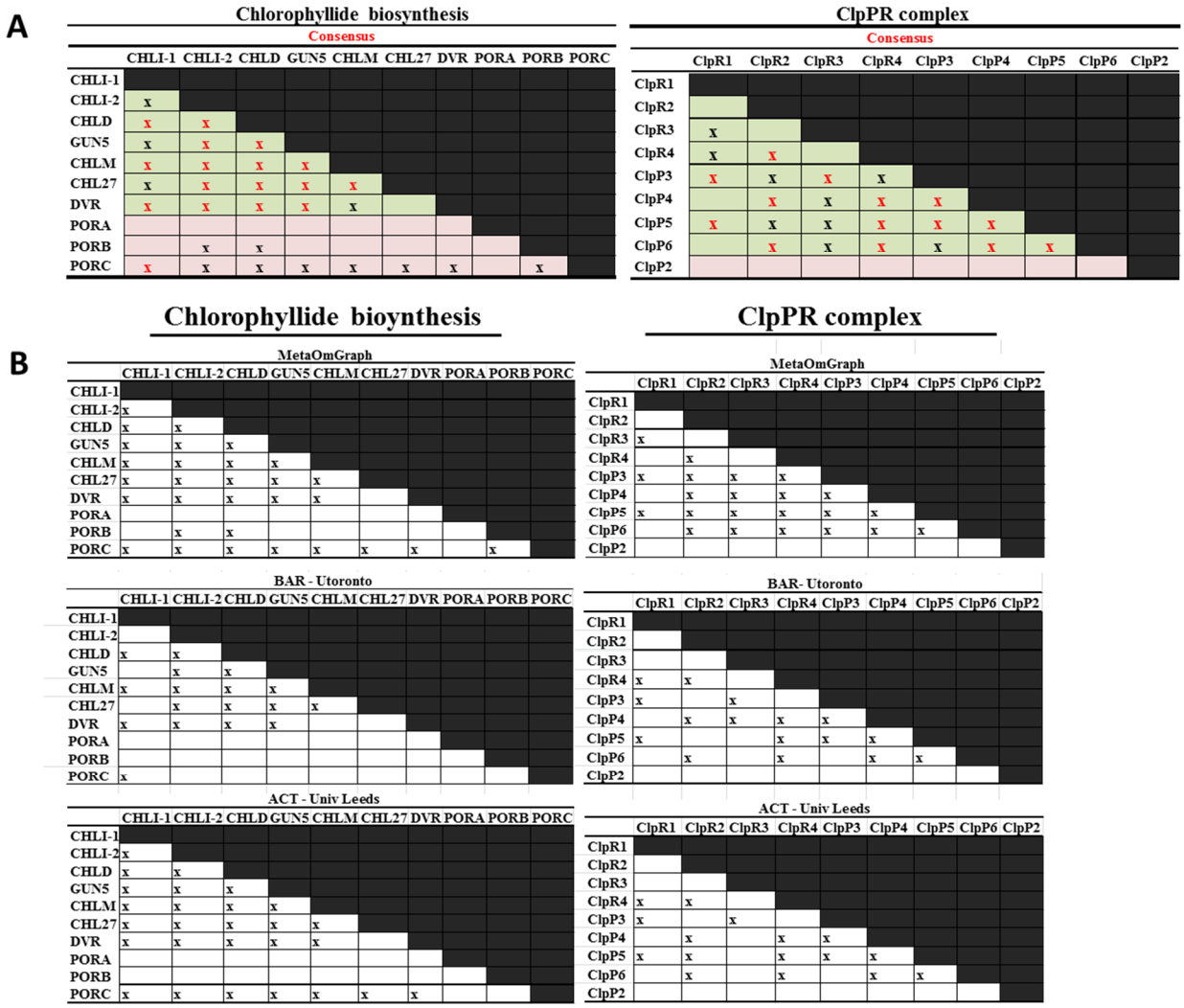

Figure 7. Coexpression within gene sets of chlorophyllide biosynthesis and the ClpPR protease complex. A, All pairwise combinations of genes in each geneset are illustrated. Gene pairs demonstrating co-expression in all three software programs are indicated with a red "x". Gene pairs demonstrating co-expression in one or two of the software programs are indicated with a black "x". Presumed true-positive interactions are indicated with green, presumed true-negatives in red. B, All co-expression pairs from each of the three software programs are shown. Enzymes of the chlorophyllide synthesis pathway are named as follows: CHLI-1, Mg-protoporphyrin IX chelatase I-1; CHLI-2, Mg-protoporphyrin IX chelatase I-2; CHLD, Mg-protoporphyrin IX chelatase D; GUN5, Mg-protoporphyrin IX chelatase H (CHLH); CHLM, Mg-protoporphyrin IX methyltransferase; CHL27, Mg-protoporphyrin IX monomethyl ester cyclase; DVR, 3,8-divinyl protochlorophyllide 8-vinyl reductase; POR, protochlorophyllide oxidoreductase.

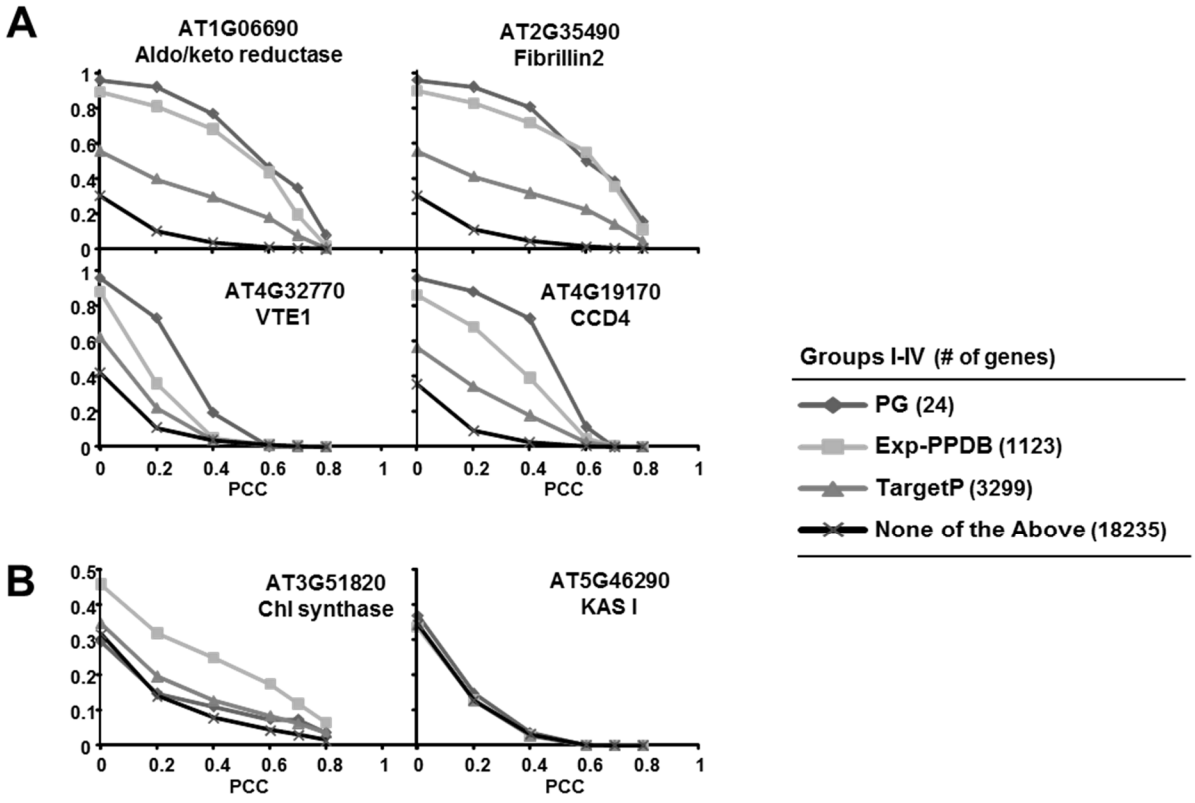

Figure 8. PG genes preferentially maintain coexpression with other PG genes at higher PCCs. Genes analyzed for co-expression correlation were annotated for inclusion in 4 groups describing sub-cellular localization: Group I: PG-localized as determined in this paper "PG", Group II: plastid-localized as curated in the Plant Proteome Database (Sun et al., 2009), based on experimental evidence "PPDB", Group III: plastid-predicted by TargetP (Emanuelsson et al., 2000), "TargetP", Group IV: all genes not fitting in any of Group I-III "none of the above". The fraction of genes above each of the given PCCs were plotted and the size of each group is indicated in the key. See the supplemental text for an explanation of abbreviations. A, Graphs of four representative PG genes are illustrated. The fraction of genes of Group I (PG) co-expressing above each PCC are consistently as high or higher than the fractions of the other 3 groups. B, Two plastidic, non-PG genes (Chl synthase, KAS I) demonstrate that Group I "PG" enrichment at each PCC value is not a general response of plastid genes.

We chose to employ the MetaOmGraph program to investigate the PG co-expression network because of its user-friendly nature and validated the final results with the other two programs. We discarded from the analysis those probes measuring multiple genes to ensure that

we were testing specific gene-gene co-expression relationships. The resulting set contained 21158 Affymetrix microarray probes, including 25 of the 30 PG core genes. PG core genes FBN1a and 1b, as well as DGAT4 had to be excluded because they were not represented by unique probes (see further in discussion), whereas the SOUL and esterase 1 genes were not represented on the microarrays.

A PG network was constructed from a genome-wide search for each of the 25 PG core genes on the Affymetrix microarray. Some of the PG genes (e.g. FBN2, 4, Aldo/keto reductase, unknown-2) had several hundred co-expressing genes above a PCC threshold of 0.7 (or in some cases even above 0.8), whereas other genes (ABC1K7, UbiE-2, M48, DGAT3, unknown SAG) had none above that threshold. Therefore, we used the twenty strongest co-expressing genes for each PG core gene to construct a PG network, rather than applying a minimal PCC threshold. All such co-expression relationships had a PCC above 0.65 with the exception of the PLAT/LH2 domain protein and the SAG protein with unknown function. Strong negative correlations between genes can be relevant, however negative PCC values never exceeded an absolute value of 0.67, and only positive correlations became therefore part of the PG network.

The resulting network contained 374 nodes (genes) and 500 edges (co-expression interactions) (Figure 9). Of the 374 nodes, 201 (54%) were assigned to the plastid based on experimental information. Interestingly, the PG core proteins differed strongly in the subcellular localization of their co-expressers. For instance, in the case of the 5 FBNs, NDC1, ABC1K2 and several others, 17-20 out of 20 of the co-expressers were plastid-localized, however core proteins VTE1, UbiE1, DGAT3, and PLAT/LH2 domain protein each had three or less plastid-localized co-expressers. This immediately suggests that the latter proteins are primarily post-transcriptionally regulated, or that their transcriptional regulation is integrated with extra-

plastidic functions and needs. To better assign functions to the PG core genes and the PG as a whole, co-expressing genes were categorized by their assigned functional category (using the MapMan bin system as the basis to organize the functions), and edges connecting to each bin were counted. Because some bins were much larger than others and thus had a much greater opportunity to be represented in the PG network, we normalized the representation of each bin by its size. As indicated in Table 3, a strong enrichment was found for plastid-localized proteases (17 in total; LON, Prep1, EGY2, FtsH1,2,5,8,9, ClpR2,R3,P4,P5,P6,S,C1,D and DegP1,8), proteins involved in cyclic/alternative electron flow (five NDH subunits, PGR5, PGRL1A,B, PTOX, PIFI) and regulators of the light reaction state transition kinase (STN7 and phosphatase TAP38), plastid-localized isoprenoid metabolism (in particular carotenoid metabolism PDS, ZDS, LYC, ZEP), chlorophyll degradation (PaO/ACD1, pheophytinase, ACD2), and plastid redox regulation (Trx-M1,2,4, Trx-F1, Fd-Trx-Reductase subunits, NADPH-reductase, PrxQ and others) (Table 3). To further substantiate the findings from the MetaOmGraph co-expression analysis, we analyzed functional enrichment of the top 20 co-expressers using the two other software programs, BAR and ACT. Clearly, the distribution of functional groups was consistent between all three programs, strengthening the significance of the MetaOmGraph analysis.

Figure 9. PG network visualization and functional enrichment. For each PG gene, the 20 strongest co-expressing genes from a genome-wide analysis by MetaOmGraph were compiled into a PG co-expression network and visualized with the Cytoscape software program, using the force-directed layout algorithm. Each gene is represented by a single node. Edges, representing co-expression interactions between PG genes and co-expressed genes, are colored according to the functional annotation of the co-expressed gene. Co-expression relationships between two PG genes are indicated with red. Visualization reveals 4 functional modules in which co-expressed genes are enriched in specific cellular/plastidic processes. Each module is shaded in grey and the enriched cellular processes are indicated. Six PG genes are not included in a functional module. For each, the number of plastid-targeted genes (out of 20) and potential relevant co-expressers are listed. Twenty seven co-expressors that are located at important positions in the network, and/or that have particularly interesting functions, are marked with numbers and are: 1 – Pheophytinase; 2 - Pheophorbide a oxygenase (PaO or ACD1); 3 - FtsH8; 4 - CCD1; 5 - ZDS; 6 - PDS1; 7 - FtsH2; 8 - DegP1; 9 - EF-TU-Lep; 10 - Fd1-like; 11 - Trx M1; 12 - Trx M2; 13, FTR beta; 14 - CcdA cytf assembly; 15 - AKRed-like; 16 - Haloacid dehalogenase domain protein; 17 - methyltransferase domain protein; 18 - Tyr kinase; 19, Beta-glucosidase 9; 20 - ZEP; 21 - NAD kinase 2; 22 - STN7; 23 - TAP38; 24 – PTOX/Immutans; 25 - NDH-N; 26 - NDF1; 27 - NDF2.

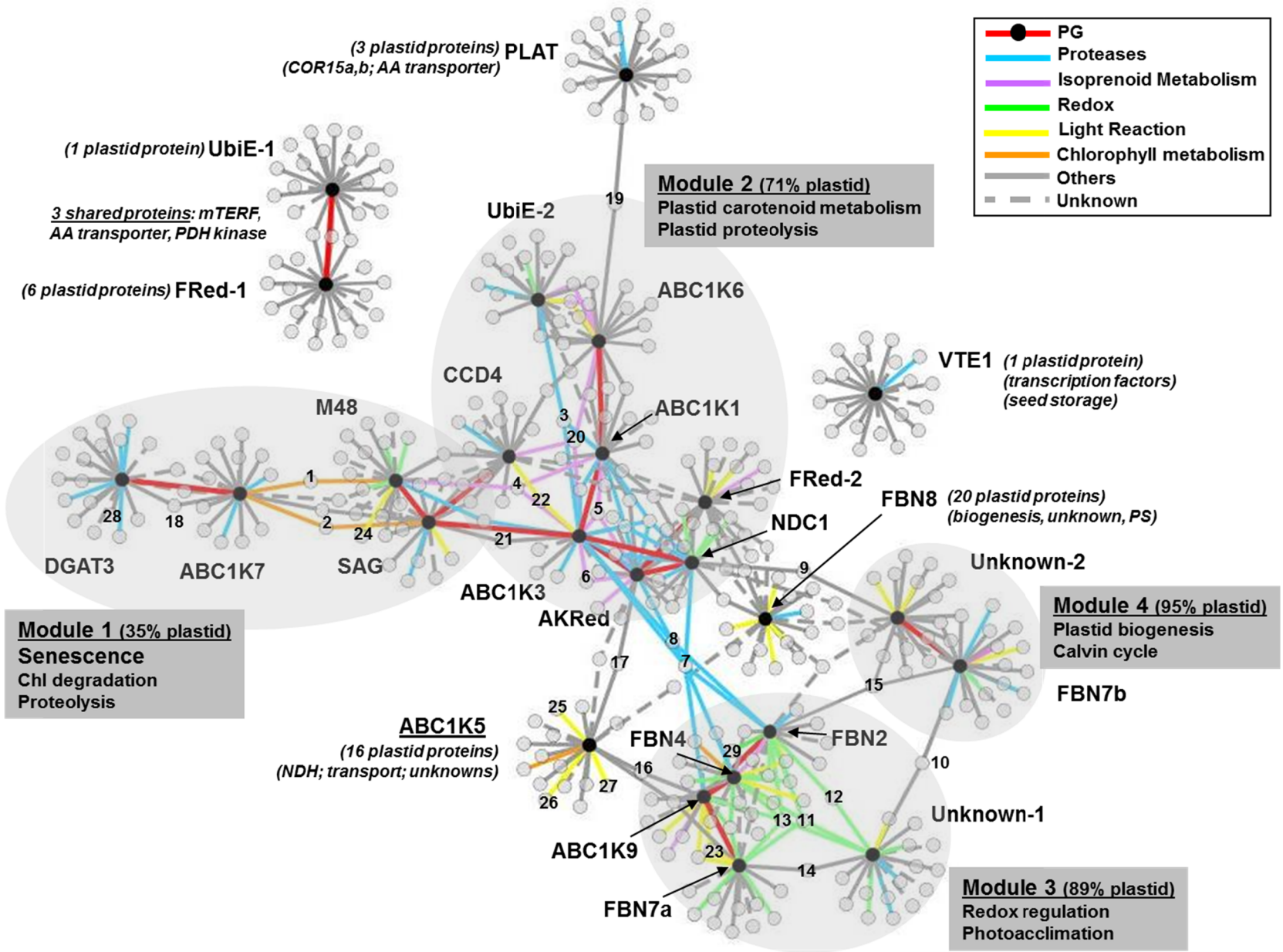
PG
Proteases
Isoprenoid Metabolism
Redox
Light Reaction
Chlorophyll metabolism
Others
Unknown
(3 plastid proteins) (COR15a,b; AA transporter) PLAT
(1 plastid protein) UbiE-1
3 shared proteins: mTERF, AA transporter, PDH kinase
(6 plastid proteins) FRed-1
Module 2 (71% plastid)
Plastid carotenoid metabolism
Plastid proteolysis
UbiE-2
ABC1K6
VTE1 (1 plastid protein) (transcription factors) (seed storage)
CCD4
M48
ABC1K1
FRed-2
FBN8 (20 plastid proteins) (biogenesis, unknown, PS)
NDC1
Unknown-2
DGAT3
ABC1K7
SAG
ABC1K3
AKRed
Module 4 (95% plastid)
Plastid biogenesis
Calvin cycle
FBN7b
Module 1 (35% plastid)
Senescence
Chl degradation
Proteolysis
ABC1K5
(16 plastid proteins)
(NDH; transport; unknowns)
FBN4
FBN2
Unknown-1
ABC1K9
FBN7a
Module 3 (89% plastid)
Redox regulation
Photoacclimation

Table 3. Functional group enrichment of the PG network produced by MetaOmGraph.

Functional group	Bin size (a)	whole network (b)	module I (b)	module II (b)	module III (b)	module IV (b)
Protein degradation	1355	0.1	0.1	**0.2**	0.1	0.1
Protein degradation - not plastid	*1313*	0.0	0.1	0.0	0.0	0.0
Protein degradation - plastid	*42*	***3.3***	***1.2***	***6.5***	***3.3***	***3.6***
Core plastoglobule (PG)	25	**3.4**	**4.0**	**4.5**	**4.8**	**2.0**
Light reaction	139	0.8	0.4	0.5	**1.4**	**1.1**
Assembly factors	*2*	*0.0*	*0.0*	*0.0*	*0.0*	*0.0*
light stress-Lil/Sep/Ohp	*8*	*0.5*	*0.0*	***1.6***	*0.0*	*0.0*
NDH dependent & independent, Immutans, PIFI	*29*	***1.5***	***1.7***	*0.4*	***2.8***	*0.0*
PSI, PSII, ATPsynt, cytb6f, FNR, electron carriers (PC, Fd)	*94*	*0.5*	*0.0*	*0.3*	*0.9*	***1.6***
thylakoid-bound regulators, including kinases and phosphatases	*5*	***3.2***	*0.0*	***5.0***	***8.0***	*0.0*
Isoprenoid metabolism	124	0.7	0.2	**1.6**	0.5	0.4
Isoprenoid metabolism - plastid	59	**1.1**	0.0	**2.5**	**1.0**	0.8
Isoprenoid metabolism - not plastid	65	0.3	0.4	0.8	0.0	0.0
Redox	187	0.7	0.4	0.3	**2.5**	0.3
Tetrapyrrole metabolism	50	0.5	**2.0**	0.0	0.4	0.0
Stress	690	0.1	0.1	0.1	0.0	0.0
Miscellaneous	1274	0.1	0.2	0.1	0.1	0.1
Protein - other	1535	0.1	0.0	0.1	0.1	0.4
plastidic	209					
non-plastidic	1326					
Not assigned	7707	0.1	0.1	0.1	0.1	0.0
Development	521	0.1	0.2	0.1	0.0	0.0
CHO metabolism (c)	441	0.3	0.0	0.2	0.2	0.9
Transport	944	0.1	0.1	0.1	0.0	0.1
Other (d)	2128	0.1	0.1	0.0	0.0	0.0
Signalling	1048	0.0	0.0	0.0	0.0	0.0
Lipid metabolism	331	0.0	0.1	0.0	0.0	0.0
DNA/RNA	2659	0.0	0.0	0.0	0.0	0.0

(a) number of genes (represented by a single probe spot on the 22K Affymetrix microarray chip) in each group

(b) Number of edges per bin, normalized by bin size, and normaized for number of PG cores gene per module. Values in bold are enriched functions

(c) includes major and minor carbohydrate metabolism, gluconeogenesis, glycolysis, TCA cycle, C1 metabolism, fermentation, oxidative pentose phosphate pathway, Calvin cycle, and all other dark reactions

(d) includes cofactor and vitamin metabolism, metal handling, xenobiotics, amino acid metabolism, nucleotide metabolism, cytoskeleton, mitochondrial electron transport, cell wall, cell, cell division, cell cycle, nitrogen metabolism, photorespiration, polyamine metabolism, sulfur assimilation, secondary metabolism (excluding isoprenoids/tetrapyrrole), and hormone metabolism

2.3.8 The PG coexpression network shows four modules The coexpression network showed that most core genes had associations with other PG genes, producing a gene expression network with 4 clusters of nodes, which we refer to as 'modules'. Modules are parts of biological networks in which nodes are densely connected with each other, but between which there are only sparse connections. Thus within each of these modules, genes co-express more tightly to each other than with genes outside the module (Figures 9; Table 3). The modular nature is an important property of biological networks. As will be detailed below, the four modules each showed enrichment for specific functions. The remainder of the PG core genes (FRed-1, UbiE-1, PLAT/LH2-1 and VTE1) had no or weaker associations with other PG genes (Figure 9); moreover, they had in common that most of their coexpressors encoded for extra-plastidic proteins.

Module-1, with four PG core genes (DGAT3, ABC1K7, SAG and M48 metalloprotease), was enriched for senescence functions, in particular chlorophyll degradation (pheophorbide a oxygenase (PaO) and pheophytinase (PPH)) and a variety of proteases outside the plastid (including a senescence-associated cystein protease), as well as the senescence-induced Clp protease chaperone ClpD1. The two chlorophyll degradation enzymes co-expressed with ABC1K7 and SAG (Figure 9 – nodes 1 and 2) and we note that a 3rd, more down-stream enzyme (red chlorophyll catabolite reductase; RCCR), was found in module-3 co-expressing with FBN4. Strikingly, only 35% of the edges in module-1 were plastid-localized, compared to 71-95% for the other modules, consistent with the observation that senescence leads to controlled breakdown of the whole cell, and is not limited to plastids. We also point out an interesting plastid-localized putative tyrosine kinase that co-expressed with both DGAT3 and ABC1K7 (Figure 9 – node

#18). The role for M48 protease is completely unknown and its co-expressors included 5 plastid proteins with unknown function, and 4 plastid-localized proteins: PPH, ClpR3, thylakoid alternative oxidase (PTOX) and a glutaredoxin-thioredoxin.

The most extensive module (module-2) was centrally located in the PG network and comprised eight PG genes (ABC1K-2,3,6, aldo-keto reductase, NDC1, flavin-reductase 2, CCD4, UbiE-2). It was particularly enriched for carotenoid metabolism enzymes (Figure 10) and plastid proteases (22 edges); 71% of the nodes encoded for plastid proteins indicating tight integration with plastid functions (Table 3; Figure 9). In addition to the plastid carotenoid enzymes, also upstream cytosolic solanesyl diphosphate synthase (SPS1) and its plastid isoform (SPS2-responsible for synthesizing the hydrophobic tail of plastoquinone –PQ9) were part of this module (we note that MEP pathway enzymes are only found in module-4). Interestingly, GOLDEN2-LIKE 1 (GPRI1) transcription factor, known to co-regulate expression of a suite of nuclear photosynthetic genes [53], was also part of this module as a co-expressor of CCD4. Within module-2, ABC1K2, AKred and NDC1 were particularly tightly connected, mostly through co-expressing plastid proteases. The top 20 co-expressors of ABC1K2 were almost exclusively involved in carotenoid metabolism (ZEP, PDS, ZDS, CCD1), and protein degradation (FtsH1,2,5,8,9, ClpR3 and ClpC, PREP1, DegP1), but also included thylakoid kinase STN7, involved in phosphorylation of LHC proteins facilitating state-transitions to optimize electron flow [54].

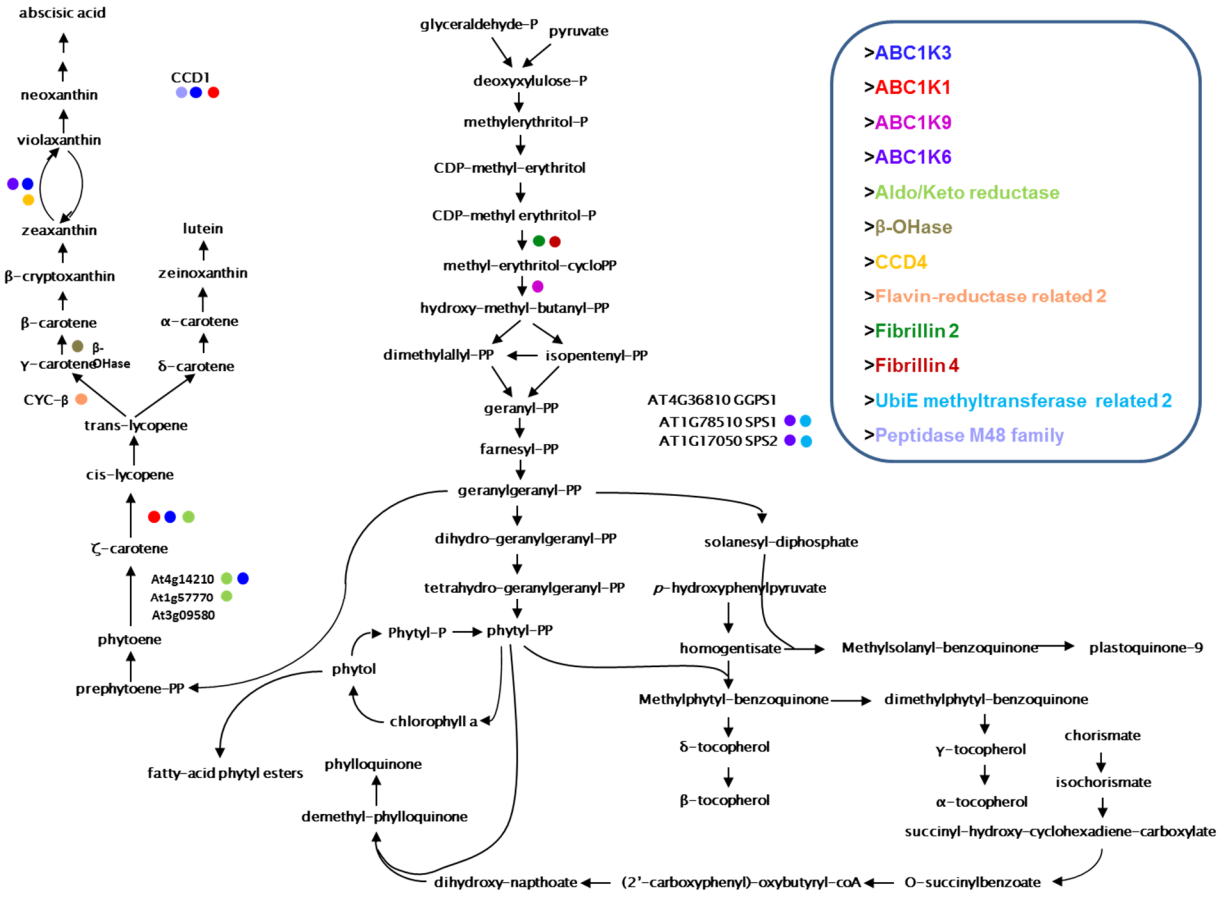

Figure 10. Coexpression relationships between PG genes and isoprenoid metabolism genes found in MetaOmGraph have been projected onto the isoprenoid pathway. The MEP pathway and downstream metabolic pathways of carotenoid, quinone, tocopherol and chlorophyll metabolism have been overlaid with their co-expressing PG genes. Colored circles indicate which PG gene(s) co-express with each gene in the pathway. GGPS: geranylgeranyl diphosphate synthase, SPS1: solanesyl diphosphate synthase isoform 1, SPS2: solanesyl diphosphate synthase isoform 2, CYC-β: lycopene β-cyclase, β-OHase: β-ring carotenoid hydroxylase, CCD1: carotenoid cleavage dioxygenase 1.

The third module involved five PG core genes (ABC1K4, FBN2, 4, 7a and unknown-1) and was particularly enriched in redox regulators and 'photoacclimation'. Eighty-nine percent of the edges encoded for assigned plastid proteins. The module was highly enriched for plastid redox regulators (including thioredoxins M-1, -2, -4, and F-1, two Fd-TRX reductase subunits, glutaredoxins) and non-linear electron flow components (NDH, PGRL1A, PIFI), as well as

several plastid proteases (ClpR2,P5 and S; DegP1, FtsH2), (Figure 9). Also the thylakoid phosphatase TAP38 and the gene coding for the 'acclimation of photosynthesis to environment 1' (APE1) were part of this module.

The fourth and smallest module contained PG core proteins FBN7b and unknown-2, and was strongly enriched for proteins involved in various aspects of plastid biogenesis, including proteases, and the Calvin cycle. Remarkably, PG core protein unknown-2, co-expressed with six different Calvin cycle genes (FBPase, FBPA, sedoheptulose-bisphosphatase, phosphoribulokinase, G3P-DH, phosphoglycerate kinase) as well as the catalytic subunit of glycine decarboxylase, critical for photorespiration. FBN7b appears to be involved in plastid/thylakoid biogenesis; among its top co-expressors are genes coding for 'thylakoid formation 1' (TF1), 'vesicle-inducing protein in plastids' (VIPP1), plastid division protein Giant Chloroplasts 1 (GC1), and several genes of protein synthesis, assembly, folding and targeting. MEP enzymes IspF and HDS were also found in this module-4, as co-expressers of FBN-2, 4 and ABC1K4.

FBN8 was positioned between modules 2 and 4 and its co-expressors (all 20 were plastid-localized) were enriched in plastid biogenesis, photosynthesis and several proteins without known function. ABC1K1 connected to both modules 2 and 4 and its co-expressors (16 were plastid-localized) were enriched in NDH subunits, transporters and various unknowns.

It is important to note that only 1 of the genes (CF1-γ) encoding for known structural proteins of the linear electron transport chain and ATP-synthase (e.g. Photosystems I or II, the cyt*b6f* complex or ATPsynthase) co-expressed with the PG core genes. However two of the three known genes that control state transitions (both STN7 and TAP38) and several structural components of cyclic (NDH and PGR components) or alternative electron flow (PTOX) were

part of the co-expression network. This suggests that the PG function is tightly integrated with cyclic electron flow or the balance between PSI and PSII activity. We note that 4 lumenal OEC-23-like proteins with unknown function, as well as two unusual low abundant LHCI-5 and LHCII-7 proteins (At1g45474 and At1g76570) were found as co-expressors, suggesting that they have functions related to optimization of the light reactions under stress conditions. Indeed, LHCI-5 is a component of the PSI-NDH supercomplex and necessary for its formation and stability, particularly under times of stress [55]. The co-expression profile was found to be very similar to NPQ4 (PsbS) and LIL3 involved in chlorophyll or tocopherol biosynthesis [56]. LHCII-7 was found to be up-regulated in response to light stress [57] and blue or far-red light treatment [58].

Three of the PG core proteins were not placed in the co-expression network because they were on the same probe (on the microarrays) as a close homologue. Indeed evaluation of DGAT4 on the same probe as a closely related non-plastid homologue (At3g26820), showed that the top 20 co-expressors were mostly involved with senescence but not in the plastid, and they did not connect well to the PG network However, homologues FBN1a and b, both PG core proteins and together on a single probe spot, connected tightly in the network, with co-expression with core protein ABC1K2, and its co-expressors RbcX and FtsH8, and also co-expressing with RD20 and POT, both co-expressors of ABC1K7. Thus FBN1a/b is located in the network between module-1 and module-2.

2.3.9 Experimental verification of the co-expression network The co-expression network suggested that a subset of the PG localized proteins (module 1) is involved in senescence responses. Therefore, we tested for 5 genes (*ACD1, PPH, DGAT3, ABC1K7, MCS)* from

module-1 if transcript accumulation is indeed up-regulated during natural senescence. As a control, we also tested two genes from module-4 (*ABC1K4* and *FBN4*) which have no obvious senescence association in the network. To that end, Arabidopsis rosette leaves were harvested during bolting and flowering, during which leaves show increased visual signs of natural leaf senescence. Because PGs are found to accumulate fatty acid phytyl esters, with the phytol generated by breakdown of chlorophyll [6], the uncharacterized esterase identified in our PG core proteome is an excellent candidate enzyme for the esterification of free phytol at the PG. The flux into phytol esterification would be expected to be highest during senescence-induced chlorophyll degradation and we thus tested whether expression of the esterase, which is not represented on the 22K microarrays, is also senescence-induced. RT-PCR experiments were then carried out on three biological replicates (Figure 11). Indeed, expression of the five genes from the senescence-associated module-1, and the esterase, but not the two genes from module-4, are induced by senescence, thus providing support for our co-expression network and our hypothesized functions for the esterase and MCS gene products.

2.4 DISCUSSION

2.4.1 The core PG proteome We identified and quantified proteins highly enriched in the thylakoid-associated PG as compared to other subplastid locations (the core PG proteome), and we associated key functions to the PG using genome-wide co-expression network analyses. PG localization for core proteins ABC1K2, 3 and M48 metalloprotease was confirmed by immunodetection. We determined that 13 proteins, previously assigned to the PG, were not particularly enriched in the PGs; instead they appeared primarily localized in the stroma or

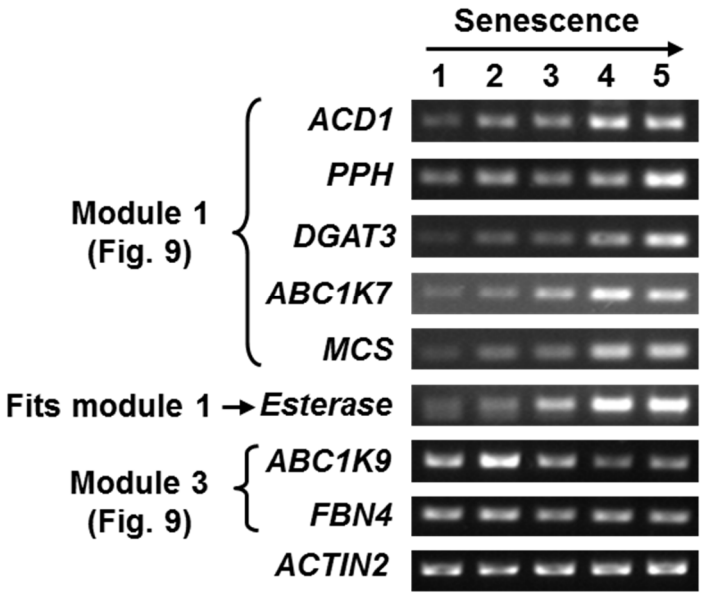

Figure 11. Gene expression of eight selected genes in *Arabidopsis* leaves during natural leaf senescence determined by RT-PCR. Transcript accumulation of five genes from module 1 (*ACD1, PPH, DGAT3, ABC1K7, MCS)*, two genes from module 4 (*ABC1K9* and *FBN4*) and the uncharacterized esterase (AT5G41120), which was not on the microarray experiments, and therefore could not be incorporated in the co-expression network. *ACTIN2* was used as internal loading control. Leaf tissue was selected from five time points during the course of natural leaf senescence: 1 = leaf rosette from plants beginning to bolt; 2 = leaf rosette from plant beginning to flower; 3 = senescing leaves ~10% chlorotic, 4 = senescing leaves ~50% chlorotic; 5 = senescing leaves ~50% chlorotic, one week later in senescence. The experiment was carried out in three independent replicates, with similar results; data for one of the replicates is shown.

thylakoid membranes. Indeed, 8 of these were not found in the co-expression network, whereas the others had only a single connection to a PG core gene (RAP38 and FBPA-2 to Unknown2; RAP41 to ABCK1; FBPA-1 to FRed2; PrxQ to FBN7b). Importantly, we extended the known PG proteome with six new proteins of low abundance, including M48 protease. These new PG proteins were well-integrated in the co-expression network, providing further support for their PG localization and function. The newly assigned PG proteins had lower abundance than

previously identified PG proteins, most likely because we used a more sensitive instrument than in previous studies.

It is possible that several PG proteins were still not observed because they remained below the detected limit. We expected several of these hypothetical proteins to be present in our co-expression network, but typically not identified in Arabidopsis chloroplast fractions (or total leaf proteomes) due to their low abundance. We therefore manually screened for such putative PG proteins. Two proteins, at1g13990 with unknown function and a DUF760 domain, as well asuncharacterized at4g11570 with a haloacid dehalogenase-like hydrolase (HAD) domain, stood out as they each had three connections to PG core genes (unknown-SAG, M48, ABC1K7 and CCD4). HAD domain proteins are a superfamily of largely uncharacterized enzymes with ~115 members in Arabidopsis. In *E. coli* with 28 HAD proteins, HAD phosphatases showed high catalytic efficiency and affinity to a wide range of phosphorylated metabolites [59]. Surprisingly, most HADs hydrolyzed small phosphodonors (acetyl phosphate, carbamoyl phosphate, and phosphoramidate), which also serve as substrates for autophosphorylation of the receiver domains of the two-component signal transduction systems [59]. Interestingly, the PG co-expression network also included a putative stromal sensor kinase domain protein (at1g67840; co-expressing with both ABC1K4 and FBN2 both in module-3) that could act together with the HAD domain protein in a possible signal transduction chain to relay information between the thylakoid and stroma/envelope.

2.4.2 Chloroplast protein distribution and recruitment of proteins to PGs To better understand the absolute distribution of PG core proteins between the PG and the thylakoid membrane, we need to consider how the surface area of the PG particle compares to the surface area of the

thylakoid membrane (since the core proteins located to the periphery of membrane and PG). From TEM analysis we roughly estimate that PG surface in light-stressed leaves (as used in this study) is between 5% and 20% of the total thylakoid + PG surface area. For proteins with a MS/MS based PG/thylakoid protein ratio of 20 (note that these thylakoids were not stripped of their PGs and thus includes the PG), this means that the absolute protein distribution between PG and thylakoid membrane ranges from 1:1 and 4:1 (PG:membrane) (if the MS/MS based ratio is 100, then 5:1 and 20:1). Thus most of the PG core proteins (average PG/thyl = ~50; Table 2) are not exclusively located to the PG core, but are also found with significant copy numbers in the thylakoid membrane surface. A possible exception was ABC1K4 which showed a MS/MS based ratio of 440 (Table 2), corresponding with a 22:1 to 88:1 PG/membrane ratio.

It is not known how proteins are recruited to the PGs. This could occur by *de novo* synthesis and direct targeting to PGs. Alternatively, proteins could be recruited from other locations (e.g. stroma or thylakoid) to the PG through (ir)reversible protein modifications or through changes in the lipid/metabolite composition of the PGs. We can draw a parallel with recruitment of proteins to lipid rafts, which are membrane microdomains with a distinct lipid and protein composition [60]. Such lipid rafts in plant plasma membranes have emerged as a regulatory mechanism governing physiological responses, in particular with a role as signal transduction platforms during stress. In the lipid rafts, proteins (typically low abundant) are brought physically together such that they form functional modules to carry out specific functions. Because the PG can rapidly change in size and number in response to (a)biotic stresses, it seems likely that both *de novo* synthesis, as well as recruitment of existing proteins could occur. In the latter case, proteins should show dual localization between PGs and other plastid compartments (as is the case for most PG core proteins), whereas the first group should

be exclusively localized to PGs with changing cellular concentrations dependent on PG size and abundance.

Indeed, we determined that some of the PG core proteins showed a far stronger enrichment to the PGs (e.g. ABC1K4 and VTE1) than others (Table 2). Dynamic changes in localization have been reported for some FBN proteins, but mechanisms are unknown. The FBN1a homolog in tobacco and pepper distributed primarily in the stroma under optimal conditions, but redistributed to the thylakoid (including PGs) in response to light or drought stress [12, 61]. Based on our experimental data and empirical relationship between physico-chemical parameters of FBN proteins and their distribution between PG and thylakoid preparations (Figure 6), we suggest that FBN10 is a good example of a protein dual-localized between PGs and the stromal-exposed thylakoid surface. The direct membrane continuity between the thylakoid and PG, demonstrated elegantly by [15], could permit movement of proteins between these two membrane systems. How unique protein compositions are maintained between them has not been demonstrated conclusively, but it is likely that protein modifications such as (de)phosphorylation, prenylation or redox regulation may alter the distribution.

FBPA1,2 and 3 were previously identified in isolated PGs [4, 8], and transient expression of GFP-tagged FBPA1 and 2 (At2g21330, At4g38970) in isolated protoplasts demonstrated association to PGs (Vidi et al., 2006). Our current quantitative, comparative analysis clearly demonstrated that these abundant FBPA mostly localized to the stroma, with only a small portion found in isolated PGs. We suggest that small amounts of these FBPA could be recruited to the PG (but their function is not understood) and that the concentration effect at the PG surface, compared to the diffuse signal from the much larger stroma volume, explains the apparent, more exclusive PG localization observed by GFP-tagging.

Our evidence that a significant number of genes involved in plastid isoprenoid/carotenoid accumulation are transcriptionally coordinated with genes encoding for PG proteins suggests that at least a subset of PG proteins are synthesized *de novo* concurrent with isoprenoid metabolism. Consistent with this notion, expression of *Erwinia uredovora* phytoene desaturase in potato tuber enhanced carotenoid metabolism, while simultaneously increasing transcript levels of the FBN homolog CDSP34 [62]

2.4.3 The PG co-expression network suggests several PG functions - An integrated model PGs are believed to function in chloroplast development, stress responses, lipid metabolism and senescence including chlorophyll degradation - reviewed in [1, 3]; [2]. Because PGs function in so many diverse processes, and because most PG proteins have no known function, it has been difficult to obtain an integrated view of the role of the PG and assign PG core proteins to specific tasks or processes. To provide a framework for PG function, and to associate putative functions or processes to PG proteins with unknown functions, we determined the co-expression network based on the twenty most tightly associated co-expressors for each PG core gene. This resulted in four modules, each with a clear enrichment for specific functions, indicating that subsets of the PG core proteins work together to carry out specific roles.

Based on the core PG proteome information and modular structure of the co-expression network, as well as extensive published information, we created a summarizing model that integrates PG functions with chloroplast photosynthesis and metabolism, chloroplast responses to abiotic stress, and senescence (Figure 12). A detailed description explaining the various pathways and processes is provided in the legend of the figure. In the remainder of this

Figure 12. A model for plastoglobule function in plastid metabolism and short and long term photo response and adaptation. Physical connectivity of the PG and thylakoid permit extensive exchange of metabolites between the two sub-compartments and possibly also facilitates recruitment of proteins from the thylakoid-stromal exposed surface to the PG. During times of high lipid or protein turnover (such as senescence, stress or plastid biogenesis) the role of the PG becomes especially pertinent. We illustrate here some of the proposed functions of the PG in these processes. Turnover of galactolipids by DAD1-like acylhydrolases will release free fatty acids transported to the PG where they can either i) be incorporated into TAG by DAGAT1/2, ii) enter the jasmonic acid synthesis pathway, in the case of linolenic acid (18:3), or iii) be esterified to free phytol into fatty acid phytyl esters (FAPEs) during concurrent chlorophyll degradation. Alternatively, the free phytol can be recycled for incorporation into tocopherols by two subsequent phytol kinases, the first of which has been identified (VTE5) (Valentin et al., 2006). During chlorophyll degradation, the tetrapyrrole head group is captured by the PG-localized SOUL/heme-binding protein (SOUL/HBP) and delivered for further degradation to the stroma. We predict that the four PG oxidoreductases (NDC1, AKRed and FRed1 and 2) are active in re-reducing oxidized lipophilic compounds sequestered in the PG. Supporting this, NDC1 has recently been demonstrated to display NAD(P)H reductase activity towards a plastoquinone (PQ-9) analog (decyl-PQ) (Eugeni-Piller et al., 2011). We expect that NDC1 and the other PG oxidoreductases are responsible for regeneration of oxidized PG quinones following ROS scavenging. PQ-9 is expected to be exchanged between the PG and thylakoid. Selective uptake of reduced (or oxidized) PQ-9 would permit a powerful control over the redox state of PQ-9 in the thylakoid and thus over a number of processes regulated by PQ-9 redox state, including photosynthetic electron flow, retrograde signaling, carotenoid desaturation, and LHCII state transition. The presence of the carotenoid cleavage dioxygenase 4 (CCD4), suggests the presence of carotenoid catabolism at the PG. Carotenoids released from the photosynthetic apparatus (photosystems and light harvesting complexes) can be directed to the PG by FBN4 (or other FBNs) for degradation by CCD4. ABC1K4, positioned as a hub in module-4 (Figure 9), is regulating the localization or function of fibrillins (FBNs) and thioredoxins (TRXs) as well as components of the cyclic electron flow apparatus (NDH- and/or PGR5-dependent). FBNs will be controlling the size of PGs (dashed arrow), while TRXs will control Calvin Cycle activity to match supply of reducing power produced from photosynthesis. Increased Calvin cycle activity will create additional demand for ATP that can be met by upregulated cyclic electron flow (CEF), either NDH- or PGR5-dependent (Livingston et al., 2010; Livingston et al., 2010). Metabolites are enclosed in grey boxes, PG-localized proteins are marked in red and co-expressers are marked in blue. Abbreviations used in the figure are listed: Thioredoxin (TRX), cyclic electron flow (CEF), fibrillin (FBN), light-harvesting complex (LHC), zeaxanthin epoxidase (ZEP), state transition kinase (STN7), phytoene desaturase (PDS), zeta-carotene desaturase (ZDS), plastoquinone-9 (PQ-9), reactive oxygen species (ROS), 9-cis-epoxycarotenoid dioxygenase (NCED), plastochromanol-8 (PC-8), triacylglycerol (TAG), lipoxygenase (LOX), fatty acid phytyl ester (FAPE), 9-,13-hyroperoxy-octadecatrienoic acid (9-

,13-HPOT), allene oxide synthase (AOS), phytol kinase (VTE5), SOUL/heme-binding protein domain (SOUL/HBP), pheophytinase (PPH), metal chelating substance (MCS*) possible represented by AT5G17450, pheophorbide a (pheide a), pheophorbide a oxygenase (PaO), 12-oxo-phytodienoic acid (OPDA), poly-unsaturated fatty acids (PUFA), abscisic acid (ABA), diacyl glycerol acyl transferase (DGAT), red chlorophyll catabolite (RCC), red chlorophyll catabolite reductase (RCCR),primary fluorescent chlorophyll catabolite (pFCC).

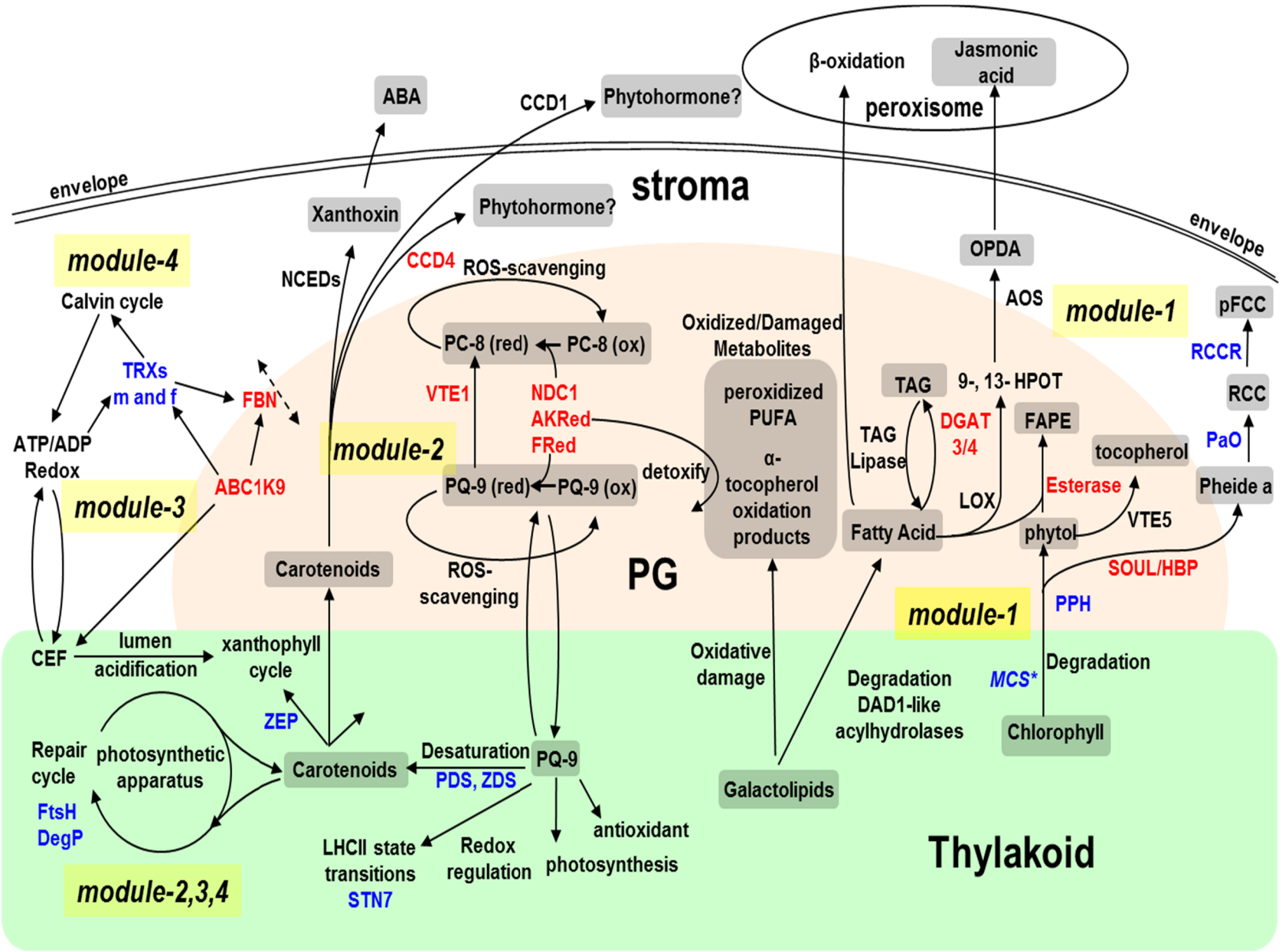
β-oxidation
Jasmonic acid
peroxisome
ABA
CCD1
Phytohormone?
envelope
stroma
envelope
Xanthoxin
Phytohormone?
module-4
Calvin cycle
NCEDs
CCD4
ROS-scavenging
OPDA
AOS
module-1
pFCC
RCCR
RCC
PaO
Pheide a
Oxidized/Damaged Metabolites
PC-8 (red)
PC-8 (ox)
TRXs m and f
FBN
VTE1
NDC1
AKRed
FRed
peroxidized PUFA
α-tocopherol oxidation products
TAG
9-, 13- HPOT
TAG Lipase
DGAT 3/4
FAPE
tocopherol
ATP/ADP Redox
module-2
ABC1K9
module-3
PQ-9 (red)
PQ-9 (ox)
detoxify
LOX
Esterase
VTE5
Fatty Acid
phytol
Carotenoids
ROS-scavenging
PG
SOUL/HBP
module-1
PPH
CEF
lumen acidification
xanthophyll cycle
Oxidative damage
Degradation
Degradation DAD1-like acylhydrolases
MCS*
ZEP
Repair cycle
photosynthetic apparatus
Carotenoids
Desaturation
PDS, ZDS
PQ-9
Chlorophyll
Galactolipids
FtsH
DegP
LHCII state transitions
STN7
Redox regulation
antioxidant
photosynthesis
Thylakoid
module-2,3,4

discussion, we will briefly summarize suggested PG functions and summarize our conclusions for FBNs and ABC1K proteins.

Function 1. The role of PG during leaf scenescence During senescence, the thylakoid membrane is dismantled, resulting in the free monogalactosyl- and digalactosyl glycerols and free fatty acids. These can be used as substrate by AOS for production of jasmonic acid (JA), or stored as TAG by DGAT3/4 (Figure 12). The PG likely serves as a transient storage space for these glycerols and fatty acids. Concomitant with breakdown of the thylakoid bilayer, thylakoid protein complexes and associated pigments such as chlorophylls are degraded. The first steps in chlorophyll degradation are the removal of Mg^{2+} from the porphyrin ring by an unknown protein, tentatively named 'metal chelating substance' (MCS), and cleavage of the phytol from the porphyrin ring by pheophytinase (PPH), one of the co-expressors in module-1 (Figure 12) [63]. The toxic free phytol has been shown to become esterified to fatty acid and deposited in the PG [6]. We speculate that the PG localized esterase could be responsible for this esterification and its transcript levels did increase during natural senescence; experiments are now underway to test this hypothesis. at5g17450, a co-expressor in senescence module-1 is a candidate for MCS because it has a metal binding domain (HMA). This protein must have a very low abundance as it has not been identified by proteomics. In all three co-expression tools, the top 20 co-expressors of at5g17450 included DAGAT-1 and PaO supporting our hypothesis. During senescence, the thylakoid membrane is dismantled resulting in the free monogalactosyl- and digalactocyl glycerols and free fatty acids. These can be used as substrate by AOS for production of jasmonic acid (JA), or stored as TAG by DAGAT1/2 (Figure 12). AOS was not part of the co-expression network and was not sufficiently enriched in the PGs to be considered a PG core protein, even if

it was assigned to the PG previously [8]. But AOS connect functionally very well to the PG suggesting that it could cycle on and off from the PG surface. We very excited to find a highly PG specific M48 protease, that was of low abundance and not studied previously. Members of the M48 class of metallo-endopeptidases in non-plant species have been found to function in N- and C-terminal processing of proteins [64-66]. The PG M48 protease could be involved in degradation of PG located proteins, it could cleave PG localized proteins such they release from the PGs.

Function 2. PG function in isoprenoid metabolism The largest set of PG core proteins and their co-expressors were involved with plastid isoprenoid metabolism, in particular carotenoid metabolism, including two PDS isoforms, ZDS, LYC-β, β-OHase, ZEP, and CCD1 (Figure 10). Particularly interesting was the finding that PG genes co-expressed with PDS and ZDS, as these enzymes transfer electrons from their carotenoid substrate to the plastoquinone pool, a major component of the PG metabolome [67-69]. The other isoprenoid genes, upstream of the carotenoid biosynthetic pathway, were both isoforms of solanesyl diphosphate synthase (SDS1,2), and MDS and HDS of the MEP pathway. Plastid-localized SDS2 is responsible for synthesizing the hydrophobic tail of plastoquinone (PQ-9). In particular ABC1K2, and to a lesser degree ABC1K3, was part of the network of these isoprenoid genes. The surprising linkage within the PG network of isoprenoid metabolism to plastid proteolysis can be easiest explained by the observation that these plastid proteases, in particular the thylakoid FtsH complex, are 'household' proteases, thus removing proteins that are unwanted or damaged, followed by release of chlorophylls and carotenoids. Indeed, it has been demonstrated that carotenoids and

Chl a are continuously synthesized and degraded in photosynthesizing leaves and indicate distinct acclimatory responses of their turnover to changing irradiance [70].

The abundant PG compounds α-tocopherol, PQ-9, and plastochromanol-8 (PC-8) are effective antioxidants *in vivo* [71-73]. All three compounds are known to accumulate in response to light stress, most of which is likely accumulating in the PG [4, 5]. Within the PG, these antioxidants can re-reduce the sequestered oxidized lipids. As part of module-2, four enzymes with (putative) oxidoreductase activity are present in the PG (NDC1, aldo/keto reductase, and flavin reductase 1 and 2) which (may) act in regeneration of spent antioxidants in the PG by reducing carbonyl groups. Consistent with this possibility, vitamin K epoxide/naphthoquinone reductase was found to specifically reduce phylloquinone and menaquinone to their quinol forms in vitro [74]. NDC1 has recently been demonstrated to display NAD(P)H reductase activity towards a plastoquinone (PQ-9) analog decyl-PQ [45]. We speculate that the four PG oxidoreductases are active in re-reducing oxidized lipophilic compounds sequestered in the PG, thereby affecting the thylakoid redox state (see function 3 below). We expect that NDC1 and the other PG oxidoreductases are responsible for regeneration of oxidized PG quinones following ROS scavenging.

The significance of PQ-9 goes far beyond its antioxidant properties. Its electron shuttling function between PSII and cytb_6f make it a prime sensor of photosynthetic electron flow. Indeed its redox state is believed to contribute to a retrograde signal to the nucleus, and is an important control over photosynthetic electron flow [54], including regulation of the state transition kinase STN7 [75-77], and is essential for the desaturation reactions of carotenoid biosynthesis [78]. Thus, the sequestering or release of PQ-9 from the PG – to regulate thylakoid pool size and

redox state - would hold a significant influence over regulation of state transitions, electron flow, carotenoid metabolism, retrograde signaling, and antioxidant effects.

Function 3. Contribution of PGs in optimization of photosynthesis, light acclimation and repair

Among the predominant genes co-expressing with members of the PG are the state transition kinase STN7 involved in balancing PSI and PSII activity, structural components of cyclic electron flow (NDH and PGR) and alternative oxidase (PTOX), nearly the complete plastidic thioredoxin regulatory system, as well as six enzymes of the Calvin cycle. This strongly suggests that the PG is intimately involved with optimization of the dark and light reactions, in particular via the redox state. Interestingly, recent work suggested that the chloroplast redox status (or ROS) regulate cyclic electron flow, which in turn helps to achieve the correct ratio of ATP and redox energy required for the Calvin cycle and chloroplast metabolism in general [79, 80]. Interestingly, the PG co-expression network also included the chloroplast sensor kinase CSK (at1g67840), co-expressing in module-3 with both ABC1K4 and FBN2, and many components of the chloroplast redox network. CSK was recently shown to be involved in redox-coupled transcriptional regulation of chloroplast genes [81]. Furthermore, zeaxanthin epoxidase (ZEP) involved in the reversible conversion of zeaxanthin to violaxanthin (via antheroxanthin) within the xanthophyll cycle was centrally located in the gene expression network with connections to ABC1K2, ABC1K6 and CCD4. We speculate that ZEP activity may be regulated by one of these ABC1K proteins. Consistently, it was suggested that ZEP activity is controlled by a direct, as yet unidentified, modification, which does not involve the state transition kinases [82]. There is some indirect evidence that phosphorylation of ZEP significantly impedes its *in vivo* activity [83]. Collectively, it appears that the PG plays a key role in short term regulation and balancing

of photosynthetic activities. TEM has clearly documented the dynamic and reversible nature of PG size and osmiophilicity in response to diverse abiotic and biotic stresses [6, 13, 84-87]. Therefore, PGs have been implicated in adaptation to environmental fluctuations via secondary metabolism and stress responses [1, 3]. Perhaps surprising, none of the well-known enzymes involved in detoxification of soluble reactive oxygen species (superoxide and hydrogen peroxide) such as superoxide dismutases, or thylakoid and stromal APX, were found in the PG co-expression network.

2.4.4 FBNs and ABC1K proteins – distribution, functions and targets The seven PG-localized FBNs (1a, 1b, 2, 4, 7a, 7b, 8) and the six ABC1K proteins constituted more than 70% of the PG protein mass. These six ABC1K proteins are expected to act as enzyme regulators, possibly via phosphorylation [42], and the notion of a regulatory function is strengthened by their position as hubs in the PG network (Figure 9). Their PG localization suggests that they are regulating enzymes that locate, at least transiently, to the PG; the co-expression network provides potential target genes that should now be experimentally tested. ABC1K1 and ABC1K3 co-express tightly with the four genes of the FtsH complex (FtsH 1/2/5/8) and thus may help orchestrate PSII repair under excess light exposure. ABC1K3 also co-expresses tightly with several members of carotenoid metabolism which are critical for PSII repair given that carotenoids have been found to continuously turnover [70]. ABC1K9 formed the hub of module-2, connecting with three FBN genes (FBN 7a, 2, and 4). FBN 4 was found to be phosphorylated in a PAMP-dependent manner [88]. Thus, ABC1K9 may directly regulate the function or localization of one or more FBNs via phosphorylation. We note that ABC1K homologue at5g64940, that we annotated as ABC1K8, was never found in the PG nor in the co-expression network. ABC1K8 was identified as a

chloroplast inner-envelope protein and reduced expression resulted in increased sensitivity toward oxidative stress and high light [89].

The FBN proteins are suggested to primarily function as structural proteins, likely determining PG size, some involved in adaptation to environmental stress and others possibly influencing metabolite and protein content. Information about their possible functions is summarized in a recent review [2]. When these three proteins were simultaneously knocked down by RNAi in *A. thaliana*, increased sensitivity to high light plus cold stress was found [90]. Curiously, this sensitivity could be relieved by jasmonic acid treatment, perhaps indicating that FBN are required for supply of substrate to AOS, the first committed step in JA biosynthesis (Figure 12). Furthermore, constitutive over-expression of FBN1a resulted in enhanced phototolerance [91]. The other highly abundant FBN (FBN4) also contributed to adaptation to light stress, since reduced expression of FBN4 in apple and *A. thaliana*, led to enhanced sensitivity to bacterial infection and methyl viologen treatment, and also resulted in altered PG lipid composition [14]. Interestingly, the PG-localized FBN1a and 4 were identified in association with LHCII subcomplexes I and III under light stress conditions [92]. A potato homolog of FBN1a, C40.4, was found associated with the PSII complex and knockdown, demonstrated decreased non-photochemical quenching, indicating a requirement for proper photosynthetic efficiency [93]. FBN4 contains a lipocalin domain which is predicted to be involved in binding and transport of small hydrophobic metabolites. The other FBN proteins show less conserved lipocalin signatures. Thus, it was suggested that in particular FBN4 could receive carotenoid or chlorophyll from damaged/degraded LHC complexes [2]. We further suggest that the FBNs subsequently transport the metabolites to the PG for recycling or degradation. It is tempting to speculate that the PG core SOUL heme-binding protein similarly

functions to receive heme molecules released from degraded photosystems and cytb_6f complexes. The seven PG-localized FBNs were distributed across the co-expression network thus providing further suggestions for functions.

2.5 MATERIALS AND METHODS

2.5.1 Preparation of PG and thylakoid material The PG isolation method was adapted from Ytterberg, et al [8]. For each PG preparation, two flats (~150 individuals) of *A. thaliana* (Col-0) were grown on soil for 2.5 weeks, under 120 µmol photons m^{-2} s^{-1} with a 16 hour photoperiod. Plants were then transferred to 520 µmol photons.m^{-2}.s^{-1} conditions during the dark period. In the morning of the 6th day leaf tissue was harvested and homogenized in grinding buffer (50 mM Hepes-KOH pH 8.0, 5 mM $MgCl_2$, 100 mM sorbitol, 5 mM ascorbic acid, 5 mM reduced cysteine, 0.05 % (w/v) BSA). Homogenate was filtered through four layers of 20-µm miracloth and thylakoid membranes were pelleted by centrifugation for 6 minutes at 1800xg. Thylakoid pellets were washed once in 4 volumes of grinding buffer and resuspended in Medium R (50 mM Hepes-KOH pH 8.0, 5 mM $MgCl_2$, cocktail of protease inhibitors) containing 0.2 M sucrose. An aliquot of resuspended thylakoid material was stored at -80^o C to be used as the pre-sonicated thylakoid fraction. The remainder was sonicated 4x 5s at output power 23 Watts (Fischer Scientific, sonic dismembrator Model 100), returning the samples to ice between each sonication event. Sonicated samples were centrifuged for 30 minutes at 150,000 xg and PGs released from the thylakoid floated to the surface of the solution. PGs were removed and combined with Medium R with 0.7M sucrose to achieve a sucrose concentration of 0.5M, which was then overlayed with Medium R with 0.2M sucrose and Medium R with no sucrose. The gradient was

centrifuged 90 minutes, 150,000 xg. The resulting floating pad of PGs was removed, flash frozen in liquid N_2, and stored at -80^o C.

2.5.2 Antiserum generation Nucleotide sequences encoding the soluble part of the M48 protein (amino acids 72-325) and the C-termini of ABC1K2 (556-711) and ABC1K3 (578-582) were amplified by PCR. The resulting DNA fragments were ligated into restriction sites of the pET21a expression vector, coding for a C-terminal His affinity tag. The vector was transformed into BL21 *E. coli* cells, and over-expressed protein was harvested from liquid culture after incubation in 1mM IPTG for 3 h at 37^{0}C. Proteins were solubilized in 200mM NaCl, 50mM Tris, and 8M Urea at pH 8 and purified on a nickel-nitrotriacetic acid agarose resin matrix, and polyclonal antibodies were raised in rabbits by injecting purified antigen.

2.5.3 Immunoblotting Protein concentrations were estimated by the BCA method [94] using a BCA kit (Pierce). Protein samples were solubilized in 1x Laemmli buffer (125 mM Tris-HCl pH 6.8, 2% SDS, 5% β-mercaptoethanol, 10% glycerol), heated for 10 mins at 75^o C, and separated in a SDS-PAGE gel (6% acrylamide stacking, 12% separation). Proteins were blotted to nitrocellulose, probed with purified anti-PeptidaseM48, anti-ABC1K2, anti-ABC1K3 or anti-VTE1 serum (a gift of Dr. Dean DellaPenna), and visualized by the horseradish peroxidase-based enhanced chemiluminescence system. Densitometric analysis of relevant spots was performed using the ImageJ software program (http://rsbweb.nih.gov/ij/).

2.5.4 Transmission Electron Microscopy Leaf tissue from 3 individuals of each genotype at each time point was harvested 1 hour after beginning of the photoperiod. Leaf margins and

midribs were excluded and the remaining leaf tissue was divided into 1x2 mm sections with a fresh razor blade. Sections were fixed in 2% glutaraldehyde, 2 % paraformaldehyde, 0.1% tannic acid, 70 mM PIPES buffer pH 6.8 for 2 hours and then washed 3 times in 70 mM PIPES buffer pH 6.8. Tissues were fixed in 1% osium tetroxide (OsO_4), 70 mM PIPES pH 6.8 for 2 hours and washed 3 times in 70 mM PIPES pH 6.8. Tissues were then stained in 2% uranyl acetate for 1 hour and washed twice in ultrapure H_2O. Fixed and stained tissues were carried through an acetone series of increasing concentrations. Dehydrated tissue was then embedded with Spurr's resin (Electron Microscopy Sciences; Hatfield, PA) in increasing concentrations of resin in acetone, according to manufacturer's instructions. Fully embedded tissue was cured in resin blocks at 60ºC overnight. Cured resin blocks were sectioned and imaged at Electron Microscopy Services; Colorado Springs, Colorado.

2.5.5 Scanning Electron Microscopy 2-3 µl of purified PG sample were spotted onto a silica wafer. A 3 µl drop of 2% OsO_4 in 70 mM potassium phosphate pH 7.2 was added to the 3 µl drop of the PG sample on the silica wafer. The buffered OsO_4 was allowed to remain in contact with the PGs for one hour at 4^o C. After one hour the wafers were floated on a droplet of 70 mM potassium phosphate buffer at pH 7.2 for 10 minutes. This was done three times at 4^o C. The wafers were then floated on drops of 2% gluteradehyde in 70mM potassium phosphate pH 7.2 for one hour at 4^o C. After one hour the wafers were floated on drops of 70mM potassium phosphate pH 7.2 for 10 minutes at 4^o C. The wafers were then floated on drops of distilled water for 10 minutes at 4^o C. The wafers were dehydrated by floating on first 25%, then 50%, then 75%, then 95% and finally drops of 100% ethanol for approximately 10 minutes each at 4^o C. The wafers were then critical point dried in 100% ethanol (Bal Tec - Leica Microsystems, Inc.,

Bannockburn, IL). The wafers were then mounted on specimen supports and sputter coated with gold/palladium (Denton Vacuum, LLC, Moorestown, NJ). The wafers were viewed at 3 kV in a Hitachi S4500 scanning electron microscope (Hitachi High-Technologies Corp., Tokyo, Japan).

2.5.6 In-solution and in-gel digestion of isolated PGs For in-solution digestion, isolated PGs were precipitated in 10% tri-chloro acetic acid (TCA) overnight at 4^{o} C. Precipitated proteins were pelleted by centrifugation and washed once with 100% acetone and once with 80% acetone, 10% methanol, 0.1% acetic acid, by incubating at -20^{o} C for 1.5 hours each. Washed pellets were resuspended in dimethyl sulfoxide and quantified by the BCA method [94] using a BCA kit (Pierce). 5 µg of protein was digested with modified trypsin (Promega), 40:1 (protein: trypsin). Salts and detergents were removed by C18 Ziptip (Millipore) and dried down in a speed-vac. Digested and washed samples were resuspended in 15 µl 2% formic acid immediately prior to loading on the LC-MS/MS instrument. For gel-based separation and in-gel digestion, PG samples were lyophilized and solubilized in a modified Laemmli solubilization buffer (125 mM Tris-HCl pH 6.8, 6% SDS, 10% β-mercaptoethanol, 20% glycerol). Samples were shaken gently at 30^{o} C for 15 minutes to ensure complete solubilization and subsequently heated at 80^{o} C for 10 min. Samples were centrifuged to remove insoluble material and proteins were separated by SDS PAGE (6% acrylamide stacking, 12% separation). Each gel lane was cut in 5 slices and proteins were digested with trypsin, as described in [95].

2.5.7 ***Proteome analysis of total leaf extracts*** Wild-type plants (Col-0) were grown on soil for 30 days under a short-day cycle (10h/14h of light/dark) at 120 µmol photons.m^{-2}.s^{-1}. The complete leaf rosettes were then harvested and proteins were immediately quantitatively extracted in

presence of SDS (in triplicate) as described in detail in [95]. Alternatively, plants were transferred were grown on soil for 2.5 weeks under similar conditions as above, but transferred to 520 µmol photons m^{-2} s^{-1} conditions. In the morning of the 6^{th} day leaf tissue was harvested and extracted as above (in triplicate).

2.5.8 Proteome analysis by nanoLC-LTQ-Orbitrap and data processing Peptides prepared from in-gel digestion and in-solution digestion were analyzed by data-dependent tandem mass spectrometry (MS/MS) using on-line LC-LTQ-Orbitrap (Thermo Electron) with dynamic exclusion, similar as described in [35]. Peak lists (.mgf format) were generated using DTA supercharge (v1.19) software (http://msquant.sourceforge.net/) and searched with Mascot v2.2 (Matrix Science) against a combined database containing the Arabidopsis genome with protein-coding gene models and 187 sequences for known contaminants (e.g. keratin, trypsin) (total 33,013 entries) and concatenated with a decoy database where all the sequences were randomized; in total this database contained 66,026 protein sequences. Off-line calibration for all precursors ions was done as described in [96]. Each of the peak lists were searched using Mascot v2.2 (maximum p-value of 0.01) for full tryptic peptides using a precursor ion tolerance set at ±6 ppm, fixed cysteine carbamido-methylation and variable methionine oxidation, protein N-terminal acetylation, asparagine/glutamine (N/Q) deamidation and maximally one missed cleavage allowed. The maximum fragment ion tolerance (MS/MS) was 0.8 Da. For semi-tryptic peptides the search was performed with a precursor ion tolerance set at ±3 ppm, fixed cysteine carbamido-methylation and variable methionine oxidation, N-terminal acetylation, glutamine deamidation and maximally one missed cleavage allowed. Minimal ion score threshold was chosen such that a peptide false discovery rate (FDR) below 1% was achieved. Using an in-

house written filter, the search results were further filtered as follows: For identification with two or more peptides, the minimum ion score threshold was set to 30. For protein identification based on a single peptide, the minimum ion score threshold was set to 33, and the mass accuracy of the precursor ion was required to be within ±3 ppm. The peptide false discovery rate (FDR) was calculated as: 2 × (decoy hits) / (target + decoy hits) and was below 1%. The FDR of proteins identified with two or more peptides was zero. Peptides with less than seven amino acids were discarded. All mass spectral data (the mgf files reformatted as PRIDE XML files) are available via the Proteomics Identifications database (PRIDE) at http://www.ebi.ac.uk/pride/.

Several Arabidopsis genes have more than one gene model, and in such cases the protein form with the highest number of matched spectra was selected; if two gene models had the same number of matched spectra, the model with the lower digit was selected. For quantification, each protein accession was scored for total spectral counts (SPC), unique SPC (uniquely matching to an accession) and adjusted SPC [95]. The latter assigns shared peptides to accessions in proportion to their relative abundance using unique spectral counts for each accession as a basis. The normalized adjSPC (NadjSPC) for each protein was calculated through division of adjSPC by the sum of all adjSPC values for the proteins from that gel lane. NadjSPC provides a relative protein abundance measure by mass, whereas NSAF estimates relative protein concentration within a particular sample.

2.5.10 Genome-wide co-expression calculations and network visualization The Pearson correlation coefficients of all pairwise combinations between PG (bait) genes and all single-gene probes of the *A.thaliana* 22K Affymetrix microarray (Affymetrix, Inc.) were calculated using three different software programs: i) the MetaOmGraph software program (http://metnetdb.org)

[50], ii) the Botany Array Resource (BAR) expression angler (http://142.150.214.117/welcome.htm) [51], and the Arabidopsis Co-expression data mining Tool (ACT) website (http://www.arabidopsis.leeds.ac.uk/act/index.php) [52]. MetaOmGraph analysis used the publicly available "Affy.ath1.data1 project" containing normalized, averaged Arabidopsis experimental datasets obtained from NASCArrays (http://affymetrix.arabidopsis.info/) and PlexDB (http://plexdb.org) from 71 experiments and 424 microarray chips from diverse environmental and genotypic conditions and tissue types and developmental stages. Correlations were calculated using the Pearson correlation algorithm. Visualization of the MetaOmGraph-derived network was performed in Cytoscape v2.8.0 (http://cytoscape.org/) [97], applying the force-directed layout algorithm. Co-expression analysis using the BAR expression angler was performed for each PG gene by searching in the 'NASCArrrays 392' dataset available at the website. Analysis at the ACT website was performed for each PG gene by using the "Co-expression analysis over available array experiments" option.

2.5.11 Analysis of transcript accumulation during natural senescence Wild-type Arabidopsis col-0 was grown on soil. Leaf tissue was selected from five time points during the course of natural leaf senescence: 1 = leaf rosette from plants beginning to bolt; 2 = leaf rosette from plant beginning to flower; 3 = senescing leaf ~10% chlorotic, 4 = senescing leaf ~50% chlorotic; 5 = senescing leaf ~50% chlorotic, one week later in senescence. Total RNA was extracted from leaf tissue using the RNeasy plant miniprep kit (Qiagen) according the manufacturer's instructions. 700 ng of total RNA was used for synthesis of cDNA using oligo $dT_{(20)}$ primer and the Superscript III cDNA synthesis kit (Invitrogen) according to the manufacturer's instructions. cDNA samples were diluted to equal concentration by normalizing according to amplification of

the actin2 gene using 20 cycles. Each gene was then amplified for 25 cycles using an equal volume of template and an appropriate gene specific primer pair. Signal intensity was quantified using the Alpha Imager 2200 v5.5 software package. The forward and reverse primers are: for *PAO/ACD1* 5'- GAT GCG AAA CTA CCA ATC GTC G -3' and 5'- CAT CAG AAG GAA CAC CAG CCG -3'; for *PPH* 5'- CAA TCA TGC TTG CTC CTG GTG -3' and 5'- CTA CCA ATC CTG GAC TCC TCC -3'; for *DGAT3* 5'- GCC AGA GGA GCT TCA TTT TAC T -3' and 5'- GGG TAT GCC CAT TGT CCT T -3': for *ABC1K7* 5'- ATC CGC ACC CAG GAA ACC TT -3'and 5'- ACA GAT CCT GCC ATA GAA AGG AGG -3': for *MCS* 5'- GAA ATC GGT GGA GGT GAA CC -3' and 5'- GGT TGG TTG GCT CAC ATG AT -3': for *ESTERASE* 5'- GCT AAC TGC TGT TAC CTC CCC -3' and 5'- CAA ACT CCG AAT GTT CTG GCC -3': for *ABC1K4* 5'- GCA GCT TGG TCT ACT GTC TC -3' and 5'- CAC ATT AAG CGC GGT AAT AAG G -3': for *FBN4* 5'- TTC TTT CCG ACC ACC GTT CT -3' and 5'- ACT TGT GTG CCA ATG TCG C -3': for *ACTIN2* 5'- CAA ACG AGG GCT GGA ACA AGA CT -3' and 5'- GCA ACT GGG ATG ATA TGG AAA AGA -3'

2.5.12 Calculation of protein physicochemical parameters Parameters were calculated by the ProtParam tool [98] available through the ExPasy website (http://expasy.org/tools/).

Supplemental Table 1. Experimental data of in-gel and in-solution PG proteome analysis

Core PG proteome (workflow Figure 4)	Accession - Selected gene model	Lab Annotation	Curated Location	Coverage in-gel (PG)	Coverage in-sol (PG)	Average NadjSPC PG	Repl. 1 NadjSPC average (in gel & in-sol)	Repl.2 NadjSPC average (in-gel & in-sol)	Repl. 3 NadjSPC average (in-gel & in-sol)	CV (NadjSPC)	In-gel - Average NadjSPC repl. 1,2,3	In-sol - Average NadjSPC repl.1,2,3
yes	AT4G19170.1	arotenoid dioxygenase (CCD4 a	plastoglobules	0.67	0.49	0.02056	0.01492	0.02159	0.02518	0.25	0.02092	0.02020
yes-new	AT3G24190.1	ABC1 kinase 6 - ABC1K6	plastoglobules	0.58	0.40	0.01597	0.01580	0.01835	0.01376	0.14	0.01756	0.01438
yes	AT1G71810.1	ABC1 kinase 1 - ABC1K1	plastoglobules	0.44	0.42	0.01069	0.01019	0.01215	0.00973	0.12	0.01172	0.00966
yes	AT1G79600.1	ABC1 kinase 2 - ABC1K2	plastoglobules	0.61	0.66	0.02652	0.02250	0.03364	0.02341	0.23	0.02261	0.03042
yes	AT4G31390.1	ABC1 kinase 3 - ABC1K3	plastoglobules	0.74	0.47	0.02771	0.02706	0.03025	0.02582	0.08	0.02400	0.03142
yes	AT5G05200.1	ABC1 kinase 4 - ABC1K4	plastoglobules	0.75	0.52	0.03226	0.03106	0.03526	0.03047	0.08	0.03444	0.03009
yes-new	AT3G07700.1	ABC1 kinase 7 - ABC1K7	plastoglobules	0.40	0.13	0.00508	0.00429	0.00430	0.00664	0.27	0.00753	0.00262
yes	AT1G06690.1	aldo/keto reductase	plastoglobules	0.65	0.39	0.00929	0.00988	0.01224	0.00573	0.35	0.01061	0.00797
yes	AT1G54570.1	cyl glycerol transferase 3 (DGAT	plastoglobules	0.57	0.37	0.01603	0.01566	0.01815	0.01428	0.12	0.01733	0.01474
yes	AT3G26840.1	ylglycerol Acyltransferase 4 (DG,	plastoglobules	0.45	0.25	0.00871	0.00973	0.00737	0.00904	0.14	0.01121	0.00622
yes-new	AT5G41120.1	ase/lipase/thioesterase (Estera	plastoglobules	0.28	0.03	0.00179	0.00193	0.00225	0.00120	0.30	0.00309	0.00050
yes	AT4G04020.1	fibrillin 1a (FBN1a)	plastoglobules	0.80	0.79	0.09986	0.10016	0.08431	0.11510	0.15	0.08464	0.11507
yes	AT4G22240.1	fibrillin 1b (FBN1b)	plastoglobules	0.74	0.78	0.05915	0.06471	0.05080	0.06193	0.12	0.04461	0.07369
yes	AT2G35490.1	fibrillin 2 (FBN2)	plastoglobules	0.44	0.45	0.04368	0.04548	0.04350	0.04208	0.04	0.05752	0.02985
yes	AT3G23400.1	fibrillin 4 (FBN4)	plastoglobules	0.55	0.50	0.07373	0.07226	0.05232	0.09659	0.30	0.05925	0.08821
yes	AT3G58010.1	fibrillin 7a (FBN7a)	plastoglobules	0.72	0.67	0.02179	0.02884	0.02571	0.01083	0.44	0.01597	0.02762
yes	AT2G42130.4	ɔ) - model .4 scores better than	plastoglobules	0.59	0.57	0.01319	0.01828	0.01452	0.00677	0.45	0.01241	0.01396
yes	AT2G46910.1	fibrillin 8 (FBN8)	plastoglobules	0.56	0.54	0.01099	0.01242	0.00995	0.01059	0.12	0.00950	0.01247
yes	AT1G32220.1	flavin reductase-related 1	plastoglobules	0.41	0.49	0.01279	0.01275	0.00991	0.01570	0.23	0.00777	0.01781
yes	AT2G34460.1	flavin reductase-related 2	plastoglobules	0.50	0.47	0.00911	0.00839	0.01173	0.00721	0.26	0.01020	0.00803
yes-new	AT4G39730.1	lipid-associated PLAT/LH2-1	plastoglobules	0.30	0.27	0.01011	0.01001	0.00720	0.01312	0.29	0.00404	0.01618
yes-new	AT3G27110.1	M48 protease	plastoglobules	0.36	0.38	0.00211	0.00121	0.00300	0.00211	0.42	0.00209	0.00212
yes	AT5G08740.1	dually targeted in plastid & mitoc	plastoglobules	0.50	0.42	0.01516	0.01568	0.01385	0.01596	0.08	0.01367	0.01665
yes	AT3G10130.1	SOUL heme-binding	plastoglobules	0.75	0.57	0.01133	0.01235	0.01016	0.01149	0.10	0.01021	0.01246
yes	AT4G32770.1	tocopherol cyclase (VTE1)	plastoglobules	0.55	0.39	0.01632	0.01621	0.01716	0.01557	0.05	0.01606	0.01657
yes	AT1G78140.1	UbiE methyltransferase related '	plastoglobules	0.52	0.56	0.00950	0.00936	0.01365	0.00549	0.43	0.00978	0.00922
yes	AT2G41040.1	UbiE methyltransferase related 2	plastoglobules	0.44	0.43	0.00903	0.00886	0.01068	0.00755	0.17	0.00723	0.01083
yes-new	AT3G43540.1	unknown protein 2 (DUF1350)	plastoglobules	0.57	0.41	0.00774	0.01008	0.00910	0.00404	0.42	0.00960	0.00588
yes-new	AT1G73750.1	unknown protein (SAG)	plastoglobules	0.32	0.20	0.00249	0.00454	0.00239	0.00055	0.80	0.00311	0.00187
yes	AT4G13200.1	unknown protein 1	plastoglobules	0.55	0.53	0.01150	0.01337	0.01158	0.00956	0.17	0.00690	0.01610
	AT2G01140.1	se-bisphosphate aldolase-3 (SF	plastid	0.16	0.00	0.00041	0.00047	0.00076	0.00000	0.93	0.00082	0.00000
	AT4G38970.1	se-bisphosphate aldolase-2 (SF	plastid stroma	0.62	0.39	0.00891	0.01092	0.01046	0.00535	0.35	0.00907	0.00876
	AT2G21330.1	se-bisphosphate aldolase-1 (SF	plastid stroma	0.68	0.40	0.01544	0.01425	0.01520	0.01686	0.09	0.01601	0.01487
	AT5G42650.1	ide synthase (AOS) (interaction	thylakoid	0.79	0.49	0.01829	0.01684	0.01783	0.02020	0.09	0.02316	0.01342
	AT2G22170.1	ɜd PLAT/LH2 - dually targeted to	ER & cytosol?	0.30	0.40	0.00432	0.00623	0.00416	0.00257	0.43	0.00132	0.00732
	AT3G12110.1	actin 11 (ACT11)		0.10	0.00	0.00003	0.00010	0.00000	0.00000	1.73	0.00007	0.00000
	AT3G46520.1	actin 12 (ACT12)		0.10	0.00	0.00003	0.00010	0.00000	0.00000	1.73	0.00007	0.00000
	AT5G59370.1	actin 4 (ACT4)		0.10	0.00	0.00003	0.00010	0.00000	0.00000	1.73	0.00007	0.00000
	AT1G17870.1	EGY3, metalloprotease		0.07	0.00	0.00014	0.00042	0.00000	0.00000	1.73	0.00028	0.00000
	AT4G33110.1	-methionine-dependent methyltransferases		0.08	0.00	0.00020	0.00014	0.00045	0.00000	1.17	0.00040	0.00000
	AT4G28520.1	cruciferin 3		0.14	0.00	0.00035	0.00000	0.00105	0.00000	1.73	0.00070	0.00000
	AT2G39330.1	jacalin-related lectin 23		0.38	0.00	0.00107	0.00057	0.00188	0.00076	0.66	0.00214	0.00000

Supplemental Table 1. (continued)

Core PG proteome (workflow Figure 4)	Accession - Selected gene model	Lab Annotation	Curated Location	Coverage in-gel (PG)	Coverage in-sol (PG)	Average NadjSPC PG	Repl. 1 NadjSPC average (in gel & in-sol)	Repl.2 NadjSPC average (in-gel & in-sol)	Repl. 3 NadjSPC average (in-gel & in-sol)	CV (NadjSPC)	In-gel - Average NadjSPC repl. 1,2,3	In-sol - Average NadjSPC repl.1,2,3
	AT3G16470.1	JR1 (Jacalin lectin family protein)	plastid or cytosolic	0.20	0.00	0.00015	0.00000	0.00045	0.00000	1.73	0.00030	0.00000
	AT2G33380.1	RD20 protein induced by ABA during dehydration, EF		0.53	0.32	0.00563	0.00564	0.00929	0.00196	0.65	0.00688	0.00438
	AT1G67360.1	rubber elongation factor (REF) family		0.68	0.00	0.00337	0.00439	0.00399	0.00175	0.42	0.00675	0.00000
	AT5G16550.1	unknown protein		0.20	0.10	0.00074	0.00035	0.00105	0.00082	0.48	0.00074	0.00075
	AT5G59960.1	unknown protein		0.06	0.00	0.00005	0.00000	0.00015	0.00000	1.73	0.00010	0.00000
	AT5G07990.1	Cytochrome P450 protein		0.05	0.00	0.00005	0.00007	0.00008	0.00000	0.87	0.00010	0.00000
	AT5G47860.1	unknown protein		0.21	0.00	0.00046	0.00092	0.00045	0.00000	1.01	0.00091	0.00000
	AT4G10000.1	glutaredoxin family protein		0.41	0.05	0.00055	0.00135	0.00029	0.00000	1.30	0.00080	0.00030
	AT2G29550.1	tubulin beta-7 chain (TUB7)		0.12	0.00	0.00018	0.00000	0.00053	0.00000	1.73	0.00035	0.00000
	AT1G50010.1	TUA2 (tubulin alpha-2 chain)	cytoskeleton	0.08	0.00	0.00002	0.00000	0.00006	0.00000	1.73	0.00004	0.00000
	AT5G19780.1	tubulin alpha-3/alpha-5 chain (T	cytoskeleton	0.07	0.00	0.00006	0.00000	0.00017	0.00000	1.73	0.00012	0.00000
	AT4G14960.1	tubulin alpha-6 chain (TUA6)	cytoskeleton	0.08	0.00	0.00002	0.00000	0.00006	0.00000	1.73	0.00004	0.00000
	AT3G09630.1	60S ribosomal protein L4/L1 (R	cytosol	0.10	0.00	0.00009	0.00000	0.00026	0.00000	1.73	0.00018	0.00000
	AT5G02870.1	60S ribosomal protein L4/L1 (R	cytosol	0.10	0.00	0.00009	0.00000	0.00026	0.00000	1.73	0.00018	0.00000
	AT5G39740.1	60S ribosomal protein L5 (RPL	cytosol	0.16	0.00	0.00013	0.00000	0.00038	0.00000	1.73	0.00025	0.00000
	AT1G19670.1	chlorophyllase 1 (CLH1) (also A	cytosol	0.13	0.00	0.00035	0.00028	0.00045	0.00033	0.25	0.00071	0.00000
	AT3G25520.1	60S ribosomal protein L5 (RPL	cytosol	0.16	0.00	0.00013	0.00000	0.00038	0.00000	1.73	0.00025	0.00000
	AT3G63520.1	9,10 (9',10') 9-cis-epoxycaroten	cytosol	0.12	0.00	0.00046	0.00014	0.00090	0.00033	0.87	0.00091	0.00000
	AT5G60390.1	elongation factor 1-alpha / EF-1	cytosol	0.26	0.00	0.00042	0.00025	0.00021	0.00080	0.78	0.00084	0.00000
	AT1G07920.1	elongation factor 1-alpha / EF-1	cytosol	0.26	0.00	0.00042	0.00025	0.00021	0.00080	0.78	0.00084	0.00000
	AT3G04120.1	glyceraldehyde-3-phosphate de	cytosol	0.52	0.00	0.00064	0.00039	0.00154	0.00000	1.25	0.00129	0.00000
	AT5G56000.1	Hsp90-4	cytosol	0.08	0.00	0.00030	0.00035	0.00045	0.00011	0.58	0.00061	0.00000
	AT5G02500.1	HSP70-1 (HSC70-1) (not plasti	cytosol	0.04	0.00	0.00005	0.00014	0.00000	0.00000	1.73	0.00009	0.00000
	AT1G72370.1	40S ribosomal protein SA (RPS	cytosol	0.17	0.00	0.00023	0.00000	0.00068	0.00000	1.73	0.00045	0.00000
	AT1G52400.1	6-phospho-beta-galactosidase	endoplasmic reticulu	0.17	0.00	0.00055	0.00000	0.00120	0.00044	1.11	0.00109	0.00000
	AT5G61790.1	calnexin 1 (CNX1)	endoplasmic reticulu	0.10	0.00	0.00024	0.00021	0.00030	0.00022	0.20	0.00049	0.00000
	AT2G20890.1	TF1 - thylakoid formation1	envelope	0.15	0.00	0.00018	0.00014	0.00030	0.00011	0.56	0.00037	0.00000
	AT3G63410.1	vte3 - MPBQ/MSBQ methyl trans	envelope-inner	0.20	0.05	0.00088	0.00042	0.00155	0.00065	0.68	0.00127	0.00048
	AT5G46110.1	TPT - IEP30 = Phosphate/triose	envelope-inner-integ	0.05	0.00	0.00034	0.00035	0.00045	0.00022	0.34	0.00068	0.00000
	AT1G06950.1	Tic110	envelope-inner-integ	0.05	0.00	0.00019	0.00021	0.00015	0.00022	0.19	0.00039	0.00000
	AT2G24820.1	Tic55 (putative Rieske iron-sulf	envelope-inner-integ	0.05	0.00	0.00017	0.00021	0.00030	0.00000	0.90	0.00034	0.00000
	AT3G56940.1	CHL27 or Crd1	envelope-inner-perip	0.11	0.00	0.00033	0.00028	0.00060	0.00011	0.75	0.00066	0.00000
	AT5G50920.1	ClpC1 (also named HSP93-V) -	envelope-inner-perip	0.34	0.04	0.00224	0.00113	0.00330	0.00229	0.48	0.00424	0.00025
	AT4G13010.1	ceQORH - oxidoreductase, Zn b	envelope-inner-perip	0.12	0.00	0.00008	0.00000	0.00023	0.00000	1.73	0.00015	0.00000
	AT3G18890.1	Tic 62 interacts with thylakoid-a	inner envelope-stron	0.22	0.10	0.00195	0.00092	0.00166	0.00328	0.62	0.00281	0.00110
	AT3G08580.1	mitochondrial ADP,ATP carrier p	mitochondria	0.30	0.18	0.00172	0.00101	0.00329	0.00087	0.79	0.00256	0.00089
	AT4G29130.1	hexokinase 1 (HXK1	mitochondria	0.14	0.00	0.00015	0.00000	0.00045	0.00000	1.73	0.00030	0.00000
	AT3G07770.1	Hsp90-6	mitochondria	0.04	0.00	0.00011	0.00000	0.00033	0.00000	1.73	0.00022	0.00000
	AT5G08670.1	H+-transporting ATP synthase b	mitochondria	0.47	0.22	0.00085	0.00005	0.00170	0.00079	0.98	0.00155	0.00014
	AT5G08690.1	H+-transporting ATP synthase b	mitochondria	0.47	0.22	0.00085	0.00005	0.00170	0.00079	0.98	0.00155	0.00014
	AT5G08680.1	H+-transporting ATP synthase b	mitochondria	0.53	0.15	0.00169	0.00257	0.00170	0.00079	0.53	0.00323	0.00014
	AT2G20360.1	NADH-DH 40 kDasubunit - Con	mitochondria	0.08	0.00	0.00010	0.00000	0.00030	0.00000	1.73	0.00020	0.00000

Supplemental Table 1. (continued)

Core PG proteome (workflow Figure 4)	Accession - Selected gene model	Lab Annotation	Curated Location	Coverage in-gel (PG)	Coverage in-sol (PG)	Average NadjSPC PG	Repl. 1 NadjSPC average (in gel & in-sol)	Repl.2 NadjSPC average (in-gel & in-sol)	Repl. 3 NadjSPC average (in-gel & in-sol)	CV (NadjSPC)	In-gel - Average NadjSPC repl. 1,2,3	In-sol - Average NadjSPC repl.1,2,3
	AT5G19760.1	oxoglutarate/malate translocato	mitochondria	0.19	0.20	0.00072	0.00060	0.00156	0.00000	1.09	0.00035	0.00109
	AT5G37510.1	NADH-DH 76kDa subunit - Con	mitochondria	0.10	0.00	0.00024	0.00000	0.00060	0.00011	1.35	0.00047	0.00000
	AT5G03290.1	isocitrate dehydrogenase [NAD	mitochondria	0.15	0.00	0.00020	0.00000	0.00060	0.00000	1.73	0.00040	0.00000
	AT5G14040.1	phosphate transporter (PHT3-1	mitochondria	0.08	0.08	0.00012	0.00000	0.00037	0.00000	1.73	0.00015	0.00010
	AT1G51980.1	mitochondrial processing pepti	mitochondria	0.33	0.00	0.00086	0.00071	0.00188	0.00000	1.10	0.00173	0.00000
	AT4G01100.1	Adenine nucleotide carrier (ADN	mitochondria	0.09	0.00	0.00005	0.00000	0.00015	0.00000	1.73	0.00010	0.00000
	AT3G02090.1	mitochondrial processing pepti	mitochondria	0.25	0.00	0.00094	0.00057	0.00203	0.00022	1.03	0.00188	0.00000
	AT5G67500.1	Voltage dependent ion channel	mitochondria	0.12	0.00	0.00007	0.00007	0.00015	0.00000	1.02	0.00015	0.00000
	AT3G01280.1	Voltage dependent ion channel	mitochondria	0.20	0.00	0.00015	0.00023	0.00023	0.00000	0.87	0.00031	0.00000
	AT5G15090.1	Voltage dependent ion channel	mitochondria	0.11	0.11	0.00028	0.00012	0.00030	0.00041	0.53	0.00018	0.00037
	AT5G66760.1	succinate dehydrogenase (ubiq	mitochondria	0.04	0.00	0.00005	0.00000	0.00015	0.00000	1.73	0.00010	0.00000
	AT4G37930.1	glycine/serine hydroxymethyltra	mitochondria	0.31	0.05	0.00141	0.00007	0.00030	0.00385	1.51	0.00199	0.00082
	AT5G23060.1	Ca2+ sensing receptor - phosp	mitochondria	0.42	0.20	0.00398	0.00207	0.00525	0.00462	0.42	0.00559	0.00237
	AT4G38510.1	probable H+-transporting ATPa	not plastid	0.00	0.06	0.00005	0.00000	0.00015	0.00000	1.73	0.00000	0.00010
	AT1G20260.2	vacuolar H+-ATPase subunit B	not plastid	0.03	0.06	0.00009	0.00000	0.00015	0.00011	0.89	0.00007	0.00010
	AT5G09810.1	actin 7 (ACT7) / actin 2	not plastid	0.25	0.00	0.00043	0.00059	0.00070	0.00000	0.87	0.00086	0.00000
	AT1G49240.1	actin 8 (ACT8)	not plastid	0.10	0.00	0.00006	0.00013	0.00006	0.00000	1.02	0.00013	0.00000
	AT2G07698.1	ATP synthase alpha chain, mito	not plastid	0.20	0.00	0.00135	0.00137	0.00196	0.00072	0.46	0.00271	0.00000
	AT5G39410.1	unknown protein	not plastid	0.10	0.00	0.00015	0.00000	0.00045	0.00000	1.73	0.00030	0.00000
	AT5G46800.1	mitochondrial carnitine/acyl (CA	not plastid	0.19	0.04	0.00026	0.00014	0.00063	0.00000	1.29	0.00040	0.00012
	AT3G13920.1	eukaryotic translation initiation f	not plastid	0.06	0.00	0.00006	0.00018	0.00000	0.00000	1.73	0.00012	0.00000
	AT1G07940.1	elongation factor 1-alpha / EF-1	not plastid	0.26	0.00	0.00042	0.00025	0.00021	0.00080	0.78	0.00084	0.00000
	AT1G07930.1	elongation factor 1-alpha (E-Tu)	not plastid	0.26	0.00	0.00042	0.00025	0.00021	0.00080	0.78	0.00084	0.00000
	AT1G57720.1	elongation factor 1B-gamma, pu	not plastid	0.11	0.00	0.00025	0.00000	0.00000	0.00076	1.73	0.00051	0.00000
	AT1G72730.1	eukaryotic translation initiation f	not plastid	0.06	0.00	0.00006	0.00018	0.00000	0.00000	1.73	0.00012	0.00000
	AT1G56070.1	elongation factor 2, EF-2	not plastid	0.05	0.03	0.00063	0.00015	0.00037	0.00137	1.03	0.00051	0.00075
	AT5G26000.1	thioglucoside glucohydrolase 1	not plastid	0.05	0.00	0.00015	0.00000	0.00045	0.00000	1.73	0.00030	0.00000
	AT5G25980.2	myrosinase or thioglucoside gl	not plastid	0.12	0.04	0.00045	0.00000	0.00060	0.00076	0.88	0.00081	0.00010
	AT5G19770.1	tubulin alpha-3/alpha-5 chain (T	not plastid	0.07	0.00	0.00006	0.00000	0.00017	0.00000	1.73	0.00012	0.00000
	AT1G04820.1	tubulin alpha-2/alpha-4 chain (T	not plastid	0.08	0.00	0.00002	0.00000	0.00006	0.00000	1.73	0.00004	0.00000
	AT1G13440.1	glyceraldehyde-3-phosphate de	nucleus	0.52	0.00	0.00064	0.00039	0.00154	0.00000	1.25	0.00129	0.00000
	AT5G09660.1	malate dehydrogenase, glyoxys	peroxisome	0.36	0.12	0.00192	0.00120	0.00187	0.00268	0.39	0.00304	0.00079
	AT1G15690.1	AVP1 (vacuolar-type H+-pumpin	plasma membrane	0.07	0.00	0.00032	0.00035	0.00038	0.00022	0.27	0.00063	0.00000
	AT1G50450.1	saccharopine dehydrogenase f	plastid	0.13	0.00	0.00033	0.00035	0.00030	0.00033	0.08	0.00065	0.00000
	AT4G34200.1	D-3-phosphoglycerate dehydro	plastid	0.06	0.00	0.00008	0.00000	0.00023	0.00000	1.73	0.00015	0.00000
	AT5G44000.1	Glutathione S-transferase relat	plastid	0.17	0.00	0.00041	0.00035	0.00045	0.00044	0.13	0.00083	0.00000
	AT4G14210.1	phytoene desaturase (PDS)	plastid	0.04	0.00	0.00011	0.00021	0.00000	0.00011	0.99	0.00021	0.00000
	AT4G01690.1	protoporphyrinogen oxidase (PI	plastid	0.06	0.00	0.00044	0.00028	0.00038	0.00065	0.44	0.00088	0.00000
	AT5G62140.1	unknown protein	plastid	0.23	0.16	0.00120	0.00144	0.00089	0.00126	0.23	0.00111	0.00129
	AT3G61870.1	unknown protein (integral mem	plastid	0.04	0.11	0.00037	0.00028	0.00060	0.00022	0.55	0.00053	0.00020
	AT4G28025.1	unknown protein	plastid	0.13	0.00	0.00023	0.00028	0.00008	0.00033	0.59	0.00046	0.00000
	AT5G35170.1	adenylate kinase	plastid	0.02	0.03	0.00012	0.00007	0.00029	0.00000	1.26	0.00005	0.00020

Supplemental Table 1. (continued)

Core PG proteome (workflow Figure 4)	Accession - Selected gene model	Lab Annotation	Curated Location	Coverage in-gel (PG)	Coverage in-sol (PG)	Average NadjSPC PG	Repl. 1 NadjSPC average (in gel & in-sol)	Repl.2 NadjSPC average (in-gel & in-sol)	Repl. 3 NadjSPC average (in-gel & in-sol)	CV (NadjSPC)	In-gel - Average NadjSPC repl. 1,2,3	In-sol - Average NadjSPC repl.1,2,3
	AT3G48870.1	ClpC2 (also named HSP93-III)	plastid stroma	0.00	0.06	0.00036	0.00030	0.00037	0.00041	0.15	0.00000	0.00072
	AT4G03520.1	thioredoxin m2	plastid stroma	0.09	0.18	0.00133	0.00221	0.00095	0.00082	0.58	0.00009	0.00256
	AT3G15360.1	thioredoxin m4	plastid stroma	0.18	0.15	0.00080	0.00225	0.00015	0.00000	1.58	0.00019	0.00141
	AT4G20360.1	elongation factor Tu (EF-Tu-1),	plastid stroma	0.16	0.14	0.00225	0.00050	0.00245	0.00381	0.74	0.00220	0.00231
	AT4G18810.1	UV-B and ozone similarly regul	plastid stroma	0.33	0.18	0.00320	0.00235	0.00454	0.00270	0.37	0.00470	0.00169
	AT3G01500.3	beta-carbonic anhydrase-1 (bet	plastid stroma	0.18	0.10	0.00118	0.00130	0.00141	0.00082	0.27	0.00102	0.00134
	AT2G04030.1	cpHSP90 (Hsp90-5)	plastid stroma	0.06	0.00	0.00031	0.00021	0.00050	0.00022	0.53	0.00062	0.00000
	AT5G26742.2	DEAD box RNA helicase (RH3)	plastid stroma	0.03	0.00	0.00007	0.00000	0.00000	0.00022	1.73	0.00015	0.00000
	AT3G26650.1	glyceraldehyde 3-phosphate de	plastid stroma	0.28	0.11	0.00063	0.00000	0.00179	0.00011	1.58	0.00084	0.00042
	AT1G12900.1	glyceraldehyde-3-phosphate de	plastid stroma	0.07	0.11	0.00025	0.00011	0.00064	0.00000	1.38	0.00007	0.00042
	AT1G42970.1	glyceraldehyde-3-phosphate de	plastid stroma	0.17	0.00	0.00030	0.00032	0.00058	0.00000	0.97	0.00060	0.00000
	AT5G35630.1	glutamate-ammonia ligase (GS	plastid stroma	0.07	0.00	0.00006	0.00007	0.00000	0.00011	0.92	0.00012	0.00000
	AT1G56500.1	haloacid dehalogenase-like hy	plastid stroma	0.05	0.00	0.00016	0.00014	0.00023	0.00011	0.38	0.00032	0.00000
	ATCG00490.1	Rubisco large subunit (RBCL)	plastid stroma	0.21	0.02	0.00136	0.00170	0.00172	0.00065	0.45	0.00252	0.00020
	AT3G45140.1	lipoxygenase AtLOX2, plastid	plastid stroma	0.09	0.00	0.00074	0.00071	0.00075	0.00076	0.04	0.00148	0.00000
	AT3G47520.1	malate dehydrogenase [NAD], p	plastid stroma	0.08	0.00	0.00018	0.00000	0.00023	0.00033	0.91	0.00037	0.00000
	AT3G12780.1	phosphoglycerate kinase-1 (PG	plastid stroma	0.08	0.00	0.00007	0.00021	0.00000	0.00000	1.73	0.00014	0.00000
	AT1G56190.1	phosphoglycerate kinase-1 (PG	plastid stroma	0.08	0.00	0.00007	0.00021	0.00000	0.00000	1.73	0.00014	0.00000
	AT2G39730.1	Rubisco activase	plastid stroma	0.57	0.53	0.02433	0.02034	0.02542	0.02723	0.15	0.02097	0.02769
	AT1G80030.1	DnaJ domain family	thylakoid	0.02	0.00	0.00005	0.00014	0.00000	0.00000	1.73	0.00009	0.00000
	ATCG01110.1	NDH H (NDH-7)	thylakoid	0.06	0.00	0.00005	0.00014	0.00000	0.00000	1.73	0.00009	0.00000
	AT5G17170.1	unknown protein Rubredoxin ar	thylakoid	0.12	0.13	0.00082	0.00036	0.00023	0.00187	1.11	0.00044	0.00120
	AT1G74470.1	geranylgeranyl reductase (GGD	thylakoid	0.38	0.20	0.00360	0.00451	0.00268	0.00361	0.25	0.00486	0.00233
	AT4G01050.1	unknown protein - Rhodanese-	thylakoid	0.10	0.03	0.00115	0.00131	0.00045	0.00170	0.55	0.00126	0.00104
	AT2G46820.1	Photosystem I protein TMP14 -	thylakoid	0.20	0.00	0.00040	0.00028	0.00038	0.00055	0.33	0.00080	0.00000
	AT3G46780.1	unknown protein (pTAC16)	thylakoid	0.36	0.15	0.00258	0.00243	0.00351	0.00181	0.33	0.00358	0.00158
	AT2G42220.1	rhodanese-like domain protein	thylakoid	0.07	0.03	0.00007	0.00022	0.00000	0.00000	1.73	0.00005	0.00010
	AT1G71500.1	Rieske [2Fe-2S] domain	thylakoid	0.16	0.16	0.00069	0.00096	0.00089	0.00022	0.59	0.00048	0.00089
	AT5G03880.1	glutaredoxin	thylakoid	0.35	0.20	0.00254	0.00287	0.00301	0.00175	0.27	0.00373	0.00135
	AT1G15980.1	NDF1- associates with NDH co	thylakoid	0.14	0.00	0.00015	0.00000	0.00045	0.00000	1.73	0.00030	0.00000
	AT4G35250.1	vestitone reductase-related	thylakoid	0.12	0.04	0.00050	0.00021	0.00075	0.00055	0.54	0.00091	0.00010
	ATCG00730.1	petD - subIV	thylakoid-integral	0.09	0.00	0.00022	0.00014	0.00030	0.00022	0.36	0.00044	0.00000
	AT4G32260.1	CFO-II - atpG	thylakoid-integral	0.28	0.08	0.00083	0.00078	0.00105	0.00065	0.24	0.00156	0.00010
	ATCG00130.1	CFO-I - atpF	thylakoid-integral	0.52	0.45	0.00339	0.00533	0.00366	0.00120	0.61	0.00260	0.00419
	AT1G29930.1	LHCII-1.3 - 100% identical to lh	thylakoid-integral	0.64	0.55	0.00197	0.00199	0.00314	0.00079	0.60	0.00134	0.00260
	AT1G29920.1	LHCII-1.2 - 100% identical to lh	thylakoid-integral	0.64	0.55	0.00131	0.00199	0.00115	0.00079	0.47	0.00134	0.00128
	AT1G29910.1	LHCII-1.1 - 100% identical to lh	thylakoid-integral	0.64	0.55	0.00131	0.00199	0.00115	0.00079	0.47	0.00134	0.00128
	AT5G01530.1	LHCII-4.1-CP29	thylakoid-integral	0.37	0.15	0.00400	0.00461	0.00301	0.00440	0.22	0.00489	0.00312
	ATCG00280.1	psbC CP43	thylakoid-integral	0.32	0.19	0.00913	0.00708	0.00858	0.01172	0.26	0.00908	0.00918
	ATCG00020.1	psbA D1	thylakoid-integral	0.19	0.15	0.00443	0.00269	0.00259	0.00801	0.70	0.00239	0.00646
	ATCG00540.1	petA - cytochrome f (cleavable s	thylakoid-integral	0.45	0.26	0.00468	0.00386	0.00386	0.00633	0.30	0.00437	0.00499
	ATCG00680.1	psbB CP47	thylakoid-integral	0.35	0.27	0.01570	0.01647	0.01625	0.01438	0.07	0.01924	0.01215

Supplemental Table 1. (continued)

Core PG proteome (workflow Figure 4)	Accession - Selected gene model	Lab Annotation	Curated Location	Coverage in-gel (PG)	Coverage in-sol (PG)	Average NadjSPC PG	Repl. 1 NadjSPC average (in gel & in-sol)	Repl.2 NadjSPC average (in-gel & in-sol)	Repl. 3 NadjSPC average (in-gel & in-sol)	CV (NadjSPC)	In-gel - Average NadjSPC repl. 1,2,3	In-sol - Average NadjSPC repl.1,2,3
	ATCG00350.1	psaA - subunit Ia	thylakoid-integral	0.13	0.04	0.00494	0.00245	0.00204	0.01031	0.94	0.00308	0.00679
	ATCG00720.1	petB - Cytochrome b6	thylakoid-integral	0.15	0.09	0.00067	0.00066	0.00093	0.00041	0.39	0.00054	0.00080
	ATCG00340.1	psaB - subunit Ib	thylakoid-integral	0.21	0.09	0.00709	0.00566	0.00687	0.00874	0.22	0.00642	0.00776
	AT1G50250.1	FtsH1	thylakoid-integral	0.25	0.00	0.00059	0.00095	0.00081	0.00000	0.87	0.00117	0.00000
	AT1G06430.1	FtsH8 TAT ltp	thylakoid-integral	0.31	0.00	0.00168	0.00205	0.00144	0.00156	0.19	0.00336	0.00000
	AT2G34430.1	LHCII-1.4	thylakoid-integral	0.52	0.56	0.00144	0.00260	0.00172	0.00000	0.92	0.00168	0.00120
	AT2G34420.1	LHCII-1.5	thylakoid-integral	0.51	0.56	0.00131	0.00153	0.00222	0.00017	0.80	0.00046	0.00215
	AT3G54890.1	LHCI-1-1 - LHCI-730	thylakoid-integral	0.15	0.26	0.00098	0.00168	0.00103	0.00022	0.75	0.00043	0.00152
	AT3G61470.1	LHCI-2.1 - LHCI-680B	thylakoid-integral	0.17	0.24	0.00163	0.00189	0.00299	0.00000	0.93	0.00038	0.00288
	AT1G61520.1	LHCI-3 - LHCI-680A CAB4	thylakoid-integral	0.25	0.27	0.00734	0.00892	0.00813	0.00497	0.28	0.00755	0.00713
	AT3G47470.1	LHCI-4 - LHCI-730	thylakoid-integral	0.30	0.15	0.00299	0.00440	0.00262	0.00196	0.42	0.00430	0.00169
	AT2G05100.1	LHCII-2.1	thylakoid-integral	0.25	0.35	0.00283	0.00345	0.00461	0.00044	0.76	0.00127	0.00440
	AT2G05070.1	LHCII-2.2	thylakoid-integral	0.16	0.35	0.00031	0.00067	0.00011	0.00014	1.04	0.00020	0.00041
	AT3G27690.1	LHCII-2.3	thylakoid-integral	0.53	0.35	0.00106	0.00256	0.00011	0.00050	1.25	0.00170	0.00041
	AT5G54270.1	LHCII-3	thylakoid-integral	0.20	0.44	0.00097	0.00091	0.00156	0.00044	0.58	0.00067	0.00126
	AT3G08940.2	LHCII-4.2 - CP29 - model .2 is t	thylakoid-integral	0.36	0.22	0.00129	0.00159	0.00140	0.00089	0.28	0.00181	0.00078
	AT2G40100.1	LHCII-4.3 -CP29	thylakoid-integral	0.30	0.11	0.00049	0.00064	0.00082	0.00000	0.89	0.00068	0.00029
	AT4G10340.1	LHCII-5 - CP26	thylakoid-integral	0.49	0.42	0.00511	0.00652	0.00468	0.00412	0.25	0.00561	0.00461
	AT1G15820.1	LHCII-6 - CP24	thylakoid-integral	0.32	0.30	0.00328	0.00435	0.00290	0.00259	0.29	0.00393	0.00264
	AT4G17600.1	Lil3.2	thylakoid-integral	0.07	0.00	0.00013	0.00007	0.00000	0.00033	1.30	0.00027	0.00000
	AT1G44575.1	psbS (NPQ4 - null mutant)	thylakoid-integral	0.37	0.26	0.00295	0.00292	0.00418	0.00175	0.41	0.00277	0.00312
	AT4G22890.1	PGRL1A	thylakoid-integral	0.21	0.07	0.00075	0.00042	0.00038	0.00145	0.81	0.00068	0.00082
	AT1G31330.1	psaF- subunit III - LTP - hydropl	thylakoid-integral	0.27	0.17	0.00291	0.00416	0.00203	0.00254	0.38	0.00204	0.00378
	AT1G55670.1	psaG - subunit V- stromal side	thylakoid-integral	0.00	0.04	0.00015	0.00044	0.00000	0.00000	1.73	0.00000	0.00029
	AT1G30380.1	psaK - subunit X	thylakoid-integral	0.00	0.27	0.00039	0.00087	0.00029	0.00000	1.14	0.00000	0.00078
	AT4G12800.1	psaL - subunit XI (also named \	thylakoid-integral	0.19	0.40	0.00140	0.00166	0.00127	0.00128	0.16	0.00165	0.00116
	ATCG00270.1	psbD D2	thylakoid-integral	0.15	0.20	0.00494	0.00473	0.00398	0.00611	0.22	0.00363	0.00625
	AT1G73990.1	SppA	thylakoid-integral	0.03	0.00	0.00010	0.00007	0.00023	0.00000	1.17	0.00020	0.00000
	AT1G77490.1	thylakoid bound APX	thylakoid-integral	0.16	0.00	0.00034	0.00042	0.00060	0.00000	0.90	0.00068	0.00000
	AT5G42270.1	FtsH5 (VAR1)	thylakoid-integral	0.38	0.08	0.00413	0.00295	0.00325	0.00621	0.44	0.00689	0.00137
	AT2G30950.1	FtsH2 (VAR2 and Pftf)	thylakoid-integral	0.44	0.13	0.00313	0.00302	0.00299	0.00339	0.07	0.00464	0.00162
	AT4G09010.1	TL29	thylakoid-peripheral-	0.12	0.00	0.00017	0.00050	0.00000	0.00000	1.73	0.00033	0.00000
	AT4G02530.1	thylakoid lumen protein TL16.5	thylakoid-peripheral-	0.09	0.00	0.00002	0.00007	0.00000	0.00000	1.73	0.00005	0.00000
	AT3G01480.1	Tlp-40 (or CYCLOPHILIN 38 - C	thylakoid-peripheral-	0.08	0.00	0.00007	0.00014	0.00008	0.00000	0.98	0.00014	0.00000
	AT3G27925.1	DegP1 - HhoA homologue or D	thylakoid-peripheral-	0.10	0.00	0.00017	0.00014	0.00038	0.00000	1.10	0.00035	0.00000
	AT1G20340.1	plastocyanin-1 (PC-1)	thylakoid-peripheral-	0.17	0.14	0.00012	0.00036	0.00000	0.00000	1.73	0.00009	0.00015
	AT5G23120.1	HCF136 Tat ltp	thylakoid-peripheral-	0.39	0.13	0.00265	0.00192	0.00378	0.00224	0.38	0.00324	0.00206
	AT5G66570.1	psbO OEC33	thylakoid-peripheral-	0.30	0.36	0.00194	0.00230	0.00193	0.00159	0.18	0.00173	0.00215
	AT4G03280.1	petC - Rieske Fe-S protein	thylakoid-peripheral-	0.14	0.11	0.00083	0.00102	0.00114	0.00033	0.53	0.00051	0.00114
	AT5G64040.1	psaN - TAT LTP	thylakoid-peripheral-	0.06	0.13	0.00091	0.00074	0.00118	0.00082	0.25	0.00005	0.00178
	AT3G50820.1	psbO OEC33-like	thylakoid-peripheral-	0.42	0.31	0.00349	0.00375	0.00136	0.00536	0.58	0.00247	0.00451
	AT1G06680.2	PsbP-1 OEC23 Tat ltp	thylakoid-peripheral-	0.25	0.09	0.00136	0.00224	0.00139	0.00044	0.67	0.00120	0.00151

Supplemental Table 1. (continued)

Core PG proteome (workflow Figure 4)	Accession - Selected gene model	Lab Annotation	Curated Location	Coverage in-gel (PG)	Coverage in-sol (PG)	Average NadjSPC PG	Repl. 1 NadjSPC average (in gel & in-sol)	Repl.2 NadjSPC average (in-gel & in-sol)	Repl. 3 NadjSPC average (in-gel & in-sol)	CV (NadjSPC)	In-gel - Average NadjSPC repl. 1,2,3	In-sol - Average NadjSPC repl.1,2,3
	AT1G54780.1	thylakoid lumen 18.3 kDa	thylakoid-peripheral-	0.27	0.24	0.00091	0.00161	0.00113	0.00000	0.90	0.00038	0.00145
	ATCG01060.1	psaC - subunit VII - stromal sid	thylakoid-peripheral-	0.00	0.51	0.00100	0.00126	0.00092	0.00082	0.23	0.00000	0.00200
	AT4G02770.1	psaD-2 subunit II - stromal side	thylakoid-peripheral-	0.64	0.26	0.00340	0.00447	0.00286	0.00287	0.27	0.00375	0.00305
	AT4G28750.1	psaE-1 subunit IV - stromal sid	thylakoid-peripheral-	0.56	0.32	0.00052	0.00066	0.00090	0.00000	0.90	0.00084	0.00020
	AT2G20260.1	psaE-2 subunit IV - stromal sid	thylakoid-peripheral-	0.28	0.00	0.00040	0.00033	0.00000	0.00087	1.10	0.00080	0.00000
	AT1G73060.1	LPA3 - PSII assembly factor ass	thylakoid-peripheral-	0.11	0.00	0.00017	0.00021	0.00030	0.00000	0.90	0.00034	0.00000
	AT1G03680.1	thioredoxin m 1	thylakoid-peripheral-	0.00	0.18	0.00020	0.00015	0.00044	0.00000	1.14	0.00000	0.00040
	AT5G66190.1	FNR-1	thylakoid-peripheral-	0.38	0.15	0.00344	0.00166	0.00285	0.00580	0.62	0.00338	0.00350
	AT1G20020.1	FNR-2 (interaction with Cytf, ma	thylakoid-peripheral-	0.30	0.05	0.00141	0.00128	0.00120	0.00175	0.21	0.00272	0.00010
	AT4G09650.1	CF1d - atpD	thylakoid-peripheral-	0.36	0.00	0.00087	0.00120	0.00098	0.00044	0.45	0.00175	0.00000
	ATCG00470.1	CF1e - atpE	thylakoid-peripheral-	0.34	0.46	0.00160	0.00249	0.00147	0.00085	0.52	0.00088	0.00233
	AT4G04640.1	CF1y - atpC	thylakoid-peripheral-	0.48	0.55	0.00676	0.00607	0.00600	0.00820	0.19	0.00735	0.00617
	ATCG00480.1	CF1b - atpB	thylakoid-peripheral-	0.91	0.85	0.04919	0.04399	0.04280	0.06078	0.20	0.04806	0.05032
	ATCG00120.1	CF1a - atpA	thylakoid-peripheral-	0.60	0.46	0.03025	0.02904	0.02665	0.03506	0.14	0.03424	0.02626
	AT3G26070.1	fibrillin 3a (FBN3a)	thylakoid-peripheral-	0.06	0.05	0.00035	0.00007	0.00015	0.00082	1.19	0.00015	0.00055
	AT1G51110.1	fibrillin 10 (FBN10)	thylakoid-peripheral-	0.24	0.00	0.00098	0.00149	0.00090	0.00055	0.49	0.00196	0.00000
	AT1G03630.1	PORC- ~constitutive expressior	thylakoid-peripheral-	0.05	0.00	0.00010	0.00014	0.00015	0.00000	0.87	0.00019	0.00000
	AT1G03130.1	psaD-1 subunit II - stromal side	thylakoid-peripheral-	0.58	0.26	0.00216	0.00199	0.00286	0.00164	0.29	0.00209	0.00223
	AT2G21410.1	VHA-A2 (VACUOLAR PROTON /	tonoplast	0.03	0.00	0.00007	0.00000	0.00000	0.00022	1.73	0.00015	0.00000
	AT1G76030.1	V-ATPase subunit B (VATB)	vacuole	0.33	0.06	0.00058	0.00000	0.00173	0.00000	1.73	0.00105	0.00010
	AT3G18780.1	actin 2 (ACT2)	vacuole	0.10	0.00	0.00006	0.00013	0.00006	0.00000	1.02	0.00013	0.00000
	AT1G12840.1	V-ATPase subunit C (VATC) (DI	vacuole	0.19	0.04	0.00047	0.00021	0.00119	0.00000	1.36	0.00054	0.00039
	AT1G47128.1	cysteine proteinase (RD21A) / tl	vacuole	0.08	0.00	0.00060	0.00050	0.00053	0.00076	0.25	0.00119	0.00000
	AT1G78900.1	ATPase 70 kDa	vacuole	0.25	0.04	0.00072	0.00021	0.00195	0.00000	1.48	0.00125	0.00020

Supplemental Table 2. Comparison of protein abundances in PG, total leaf, thylakoid and stroma

Core PG proteome (workflow Figure 4)	Accession - Selected gene model	Lab Annotation	Curated Location	PG/Total Leaf (NadjSPC)	PG/Thy (NadjSPC)	PG/Stroma (NadjSPC)	PG/Total Leaf (NadjSPC)	PG/Thy (NadjSPC)	PG/Stroma (NadjSPC)
yes	AT4G19170.1	ycarotenoid dioxygenase (CCD4 al	plastoglobules	pass (>100)	pass (>10-<50))	pass (>20-<50)	726.9	17.9	41.7
yes-new	AT3G24190.1	ABC1 kinase 6 - ABC1K6	plastoglobules	pass (>100)	pass (>10-<50))	pass (>100)	234.2	15.3	322.0
yes	AT1G71810.1	ABC1 kinase 1 - ABC1K1	plastoglobules	pass (>100)	pass (>10-<50))	pass (>100)	ND in leaf	17.2	ND in stroma
yes	AT1G79600.1	ABC1 kinase 2 - ABC1K2	plastoglobules	pass (>100)	pass (>10-<50))	pass (>100)	3793.0	11.0	ND in stroma
yes	AT4G31390.1	ABC1 kinase 3 - ABC1K3	plastoglobules	pass (>100)	pass (>10-<50))	pass (>100)	3963.8	15.6	ND in stroma
yes	AT5G05200.1	ABC1 kinase 4 - ABC1K4	plastoglobules	pass (>100)	pass (>100)	pass (>100)	ND in leaf	439.5	ND in stroma
yes-new	AT3G07700.1	ABC1 kinase 7 - ABC1K7	plastoglobules	pass (>100)	pass (>10-<50))	pass (>100)	ND in leaf	37.4	ND in stroma
yes	AT1G06690.1	aldo/keto reductase	plastoglobules	pass (>100)	pass (>10-<50))	pass (>100)	119.6	12.9	764.7
yes	AT1G54570.1	acyl glycerol transferase 3 (DGAT	plastoglobules	pass (>100)	pass (>10-<50))	pass (>100)	ND in leaf	30.8	ND in stroma
yes	AT3G26840.1	cylglycerol Acyltransferase 4 (DGA	plastoglobules	pass (>100)	pass (>5)	pass (>100)	ND in leaf	ND in thyl	ND in stroma
yes-new	AT5G41120.1	erase/lipase/thioesterase (Esteras	plastoglobules	pass (>100)	pass (>5)	pass (>100)	ND in leaf	ND in thyl	ND in stroma
yes	AT4G04020.1	fibrillin 1a (FBN1a)	plastoglobules	pass (>100)	pass (>10-<50))	pass (>100)	170.1	34.0	176.2
yes	AT4G22240.1	fibrillin 1b (FBN1b)	plastoglobules	pass (>100)	pass (>10-<50))	pass (>100)	569.6	39.9	712.8
yes	AT2G35490.1	fibrillin 2 (FBN2)	plastoglobules	pass (>100)	pass (>50-<100))	pass (>100)	151.5	59.0	1187.7
yes	AT3G23400.1	fibrillin 4 (FBN4)	plastoglobules	pass (>50-<100)	pass (>10-<50))	pass (>100)	79.1	32.0	121.2
yes	AT3G58010.1	fibrillin 7a (FBN7a)	plastoglobules	pass (>100)	pass (>10-<50))	pass (>100)	342.2	14.8	145.6
yes	AT2G42130.4	7b) - model .4 scores better than m	plastoglobules	pass (>50-<100)	pass (>10-<50))	pass (>20-<50)	55.5	10.6	23.5
yes	AT2G46910.1	fibrillin 8 (FBN8)	plastoglobules	pass (>100)	pass (>10-<50))	pass (>100)	388.4	29.4	434.1
yes	AT1G32220.1	flavin reductase-related 1	plastoglobules	pass (>50-<100)	pass (>10-<50))	pass (>100)	96.9	21.9	102.3
yes	AT2G34460.1	flavin reductase-related 2	plastoglobules	pass (>10-50)	pass (>5 -<10)	pass (>50-<100)	28.4	5.6	75.2
yes-new	AT4G39730.1	lipid-associated PLAT/LH2-1	plastoglobules	pass (>10-50)	pass (>5)	pass (>100)	48.5	ND in thyl	ND in stroma
yes-new	AT3G27110.1	M48 protease	plastoglobules	pass (>100)	pass (>10-<50))	pass (>100)	ND in leaf	16.9	ND in stroma
yes	AT5G08740.1	- dually targeted in plastid & mitoch	plastoglobules	pass (>100)	pass (>10-<50))	pass (>100)	2119.4	18.9	ND in stroma
yes	AT3G10130.1	SOUL heme-binding	plastoglobules	pass (>100)	pass (>50-<100))	pass (>100)	ND in leaf	60.6	ND in stroma
yes	AT4G32770.1	tocopherol cyclase (VTE1)	plastoglobules	pass (>100)	pass (>100)	pass (>100)	ND in leaf	131.0	ND in stroma
yes	AT1G78140.1	UbiE methyltransferase related 1	plastoglobules	pass (>100)	pass (>10-<50))	pass (>100)	ND in leaf	48.0	ND in stroma
yes	AT2G41040.1	UbiE methyltransferase related 2	plastoglobules	pass (>100)	pass (>50-<100))	pass (>100)	ND in leaf	72.5	ND in stroma
yes-new	AT3G43540.1	unknown protein 2 (DUF1350)	plastoglobules	pass (>100)	pass (>10-<50))	pass (>50-<100)	410.5	13.5	79.9
yes-new	AT1G73750.1	unknown protein (SAG)	plastoglobules	pass (>100)	pass (>5)	pass (>100)	ND in leaf	ND in thyl	ND in stroma
yes	AT4G13200.1	unknown protein 1	plastoglobules	pass (>50-<100)	pass (>10-<50))	pass (>100)	76.0	10.6	ND in stroma
	AT2G01140.1	ose-bisphosphate aldolase-3 (SFB	plastid	pass (>10-50)	pass (>5)		11.7	ND in thyl	0.6
	AT4G38970.1	ose-bisphosphate aldolase-2 (SFB	plastid stroma				1.3	1.8	0.7
	AT2G21330.1	ose-bisphosphate aldolase-1 (SFB	plastid stroma				7.7	4.3	2.3
	AT5G42650.1	oxide synthase (AOS) (interaction w	thylakoid	pass (>10-50)		pass (>20-<50)	14.1	4.4	46.1
	AT2G22170.1	ed PLAT/LH2 - dually targeted to ER & cytosol?		pass (>100)	pass (>5)	pass (>100)	122.1	ND in thyl	ND in stroma
	AT3G12110.1	actin 11 (ACT11)		pass (>100)	pass (>5)	pass (>100)	ND in leaf	ND in thyl	ND in stroma
	AT3G46520.1	actin 12 (ACT12)		pass (>100)	pass (>5)	pass (>100)	ND in leaf	ND in thyl	ND in stroma
	AT5G59370.1	actin 4 (ACT4)		pass (>100)	pass (>5)	pass (>100)	ND in leaf	ND in thyl	ND in stroma
	AT1G17870.1	EGY3, metalloprotease		pass (>100)	pass (>5)	pass (>100)	ND in leaf	ND in thyl	ND in stroma
	AT4G33110.1	l-L-methionine-dependent methyltransferases		pass (>10-50)	pass (>5)	pass (>100)	28.0	ND in thyl	ND in stroma
	AT4G28520.1	cruciferin 3		pass (>100)	pass (>5)	pass (>100)	ND in leaf	ND in thyl	ND in stroma
	AT2G39330.1	jacalin-related lectin 23		pass (>100)	pass (>5)	pass (>100)	ND in leaf	ND in thyl	ND in stroma

Supplemental Table 2. (continued)

Core PG proteome (workflow Figure 4)	Accession - Selected gene model	Lab Annotation	Curated Location	PG/Total Leaf (NadjSPC)	PG/Thy (NadjSPC)	PG/Stroma (NadjSPC)	PG/Total Leaf (NadjSPC)	PG/Thy (NadjSPC)	PG/Stroma (NadjSPC)
	AT3G16470.1	JR1 (Jacalin lectin family protein)	plastid or cytosolic?		pass (>5)		0.3	ND in thyl	6.2
	AT2G33380.1	RD20 protein induced by ABA during dehydration, EF-ha		pass (>100)	pass (>5)	pass (>100)	ND in leaf	ND in thyl	ND in stroma
	AT1G67360.1	rubber elongation factor (REF) family		pass (>100)	pass (>5)	pass (>100)	ND in leaf	ND in thyl	ND in stroma
	AT5G16550.1	unknown protein		pass (>100)	pass (>5)	pass (>100)	ND in leaf	ND in thyl	ND in stroma
	AT5G59960.1	unknown protein		pass (>100)	pass (>5)	pass (>100)	ND in leaf	ND in thyl	ND in stroma
	AT5G07990.1	Cytochrome P450 protein		pass (>100)	pass (>5)	pass (>100)	ND in leaf	ND in thyl	ND in stroma
	AT5G47860.1	unknown protein		pass (>100)	pass (>5)		ND in leaf	ND in thyl	9.3
	AT4G10000.1	glutaredoxin family protein		pass (>10-50)		pass (>100)	21.1	1.5	ND in stroma
	AT2G29550.1	tubulin beta-7 chain (TUB7)			pass (>5)	pass (>100)	1.3	ND in thyl	ND in stroma
	AT1G50010.1	TUA2 (tubulin alpha-2 chain)	cytoskeleton		pass (>5)	pass (>100)	0.0	ND in thyl	ND in stroma
	AT5G19780.1	tubulin alpha-3/alpha-5 chain (TUA	cytoskeleton		pass (>5)	pass (>100)	0.1	ND in thyl	ND in stroma
	AT4G14960.1	tubulin alpha-6 chain (TUA6)	cytoskeleton		pass (>5)	pass (>100)	0.0	ND in thyl	ND in stroma
	AT3G09630.1	60S ribosomal protein L4/L1 (RPL4	cytosol		pass (>5)	pass (>100)	0.2	ND in thyl	ND in stroma
	AT5G02870.1	60S ribosomal protein L4/L1 (RPL4	cytosol		pass (>5)	pass (>100)	0.2	ND in thyl	ND in stroma
	AT5G39740.1	60S ribosomal protein L5 (RPL5B)	cytosol		pass (>5)	pass (>100)	1.1	ND in thyl	ND in stroma
	AT1G19670.1	chlorophyllase 1 (CLH1) (also ATH	cytosol		pass (>5)	pass (>100)	3.9	ND in thyl	ND in stroma
	AT3G25520.1	60S ribosomal protein L5 (RPL5)	cytosol		pass (>5)	pass (>100)	0.3	ND in thyl	ND in stroma
	AT3G63520.1	9,10 (9',10') 9-cis-epoxycarotenoid	cytosol		pass (>5)	pass (>100)	5.9	ND in thyl	ND in stroma
	AT5G60390.1	elongation factor 1-alpha / EF-1-al	cytosol		pass (>5)	pass (>100)	0.6	ND in thyl	ND in stroma
	AT1G07920.1	elongation factor 1-alpha / EF-1-al	cytosol		pass (>5)	pass (>100)	0.6	ND in thyl	ND in stroma
	AT3G04120.1	glyceraldehyde-3-phosphate dehyd	cytosol		pass (>5)		0.3	ND in thyl	2.4
	AT5G56000.1	Hsp90-4	cytosol		pass (>5)	pass (>100)	3.2	ND in thyl	ND in stroma
	AT5G02500.1	HSP70-1 (HSC70-1) (not plastid) -	cytosol		pass (>5)		0.0	ND in thyl	0.1
	AT1G72370.1	40S ribosomal protein SA (RPSaA	cytosol		pass (>5)	pass (>100)	0.3	ND in thyl	ND in stroma
	AT1G52400.1	6-phospho-beta-galactosidase (BG	endoplasmic reticulum		pass (>5)		1.6	ND in thyl	7.3
	AT5G61790.1	calnexin 1 (CNX1)	endoplasmic reticulum		pass (>5)	pass (>100)	0.6	ND in thyl	ND in stroma
	AT2G20890.1	TF1 - thylakoid formation1	envelope				0.4	0.1	0.6
	AT3G63410.1	vte3 - MPBQ/MSBQ methyl transf	envelope-inner				1.2	0.6	1.1
	AT5G46110.1	TPT - IEP30 = Phosphate/triose-ph	envelope-inner-integral				2.4	0.2	0.6
	AT1G06950.1	Tic110	envelope-inner-integral				0.2	0.0	0.2
	AT2G24820.1	Tic55 (putative Rieske iron-sulfur p	envelope-inner-integral				6.0	0.6	4.7
	AT3G56940.1	CHL27 or Crd1	envelope-inner-peripheral-stromal-side			pass (>100)	0.3	0.2	ND in stroma
	AT5G50920.1	ClpC1 (also named HSP93-V) - sir	envelope-inner-peripheral-stromal-side				0.4	0.4	0.2
	AT4G13010.1	ceQORH - oxidoreductase, Zn bin	envelope-inner-peripheral-stromal-side			pass (>100)	1.4	0.6	ND in stroma
	AT3G18890.1	Tic 62 interacts with thylakoid-assc	inner envelope-stromal side			pass (>50-<100)	2.5	0.6	77.2
	AT3G08580.1	mitochondrial ADP,ATP carrier pro	mitochondria			pass (>100)	0.8	4.6	ND in stroma
	AT4G29130.1	hexokinase 1 (HXK1	mitochondria		pass (>5)	pass (>100)	5.4	ND in thyl	ND in stroma
	AT3G07770.1	Hsp90-6	mitochondria		pass (>5)		2.7	ND in thyl	6.0
	AT5G08670.1	H+-transporting ATP synthase beta	mitochondria		pass (>10-<50))	pass (>100)	0.5	11.6	ND in stroma
	AT5G08690.1	H+-transporting ATP synthase beta	mitochondria		pass (>10-<50))	pass (>100)	0.5	11.6	ND in stroma
	AT5G08680.1	H+-transporting ATP synthase beta	mitochondria		pass (>10-<50))	pass (>100)	0.9	23.1	ND in stroma
	AT2G20360.1	NADH-DH 40 kDasubunit - Comple	mitochondria		pass (>5)	pass (>100)	0.3	ND in thyl	ND in stroma

Supplemental Table 2. (continued)

Core PG proteome (workflow Figure 4)	Accession - Selected gene model	Lab Annotation	Curated Location	PG/Total Leaf (NadjSPC)	PG/Thy (NadjSPC)	PG/Stroma (NadjSPC)	PG/Total Leaf (NadjSPC)	PG/Thy (NadjSPC)	PG/Stroma (NadjSPC)
	AT5G19760.1	oxoglutarate/malate translocator ([	mitochondria		pass (>5)	pass (>100)	1.0	ND in thyl	ND in stroma
	AT5G37510.1	NADH-DH 76kDa subunit - Comple	mitochondria		pass (>5)	pass (>100)	0.6	ND in thyl	ND in stroma
	AT5G03290.1	isocitrate dehydrogenase [NAD+],	mitochondria		pass (>5)	pass (>100)	5.3	ND in thyl	ND in stroma
	AT5G14040.1	phosphate transporter (PHT3-1 or	mitochondria		pass (>5)	pass (>100)	0.3	ND in thyl	ND in stroma
	AT1G51980.1	mitochondrial processing peptidas	mitochondria		pass (>5)	pass (>100)	7.0	ND in thyl	ND in stroma
	AT4G01100.1	Adenine nucleotide carrier (ADNT1	mitochondria		pass (>5)	pass (>100)	3.6	ND in thyl	ND in stroma
	AT3G02090.1	mitochondrial processing peptidas	mitochondria		pass (>5)	pass (>100)	1.5	ND in thyl	ND in stroma
	AT5G67500.1	Voltage dependent ion channel VD	mitochondria		pass (>5)	pass (>100)	0.5	ND in thyl	ND in stroma
	AT3G01280.1	Voltage dependent ion channel VD	mitochondria		pass (>5)	pass (>100)	0.4	ND in thyl	ND in stroma
	AT5G15090.1	Voltage dependent ion channel VD	mitochondria		pass (>5)	pass (>100)	0.7	ND in thyl	ND in stroma
	AT5G66760.1	succinate dehydrogenase (ubiquin	mitochondria		pass (>5)	pass (>100)	0.9	ND in thyl	ND in stroma
	AT4G37930.1	glycine/serine hydroxymethyltransf	mitochondria		pass (>5)	pass (>100)	0.5	ND in thyl	ND in stroma
	AT5G23060.1	Ca2+ sensing receptor - phosphop	mitochondria			pass (>100)	2.4	0.6	327.8
	AT4G38510.1	probable H+-transporting ATPase	not plastid		pass (>5)	pass (>100)	0.1	ND in thyl	ND in stroma
	AT1G20260.2	vacuolar H+-ATPase subunit B	not plastid		pass (>5)	pass (>100)	0.6	ND in thyl	ND in stroma
	AT5G09810.1	actin 7 (ACT7) / actin 2	not plastid		pass (>5)	pass (>100)	0.5	ND in thyl	ND in stroma
	AT1G49240.1	actin 8 (ACT8)	not plastid		pass (>5)	pass (>100)	0.1	ND in thyl	ND in stroma
	AT2G07698.1	ATP synthase alpha chain, mitoch	not plastid		pass (>10-<50))	pass (>100)	1.8	21.7	ND in stroma
	AT5G39410.1	unknown protein	not plastid		pass (>5)	pass (>100)	3.3	ND in thyl	ND in stroma
	AT5G46800.1	mitochondrial carnitine/acyl (CAC)	not plastid		pass (>5)	pass (>100)	0.9	ND in thyl	ND in stroma
	AT3G13920.1	eukaryotic translation initiation fact	not plastid		pass (>5)	pass (>100)	0.0	ND in thyl	ND in stroma
	AT1G07940.1	elongation factor 1-alpha / EF-1-al	not plastid		pass (>5)	pass (>100)	0.6	ND in thyl	ND in stroma
	AT1G07930.1	elongation factor 1-alpha (E-Tu)	not plastid		pass (>5)	pass (>100)	0.6	ND in thyl	ND in stroma
	AT1G57720.1	elongation factor 1B-gamma, putat	not plastid		pass (>5)	pass (>100)	0.3	ND in thyl	ND in stroma
	AT1G72730.1	eukaryotic translation initiation fact	not plastid		pass (>5)		0.3	ND in thyl	1.2
	AT1G56070.1	elongation factor 2, EF-2	not plastid		pass (>5 -<10)		0.1	5.1	4.3
	AT5G26000.1	thioglucoside glucohydrolase 1 (TC	not plastid		pass (>5)		0.0	ND in thyl	0.1
	AT5G25980.2	myrosinase or thioglucoside glucol	not plastid		pass (>5)		0.1	ND in thyl	1.0
	AT5G19770.1	tubulin alpha-3/alpha-5 chain (TUA	not plastid		pass (>5)	pass (>100)	0.1	ND in thyl	ND in stroma
	AT1G04820.1	tubulin alpha-2/alpha-4 chain (TUA	not plastid		pass (>5)	pass (>100)	0.0	ND in thyl	ND in stroma
	AT1G13440.1	glyceraldehyde-3-phosphate dehy	nucleus		pass (>5)		0.3	ND in thyl	0.8
	AT5G09660.1	malate dehydrogenase, glyoxysom	peroxisome				0.7	2.0	2.6
	AT1G15690.1	AVP1 (vacuolar-type H+-pumping	plasma membrane		pass (>5)	pass (>100)	0.4	ND in thyl	ND in stroma
	AT1G50450.1	saccharopine dehydrogenase fami	plastid		pass (>5 -<10)	pass (>100)	4.6	5.3	ND in stroma
	AT4G34200.1	D-3-phosphoglycerate dehydrogen	plastid				0.2	0.1	0.0
	AT5G44000.1	Glutathione S-transferase related p	plastid	pass (>100)	pass (>5)	pass (>100)	ND in leaf	ND in thyl	ND in stroma
	AT4G14210.1	phytoene desaturase (PDS)	plastid			pass (>100)	5.1	1.5	ND in stroma
	AT4G01690.1	protoporphyrinogen oxidase (PPO)	plastid			pass (>100)	0.7	0.3	ND in stroma
	AT5G62140.1	unknown protein	plastid	pass (>10-50)		pass (>100)	14.9	3.8	ND in stroma
	AT3G61870.1	unknown protein (integral membra	plastid			pass (>100)	3.1	0.7	ND in stroma
	AT4G28025.1	unknown protein	plastid			pass (>100)	4.0	0.7	ND in stroma
	AT5G35170.1	adenylate kinase	plastid				0.2	0.2	1.1

Supplemental Table 2. (continued)

Core PG proteome (workflow Figure 4)	Accession - Selected gene model	Lab Annotation	Curated Location	PG/Total Leaf (NadjSPC)	PG/Thy (NadjSPC)	PG/Stroma (NadjSPC)	PG/Total Leaf (NadjSPC)	PG/Thy (NadjSPC)	PG/Stroma (NadjSPC)
	AT3G48870.1	ClpC2 (also named HSP93-III)	plastid stroma				0.6	0.6	0.6
	AT4G03520.1	thioredoxin m2	plastid stroma				4.6	3.4	1.8
	AT3G15360.1	thioredoxin m4	plastid stroma	pass (>10-50)	pass (>5 -<10)		14.2	6.4	2.3
	AT4G20360.1	elongation factor Tu (EF-Tu-1), pla	plastid stroma				0.2	0.5	0.2
	AT4G18810.1	UV-B and ozone similarly regulate	plastid stroma	pass (>10-50)	pass (>10-<50))		19.1	10.9	6.6
	AT3G01500.3	beta-carbonic anhydrase-1 (beta C	plastid stroma				0.1	0.3	0.1
	AT2G04030.1	cpHSP90 (Hsp90-5)	plastid stroma				0.1	0.2	0.1
	AT5G26742.2	DEAD box RNA helicase (RH3)	plastid stroma				0.1	0.1	0.0
	AT3G26650.1	glyceraldehyde 3-phosphate dehyc	plastid stroma				0.1	0.1	0.0
	AT1G12900.1	glyceraldehyde-3-phosphate dehyc	plastid stroma				0.1	0.2	0.0
	AT1G42970.1	glyceraldehyde-3-phosphate dehyc	plastid stroma				0.0	0.0	0.0
	AT5G35630.1	glutamate-ammonia ligase (GS2),	plastid stroma				0.0	0.0	0.0
	AT1G56500.1	haloacid dehalogenase-like hydrol	plastid stroma				0.7	0.1	0.7
	ATCG00490.1	Rubisco large subunit (RBCL)	plastid stroma				0.0	0.0	0.0
	AT3G45140.1	lipoxygenase AtLOX2, plastid	plastid stroma				0.1	0.1	0.0
	AT3G47520.1	malate dehydrogenase [NAD], plas	plastid stroma				0.3	0.1	0.1
	AT3G12780.1	phosphoglycerate kinase-1 (PGK-1	plastid stroma				0.0	0.0	0.0
	AT1G56190.1	phosphoglycerate kinase-1 (PGK-2	plastid stroma				0.0	0.1	0.0
	AT2G39730.1	Rubisco activase	plastid stroma				1.0	2.0	0.8
	AT1G80030.1	DnaJ domain family	thylakoid	pass (>100)		pass (>100)	ND in leaf	0.4	ND in stroma
	ATCG01110.1	NDH H (NDH-7)	thylakoid				0.1	0.0	0.1
	AT5G17170.1	unknown protein Rubredoxin and F	thylakoid			pass (>100)	1.5	0.5	ND in stroma
	AT1G74470.1	geranylgeranyl reductase (GGDR)	thylakoid			pass (>20-<50)	2.2	1.4	30.6
	AT4G01050.1	unknown protein - Rhodanese-like	thylakoid			pass (>50-<100)	1.5	0.6	94.8
	AT2G46820.1	Photosystem I protein TMP14 - PS	thylakoid				1.2	0.5	6.0
	AT3G46780.1	unknown protein (pTAC16)	thylakoid				1.0	0.5	4.0
	AT2G42220.1	rhodanese-like domain protein	thylakoid				0.2	0.1	3.0
	AT1G71500.1	Rieske [2Fe-2S] domain	thylakoid			pass (>10-<20)	0.7	0.2	11.1
	AT5G03880.1	glutaredoxin	thylakoid			pass (>100)	4.7	2.1	ND in stroma
	AT1G15980.1	NDF1- associates with NDH compl	thylakoid			pass (>100)	2.1	0.2	ND in stroma
	AT4G35250.1	vestitone reductase-related	thylakoid				1.1	0.2	6.0
	ATCG00730.1	petD - subIV	thylakoid-integral				0.8	0.3	6.0
	AT4G32260.1	CFO-II - atpG	thylakoid-integral			pass (>20-<50)	0.7	0.3	22.5
	ATCG00130.1	CFO-I - atpF	thylakoid-integral				1.7	0.6	9.2
	AT1G29930.1	LHCII-1.3 - 100% identical to lhcb-	thylakoid-integral				0.5	0.2	5.1
	AT1G29920.1	LHCII-1.2 - 100% identical to lhcb-	thylakoid-integral				0.4	0.3	3.4
	AT1G29910.1	LHCII-1.1 - 100% identical to lhcb-	thylakoid-integral				0.4	0.3	3.4
	AT5G01530.1	LHCII-4.1-CP29	thylakoid-integral				1.1	0.3	9.2
	ATCG00280.1	psbC CP43	thylakoid-integral				1.1	0.3	4.5
	ATCG00020.1	psbA D1	thylakoid-integral			pass (>10-<20)	1.0	0.4	13.9
	ATCG00540.1	petA - cytochrome f (cleavable ss	thylakoid-integral			pass (>10-<20)	1.7	0.5	13.2
	ATCG00680.1	psbB CP47	thylakoid-integral			pass (>10-<20)	1.3	0.5	15.7

Supplemental Table 2. (continued)

Core PG proteome (workflow Figure 4)	Accession - Selected gene model	Lab Annotation	Curated Location	PG/Total Leaf (NadjSPC)	PG/Thy (NadjSPC)	PG/Stroma (NadjSPC)	PG/Total Leaf (NadjSPC)	PG/Thy (NadjSPC)	PG/Stroma (NadjSPC)
	ATCG00350.1	psaA - subunit Ia	thylakoid-integral			pass (>10-<20)	4.7	0.6	10.5
	ATCG00720.1	petB - Cytochrome b6	thylakoid-integral				0.3	0.1	0.9
	ATCG00340.1	psaB - subunit Ib	thylakoid-integral			pass (>10-<20)	2.0	0.5	10.2
	AT1G50250.1	FtsH1	thylakoid-integral				0.6	0.2	2.8
	AT1G06430.1	FtsH8 TAT ITP	thylakoid-integral			pass (>10-<20)	2.4	0.8	11.5
	AT2G34430.1	LHCII-1.4	thylakoid-integral				0.5	0.2	3.8
	AT2G34420.1	LHCII-1.5	thylakoid-integral				0.6	0.6	3.6
	AT3G54890.1	LHCI-1-1 - LHCI-730	thylakoid-integral				0.3	0.2	1.8
	AT3G61470.1	LHCI-2.1 - LHCI-680B	thylakoid-integral				0.6	0.5	1.9
	AT1G61520.1	LHCI-3 - LHCI-680A CAB4	thylakoid-integral				1.2	0.8	8.3
	AT3G47470.1	LHCI-4 - LHCI-730	thylakoid-integral				0.6	0.3	2.0
	AT2G05100.1	LHCII-2.1	thylakoid-integral				1.3	1.1	7.9
	AT2G05070.1	LHCII-2.2	thylakoid-integral				0.1	0.1	0.8
	AT3G27690.1	LHCII-2.3	thylakoid-integral				0.3	1.7	4.4
	AT5G54270.1	LHCII-3	thylakoid-integral				0.2	0.2	1.2
	AT3G08940.2	LHCII-4.2 - CP29 - model .2 is bett	thylakoid-integral				0.5	0.2	2.7
	AT2G40100.1	LHCII-4.3 -CP29	thylakoid-integral			pass (>20-<50)	4.7	0.4	40.0
	AT4G10340.1	LHCII-5 - CP26	thylakoid-integral				0.5	0.3	2.7
	AT1G15820.1	LHCII-6 - CP24	thylakoid-integral				0.5	0.3	2.9
	AT4G17600.1	Lil3.2	thylakoid-integral			pass (>100)	0.3	0.3	ND in stroma
	AT1G44575.1	psbS (NPQ4 - null mutant)	thylakoid-integral				1.3	0.3	2.4
	AT4G22890.1	PGRL1A	thylakoid-integral			pass (>100)	0.6	0.3	ND in stroma
	AT1G31330.1	psaF- subunit III - LTP - hydrophot	thylakoid-integral				0.4	0.4	3.7
	AT1G55670.1	psaG - subunit V- stromal side	thylakoid-integral				0.1	0.1	1.0
	AT1G30380.1	psaK - subunit X	thylakoid-integral			pass (>10-<20)	4.6	1.0	10.6
	AT4G12800.1	psaL - subunit XI (also named V)	thylakoid-integral				0.4	0.4	3.8
	ATCG00270.1	psbD D2	thylakoid-integral				0.7	0.2	4.5
	AT1G73990.1	SppA	thylakoid-integral			pass (>100)	4.7	0.2	ND in stroma
	AT1G77490.1	thylakoid bound APX	thylakoid-integral				1.6	0.2	4.6
	AT5G42270.1	FtsH5 (VAR1)	thylakoid-integral			pass (>100)	1.6	0.6	ND in stroma
	AT2G30950.1	FtsH2 (VAR2 and Pftf)	thylakoid-integral			pass (>20-<50)	1.1	0.3	42.4
	AT4G09010.1	TL29	thylakoid-peripheral-lumenal-side				0.2	0.0	0.7
	AT4G02530.1	thylakoid lumen protein TL16.5	thylakoid-peripheral-lumenal-side				0.0	0.0	0.1
	AT3G01480.1	Tlp-40 (or CYCLOPHILIN 38 - CYP	thylakoid-peripheral-lumenal-side				0.1	0.0	0.1
	AT3G27925.1	DegP1 - HhoA homologue or DegC	thylakoid-peripheral-lumenal-side				1.0	0.1	0.3
	AT1G20340.1	plastocyanin-1 (PC-1)	thylakoid-peripheral-lumenal-side				0.1	0.1	0.1
	AT5G23120.1	HCF136 Tat ltp	thylakoid-peripheral-lumenal-side				2.0	0.6	1.1
	AT5G66570.1	psbO OEC33	thylakoid-peripheral-lumenal-side				0.6	0.1	1.8
	AT4G03280.1	petC - Rieske Fe-S protein	thylakoid-peripheral-lumenal-side				0.4	0.1	1.4
	AT5G64040.1	psaN - TAT LTP	thylakoid-peripheral-lumenal-side				1.2	0.4	5.7
	AT3G50820.1	psbO OEC33-like	thylakoid-peripheral-lumenal-side				1.2	0.5	5.4
	AT1G06680.2	PsbP-1 OEC23 Tat ITP	thylakoid-peripheral-lumenal-side				0.3	0.1	0.6

Supplemental Table 2. (continued)

Core PG proteome (workflow Figure 4)	Accession - Selected gene model	Lab Annotation	Curated Location	PG/Total Leaf (NadjSPC)	PG/Thy (NadjSPC)	PG/Stroma (NadjSPC)	PG/Total Leaf (NadjSPC)	PG/Thy (NadjSPC)	PG/Stroma (NadjSPC)
	AT1G54780.1	thylakoid lumen 18.3 kDa	thylakoid-peripheral-lumenal-side				0.6	0.2	2.5
	ATCG01060.1	psaC - subunit VII - stromal side	thylakoid-peripheral-stromal side				1.6	3.0	4.1
	AT4G02770.1	psaD-2 subunit II - stromal side-tig	thylakoid-peripheral-stromal side			pass (>20-<50)	1.9	0.4	50.9
	AT4G28750.1	psaE-1 subunit IV - stromal side	thylakoid-peripheral-stromal side				0.4	0.3	2.0
	AT2G20260.1	psaE-2 subunit IV - stromal side	thylakoid-peripheral-stromal side				0.6	0.1	5.5
	AT1G73060.1	LPA3 - PSII assembly factor assoc	thylakoid-peripheral-stromal side				0.9	0.1	0.2
	AT1G03680.1	thioredoxin m1	thylakoid-peripheral-stromal-side				0.4	0.4	0.2
	AT5G66190.1	FNR-1	thylakoid-peripheral-stromal-side				1.5	0.6	1.9
	AT1G20020.1	FNR-2 (interaction with Cytf, mayb	thylakoid-peripheral-stromal-side				0.8	0.5	0.5
	AT4G09650.1	CF1d - atpD	thylakoid-peripheral-stromal-side				0.4	0.1	1.0
	ATCG00470.1	CF1e - atpE	thylakoid-peripheral-stromal-side				0.7	0.5	7.0
	AT4G04640.1	CF1y - atpC	thylakoid-peripheral-stromal-side			pass (>10-<20)	2.6	0.6	12.7
	ATCG00480.1	CF1b - atpB	thylakoid-peripheral-stromal-side			pass (>10-<20)	1.7	0.9	15.1
	ATCG00120.1	CF1a - atpA	thylakoid-peripheral-stromal-side			pass (>10-<20)	1.6	1.4	15.3
	AT3G26070.1	fibrillin 3a (FBN3a)	thylakoid-peripheral-stromal-side			pass (>100)	0.9	0.1	ND in stroma
	AT1G51110.1	fibrillin 10 (FBN10)	thylakoid-peripheral-stromal-side			pass (>100)	4.7	1.8	ND in stroma
	AT1G03630.1	PORC- ~constitutive expression	thylakoid-peripheral-stromal-side				0.4	0.1	0.4
	AT1G03130.1	psaD-1 subunit II - stromal side-tig	thylakoid-peripheral-stromal-side			pass (>10-<20)	1.2	1.5	17.7
	AT2G21410.1	VHA-A2 (VACUOLAR PROTON A	tonoplast		pass (>5)	pass (>100)	1.3	ND in thyl	ND in stroma
	AT1G76030.1	V-ATPase subunit B (VATB)	vacuole		pass (>5)	pass (>100)	0.6	ND in thyl	ND in stroma
	AT3G18780.1	actin 2 (ACT2)	vacuole		pass (>5)	pass (>100)	0.1	ND in thyl	ND in stroma
	AT1G12840.1	V-ATPase subunit C (VATC) (DET	vacuole		pass (>5 -<10)	pass (>10-<20)	0.8	7.5	15.3
	AT1G47128.1	cysteine proteinase (RD21A) / thio	vacuole		pass (>5)	pass (>100)	3.0	ND in thyl	ND in stroma
	AT1G78900.1	ATPase 70 kDa	vacuole		pass (>5)	pass (>100)	0.2	ND in thyl	ND in stroma

Supplemental Table 3. MetaOmGraph co-expression results - Top 20

PG gene	PG Name	Co-Expresser	PCC Value	Module	Co-Expresser	Lab annotation	Curated Loc.	BIN1	BIN NAME1
At1g54570	Diacylglycerol Acyltransferase 3 (DGAT3)	AT1G02470	0.9317	I	AT1G02470.1	Polyketide cyclase/dehydrase/lipid transport protein		35.2	not assigned.unknown
At1g54570	Diacylglycerol Acyltransferase 3 (DGAT3)	AT3G10320	0.8849	I	AT3G10320.1	Glycosyltransferase 61 protein		35.2	not assigned.unknown
At1g54570	Diacylglycerol Acyltransferase 3 (DGAT3)	AT5G45890	0.8446	I	AT5G45890.1	cystein protease - SAG		29.5.3	protein.degradation.cysteine protea
At1g54570	Diacylglycerol Acyltransferase 3 (DGAT3)	AT4G18980	0.8369	I	AT4G18980.1	AtS40-3		35.2	not assigned.unknown
At1g54570	Diacylglycerol Acyltransferase 3 (DGAT3)	AT4G32250	0.8141	I	AT4G32250.1	protein Tyrosine kinase	plastid	29.4.1	protein.postranslational modificatic
At1g54570	Diacylglycerol Acyltransferase 3 (DGAT3)	AT2G28085	0.7949	I	AT2G28085.1	SAUR-like auxin-responsive protein		17.2.3	hormone metabolism.auxin.induce
At1g54570	Diacylglycerol Acyltransferase 3 (DGAT3)	AT3G45010	0.7738	I	AT3G45010.1	serine carboxypeptidase-like 48		29.5	protein.degradation
At1g54570	Diacylglycerol Acyltransferase 3 (DGAT3)	AT5G45900	0.7698	I	AT5G45900.1	ThiF protein		29.5.2	protein.degradation.autophagy
At1g54570	Diacylglycerol Acyltransferase 3 (DGAT3)	AT4G24000	0.7358	I	AT4G24000.1	cellulose synthase like G2		10.2.1	cell wall.cellulose synthesis.cellulo
At1g54570	Diacylglycerol Acyltransferase 3 (DGAT3)	AT5G53350	0.7319	I	AT5G53350.1	ClpX1 - likely mitochondria	mitochondria	29.5.5	protein.degradation.serine proteas
At1g54570	Diacylglycerol Acyltransferase 3 (DGAT3)	AT1G69490	0.7296	I	AT1G69490.1	NAC-like, activated by AP3/PI		33.99	development.unspecified
At1g54570	Diacylglycerol Acyltransferase 3 (DGAT3)	AT1G30220	0.7207	I	AT1G30220.1	inositol transporter 2		34.2	transport.sugars
At1g54570	Diacylglycerol Acyltransferase 3 (DGAT3)	AT1G22380	0.7189	I	AT1G22380.1	UDP-glucosyl transferase 85A3		26.2	misc.UDP glucosyl and glucoronyl
At1g54570	Diacylglycerol Acyltransferase 3 (DGAT3)	AT4G02940	0.7167	I	AT4G02940.1	oxidoreductase, 2OG-Fe(II) oxygenase protein		35.1	not assigned.no ontology
At1g54570	Diacylglycerol Acyltransferase 3 (DGAT3)	AT5G17450	0.7142	I	AT5G17450.1	Heavy metal transport/detoxification protein		15.2	metal handling.binding, chelation a
At1g54570	Diacylglycerol Acyltransferase 3 (DGAT3)	AT1G35310	0.7123	I	AT1G35310.1	MLP-like protein 168		20.2.99	stress.abiotic.unspecified
At1g54570	Diacylglycerol Acyltransferase 3 (DGAT3)	AT3G28050	0.7115	I	AT3G28050.1	nodulin MtN21 /EamA-like transporter		33.99	development.unspecified
At1g54570	Diacylglycerol Acyltransferase 3 (DGAT3)	AT2G26230	0.7104	I	AT2G26230.1	uricase / urate oxidase / no	peroxisome	23.2	nucleotide metabolism.degradatior
At1g54570	Diacylglycerol Acyltransferase 3 (DGAT3)	AT4G39480	0.7099	I	AT4G39480.1	cytochrome P450		26.1	misc.cytochrome P450
At1g54570	Diacylglycerol Acyltransferase 3 (DGAT3)	AT5G40690	0.7051	I	AT5G40690.1	unknown protein		35.2	not assigned.unknown
At1g73750	Unknown SAG	AT5G63800	0.7682	I	AT5G63800.1	beta-galactosidase 6 (BGA	not plastid	26.3	misc.gluco-, galacto- and mannosi
At1g73750	Unknown SAG	AT2G23840	0.7483	I	AT2G23840.1	HNH endonuclease		28.1	DNA.synthesis/chromatin structure
At1g73750	Unknown SAG	AT2G42750	0.6976	I	AT2G42750.1	DnaJ-domain protein		26.29*	misc.DnaJ domain with unknown fu
At1g73750	Unknown SAG	AT4G11570	0.6793	I	AT4G11570.1	haloacid dehalogenase-like	likely plastid	3.2	minor CHO metabolism.trehalose
At1g73750	Unknown SAG	AT3G44880	0.6761	I	AT3G44880.1	Pheophorbide a oxygenase	envelope-inner	19.50*	tetrapyrrole degradation
At1g73750	Unknown SAG	***AT3G27110***	0.6623	I	AT3G27110.1	M48 protease	plastoglobules	29.5	protein.degradation
At1g73750	Unknown SAG	AT5G19140	0.6587	I	AT5G19140.1	auxin/aluminum-responsive	not plastid	15	metal handling
At1g73750	Unknown SAG	AT4G11960	0.6486	I	AT4G11960.1	PGRL1B	thylakoid-integral	1.1.40	PS.lightreaction.cyclic electron flov
At1g73750	Unknown SAG	***AT1G79600***	0.6458	I	AT1G79600.1	ABC1 kinase 3 - ABC1K3	plastoglobules	26.56*	misc.ABC1k family
At1g73750	Unknown SAG	AT1G13990	0.6456	I	AT1G13990.1	unknown protein (DUF760)	plastid	35.2	not assigned.unknown
At1g73750	Unknown SAG	AT1G26920	0.6447	I	AT1G26920.1	unknown protein		35.2	not assigned.unknown
At1g73750	Unknown SAG	AT5G18760	0.6428	I	AT5G18760.1	RING/U-box superprotein		29.5.11.4.2	protein.degradation.ubiquitin.E3.RI
At1g73750	Unknown SAG	***AT4G19170***	0.6410	I	AT4G19170.1	9-cis-epoxycarotenoid diox	plastoglobules	16.1.4	secondary metabolism.isoprenoids
At1g73750	Unknown SAG	AT1G01240	0.6395	I	AT1G01240.1	unknown protein		35.2	not assigned.unknown
At1g73750	Unknown SAG	AT3G03470	0.6379	I	AT3G03470.1	cytochrome P450		26.1	misc.cytochrome P450
At1g73750	Unknown SAG	AT1G21640	0.6365	I	AT1G21640.1	NADK2 - NADPH synthesis	plastid stroma	18.21*	Co-factor and vitamine metabolism
At1g73750	Unknown SAG	AT3G19900	0.6352	I	AT3G19900.1	unknown protein	stroma	35.2	not assigned.unknown
At1g73750	Unknown SAG	AT4G29010	0.6311	I	AT4G29010.1	enoyl-CoA hydratase - AIM	peroxisome	11.9.4.9	lipid metabolism.lipid degradation.b
At1g73750	Unknown SAG	AT1G09240	0.6301	I	AT1G09240.1	nicotianamine synthase 3		15.2	metal handling.binding, chelation a
At1g73750	Unknown SAG	AT3G26280	0.6284	I	AT3G26280.1	cytochrome P450		26.1	misc.cytochrome P450

Supplemental Table 3. (continued)

PG gene	PG Name	Co-Expresser	PCC Value	Module	Co-Expresser	Lab annotation	Curated Loc.	BIN1	BIN NAME1
At3g07700	ABC1K7	AT2G33380	0.7578	I	AT2G33380.1	RD20 protein induced by ABA during dehydration, EF-hand dom		30.3	signalling.calcium
At3g07700	ABC1K7	AT1G69870	0.7460	I	AT1G69870.1	proton-dependent oligopep	plasma membrane	34.13	transport.peptides and oligopeptide
At3g07700	ABC1K7	AT3G03470	0.7444	I	AT3G03470.1	cytochrome P450		26.1	misc.cytochrome P450
At3g07700	ABC1K7	AT3G44880	0.7392	I	AT3G44880.1	Pheophorbide a oxygenase	envelope-inner	19.50*	tetrapyrrole degradation
At3g07700	ABC1K7	AT4G32250	0.7384	I	AT4G32250.1	protein tyrosine kinase	plastid	29.4.1	protein.postranslational modificatic
At3g07700	ABC1K7	AT1G69610	0.7317	I	AT1G69610.1	unknown protein (DUF1666)		35.2	not assigned.unknown
At3g07700	ABC1K7	AT1G13990	0.7191	I	AT1G13990.1	unknown protein (DUF760)	plastid	35.2	not assigned.unknown
At3g07700	ABC1K7	AT4G02940	0.7083	I	AT4G02940.1	oxidoreductase, 2OG-Fe(II) oxygenase protein		35.1	not assigned.no ontology
At3g07700	ABC1K7	AT1G58360	0.7012	I	AT1G58360.1	amino acid permease 1		34.3	transport.amino acids
At3g07700	ABC1K7	AT3G10320	0.7009	I	AT3G10320.1	Glycosyltransferase 61 protein		35.2	not assigned.unknown
At3g07700	ABC1K7	AT5G65870	0.6990	I	AT5G65870.1	phytosulfokine 5 precursor		33.99	development.unspecified
At3g07700	ABC1K7	AT2G17730	0.6916	I	AT2G17730.1	NIP1 - interacts with NEP F	thylakoid	28.3*	DNA.plastid nucleoid interacting
At3g07700	ABC1K7	AT3G10420	0.6894	I	AT3G10420.1	AAA domain protein		35.1	not assigned.no ontology
At3g07700	ABC1K7	AT4G27830	0.6863	I	AT4G27830.1	beta glucosidase		26.3	misc.gluco-, galacto- and mannosi
At3g07700	ABC1K7	AT2G23450	0.6768	I	AT2G23450.1	protein kinase family protein		30.2.25	signalling.receptor kinases.wall ass
At3g07700	ABC1K7	AT5G13800	0.6729	I	AT5G13800.1	pheophytin pheophorbide h	thylakoid	19.50*	tetrapyrrole degradation
At3g07700	ABC1K7	AT5G08750	0.6715	I	AT5G08750.1	RING/FYVE/PHD zinc finger superprotein		29.5.11.4.2	protein.degradation.ubiquitin.E3.RI
At3g07700	ABC1K7	AT5G51070	0.6707	I	AT5G51070.1	ClpD (Erd1)	plastid stroma	29.5.5	protein.degradation.serine proteas
At3g07700	ABC1K7	***AT1G54570***	0.6681	I	AT1G54570.1	Diacyl glycerol transferase	plastoglobules	11.10	lipid metabolism.glycolipid synthes
At3g07700	ABC1K7	AT4G08290	0.6674	I	AT4G08290.1	nodulin MtN21 /EamA-like transporter		33.99	development.unspecified
At3g27110	M48 protease	AT1G31170	0.7588	I	AT1G31170.1	sulfiredoxin (Srx)	plastid	21	redox
At3g27110	M48 protease	AT1G09130	0.7553	I	AT1G09130.1	ClpR3	plastid stroma	29.5.5	protein.degradation.serine proteas
At3g27110	M48 protease	AT4G03410	0.7539	I	AT4G03410.1	Peroxisomal membrane 22 kDa (Mpv17/PMP22) protein		35.1	not assigned.no ontology
At3g27110	M48 protease	AT3G19900	0.7536	I	AT3G19900.1	unknown protein	stroma	35.2	not assigned.unknown
At3g27110	M48 protease	AT4G11570	0.7369	I	AT4G11570.1	haloacid dehalogenase-like	likely plastid	3.2	minor CHO metabolism.trehalose
At3g27110	M48 protease	AT4G27990	0.7329	I	AT4G27990.1	YGGT-B protein (likely not	plastid	35.1	not assigned.no ontology
At3g27110	M48 protease	AT3G63520	0.7323	I	AT3G63520.1	9,10 (9',10') 9-cis-epoxycar	cytosol	16.1.4.10	secondary metabolism.isoprenoids
At3g27110	M48 protease	AT1G09240	0.7273	I	AT1G09240.1	nicotianamine synthase 3		15.2	metal handling.binding, chelation a
At3g27110	M48 protease	AT1G13990	0.7257	I	AT1G13990.1	unknown protein (DUF760)	plastid	35.2	not assigned.unknown
At3g27110	M48 protease	AT1G77930	0.7250	I	AT1G77930.1	DnaJ-domain protein		26.29*	misc.DnaJ domain with unknown fu
At3g27110	M48 protease	AT3G12800	0.7245	I	AT3G12800.1	short-chain dehydrogenase	peroxisome	26.22	misc.short chain dehydrogenase/re
At3g27110	M48 protease	AT5G63800	0.7235	I	AT5G63800.1	beta-galactosidase 6 (BGA	not plastid	26.3	misc.gluco-, galacto- and mannosi
At3g27110	M48 protease	AT1G78200	0.7222	I	AT1G78200.1	Protein phosphatase 2C protein (PlasmaMembrane?)		29.4	protein.postranslational modificatic
At3g27110	M48 protease	AT5G04260	0.7192	I	AT5G04260.1	glutaredoxin-thioredoxin pr	plastid stroma	21.1	redox.thioredoxin
At3g27110	M48 protease	AT1G06650	0.7122	I	AT1G06650.1	2-oxoglutarate-dependent d		21.2	redox.ascorbate and glutathione
At3g27110	M48 protease	AT3G03890	0.7095	I	AT3G03890.1	unknown protein; Pyridox_d	plastid stroma	35.2	not assigned.unknown
At3g27110	M48 protease	AT3G56630	0.7037	I	AT3G56630.1	cytochrome P450		26.10	misc.cytochrome P450
At3g27110	M48 protease	AT2G20920	0.7033	I	AT2G20920.1	unknown protein	plastid	35.2	not assigned.unknown
At3g27110	M48 protease	AT4G22260	0.7027	I	AT4G22260.1	Plastid Terminal oxidase (F	thylakoid-integral	1.1.40	PS.lightreaction.cyclic electron flov
At3g27110	M48 protease	AT5G13800	0.7008	I	AT5G13800.1	pheophytin pheophorbide h	thylakoid	19.50*	tetrapyrrole degradation

Supplemental Table 3. (continued)

PG gene	PG Name	Co-Expresser	PCC Value	Module	Co-Expresser	Lab annotation	Curated Loc.	BIN1	BIN NAME1
At1g06690	Aldo/keto reductase (AKRed)	AT4G29590	0.8805	II	AT4G29590.1	methyltransferase domain p	plastid	29.4	protein.postranslational modificatic
At1g06690	Aldo/keto reductase (AKRed)	AT5G42270	0.8730	II	AT5G42270.1	FtsH5 (VAR1)	thylakoid-integral	29.5.7	protein.degradation.metalloproteas
At1g06690	Aldo/keto reductase (AKRed)	AT4G36530	0.8477	II	AT4G36530.2	hydrolase, alpha/beta fold protein		35.1	not assigned.no ontology
At1g06690	Aldo/keto reductase (AKRed)	AT1G57770	0.8441	II	AT1G57770.1	phytoene desaturase (PDS	plastid	16.1.4	secondary metabolism.isoprenoids
At1g06690	Aldo/keto reductase (AKRed)	AT1G50250	0.8358	II	AT1G50250.1	FtsH1	thylakoid-integral	29.5.7	protein.degradation.metalloproteas
At1g06690	Aldo/keto reductase (AKRed)	AT4G14210	0.8343	II	AT4G14210.1	phytoene desaturase (PDS	plastid	16.1.4.2	secondary metabolism.isoprenoids
At1g06690	Aldo/keto reductase (AKRed)	AT4G35250	0.8342	II	AT4G35250.1	vestitone reductase-related	thylakoid	35.1	not assigned.no ontology
At1g06690	Aldo/keto reductase (AKRed)	AT1G55480	0.8326	II	AT1G55480.1	unknown protein	thylakoid-peripheral-stromal-side	35.2	not assigned.unknown
At1g06690	Aldo/keto reductase (AKRed)	AT1G62750	0.8223	II	AT1G62750.1	elongation factor Tu-G (EF-	plastid stroma	29.2.4	protein.synthesis.elongation
At1g06690	Aldo/keto reductase (AKRed)	***AT2G34460***	0.8177	II	AT2G34460.1	flavin reductase-related 2	plastoglobules	35.1	not assigned.no ontology
At1g06690	Aldo/keto reductase (AKRed)	AT3G04870	0.8176	II	AT3G04870.1	zeta-carotene desaturase (	plastid	16.1.4.3	secondary metabolism.isoprenoids
At1g06690	Aldo/keto reductase (AKRed)	AT1G79510	0.8163	II	AT1G79510.1	unknown protein (DUF2358)		35.2	not assigned.unknown
At1g06690	Aldo/keto reductase (AKRed)	***AT1G79600***	0.8136	II	AT1G79600.1	ABC1 kinase 3 - ABC1K3	plastoglobules	26.56*	misc.ABC1k family
At1g06690	Aldo/keto reductase (AKRed)	AT2G30950	0.8136	II	AT2G30950.1	FtsH2 (VAR2 and Pftf)	thylakoid-integral	29.5.7	protein.degradation.metalloproteas
At1g06690	Aldo/keto reductase (AKRed)	AT3G19170	0.8112	II	AT3G19170.1	AtPrep1 - (AtZnMP) metallc	stroma & mitochondria	29.5.7	protein.degradation.metalloproteas
At1g06690	Aldo/keto reductase (AKRed)	AT5G13650	0.8077	II	AT5G13650.1	elongation factor protein, ty	plastid stroma	29.2.4	protein.synthesis.elongation
At1g06690	Aldo/keto reductase (AKRed)	AT4G11175	0.8075	II	AT4G11175.1	translation initiation factor I	plastid stroma	29.2.3	protein.synthesis.initiation
At1g06690	Aldo/keto reductase (AKRed)	AT1G80030	0.8033	II	AT1G80030.1	DnaJ domain family	thylakoid	26.29*	misc.DnaJ domain with unknown fu
At1g06690	Aldo/keto reductase (AKRed)	AT2G32640	0.8030	II	AT2G32640.1	lycopene cyclase domain	thylakoid	35.2	not assigned.unknown
At1g06690	Aldo/keto reductase (AKRed)	AT1G18060	0.8024	II	AT1G18060.1	fibrillin-like protein	thylakoid	35.2	not assigned.unknown
At1g79600	ABC1K3	AT1G06430	0.8462	II	AT1G06430.1	FtsH8 TAT ITP	thylakoid-integral	29.5.7	protein.degradation.metalloproteas
At1g79600	ABC1K3	AT2G30950	0.8292	II	AT2G30950.1	FtsH2 (VAR2 and Pftf)	thylakoid-integral	29.5.7	protein.degradation.metalloproteas
At1g79600	ABC1K3	AT1G50250	0.8259	II	AT1G50250.1	FtsH1	thylakoid-integral	29.5.7	protein.degradation.metalloproteas
At1g79600	ABC1K3	AT5G67030	0.8259	II	AT5G67030.1	zeaxanthin epoxidase preci	thylakoid	16.1.4	secondary metabolism.isoprenoids
At1g79600	ABC1K3	AT3G04870	0.8201	II	AT3G04870.1	zeta-carotene desaturase (	plastid	16.1.4.3	secondary metabolism.isoprenoids
At1g79600	ABC1K3	AT1G68830	0.8198	II	AT1G68830.1	STN7 kinase state transitio	thylakoid-integral	1.1.30	PS.lightreaction.state transition
At1g79600	ABC1K3	AT5G42270	0.8190	II	AT5G42270.1	FtsH5 (VAR1)	thylakoid-integral	29.5.7	protein.degradation.metalloproteas
At1g79600	ABC1K3	AT4G14210	0.8182	II	AT4G14210.1	phytoene desaturase (PDS	plastid	16.1.4.2	secondary metabolism.isoprenoids
At1g79600	ABC1K3	***AT1G06690***	0.8136	***II***	AT1G06690.1	aldo/keto reductase	plastoglobules	35.1	not assigned.no ontology
At1g79600	ABC1K3	AT3G63520	0.8112	II	AT3G63520.1	9,10 (9',10') 9-cis-epoxycar	cytosol	16.1.4.10	secondary metabolism.isoprenoids
At1g79600	ABC1K3	AT1G09130	0.8091	II	AT1G09130.1	ClpR3	plastid stroma	29.5.5	protein.degradation.serine proteas
At1g79600	ABC1K3	***AT5G08740***	0.8052	***II***	AT5G08740.1	NDC1 - dually targeted in p	plastoglobules & mitochondria	35.2	not assigned.unknown
At1g79600	ABC1K3	AT3G19170	0.8029	II	AT3G19170.1	AtPrep1 - (AtZnMP) metallc	stroma & mitochondria	29.5.7	protein.degradation.metalloproteas
At1g79600	ABC1K3	AT1G21640	0.8004	II	AT1G21640.1	NADK2 - NADPH synthesis	plastid stroma	18.21*	Co-factor and vitamine metabolism
At1g79600	ABC1K3	AT5G50920	0.7988	II	AT5G50920.1	ClpC1 (also named HSP93	envelope-inner-peripheral-stromal-side	29.5.5	protein.degradation.serine proteas
At1g79600	ABC1K3	AT5G19855	0.7949	II	AT5G19855.1	RbcX protein - needed for I	stroma	29.8	protein assembly and cofactor liga
At1g79600	ABC1K3	AT3G27925	0.7916	II	AT3G27925.1	DegP1 - HhoA homologue	thylakoid-peripheral-lumenal-side	29.5.5	protein.degradation.serine proteas
At1g79600	ABC1K3	AT1G50020	0.7861	II	AT1G50020.1	unknown protein	plastid	35.2	not assigned.unknown
At1g79600	ABC1K3	AT5G58870	0.7845	II	AT5G58870.1	FtsH9	plastid	29.5.7	protein.degradation.metalloproteas
At1g79600	ABC1K3	AT4G36530	0.7835	II	AT4G36530.2	hydrolase, alpha/beta fold protein		35.1	not assigned.no ontology

Supplemental Table 3. (continued)

PG gene	PG Name	Co-Expresser	PCC Value	Module	Co-Expresser	Lab annotation	Curated Loc.	BIN1	BIN NAME1
At2g34460	Flavin-reductase related 2 (FRed-2)	AT5G42070	0.9009	II	AT5G42070.1	unknown protein	plastid	35.2	not assigned.unknown
At2g34460	Flavin-reductase related 2 (FRed-2)	AT2G04039	0.8984	II	AT2G04039.1	unknown protein	plastid	35.2	not assigned.unknown
At2g34460	Flavin-reductase related 2 (FRed-2)	AT5G08050	0.8983	II	AT5G08050.1	unknown protein	thylakoid	35.2	not assigned.unknown
At2g34460	Flavin-reductase related 2 (FRed-2)	AT2G05620	0.8973	II	AT2G05620.1	PGR5	thylakoid-peripheral-stromal side	1.1.40	PS.lightreaction.cyclic electron flov
At2g34460	Flavin-reductase related 2 (FRed-2)	AT1G23740	0.8903	II	AT1G23740.1	oxidoreductase, zinc-bindin	plastid stroma	26.7	misc.oxidases - copper, flavone et
At2g34460	Flavin-reductase related 2 (FRed-2)	AT1G18060	0.8892	II	AT1G18060.1	fibrillin-like protein	thylakoid	35.2	not assigned.unknown
At2g34460	Flavin-reductase related 2 (FRed-2)	AT5G02120	0.8826	II	AT5G02120.1	Ohp1 or Lil2/Hlip/Scp	thylakoid-integral	1.1.8*	light stress chlorophyll binding
At2g34460	Flavin-reductase related 2 (FRed-2)	AT2G21330	0.8810	II	AT2G21330.1	fructose-bisphosphate aldo	plastid stroma	1.3.6	PS.calvin cyle.aldolase
At2g34460	Flavin-reductase related 2 (FRed-2)	AT5G57345	0.8796	II	AT5G57345.1	unknown protein		35.2	not assigned.unknown
At2g34460	Flavin-reductase related 2 (FRed-2)	AT3G01060	0.8779	II	AT3G01060.1	unknown protein (likely plas	likely plastid	35.2	not assigned.unknown
At2g34460	Flavin-reductase related 2 (FRed-2)	AT4G35250	0.8745	II	AT4G35250.1	vestitone reductase-related	thylakoid	35.1	not assigned.no ontology
At2g34460	Flavin-reductase related 2 (FRed-2)	AT3G15850	0.8739	II	AT3G15850.1	fatty acid desaturase 5		11.2.1	lipid metabolism.FA desaturation.d
At2g34460	Flavin-reductase related 2 (FRed-2)	AT1G75690	0.8725	II	AT1G75690.1	sco2 - snowy cotyledon 2	plastid	26.29*	misc.DnaJ domain with unknown fu
At2g34460	Flavin-reductase related 2 (FRed-2)	AT4G11175	0.8721	II	AT4G11175.1	translation initiation factor I	plastid stroma	29.2.3	protein.synthesis.initiation
At2g34460	Flavin-reductase related 2 (FRed-2)	AT3G10230	0.8708	II	AT3G10230.1	lycopene beta cyclase (LYC	plastid	16.1.4.5	secondary metabolism.isoprenoids
At2g34460	Flavin-reductase related 2 (FRed-2)	AT3G54900	0.8707	II	AT3G54900.1	Glutaredoxin (formerly CAX	plastid	21.5	redox.periredoxins
At2g34460	Flavin-reductase related 2 (FRed-2)	AT4G09350	0.8692	II	AT4G09350.1	DnaJ domain-containing pr	maybe plastid	20.2.1	stress.abiotic.heat
At2g34460	Flavin-reductase related 2 (FRed-2)	AT5G38520	0.8664	II	AT5G38520.1	hydrolase	thylakoid	35.1	not assigned.no ontology
At2g34460	Flavin-reductase related 2 (FRed-2)	AT1G74730	0.8648	II	AT1G74730.1	unknown protein	thylakoid	35.2	not assigned.unknown
At2g34460	Flavin-reductase related 2 (FRed-2)	AT5G51110	0.8640	II	AT5G51110.1	unknown protein	plastid stroma	35.2	not assigned.unknown
At2g41040	UbiE methyltransferase related 2 (UbiE-2)	AT1G78510	0.7868	II	AT1G78510.1	solanesyl diphosphate synt	ER	16.1.5	secondary metabolism.isoprenoids
At2g41040	UbiE methyltransferase related 2 (UbiE-2)	AT1G76570	0.7602	II	AT1G76570.1	LHCII-7	thylakoid-integral	1.1.1.1	PS.lightreaction.photosystem II.LH
At2g41040	UbiE methyltransferase related 2 (UbiE-2)	AT3G56290	0.7454	II	AT3G56290.1	unknown protein		35.2	not assigned.unknown
At2g41040	UbiE methyltransferase related 2 (UbiE-2)	AT5G19850	0.7436	II	AT5G19850.1	alpha/beta-Hydrolases superprotein		35.1	not assigned.no ontology
At2g41040	UbiE methyltransferase related 2 (UbiE-2)	AT1G17050	0.7430	II	AT1G17050.1	solanesyl diphosphate synt	plastid stroma	16.1.1	secondary metabolism.isoprenoids
At2g41040	UbiE methyltransferase related 2 (UbiE-2)	AT1G32900	0.7305	II	AT1G32900.1	starch synthase, putative	plastid stroma	2.1.2.2	major CHO metabolism.synthesis.s
At2g41040	UbiE methyltransferase related 2 (UbiE-2)	AT5G50100	0.7264	II	AT5G50100.1	unknown protein (DUF393)		35.2	not assigned.unknown
At2g41040	UbiE methyltransferase related 2 (UbiE-2)	AT4G26850	0.7255	II	AT4G26850.1	mannose-1-phosphate guanylyltransferase (GDP)s		21.2.1.2	redox.ascorbate and glutathione.as
At2g41040	UbiE methyltransferase related 2 (UbiE-2)	AT1G02820	0.7228	II	AT1G02820.1	Late embryogenesis abundant 3 (LEA3) protein		33.2	development.late embryogenesis a
At2g41040	UbiE methyltransferase related 2 (UbiE-2)	AT1G06430	0.7215	II	AT1G06430.1	FtsH8 TAT ITP	thylakoid-integral	29.5.7	protein.degradation.metalloproteas
At2g41040	UbiE methyltransferase related 2 (UbiE-2)	AT1G66330	0.7193	II	AT1G66330.1	senescence-associated protein		33.99	development.unspecified
At2g41040	UbiE methyltransferase related 2 (UbiE-2)	AT3G21670	0.7151	II	AT3G21670.1	Major facilitator superprotein		34.4	transport.nitrate
At2g41040	UbiE methyltransferase related 2 (UbiE-2)	AT3G61220	0.7093	II	AT3G61220.1	short-chain dehydrogenase	not plastid	26.22	misc.short chain dehydrogenase/re
At2g41040	UbiE methyltransferase related 2 (UbiE-2)	AT5G24120	0.7082	II	AT5G24120.1	SIG5 sigma factor (SigE)	plastid	27.2	RNA.transcription
At2g41040	UbiE methyltransferase related 2 (UbiE-2)	AT5G58770	0.7063	II	AT5G58770.1	putative prenyltransferase	stroma	35.1	not assigned.no ontology
At2g41040	UbiE methyltransferase related 2 (UbiE-2)	AT5G01260	0.7026	II	AT5G01260.1	Carbohydrate-binding-like fold		2.2.2.4	major CHO metabolism.degradatic
At2g41040	UbiE methyltransferase related 2 (UbiE-2)	AT1G07180	0.6951	II	AT1G07180.1	ATNDI1/NDA1 (ALTERNAT	mitochondria & peroxisome	9.2.1	mitochondrial electron transport / A
At2g41040	UbiE methyltransferase related 2 (UbiE-2)	AT3G17800	0.6940	II	AT3G17800.1	unknown protein (DUF760)	plastid	35.2	not assigned.unknown
At2g41040	UbiE methyltransferase related 2 (UbiE-2)	AT5G17600	0.6902	II	AT5G17600.1	RING/U-box superprotein		29.5.11.4.2	protein.degradation.ubiquitin.E3.RI
At2g41040	UbiE methyltransferase related 2 (UbiE-2)	AT2G37240	0.6861	II	AT2G37240.1	unknown protein	plastid stroma	35.1	not assigned.no ontology

Supplemental Table 3. (continued)

PG gene	PG Name	Co-Expresser	PCC Value	Module	Co-Expresser	Lab annotation	Curated Loc.	BIN1	BIN NAME1
At3g24190	ABC1K6	AT1G17050	0.8739	II	AT1G17050.1	solanesyl diphosphate synt	plastid stroma	16.1.1	secondary metabolism.isoprenoids
At3g24190	ABC1K6	AT1G53090	0.8176	II	AT1G53090.1	SPA1-related 4		30.11	signalling.light
At3g24190	ABC1K6	AT1G78510	0.8122	II	AT1G78510.1	solanesyl diphosphate synt	ER	16.1.5	secondary metabolism.isoprenoids
At3g24190	ABC1K6	AT2G21320	0.8087	II	AT2G21320.1	B-box zinc finger protein		27.3.7	RNA.regulation of transcription.C2
At3g24190	ABC1K6	AT5G50100	0.8049	II	AT5G50100.1	unknown protein (DUF393)		35.2	not assigned.unknown
At3g24190	ABC1K6	AT1G02820	0.8048	II	AT1G02820.1	Late embryogenesis abundant 3 (LEA3) protein		33.2	development.late embryogenesis a
At3g24190	ABC1K6	AT3G09650	0.7994	II	AT3G09650.1	HCF152 (HIGH CHLOROP	plastid stroma	27.1	RNA.processing
At3g24190	ABC1K6	AT5G57960	0.7979	II	AT5G57960.1	HFlx - GTPase	plastid stroma	29.2.7*	protein.synthesis.ribosome biogen
At3g24190	ABC1K6	AT1G76570	0.7961	II	AT1G76570.1	LHCII-7	thylakoid-integral	1.1.1.1	PS.lightreaction.photosystem II.LH
At3g24190	ABC1K6	AT1G32900	0.7876	II	AT1G32900.1	starch synthase, putative	plastid stroma	2.1.2.2	major CHO metabolism.synthesis.s
At3g24190	ABC1K6	AT1G70610	0.7872	II	AT1G70610.1	ABC protein - transmembra	envelope	34.8	transport.metabolite transporters a
At3g24190	ABC1K6	AT4G27820	0.7849	II	AT4G27820.1	glycosyl hydrolase 1 (likely peroxisome)		26.3	misc.gluco-, galacto- and mannosi
At3g24190	ABC1K6	AT5G19850	0.7817	II	AT5G19850.1	alpha/beta-Hydrolases superprotein		35.1	not assigned.no ontology
At3g24190	ABC1K6	AT3G21670	0.7809	II	AT3G21670.1	Major facilitator superprotein		34.4	transport.nitrate
At3g24190	ABC1K6	AT5G67030	0.7805	II	AT5G67030.1	zeaxanthin epoxidase prec	thylakoid	16.1.4	secondary metabolism.isoprenoids
At3g24190	ABC1K6	AT5G64840	0.7782	II	AT5G64840.1	ABC transporter family prot	plastid	34.16	transport.ABC transporters and mu
At3g24190	ABC1K6	AT4G39800	0.7758	II	AT4G39800.1	inositol-3-phosphate syntha		3.4.3	minor CHO metabolism.myo-inosit
At3g24190	ABC1K6	AT5G35970	0.7744	II	AT5G35970.1	Deadbox DNA helicase-rela	plastid stroma	28.5*	DNA.DEAD BOX helicase
At3g24190	ABC1K6	***AT4G31390***	0.7739	***II***	AT4G31390.1	ABC1 kinase 1 - ABC1K1	plastoglobules	26.56*	misc.ABC1k family
At3g24190	ABC1K6	AT1G07010	0.7709	II	AT1G07010.1	Calcineurin-like metallo-phosphoesterase protein		26.27	misc.calcineurin-like phosphoester
At4g19170	CCD4	AT2G42750	0.7849	II	AT2G42750.1	DnaJ-domain protein		26.29*	misc.DnaJ domain with unknown fu
At4g19170	CCD4	AT2G29650	0.7818	II	AT2G29650.1	ANTR1 - Pi transporter; als	envelope-inner-integral	34.7	transport.phosphate
At4g19170	CCD4	AT5G61670	0.7742	II	AT5G61670.1	DnaJ-domain protein (homolog OR)		26.29*	misc.DnaJ domain with unknown fu
At4g19170	CCD4	AT5G57345	0.7717	II	AT5G57345.1	unknown protein		35.2	not assigned.unknown
At4g19170	CCD4	AT5G67030	0.7517	II	AT5G67030.1	zeaxanthin epoxidase prec	thylakoid	16.1.4	secondary metabolism.isoprenoids
At4g19170	CCD4	AT4G11570	0.7503	II	AT4G11570.1	haloacid dehalogenase-like	likely plastid	3.2	minor CHO metabolism.trehalose
At4g19170	CCD4	AT4G10770	0.7443	II	AT4G10770.1	oligopeptide transporter 7		34.13	transport.peptides and oligopeptide
At4g19170	CCD4	AT5G57040	0.7426	II	AT5G57040.1	lactoylglutathione lyase fam	plastid	13.2.3.2	amino acid metabolism.degradatio
At4g19170	CCD4	AT1G68830	0.7389	II	AT1G68830.1	STN7 kinase state transitio	thylakoid-integral	1.1.30	PS.lightreaction.state transition
At4g19170	CCD4	AT2G23840	0.7355	II	AT2G23840.1	HNH endonuclease		28.1	DNA.synthesis/chromatin structure
At4g19170	CCD4	AT4G09900	0.7351	II	AT4G09900.1	methyl esterase 12		35.1	not assigned.no ontology
At4g19170	CCD4	AT1G71480	0.7299	II	AT1G71480.1	nuclear transport factor 2 (N	plastid	29.3.1	protein.targeting.nucleus
At4g19170	CCD4	AT1G77930	0.7290	II	AT1G77930.1	DnaJ-domain protein		26.29*	misc.DnaJ domain with unknown fu
At4g19170	CCD4	AT1G75460	0.7203	II	AT1G75460.1	ATP-dependent protease L	plastid	29.5	protein.degradation
At4g19170	CCD4	AT2G20570	0.7173	II	At2g20570.1	GPRI1 (GOLDEN2-LIKE 1); transcription factor		27.3.20	RNA.regulation of transcription.G2
At4g19170	CCD4	AT2G29360	0.7144	II	AT2G29360.1	tropinone reductase, putativ		26.8	misc.nitrilases, *nitrile lyases, berb
At4g19170	CCD4	AT3G16520	0.7091	II	AT3G16520.1	UDP-glucoronosyl/UDP-glu		26.2	misc.UDP glucosyl and glucoronyl
At4g19170	CCD4	AT3G01060	0.7059	II	AT3G01060.1	unknown protein (likely plas	likely plastid	35.2	not assigned.unknown
At4g19170	CCD4	AT5G35970	0.7051	II	AT5G35970.1	Deadbox DNA helicase-rela	plastid stroma	28.5*	DNA.DEAD BOX helicase
At4g19170	CCD4	AT3G26310	0.7035	II	AT3G26310.1	cytochrome P450		26.1	misc.cytochrome P450

Supplemental Table 3. (continued)

PG gene	PG Name	Co-Expresser	PCC Value	Module	Co-Expresser	Lab annotation	Curated Loc.	BIN1	BIN NAME1
At4g31390	ABC1K1	AT5G13650	0.8441	II	AT5G13650.1	elongation factor protein, ty	plastid stroma	29.2.4	protein.synthesis.elongation
At4g31390	ABC1K1	AT1G79510	0.8163	II	AT1G79510.1	unknown protein (DUF2358)		35.2	not assigned.unknown
At4g31390	ABC1K1	AT4G18810	0.8103	II	AT4G18810.1	UV-B and ozone similarly r	plastid stroma	20.2.99	stress.abiotic.unspecified
At4g31390	ABC1K1	AT1G06430	0.8102	II	AT1G06430.1	FtsH8 TAT ITP	thylakoid-integral	29.5.7	protein.degradation.metalloproteas
At4g31390	ABC1K1	AT3G04870	0.7986	II	AT3G04870.1	zeta-carotene desaturase (	plastid	16.1.4.3	secondary metabolism.isoprenoids
At4g31390	ABC1K1	AT1G50250	0.7947	II	AT1G50250.1	FtsH1	thylakoid-integral	29.5.7	protein.degradation.metalloproteas
At4g31390	ABC1K1	AT5G57960	0.7927	II	AT5G57960.1	HFlx - GTPase	plastid stroma	29.2.7*	protein.synthesis.ribosome biogen
At4g31390	ABC1K1	AT4G04770	0.7870	II	AT4G04770.1	ATNAP1 or AtABC1, LAF6	plastid	14	S-assimilation
At4g31390	ABC1K1	AT5G42270	0.7799	II	AT5G42270.1	FtsH5 (VAR1)	thylakoid-integral	29.5.7	protein.degradation.metalloproteas
At4g31390	ABC1K1	AT4G10120	0.7793	II	AT4G10120.1	ATSPS4F; sucrose-phosphate synthase/ transferase		2.1.1.1	major CHO metabolism.synthesis.s
At4g31390	ABC1K1	AT1G53090	0.7755	II	AT1G53090.1	SPA1-related 4		30.11	signalling.light
At4g31390	ABC1K1	***AT3G24190***	0.7739	***II***	AT3G24190.1	ABC1 kinase 6 - ABC1K6	plastid	26.56*	misc.ABC1k family
At4g31390	ABC1K1	AT1G07010	0.7737	II	AT1G07010.1	Calcineurin-like metallo-phosphoesterase protein		26.27	misc.calcineurin-like phosphoester
At4g31390	ABC1K1	AT3G63520	0.7728	II	AT3G63520.1	9,10 (9',10') 9-cis-epoxycar	cytosol	16.1.4.10	secondary metabolism.isoprenoids
At4g31390	ABC1K1	AT2G37240	0.7715	II	AT2G37240.1	unknown protein	plastid stroma	35.1	not assigned.no ontology
At4g31390	ABC1K1	AT4G28740	0.7639	II	AT4G28740.1	similar to LPA1 (LOW PSII	likely plastid	35.2	not assigned.unknown
At4g31390	ABC1K1	AT5G58870	0.7633	II	AT5G58870.1	FtsH9	plastid	29.5.7	protein.degradation.metalloproteas
At4g31390	ABC1K1	AT3G21760	0.7544	II	AT3G21760.1	UDP-Glycosyltransferase superprotein		26.2	misc.UDP glucosyl and glucoronyl
At4g31390	ABC1K1	***AT1G79600***	0.7531	***II***	AT1G79600.1	ABC1 kinase 3 - ABC1K3	plastoglobules	26.56*	misc.ABC1k family
At4g31390	ABC1K1	AT2G22360	0.7522	II	AT2G22360.1	DnaJ domain family	thylakoid	26.29*	misc.DnaJ domain with unknown f
At5g08740	NAD(P)H-dehydrogenase C1 (NDC1)	AT5G42270	0.8626	II	AT5G42270.1	FtsH5 (VAR1)	thylakoid-integral	29.5.7	protein.degradation.metalloproteas
At5g08740	NAD(P)H-dehydrogenase C1 (NDC1)	AT3G19170	0.8340	II	AT3G19170.1	AtPrep1 - (AtZnMP) metallo	stroma & mitochondria	29.5.7	protein.degradation.metalloproteas
At5g08740	NAD(P)H-dehydrogenase C1 (NDC1)	AT1G80030	0.8204	II	AT1G80030.1	DnaJ domain family	thylakoid	26.29*	misc.DnaJ domain with unknown f
At5g08740	NAD(P)H-dehydrogenase C1 (NDC1)	AT3G54660	0.8189	II	AT3G54660.1	gluthatione reductase,	plastid stroma	21.2.2	redox.ascorbate and glutathione.gl
At5g08740	NAD(P)H-dehydrogenase C1 (NDC1)	AT5G08650	0.8132	II	AT5G08650.1	Elongation factor Tu with G	plastid stroma	29.2.4	protein.synthesis.elongation
At5g08740	NAD(P)H-dehydrogenase C1 (NDC1)	AT4G18810	0.8101	II	AT4G18810.1	UV-B and ozone similarly r	plastid stroma	20.2.99	stress.abiotic.unspecified
At5g08740	NAD(P)H-dehydrogenase C1 (NDC1)	AT5G20140	0.8071	II	AT5G20140.1	SOUL heme-binding	thylakoid	21.3	redox.heme
At5g08740	NAD(P)H-dehydrogenase C1 (NDC1)	***AT1G79600***	0.8052	***II***	AT1G79600.1	ABC1 kinase 3 - ABC1K3	plastoglobules	26.56*	misc.ABC1k family
At5g08740	NAD(P)H-dehydrogenase C1 (NDC1)	AT2G41680	0.8045	II	AT2G41680.1	AtNTRC - NADPH reductas	plastid stroma	21.1	redox.thioredoxin
At5g08740	NAD(P)H-dehydrogenase C1 (NDC1)	AT1G50250	0.8039	II	AT1G50250.1	FtsH1	thylakoid-integral	29.5.7	protein.degradation.metalloproteas
At5g08740	NAD(P)H-dehydrogenase C1 (NDC1)	AT2G21280	0.8013	II	AT2G21280.1	GC1 (Giant Chloroplast 1)	envelope-inner-peripheral-stromal-side	31.2.5	cell.division.plastid
At5g08740	NAD(P)H-dehydrogenase C1 (NDC1)	AT1G62750	0.8001	II	AT1G62750.1	elongation factor Tu-G (EF-	plastid stroma	29.2.4	protein.synthesis.elongation
At5g08740	NAD(P)H-dehydrogenase C1 (NDC1)	***AT1G06690***	0.7994	***II***	AT1G06690.1	aldo/keto reductase	plastoglobules	35.1	not assigned.no ontology
At5g08740	NAD(P)H-dehydrogenase C1 (NDC1)	AT5G48220	0.7974	II	AT5G48220.1	indole-3-glycerol phosphate	plastid stroma	13.1.6.5.4	amino acid metabolism.synthesis.a
At5g08740	NAD(P)H-dehydrogenase C1 (NDC1)	AT5G23120	0.7947	II	AT5G23120.1	HCF136 Tat ltp	thylakoid-peripheral-lumenal-side	29.8	protein assembly and cofactor liga
At5g08740	NAD(P)H-dehydrogenase C1 (NDC1)	AT4G35250	0.7941	II	AT4G35250.1	vestitone reductase-related	thylakoid	35.1	not assigned.no ontology
At5g08740	NAD(P)H-dehydrogenase C1 (NDC1)	AT1G11750	0.7932	II	AT1G11750.1	ClpP6	plastid stroma	29.5.5	protein.degradation.serine proteas
At5g08740	NAD(P)H-dehydrogenase C1 (NDC1)	AT2G30950	0.7926	II	AT2G30950.1	FtsH2 (VAR2 and Pftf)	thylakoid-integral	29.5.7	protein.degradation.metalloproteas
At5g08740	NAD(P)H-dehydrogenase C1 (NDC1)	AT2G01110	0.7913	II	AT2G01110.1	TATC-like	thylakoid-integral	29.3.3	protein.targeting.chloroplast
At5g08740	NAD(P)H-dehydrogenase C1 (NDC1)	AT1G32500	0.7878	II	AT1G32500.1	SufD (AtNap6) - ABC prote	plastid stroma	14	S-assimilation

Supplemental Table 3. (continued)

PG gene	PG Name	Co-Expresser	PCC Value	Module	Co-Expresser	Lab annotation	Curated Loc.	BIN1	BIN NAME1
At2g35490	Fibrillin 2 (FBN2)	AT1G63970	0.9168	III	AT1G63970.1	2C-methyl-D-erythritol 2,4-c	plastid stroma	16.1.1.5	secondary metabolism.isoprenoids
At2g35490	Fibrillin 2 (FBN2)	AT2G30950	0.9046	III	AT2G30950.1	FtsH2 (VAR2 and Pftf)	thylakoid-integral	29.5.7	protein.degradation.metalloproteas
At2g35490	Fibrillin 2 (FBN2)	AT1G03680	0.8995	III	AT1G03680.1	thioredoxin m1	thylakoid-peripheral-stromal-side	21.1	redox.thioredoxin
At2g35490	Fibrillin 2 (FBN2)	AT1G02560	0.8957	III	AT1G02560.1	ClpP5	plastid stroma	29.5.5	protein.degradation.serine proteas
At2g35490	Fibrillin 2 (FBN2)	AT2G31040	0.8910	III	AT2G31040.1	unknown protein	likely plastid	35.2	not assigned.unknown
At2g35490	Fibrillin 2 (FBN2)	AT5G58330	0.8891	III	AT5G58330.1	malate dehydrogenase [NA	plastid stroma	8.2.99	TCA / org.transformation.other org
At2g35490	Fibrillin 2 (FBN2)	AT4G03520	0.8890	III	AT4G03520.1	thioredoxin m2	plastid stroma	21.1	redox.thioredoxin
At2g35490	Fibrillin 2 (FBN2)	AT1G54520	0.8840	III	AT1G54520.1	unknown protein (DUF1517	plastid	35.2	not assigned.unknown
At2g35490	Fibrillin 2 (FBN2)	AT2G04700	0.8827	III	AT2G04700.1	ferredoxin-thioredoxin redu	stroma	21.1	redox.thioredoxin
At2g35490	Fibrillin 2 (FBN2)	AT3G15360	0.8780	III	AT3G15360.1	thioredoxin m4	plastid stroma	21.1	redox.thioredoxin
At2g35490	Fibrillin 2 (FBN2)	***AT5G05200***	0.8777	***III***	AT5G05200.1	ABC1 kinase 4 - ABC1K4	plastoglobules	26.56*	misc.ABC1k family
At2g35490	Fibrillin 2 (FBN2)	AT5G27560	0.8733	III	AT5G27560.1	unknown protein	plastid	35.2	not assigned.unknown
At2g35490	Fibrillin 2 (FBN2)	AT5G38660	0.8696	III	AT5G38660.1	APE1- (ACCLIMATION OF	thylakoid	35.2	not assigned.unknown
At2g35490	Fibrillin 2 (FBN2)	AT4G04640	0.8676	III	AT4G04640.1	CF1y - atpC	thylakoid-peripheral-stromal-side	1.1.4	PS.lightreaction.ATP synthase
At2g35490	Fibrillin 2 (FBN2)	AT3G27925	0.8672	III	AT3G27925.1	DegP1 - HhoA homologue	thylakoid-peripheral-lumenal-side	29.5.5	protein.degradation.serine proteas
At2g35490	Fibrillin 2 (FBN2)	AT2G27680	0.8671	III	AT2G27680.1	aldo/keto reductase family	plastid stroma	3.5	minor CHO metabolism.others
At2g35490	Fibrillin 2 (FBN2)	AT3G02730	0.8660	III	AT3G02730.1	thioredoxin f1 (Trx F1)	plastid stroma	21.1	redox.thioredoxin
At2g35490	Fibrillin 2 (FBN2)	AT1G32160	0.8643	III	AT1G32160.1	unknown protein		35.2	not assigned.unknown
At2g35490	Fibrillin 2 (FBN2)	AT1G67840	0.8637	III	AT1G67840.1	chloroplast sensor kinase p	stroma	35.1	not assigned.no ontology
At2g35490	Fibrillin 2 (FBN2)	AT4G14910	0.8634	III	AT4G14910.1	HISTIDINE BIOSYNTHESIS 5B		13.1.7.5	amino acid metabolism.synthesis.h
At3g23400	Fibrillin 4 (FBN4)	AT2G04700	0.8865	III	AT2G04700.1	ferredoxin-thioredoxin redu	stroma	21.1	redox.thioredoxin
At3g23400	Fibrillin 4 (FBN4)	AT3G15360	0.8863	III	AT3G15360.1	thioredoxin m4	plastid stroma	21.1	redox.thioredoxin
At3g23400	Fibrillin 4 (FBN4)	AT3G02730	0.8829	III	AT3G02730.1	thioredoxin f1 (Trx F1)	plastid stroma	21.1	redox.thioredoxin
At3g23400	Fibrillin 4 (FBN4)	AT1G63970	0.8682	III	AT1G63970.1	2C-methyl-D-erythritol 2,4-c	plastid stroma	16.1.1.5	secondary metabolism.isoprenoids
At3g23400	Fibrillin 4 (FBN4)	AT2G30950	0.8681	III	AT2G30950.1	FtsH2 (VAR2 and Pftf)	thylakoid-integral	29.5.7	protein.degradation.metalloproteas
At3g23400	Fibrillin 4 (FBN4)	AT5G37360	0.8665	III	AT5G37360.1	unknown protein	thylakoid	35.2	not assigned.unknown
At3g23400	Fibrillin 4 (FBN4)	AT1G54520	0.8656	III	AT1G54520.1	unknown protein (DUF1517	plastid	35.2	not assigned.unknown
At3g23400	Fibrillin 4 (FBN4)	AT5G38660	0.8648	III	AT5G38660.1	APE1- (ACCLIMATION OF	thylakoid	35.2	not assigned.unknown
At3g23400	Fibrillin 4 (FBN4)	AT5G65840	0.8620	III	AT5G65840.1	putative - alkyl hydroperoxi	plastid stroma	21	redox
At3g23400	Fibrillin 4 (FBN4)	AT1G03680	0.8596	III	AT1G03680.1	thioredoxin m1	thylakoid-peripheral-stromal-side	21.1	redox.thioredoxin
At3g23400	Fibrillin 4 (FBN4)	AT3G55040	0.8578	III	AT3G55040.1	gluthatione Transferase La	plastid stroma	26.9	misc.glutathione S transferases
At3g23400	Fibrillin 4 (FBN4)	AT2G27290	0.8559	III	AT2G27290.1	unknown protein	plastid	35.2	not assigned.unknown
At3g23400	Fibrillin 4 (FBN4)	AT5G66190	0.8548	III	AT5G66190.1	FNR-1	thylakoid-peripheral-stromal-side	1.1.7	PS.lightreaction.ferredoxin reducta
At3g23400	Fibrillin 4 (FBN4)	AT5G03880	0.8543	III	AT5G03880.1	glutaredoxin	thylakoid	21.4	redox.glutaredoxins
At3g23400	Fibrillin 4 (FBN4)	***AT5G05200***	0.8543	***III***	AT5G05200.1	ABC1 kinase 9 - ABC1K9	plastoglobules	26.56*	misc.ABC1k family
At3g23400	Fibrillin 4 (FBN4)	AT5G14970	0.8523	III	AT5G14970.1	unknown protein		35.2	not assigned.unknown
At3g23400	Fibrillin 4 (FBN4)	AT4G22890	0.8517	III	AT4G22890.1	PGRL1A	thylakoid-integral	1.1.40	PS.lightreaction.cyclic electron flov
At3g23400	Fibrillin 4 (FBN4)	AT4G37000	0.8517	III	AT4G37000.1	red chlorophyll catabolite re	plastid stroma	19.50*	tetrapyrrole degradation
At3g23400	Fibrillin 4 (FBN4)	AT4G04640	0.8496	III	AT4G04640.1	CF1y - atpC	thylakoid-peripheral-stromal-side	1.1.4	PS.lightreaction.ATP synthase
At3g23400	Fibrillin 4 (FBN4)	AT5G09660	0.8496	III	AT5G09660.1	malate dehydrogenase, gly	peroxisome	6.3	gluconeogenesis.Malate DH

Supplemental Table 3. (continued)

PG gene	PG Name	Co-Expresser	PCC Value	Module	Co-Expresser	Lab annotation	Curated Loc.	BIN1	BIN NAME1
At3g58010	Fibrillin 7a (FBN7a)	AT5G03880	0.8706	III	AT5G03880.1	glutaredoxin	thylakoid	21.4	redox.glutaredoxins
At3g58010	Fibrillin 7a (FBN7a)	AT2G04700	0.8651	III	AT2G04700.1	ferredoxin-thioredoxin redu	stroma	21.1	redox.thioredoxin
At3g58010	Fibrillin 7a (FBN7a)	AT4G27800	0.8627	III	AT4G27800.1	TAP38, protein phosphatas	thylakoid-peripheral-stromal-side	1.1.30	PS.lightreaction.state transition
At3g58010	Fibrillin 7a (FBN7a)	AT4G25650	0.8596	III	AT4G25650.1	Tic55-related protein (PTC5	plastid	29.3.3	protein.targeting.chloroplast
At3g58010	Fibrillin 7a (FBN7a)	AT3G62410	0.8592	III	AT3G62410.1	CP12 domain-containing pr	plastid stroma	1.3	PS.calvin cyle
At3g58010	Fibrillin 7a (FBN7a)	***AT5G05200***	0.8568	***III***	AT5G05200.1	ABC1 kinase 4 - ABC1K4	plastoglobules	26.56*	misc.ABC1k family
At3g58010	Fibrillin 7a (FBN7a)	AT4G21210	0.8556	III	AT4G21210.1	PPDK kinase/phosphatase	plastid stroma	29.4	protein.postranslational modificatic
At3g58010	Fibrillin 7a (FBN7a)	AT4G13140	0.8523	III	AT4G13140.1	unknown protein		35.2	not assigned.unknown
At3g58010	Fibrillin 7a (FBN7a)	AT4G10000	0.8513	III	AT4G10000.1	Glutathione S-transferase M	plastid	21.4	redox.glutaredoxins
At3g58010	Fibrillin 7a (FBN7a)	AT1G54520	0.8461	III	AT1G54520.1	unknown protein (DUF1517	plastid	35.2	not assigned.unknown
At3g58010	Fibrillin 7a (FBN7a)	AT3G01920	0.8429	III	AT3G01920.1	yrdC family protein	plastid	29.2.7*	protein.synthesis.ribosome biogen
At3g58010	Fibrillin 7a (FBN7a)	AT3G04890	0.8426	III	AT3G04890.1	unknown protein (DUF2358	plastid	35.2	not assigned.unknown
At3g58010	Fibrillin 7a (FBN7a)	AT2G29630	0.8424	III	AT2G29630.1	thiamine biosynthesis (thiC	plastid stroma	18.2	Co-factor and vitamine metabolism
At3g58010	Fibrillin 7a (FBN7a)	AT1G03680	0.8406	III	AT1G03680.1	thioredoxin m1	thylakoid-peripheral-stromal-side	21.1	redox.thioredoxin
At3g58010	Fibrillin 7a (FBN7a)	AT3G55040	0.8391	III	AT3G55040.1	gluthatione Transferase La	plastid stroma	26.9	misc.glutathione S transferases
At3g58010	Fibrillin 7a (FBN7a)	AT2G31040	0.8380	III	AT2G31040.1	unknown protein	likely plastid	35.2	not assigned.unknown
At3g58010	Fibrillin 7a (FBN7a)	AT5G23440	0.8353	III	AT5G23440.1	ferredoxin-thioredoxin redu	plastid stroma	21.1	redox.thioredoxin
At3g58010	Fibrillin 7a (FBN7a)	AT2G41090	0.8347	III	AT2G41090.1	Calcium-binding EF-hand protein		30.3	signalling.calcium
At3g58010	Fibrillin 7a (FBN7a)	AT5G54290	0.8337	III	AT5G54290.1	CcdA - thiol Disulfide transp	thylakoid-integral	29.8	protein assembly and cofactor liga
At3g58010	Fibrillin 7a (FBN7a)	AT3G15840	0.8334	III	AT3G15840.1	PIFI (post-illumination chl f	plastid	1.1.40	PS.lightreaction.cyclic electron flov
At4g13200	Unknown-1	AT3G51510	0.8245	III	AT3G51510.1	unknown protein - C/M	thylakoid	35.2	not assigned.unknown
At4g13200	Unknown-1	AT5G54290	0.8056	III	AT5G54290.1	CcdA - thiol Disulfide transp	thylakoid-integral	29.8	protein assembly and cofactor liga
At4g13200	Unknown-1	AT3G26900	0.8032	III	AT3G26900.1	shikimate kinase SKL1	plastid stroma	13.1.6.1.5	amino acid metabolism.synthesis.a
At4g13200	Unknown-1	AT4G13220	0.7996	III	AT4G13220.1	unknown protein		35.2	not assigned.unknown
At4g13200	Unknown-1	AT2G35410	0.7958	III	AT2G35410.1	putative RNA binding prote	plastid stroma	27.4	RNA.RNA binding
At4g13200	Unknown-1	AT4G08280	0.7931	III	AT4G08280.1	Glutaredoxin-like protein (DUF836)		21.4	redox.glutaredoxins
At4g13200	Unknown-1	AT4G03520	0.7922	III	AT4G03520.1	thioredoxin m2	plastid stroma	21.1	redox.thioredoxin
At4g13200	Unknown-1	AT2G04700	0.7921	III	AT2G04700.1	ferredoxin-thioredoxin redu	stroma	21.1	redox.thioredoxin
At4g13200	Unknown-1	AT1G04640	0.7899	III	AT1G04640.1	lipoyl transferase -lip2 mito	mitochondria	18.11	Co-factor and vitamine metabolism
At4g13200	Unknown-1	AT3G22210	0.7898	III	AT3G22210.1	unknown protein	not plastid	35.2	not assigned.unknown
At4g13200	Unknown-1	AT3G25805	0.7897	III	AT3G25805.1	unknown protein		35.2	not assigned.unknown
At4g13200	Unknown-1	AT4G10300	0.7885	III	AT4G10300.1	unknown protein (domains	plastid	35.2	not assigned.unknown
At4g13200	Unknown-1	AT5G16710	0.7842	III	AT5G16710.1	dehydroascorbate reductas	plastid stroma	21.2.1	redox.ascorbate and glutathione.as
At4g13200	Unknown-1	AT1G32550	0.7825	III	AT1G32550.1	Fd-like-1	plastid	26.30	misc.other Ferredoxins and Rieske
At4g13200	Unknown-1	AT1G03680	0.7809	III	AT1G03680.1	thioredoxin m1	thylakoid-peripheral-stromal-side	21.1	redox.thioredoxin
At4g13200	Unknown-1	AT1G32070	0.7793	III	AT1G32070.1	GCN5-related N-acetyltransferase (GNAT) - maybe plastid		26.24	misc.GCN5-related N-acetyltransfe
At4g13200	Unknown-1	AT1G74880	0.7791	III	AT1G74880.1	NDH O	thylakoid	1.1.6	PS.lightreaction.NADH DH
At4g13200	Unknown-1	AT1G68660	0.7768	III	AT1G68660.1	ClpS (formerly ClpT) - E. co	plastid stroma	29.5.5	protein.degradation.serine proteas
At4g13200	Unknown-1	AT1G12410	0.7759	III	AT1G12410.1	ClpR2	plastid stroma	29.5.5	protein.degradation.serine proteas
At4g13200	Unknown-1	AT1G06510	0.7748	III	AT1G06510.1	unknown protein	likely stroma	35.2	not assigned.unknown

Supplemental Table 3. (continued)

PG gene	PG Name	Co-Expresser	PCC Value	Module	Co-Expresser	Lab annotation	Curated Loc.	BIN1	BIN NAME1
At5g05200	ABC1K9	AT2G31040	0.9161	III	AT2G31040.1	unknown protein	likely plastid	35.2	not assigned.unknown
At5g05200	ABC1K9	AT3G15840	0.9074	III	AT3G15840.1	PIFI (post-illumination chl f	plastid	1.1.40	PS.lightreaction.cyclic electron flov
At5g05200	ABC1K9	AT1G54520	0.8957	III	AT1G54520.1	unknown protein (DUF1517	plastid	35.2	not assigned.unknown
At5g05200	ABC1K9	AT2G30950	0.8820	III	AT2G30950.1	FtsH2 (VAR2 and Pftf)	thylakoid-integral	29.5.7	protein.degradation.metalloproteas
At5g05200	ABC1K9	AT1G06460	0.8799	III	AT1G06460.1	31.2 kDa small heat shock	peroxisome	20.2.1	stress.abiotic.heat
At5g05200	ABC1K9	***AT2G35490***	0.8777	III	AT2G35490.1	fibrillin 2 (FBN2)	plastoglobules	26.31*	misc.fibrillins
At5g05200	ABC1K9	AT2G04700	0.8692	III	AT2G04700.1	ferredoxin-thioredoxin redu	stroma	21.1	redox.thioredoxin
At5g05200	ABC1K9	AT3G18500	0.8683	III	AT3G18500.1	DNAse I-like superprotein		35.1	not assigned.no ontology
At5g05200	ABC1K9	AT4G27800	0.8622	III	AT4G27800.1	TAP38, protein phosphatas	thylakoid-peripheral-stromal-side	1.1.30	PS.lightreaction.state transition
At5g05200	ABC1K9	AT5G14970	0.8585	III	AT5G14970.1	unknown protein		35.2	not assigned.unknown
At5g05200	ABC1K9	***AT3G58010***	0.8568	III	AT3G58010.1	fibrillin 7a (FBN7a)	plastoglobules	26.31*	misc.fibrillins
At5g05200	ABC1K9	AT1G20020	0.8546	III	AT1G20020.1	FNR-2 (interaction with Cyt	thylakoid-peripheral-stromal-side	1.1.7	PS.lightreaction.ferredoxin reducta
At5g05200	ABC1K9	***AT3G23400***	0.8543	III	AT3G23400.1	fibrillin 4 (FBN4)	plastoglobules	26.31*	misc.fibrillins
At5g05200	ABC1K9	AT5G02790	0.8526	III	AT5G02790.1	gluthatione Transferase La	cytosol	26.9	misc.glutathione S transferases
At5g05200	ABC1K9	AT3G25690	0.8520	III	AT3G25690.1	CHUP1 (CHLOROPLAST U	envelope-outer	35.1.41	not assigned.no ontology.hydroxyp
At5g05200	ABC1K9	AT3G55040	0.8520	III	AT3G55040.1	gluthatione Transferase La	plastid stroma	26.9	misc.glutathione S transferases
At5g05200	ABC1K9	AT1G67840	0.8515	III	AT1G67840.1	chloroplast sensor kinase p	stroma	35.1	not assigned.no ontology
At5g05200	ABC1K9	AT5G60600	0.8483	III	AT5G60600.1	4-hydroxy-3-methylbutyl dip	plastid stroma	16.1.1.6	secondary metabolism.isoprenoids
At5g05200	ABC1K9	AT5G03880	0.8473	III	AT5G03880.1	glutaredoxin	thylakoid	21.4	redox.glutaredoxins
At5g05200	ABC1K9	AT1G56500	0.7707	III	AT1G56500.1	haloacid dehalogenase-like	plastid stroma	3.2	minor CHO metabolism.trehalose
At2g42130	Fibrillin 7b (FBN7b)	AT5G30510	0.9229	IV	AT5G30510.1	30S ribosomal protein S1	plastid ribosome	29.2.1.1.3.1.	protein.synthesis.ribosomal proteir
At2g42130	Fibrillin 7b (FBN7b)	AT5G45390	0.9123	IV	AT5G45390.1	ClpP4	plastid stroma	29.5.5	protein.degradation.serine proteas
At2g42130	Fibrillin 7b (FBN7b)	AT2G27680	0.9090	IV	AT2G27680.1	aldo/keto reductase family	plastid stroma	3.5	minor CHO metabolism.others
At2g42130	Fibrillin 7b (FBN7b)	AT2G20890	0.9087	IV	AT2G20890.1	TF1 - thylakoid formation1	plastid	29.3.3	protein.targeting.chloroplast
At2g42130	Fibrillin 7b (FBN7b)	AT5G11450	0.9086	IV	AT5G11450.1	OEC23-like-6 Tat lTP TP21	thylakoid-peripheral-lumenal-side	1.1.1.2	PS.lightreaction.photosystem II.PS
At2g42130	Fibrillin 7b (FBN7b)	AT5G39830	0.9078	IV	AT5G39830.1	DegP8 - HhoA homologue	thylakoid-peripheral-lumenal-side	29.5.5	protein.degradation.serine proteas
At2g42130	Fibrillin 7b (FBN7b)	AT5G50250	0.9054	IV	AT5G50250.1	ribonucleoprotein CP31B	plastid stroma	27.1.5*	RNA.editing
At2g42130	Fibrillin 7b (FBN7b)	AT4G15110	0.9027	IV	AT4G15110.1	beta hydroxylase (CYP97E	plastid	16.1.4	secondary metabolism.isoprenoids
At2g42130	Fibrillin 7b (FBN7b)	AT5G19370	0.9016	IV	AT5G19370.1	rhodanese & rotamase don	plastid	26.23	misc.rhodanese
At2g42130	Fibrillin 7b (FBN7b)	AT3G26060	0.9010	IV	AT3G26060.1	Peroxiredoxin Q (Prx Q) (m	plastid	21.5	redox.periredoxins
At2g42130	Fibrillin 7b (FBN7b)	AT2G21280	0.9005	IV	AT2G21280.1	GC1 (Giant Chloroplast 1)	envelope-inner-peripheral-stromal-side	31.2.5	cell.division.plastid
At2g42130	Fibrillin 7b (FBN7b)	AT1G32550	0.9001	IV	AT1G32550.1	Fd-like-1	plastid	26.30	misc.other Ferredoxins and Rieske
At2g42130	Fibrillin 7b (FBN7b)	AT3G62030	0.8995	IV	AT3G62030.1	peptidylprolyl isomerase R(	plastid stroma	29.6	protein.folding
At2g42130	Fibrillin 7b (FBN7b)	AT1G22700	0.8990	IV	AT1G22700.1	Pyg7 - TPR protein - PSI a	thylakoid-integral	29.8	protein assembly and cofactor liga
At2g42130	Fibrillin 7b (FBN7b)	AT5G05740	0.8987	IV	AT5G05740.1	EGY2, metalloprotease	thylakoid	29.5.7	protein.degradation.metalloproteas
At2g42130	Fibrillin 7b (FBN7b)	AT3G24590	0.8973	IV	AT3G24590.1	Plsp1	thylakoid-peripheral-lumenal-side	29.9*	protein.processing
At2g42130	Fibrillin 7b (FBN7b)	AT2G15290	0.8966	IV	AT2G15290.1	Tic21 (cia5) also named PI	envelope-inner-integral	34.12	transport.metal
At2g42130	Fibrillin 7b (FBN7b)	AT4G24750	0.8965	IV	AT4G24750.1	rhodanese domain protein	plastid	35.2	not assigned.unknown
At2g42130	Fibrillin 7b (FBN7b)	AT5G54600	0.8955	IV	AT5G54600.1	50S ribosomal protein L24	plastid ribosome	29.2.1.1.1.2.	protein.synthesis.ribosomal proteir
At2g42130	Fibrillin 7b (FBN7b)	AT1G64150	0.8919	IV	AT1G64150.1	unknown protein		35.2	not assigned.unknown

Supplemental Table 3. (continued)

PG gene	PG Name	Co-Expresser	PCC Value	Module	Co-Expresser	Lab annotation	Curated Loc.	BIN1	BIN NAME1
At3g43540	Unknown-2	AT1G42970	0.8652	IV	AT1G42970.1	glyceraldehyde-3-phosphat	plastid stroma	1.3.4	PS.calvin cyle.GAP
At3g43540	Unknown-2	AT4G01800	0.8646	IV	AT4G01800.1	cpSecA	plastid stroma	29.3.3	protein.targeting.chloroplast
At3g43540	Unknown-2	AT1G11860	0.8573	IV	AT1G11860.1	aminomethyltransferase-re	not plastid	13.2.5.2	amino acid metabolism.degradatio
At3g43540	Unknown-2	AT3G54050	0.8567	IV	AT3G54050.1	fructose-bisphosphatase (F	plastid stroma	1.3.7	PS.calvin cyle.FBPase
At3g43540	Unknown-2	AT4G39710	0.8565	IV	AT4G39710.1	Isomerase	thylakoid-peripheral-lumenal-side	29.6	protein.folding
At3g43540	Unknown-2	AT3G55800	0.8531	IV	AT3G55800.1	sedoheptulose-bisphospha	plastid stroma	1.3.9	PS.calvin cyle.seduheptulose bisph
At3g43540	Unknown-2	AT1G09340	0.8494	IV	AT1G09340.1	Rap38 or CSP41B	plastid stroma	27	RNA
At3g43540	Unknown-2	AT3G55330	0.8489	IV	AT3G55330.1	OEC23-like-4 Tat ITP TL25	thylakoid-peripheral-lumenal-side	1.1.1.2	PS.lightreaction.photosystem II.PS
At3g43540	Unknown-2	AT1G32060	0.8483	IV	AT1G32060.1	phosphoribulokinase-2 (PR	plastid stroma	1.3.12	PS.calvin cyle.PRK
At3g43540	Unknown-2	AT2G27680	0.8459	IV	AT2G27680.1	aldo/keto reductase family	plastid stroma	3.5	minor CHO metabolism.others
At3g43540	Unknown-2	AT1G45474	0.8453	IV	AT1G45474.1	LHCI-5 - new	thylakoid-integral	1.1.2.1	PS.lightreaction.photosystem I.LH
At3g43540	Unknown-2	AT1G65260	0.8445	IV	AT1G65260.1	Vipp1 - mutant HCF155 - P	envelope	29.3.3	protein.targeting.chloroplast
At3g43540	Unknown-2	AT4G38970	0.8439	IV	AT4G38970.1	fructose-bisphosphate aldo	plastid stroma	1.3.6	PS.calvin cyle.aldolase
At3g43540	Unknown-2	AT5G08650	0.8434	IV	AT5G08650.1	Elongation factor Tu with G	plastid stroma	29.2.4	protein.synthesis.elongation
At3g43540	Unknown-2	***AT2G42130***	0.8412	IV	AT2G42130.4	fibrillin 7b (FBN7b) - model	plastoglobules	26.31*	misc.fibrillins
At3g43540	Unknown-2	AT5G30510	0.8410	IV	AT5G30510.1	30S ribosomal protein S1	plastid ribosome	29.2.1.1.3.1.	protein.synthesis.ribosomal proteir
At3g43540	Unknown-2	AT5G27560	0.8379	IV	AT5G27560.1	unknown protein	plastid	35.2	not assigned.unknown
At3g43540	Unknown-2	AT3G12780	0.8367	IV	AT3G12780.1	phosphoglycerate kinase-1	plastid stroma	1.3.3	PS.calvin cyle.phosphoglycerate ki
At3g43540	Unknown-2	AT2G20890	0.8363	IV	AT2G20890.1	TF1 - thylakoid formation1	plastid	29.3.3	protein.targeting.chloroplast
At3g43540	Unknown-2	AT2G30170	0.8361	IV	AT2G30170.1	phosphatase domain PP2C	plastid	29.4	protein.postranslational modificatic
At1g32220	Flavin-reductase related 1 (FRed-1)	AT5G45820	0.8252		AT5G45820.1	CBL-interacting protein kinase 20		29.4	protein.postranslational modificatic
At1g32220	Flavin-reductase related 1 (FRed-1)	AT5G61410	0.8050		AT5G61410.1	ribulose-5-phosphate-3-epi	plastid stroma	1.3.11	PS.calvin cyle.RPE
At1g32220	Flavin-reductase related 1 (FRed-1)	AT1G44000	0.7988		AT1G44000.1	unknown protein		35.2	not assigned.unknown
At1g32220	Flavin-reductase related 1 (FRed-1)	AT4G27600	0.7974		AT4G27600.1	pfkB-like carbohydrate kinase protein		3.5	minor CHO metabolism.others
At1g32220	Flavin-reductase related 1 (FRed-1)	AT1G26180	0.7871		AT1G26180.1	unknown protein		35.2	not assigned.unknown
At1g32220	Flavin-reductase related 1 (FRed-1)	AT4G19830	0.7856		AT4G19830.1	Isomerase		29.6	protein.folding
At1g32220	Flavin-reductase related 1 (FRed-1)	***AT1G78140***	0.7815		AT1G78140.1	UbiE methyltransferase rel	plastoglobules	35.1	not assigned.no ontology
At1g32220	Flavin-reductase related 1 (FRed-1)	AT2G20860	0.7715		AT2G20860.1	lipoyl synthase -lip1 mitoch	mitochondria	18.11	Co-factor and vitamine metabolism
At1g32220	Flavin-reductase related 1 (FRed-1)	AT3G06483	0.7644		AT3G06483.1	pyruvate dehydrogenase (li	mitochondria	18	Co-factor and vitamine metabolism
At1g32220	Flavin-reductase related 1 (FRed-1)	AT5G59610	0.7630		AT5G59610.1	DnaJ-domain protein	likely plastid	26.29*	misc.DnaJ domain with unknown f
At1g32220	Flavin-reductase related 1 (FRed-1)	AT1G43670	0.7628		AT1G43670.1	D-fructose-1,6-bisphosphal	not plastid	2.1.1.3	major CHO metabolism.synthesis.s
At1g32220	Flavin-reductase related 1 (FRed-1)	AT4G09620	0.7509		AT4G09620.1	mTERF domain protein	plastid	27.3.99	RNA.regulation of transcription.unc
At1g32220	Flavin-reductase related 1 (FRed-1)	AT1G76110	0.7480		AT1G76110.1	HMG (high mobility group) box protein with ARID/BRIGHT DNA-b		27.3.62	RNA.regulation of transcription.Nu
At1g32220	Flavin-reductase related 1 (FRed-1)	AT5G12130	0.7472		AT5G12130.1	TerC - PDE149 (PIGMENT	thylakoid-integral	29.3.3	protein.targeting.chloroplast
At1g32220	Flavin-reductase related 1 (FRed-1)	AT2G25870	0.7431		AT2G25870.1	haloacid dehalogenase-like	plastid	3.2	minor CHO metabolism.trehalose
At1g32220	Flavin-reductase related 1 (FRed-1)	AT5G01410	0.7387		AT5G01410.1	PDX1.3 (Vitamine b6 synth	cytosol	18.20*	Co-factor and vitamine metabolism
At1g32220	Flavin-reductase related 1 (FRed-1)	AT5G63040	0.7363		AT5G63040.1	unknown protein (likely plastid)		35.2	not assigned.unknown
At1g32220	Flavin-reductase related 1 (FRed-1)	AT2G33255	0.7339		AT2G33255.1	haloacid dehalogenase-like hydrolase		3.2	minor CHO metabolism.trehalose
At1g32220	Flavin-reductase related 1 (FRed-1)	AT5G02180	0.7326		AT5G02180.1	Transmembrane amino acid transporter		34.3	transport.amino acids
At1g32220	Flavin-reductase related 1 (FRed-1)	AT1G62960	0.7316		AT1G62960.1	ACC synthase 10		17.5.1.1	hormone metabolism.ethylene.syn

Supplemental Table 3. (continued)

PG gene	PG Name	Co-Expresser	PCC Value	Module	Co-Expresser	Lab annotation	Curated Loc.	BIN1	BIN NAME1
At1g71810	ABC1K5	AT1G56500	0.8645		AT1G56500.1	haloacid dehalogenase-like	plastid stroma	3.2	minor CHO metabolism.trehalose
At1g71810	ABC1K5	AT4G29590	0.8574		AT4G29590.1	methyltransferase domain p	plastid	29.4	protein.postranslational modificatic
At1g71810	ABC1K5	AT1G32080	0.8544		AT1G32080.1	envelope protein (MEP1)	envelope-inner-integral	34.8	transport.metabolite transporters a
At1g71810	ABC1K5	AT1G54350	0.8519		AT1G54350.1	ABC transporter family prot	plastid	34.8	transport.metabolite transporters a
At1g71810	ABC1K5	AT5G58260	0.8504		AT5G58260.1	NDH N	thylakoid	1.1.6	PS.lightreaction.NADH DH
At1g71810	ABC1K5	AT1G26230	0.8443		AT1G26230.1	Cpn60-beta-4	plastid	29.6	protein.folding
At1g71810	ABC1K5	AT1G01790	0.8443		AT1G01790.1	K+ efflux antiporter, putitive	envelope-inner-integral	34.8	transport.metabolite transporters a
At1g71810	ABC1K5	AT1G55480	0.8427		AT1G55480.1	unknown protein	thylakoid-peripheral-stromal-side	35.2	not assigned.unknown
At1g71810	ABC1K5	AT2G30390	0.8404		AT2G30390.1	ferrochelatase II	plastid	19.20	tetrapyrrole synthesis.ferrochelatas
At1g71810	ABC1K5	AT3G48420	0.8375		AT3G48420.1	haloacid dehalogenase-like	plastid stroma	3.2	minor CHO metabolism.trehalose
At1g71810	ABC1K5	AT2G32500	0.8370		AT2G32500.1	unknown protein (Dabb dor		35.2	not assigned.unknown
At1g71810	ABC1K5	AT1G64770	0.8349		AT1G64770.1	NDF2- associates with the	thylakoid	1.1.6	PS.lightreaction.NADH DH
At1g71810	ABC1K5	AT1G31190	0.8332		AT1G31190.1	Inositol monophophatase-1	plastid stroma	3.4.5	minor CHO metabolism.myo-inosit
At1g71810	ABC1K5	AT1G15980	0.8330		AT1G15980.1	NDF1- associates with NDH	thylakoid	1.1.6	PS.lightreaction.NADH DH
At1g71810	ABC1K5	AT4G17360	0.8323		AT4G17360.1	Formyl transferase		18.5	Co-factor and vitamine metabolism
At1g71810	ABC1K5	AT4G33010	0.8309		AT4G33010.1	glycine decarboxylase/glyci	mitochondria	13.2.5.2	amino acid metabolism.degradatio
At1g71810	ABC1K5	AT3G55040	0.8281		AT3G55040.1	gluthatione Transferase La	plastid stroma	26.9	misc.glutathione S transferases
At1g71810	ABC1K5	AT4G12830	0.8239		AT4G12830.1	hydrolase, alpha/beta fold p	plastid	35.1	not assigned.no ontology
At1g71810	ABC1K5	AT3G63140	0.8238		AT3G63140.1	Rap41 or CSP41A	plastid stroma	27.3.99	RNA.regulation of transcription.unc
At1g71810	ABC1K5	AT5G62840	0.8234		AT5G62840.1	phosphoglycerate/bisphosphoglycerate mutase (PGAM)		4.11	glycolysis.phosphoglycerate mutas
At1g78140	UbiE methyltransferase related 1 (UbiE-1)	AT1G75770	0.9082		AT1G75770.1	unknown protein		35.2	not assigned.unknown
At1g78140	UbiE methyltransferase related 1 (UbiE-1)	AT3G06483	0.8881		AT3G06483.1	pyruvate dehydrogenase (li	mitochondria	18	Co-factor and vitamine metabolism
At1g78140	UbiE methyltransferase related 1 (UbiE-1)	AT5G02180	0.8778		AT5G02180.1	Transmembrane amino acid transporter		34.3	transport.amino acids
At1g78140	UbiE methyltransferase related 1 (UbiE-1)	AT3G11900	0.8778		AT3G11900.1	aromatic and neutral transporter 1		34.3	transport.amino acids
At1g78140	UbiE methyltransferase related 1 (UbiE-1)	AT3G45810	0.8535		AT3G45810.1	ferric reductase-like transmembrane protein		20.1.1	stress.biotic.respiratory burst
At1g78140	UbiE methyltransferase related 1 (UbiE-1)	AT5G40670	0.8472		AT5G40670.1	PQ-loop repeat transmembrane protein		35.1	not assigned.no ontology
At1g78140	UbiE methyltransferase related 1 (UbiE-1)	AT1G44120	0.8462		AT1G44120.1	Armadillo/beta-catenin-like repeat ; C2 calcium/lipid-binding doma		35.1.3	not assigned.no ontology.armadillo
At1g78140	UbiE methyltransferase related 1 (UbiE-1)	AT4G12430	0.8444		AT4G12430.1	trehalose-6-phosphate pho		3.2.2	minor CHO metabolism.trehalose.T
At1g78140	UbiE methyltransferase related 1 (UbiE-1)	AT5G54150	0.8442		AT5G54150.1	unknown protein		35.2	not assigned.unknown
At1g78140	UbiE methyltransferase related 1 (UbiE-1)	AT1G19890	0.8414		AT1G19890.1	male-gamete-specific histone H3		28.1.3	DNA.synthesis/chromatin structure
At1g78140	UbiE methyltransferase related 1 (UbiE-1)	AT1G04600	0.8403		AT1G04600.1	myosin XI A		31.1	cell.organisation
At1g78140	UbiE methyltransferase related 1 (UbiE-1)	AT4G09620	0.8390		AT4G09620.1	mTERF domain protein	plastid	27.3.99	RNA.regulation of transcription.unc
At1g78140	UbiE methyltransferase related 1 (UbiE-1)	AT5G57320	0.8385		AT5G57320.1	gelsonin repeat protein		31.1	cell.organisation
At1g78140	UbiE methyltransferase related 1 (UbiE-1)	AT5G03690	0.8372		AT5G03690.1	fructose-bisphosphate aldolase (FBPA) (not plastid)		4.7	glycolysis.aldolase
At1g78140	UbiE methyltransferase related 1 (UbiE-1)	AT5G60740	0.8372		AT5G60740.1	ABC transporter protein		34.16	transport.ABC transporters and mu
At1g78140	UbiE methyltransferase related 1 (UbiE-1)	AT5G17780	0.8365		AT5G17780.1	alpha/beta-Hydrolases superprotein		35.1	not assigned.no ontology
At1g78140	UbiE methyltransferase related 1 (UbiE-1)	AT4G17483	0.8358		AT4G17483.1	alpha/beta-Hydrolases superprotein		29.4	protein.postranslational modificatic
At1g78140	UbiE methyltransferase related 1 (UbiE-1)	AT4G33440	0.8354		AT4G33440.1	Pectin lyase-like superprotein		10.6.3	cell wall.degradation.pectate lyase
At1g78140	UbiE methyltransferase related 1 (UbiE-1)	AT1G50990	0.8351		AT1G50990.1	Protein kinase protein		29.4	protein.postranslational modificatic
At1g78140	UbiE methyltransferase related 1 (UbiE-1)	AT4G34940	0.8339		AT4G34940.1	armadillo repeat only 1		35.1.3	not assigned.no ontology.armadillo

Supplemental Table 3. (continued)

PG gene	PG Name	Co-Expresser	PCC Value	Module	Co-Expresser	Lab annotation	Curated Loc.	BIN1	BIN NAME1
At2g46910	Fibrillin 8 (FBN8)	AT1G76450	0.9081		AT1G76450.1	OEC23-like-2 Tat ITP	thylakoid-peripheral-lumenal-side	1.1.1.2	PS.lightreaction.photosystem II.PS
At2g46910	Fibrillin 8 (FBN8)	AT1G67700	0.9062		AT1G67700.1	unknown protein	plastid	35.2	not assigned.unknown
At2g46910	Fibrillin 8 (FBN8)	AT5G07020	0.9006		AT5G07020.1	proline-rich protein family	thylakoid	35.1.42	not assigned.no ontology.proline ri
At2g46910	Fibrillin 8 (FBN8)	AT5G51110	0.8931		AT5G51110.1	unknown protein	plastid stroma	35.2	not assigned.unknown
At2g46910	Fibrillin 8 (FBN8)	AT1G75690	0.8902		AT1G75690.1	sco2 - snowy cotyledon 2	plastid	26.29*	misc.DnaJ domain with unknown fu
At2g46910	Fibrillin 8 (FBN8)	AT5G47840	0.8886		AT5G47840.1	adenylate kinase or ATP-A	plastid stroma	23.4.1	nucleotide metabolism.phosphotra
At2g46910	Fibrillin 8 (FBN8)	AT3G56650	0.8879		AT3G56650.1	OEC23-like-1	thylakoid-peripheral-lumenal-side	1.1.1.2	PS.lightreaction.photosystem II.PS
At2g46910	Fibrillin 8 (FBN8)	AT4G32590	0.8875		AT4G32590.1	NDH-F4-related - 2Fe-2S ferredoxin-domain protein		1.1.6	PS.lightreaction.NADH DH
At2g46910	Fibrillin 8 (FBN8)	AT2G21960	0.8843		AT2G21960.1	unknown protein	plastid	35.2	not assigned.unknown
At2g46910	Fibrillin 8 (FBN8)	AT2G30170	0.8821		AT2G30170.1	phosphatase domain PP2C	plastid	29.4	protein.postranslational modificatic
At2g46910	Fibrillin 8 (FBN8)	AT5G43750	0.8816		AT5G43750.1	unknown protein	thylakoid	35.2	not assigned.unknown
At2g46910	Fibrillin 8 (FBN8)	AT2G34860	0.8813		AT2G34860.1	DnaJ central domain (4 rep	plastid	26.29*	misc.DnaJ domain with unknown fu
At2g46910	Fibrillin 8 (FBN8)	AT5G38520	0.8813		AT5G38520.1	hydrolase	thylakoid	35.1	not assigned.no ontology
At2g46910	Fibrillin 8 (FBN8)	AT5G23120	0.8783		AT5G23120.1	HCF136 Tat ltp	thylakoid-peripheral-lumenal-side	29.8	protein assembly and cofactor liga
At2g46910	Fibrillin 8 (FBN8)	AT5G08050	0.8782		AT5G08050.1	unknown protein	thylakoid	35.2	not assigned.unknown
At2g46910	Fibrillin 8 (FBN8)	AT3G48420	0.8766		AT3G48420.1	haloacid dehalogenase-like	plastid stroma	3.2	minor CHO metabolism.trehalose
At2g46910	Fibrillin 8 (FBN8)	AT5G27560	0.8760		AT5G27560.1	unknown protein	plastid	35.2	not assigned.unknown
At2g46910	Fibrillin 8 (FBN8)	AT4G34090	0.8759		AT4G34090.1	unknown protein	plastid stroma	35.2	not assigned.unknown
At2g46910	Fibrillin 8 (FBN8)	AT5G45680	0.8754		AT5G45680.1	AtFKBP13 - ITP-TAT (invol	thylakoid-peripheral-lumenal-side	29.8	protein assembly and cofactor liga
At2g46910	Fibrillin 8 (FBN8)	AT1G05385	0.8739		AT1G05385.1	Psb27 homologue LPA19	thylakoid-peripheral-lumenal-side	29.8	protein assembly and cofactor liga
At4g32770	VTE1	AT1G01250	0.8223		AT1G01250.1	Integrase-type DNA-binding protein		27.3.3	RNA.regulation of transcription.AP
At4g32770	VTE1	AT4G26700	0.8100		AT4G26700.1	ATFIM1 (Arabidopsis thaliana fimbrin 1); actin binding		31.1	cell.organisation
At4g32770	VTE1	AT5G20940	0.7841		AT5G20940.1	Glycosyl hydrolase protein		26.3	misc.gluco-, galacto- and mannosi
At4g32770	VTE1	AT4G36700	0.7714		AT4G36700.1	RmlC-like cupins superprotein		35.1	not assigned.no ontology
At4g32770	VTE1	AT3G63040	0.7665		AT3G63040.1	unknown protein		35.2	not assigned.unknown
At4g32770	VTE1	AT5G62800	0.7661		AT5G62800.1	Protein with RING/U-box and TRAF-like domains		33.99	development.unspecified
At4g32770	VTE1	AT1G68380	0.7647		AT1G68380.1	Core-2/I-branching beta-1,6-N-acetylglucosaminyltransferase pro		35.2	not assigned.unknown
At4g32770	VTE1	AT1G70580	0.7621		AT1G70580.1	alanine aminotransferase-2	peroxisome	1.2.3	PS.aminotransferases peroxisoma
At4g32770	VTE1	AT3G03240	0.7613		AT3G03240.1	alpha/beta-Hydrolases superprotein		35.1	not assigned.no ontology
At4g32770	VTE1	AT3G62730	0.7560		AT3G62730.1	unknown protein		20.2.3	stress.abiotic.drought/salt
At4g32770	VTE1	AT1G62290	0.7559		AT1G62290.1	aspartyl protease family protein		29.5.4	protein.degradation.aspartate prot
At4g32770	VTE1	AT5G50770	0.7551		AT5G50770.1	hydroxysteroid dehydrogenase 6		26.22	misc.short chain dehydrogenase/re
At4g32770	VTE1	AT1G67100	0.7544		AT1G67100.1	LOB domain-containing protein 40		27.3.37	RNA.regulation of transcription.AS
At4g32770	VTE1	AT3G26790	0.7537		AT3G26790.1	AP2/B3-like transcriptional factor		27.3.1	RNA.regulation of transcription.AB
At4g32770	VTE1	AT4G21860	0.7503		AT4G21860.1	methionine sulfoxide reduct	plastid stroma	29.11*	protein.methione sulfoxide reducta
At4g32770	VTE1	AT1G47540	0.7503		AT1G47540.1	Scorpion toxin-like knottin protein		20.1.7.6	stress.biotic.PR-proteins.proteinas
At4g32770	VTE1	AT1G11170	0.7493		AT1G11170.1	unknown protein		35.2	not assigned.unknown
At4g32770	VTE1	AT1G08810	0.7486		AT1G08810.1	myb domain protein 60		27.3.25	RNA.regulation of transcription.MY
At4g32770	VTE1	AT5G07190	0.7463		AT5G07190.1	seed gene 3		33.99	development.unspecified
At4g32770	VTE1	AT4G27150	0.7461		AT4G27150.1	seed storage albumin 2		33.1	development.storage proteins

Supplemental Table 3. (continued)

PG gene	PG Name	Co-Expresser	PCC Value	Module	Co-Expresser	Lab annotation	Curated Loc.	BIN1	BIN NAME1
At4g39730	PLAT domain protein	AT3G09540	0.6665		AT3G09540.1	Pectin lyase-like superprotein		10.6.3	cell wall.degradation.pectate lyase
At4g39730	PLAT domain protein	AT4G27520	0.6336		AT4G27520.1	plastocyanin-like domain-c	not plastid	26.19	misc.plastocyanin-like
At4g39730	PLAT domain protein	AT2G35960	0.6283		AT2G35960.1	NDR1/HIN1-like 12		35.1	not assigned.no ontology
At4g39730	PLAT domain protein	AT2G15970	0.6266		AT2G15970.1	COR413-PM1 (cold regulated 413 plasma membrane 1)		20.2.2	stress.abiotic.cold
At4g39730	PLAT domain protein	AT1G18360	0.6256		AT1G18360.1	alpha/beta-Hydrolases superprotein		35.1	not assigned.no ontology
At4g39730	PLAT domain protein	AT2G42530	0.6241		AT2G42530.1	cold-regulated protein (cor	plastid stroma	20.2.2	stress.abiotic.cold
At4g39730	PLAT domain protein	AT5G01790	0.6198		AT5G01790.1	unknown protein		35.2	not assigned.unknown
At4g39730	PLAT domain protein	AT1G13930	0.6091		AT1G13930.1	abundant unknown protein - weak similarity to 60S ribosomal su		20.2.3	stress.abiotic.drought/salt
At4g39730	PLAT domain protein	AT5G59130	0.6038		AT5G59130.1	Subtilase protein		29.5.1	protein.degradation.subtilases
At4g39730	PLAT domain protein	AT5G64770	0.6022		AT5G64770.1	root meristem growth factor (RGF)		35.2	not assigned.unknown
At4g39730	PLAT domain protein	AT4G37470	0.5949		AT4G37470.1	hydrolase, alpha/beta fold protein		35.1	not assigned.no ontology
At4g39730	PLAT domain protein	AT2G42540	0.5872		AT2G42540.1	cold-regulated protein (cor	plastid stroma	20.2.2	stress.abiotic.cold
At4g39730	PLAT domain protein	AT3G44450	0.5846		AT3G44450.1	unknown protein		35.2	not assigned.unknown
At4g39730	PLAT domain protein	AT4G18390	0.5844		AT4G18390.1	TEOSINTE BRANCHED 1, cycloidea and PCF transcription factor		27.3.29	RNA.regulation of transcription.TC
At4g39730	PLAT domain protein	AT2G28900	0.5823		AT2G28900.1	Amino acid transported (Of	envelope-outer	34.8	transport.metabolite transporters a
At4g39730	PLAT domain protein	AT4G27820	0.5740		AT4G27820.1	glycosyl hydrolase 1 (likely peroxisome)		26.3	misc.gluco-, galacto- and mannosi
At4g39730	PLAT domain protein	AT5G19250	0.5724		AT5G19250.1	Glycoprotein membrane precursor GPI-anchored		35.2	not assigned.unknown
At4g39730	PLAT domain protein	AT3G46970	0.5702		AT3G46970.1	starch phosphorylase-2 (At	not plastid	2.2.2.2	major CHO metabolism.degradatic
At4g39730	PLAT domain protein	AT5G65990	0.5694		AT5G65990.1	Transmembrane amino acid transporter protein		34.3	transport.amino acids
At4g39730	PLAT domain protein	AT5G52320	0.5595		AT5G52320.1	cytochrome P450		26.1	misc.cytochrome P450

Supplemental Table 4. Functional group enrichment of plastoglobule co-expressers using different co-expression software programs

Functional group	Bin size (a)	whole network (b)	MetaOm Graph (b)	BAR (b)	ACT (b)
Protein degradation	1355	0.1	0.1	0.1	0.0
Protein degradation - plastid	*42*	**3.3**	**2.9**	**2.7**	**1.0**
Protein degradation - not plastid	*1313*	0.0	0.0	0.0	0.0
PG	25	**3.4**	**2.7**	**3.0**	**0.6**
Light reaction	139	0.8	0.9	0.7	0.2
light stress-Lil/Sep/Ohp	*8*	0.5	0.0	0.5	0.0
NDH dependent & independent, Immutans, PIFI	*29*	**1.5**	**1.8**	**1.1**	**0.4**
PSI, PSII, ATPsynt, cytb6f, FNR, electron carriers (PC, Fd)	*94*	0.5	0.6	0.4	0.0
thylakoid-bound regulators, including kinases and phosphatases	*5*	**3.2**	**4.0**	**4.0**	**3.2**
Isoprenoid metabolism	124	0.7	0.6	0.4	0.3
Isoprenoid metabolism - plastid	*59*	**1.1**	**0.9**	**0.5**	**0.4**
Isoprenoid metabolism - not plastid	*65*	0.3	0.4	0.2	0.1
Redox	187	0.7	0.6	0.7	0.2
CHO metabolism (c)	441	0.3	0.3	0.3	0.1
Stress	690	0.1	0.1	0.1	0.0
Other (d)	1274	0.1	0.1	0.1	0.0
Protein - other	1535	0.1	0.1	0.1	0.0
Protein - other - plastid	*211*	0.7	0.7	0.7	0.2
Protein - other - not plastid	*1326*	0.0	0.0	0.0	0.0
Not assigned	7707	0.1	0.1	0.1	0.0
Development	521	0.1	0.0	0.0	0.0
Tetrapyrrole metabolism	50	0.5	0.4	0.5	0.2
Transport	944	0.1	0.1	0.1	0.0
Signalling	1048	0.0	0.0	0.0	0.0
Lipid metabolism	331	0.0	0.0	0.0	0.0
DNA/RNA	2659	0.0	0.0	0.0	0.0

(a) number of genes (represented by a single probe spot on the 22K Affymetrix microarray chip) in each bin

(b) Number of edges per bin, normalized by bin size, and normalized for number of PG cores gene per module. Values in bold are enriched functions

(c) includes major and minor carbohydrate metabolism, gluconeogenesis, glycolysis, TCA cycle, C1 metabolism, fermentation, oxidative pentose phosphate pathway, Calvin cycle, and all other dark reactions

(d) includes cofactor and vitamin metabolism, metal handling, xenobiotics, amino acid metabolism, nucleotide metabolism, cytoskeleton, mitochondrial electron transport, cell wall, cell, cell division, cell cycle, nitrogen metabolism, photorespiration, polyamine metabolism, sulfur assimilation, secondary metabolism (excluding isoprenoids/tetrapyrrole), and hormone metabolism

(e) all connections present in all three software programs

2.6 LITERATURE CITED

1. Brehelin, C., F. Kessler, and K.J. van Wijk, *Plastoglobules: versatile lipoprotein particles in plastids.* Trends Plant Sci, 2007. **12**(6): p. 260-6.

2. Singh, D.K. and T.W. McNellis, *Fibrillin protein function: the tip of the iceberg?* Trends in Plant Science, 2011. **16**(8): p. 432-41.

3. Brehelin, C. and F. Kessler, *The Plastoglobule: A Bag Full of Lipid Biochemistry Tricks.* Photochemistry and Photobiology, 2008. **84**(6): p. 1388-1394.

4. Vidi, P.A., et al., *Tocopherol cyclase (VTE1) localization and vitamin E accumulation in chloroplast plastoglobule lipoprotein particles.* J Biol Chem, 2006. **281**(16): p. 11225-34.

5. Zbierzak, A.M., et al., *Intersection of the tocopherol and plastoquinol metabolic pathways at the plastoglobule.* Biochemical Journal, 2009. **425**(2): p. 389-399.

6. Gaude, N., et al., *Nitrogen deficiency in Arabidopsis affects galactolipid composition and gene expression and results in accumulation of fatty acid phytyl esters.* Plant J, 2007. **49**(4): p. 729-39.

7. Lohmann, A., et al., *Deficiency in phylloquinone (vitamin K(1)) methylation affects prenyl quinone distribution, photosystem I abundance, and anthocyanin accumulation in the Arabidopsis AtmenG mutant.* J Biol Chem, 2006. **281**(52): p. 40461-72.

8. Ytterberg, A.J., J.B. Peltier, and K.J. van Wijk, *Protein profiling of plastoglobules in chloroplasts and chromoplasts; a surprising site for differential accumulation of metabolic enzymes.* Plant Physiol, 2006. **140**(3): p. 984-997.

9. Poon, W.W., et al., *Identification of Escherichia coli ubiB, a gene required for the first monooxygenase step in ubiquinone biosynthesis.* J Bacteriol, 2000. **182**(18): p. 5139-46.

10. Xie, L.X., et al., *Expression of the human atypical kinase ADCK3 rescues coenzyme Q biosynthesis and phosphorylation of Coq polypeptides in yeast coq8 mutants.* Biochimica et Biophysica Acta (BBA) - Molecular and Cell Biology of Lipids, 2011. **1811**(5): p. 348-360.

11. Tauche, A., U. Krause-Buchholz, and G. Rodel, *Ubiquinone biosynthesis in Saccharomyces cerevisiae: the molecular organization of O-methylase Coq3p depends on Abc1p/Coq8p.* FEMS Yeast Research, 2008. **8**(8): p. 1263-1275.

12. Simkin, A.J., et al., *Fibrillin influence on plastid ultrastructure and pigment content in tomato fruit.* Phytochemistry, 2007. **68**(11): p. 1545-56.

13. Zhang, R., et al., *Moderate heat stress of Arabidopsis thaliana leaves causes chloroplast swelling and plastoglobule formation.* Photosynthesis Research, 2010. **105**(2): p. 123-134.

14. Singh, D.K., et al., *FIBRILLIN 4 is required for plastoglobule development and stress resistance in apple and Arabidopsis.* Plant Physiol., 2010. **154**(3): p. 1281-1293.

15. Austin, J.R., 2nd, et al., *Plastoglobules are lipoprotein subcompartments of the chloroplast that are permanently coupled to thylakoid membranes and contain biosynthetic enzymes.* Plant Cell, 2006. **18**(7): p. 1693-703.

16. Takabayashi, A., et al., *Three novel subunits of Arabidopsis chloroplastic NAD(P)H dehydrogenase identified by bioinformatic and reverse genetic approaches.* The Plant Journal, 2009. **57**(2): p. 207-219.

17. Dalcorso, G., et al., *A Complex Containing PGRL1 and PGR5 Is Involved in the Switch between Linear and Cyclic Electron Flow in Arabidopsis.* Cell, 2008. **132**(2): p. 273-85.

18. Biehl, A., et al., *Analysis of 101 nuclear transcriptomes reveals 23 distinct regulons and their relationship to metabolism, chromosomal gene distribution and co-ordination of nuclear and plastid gene expression.* Gene, 2005. **344**: p. 33-41.

19. Lin, W.-D., et al., *Coexpression-Based Clustering of Arabidopsis Root Genes Predicts Functional Modules in Early Phosphate Deficiency Signaling.* Plant Physiology, 2011. **155**(3): p. 1383-1402.

20. Vanderauwera, S., et al., *Genome-Wide Analysis of Hydrogen Peroxide-Regulated Gene Expression in Arabidopsis Reveals a High Light-Induced Transcriptional Cluster Involved in Anthocyanin Biosynthesis.* Plant Physiol, 2005. **139**(2): p. 806-821.

21. Rohde, A., et al., *Molecular Phenotyping of the pal1 and pal2 Mutants of Arabidopsis thaliana Reveals Far-Reaching Consequences on Phenylpropanoid, Amino Acid, and Carbohydrate Metabolism.* The Plant Cell, 2004. **16**(10): p. 2749-2771.

22. Cartieaux, F., et al., *Transcriptome analysis of Arabidopsis colonized by a plant-growth promoting rhizobacterium reveals a general effect on disease resistance.* The Plant Journal, 2003. **36**(2): p. 177-188.

23. Bischoff, V., et al., *TRICHOME BIREFRINGENCE and Its Homolog AT5G01360 Encode Plant-Specific DUF231 Proteins Required for Cellulose Biosynthesis in Arabidopsis.* Plant Physiology, 2010. **153**(2): p. 590-602.

24. Ozaki, S., et al., *Coexpression Analysis of Tomato Genes and Experimental Verification of Coordinated Expression of Genes Found in a Functionally Enriched Coexpression Module.* DNA Research, 2010. **17**(2): p. 105-116.

25. Fu, F.-F. and H.-W. Xue, *Coexpression Analysis Identifies Rice Starch Regulator1, a Rice AP2/EREBP Family Transcription Factor, as a Novel Rice Starch Biosynthesis Regulator.* Plant Physiology, 2010. **154**(2): p. 927-938.

26. Sawada, Y., et al., *Arabidopsis Bile Acid:Sodium Symporter Family Protein 5 is Involved in Methionine-Derived Glucosinolate Biosynthesis.* Plant and Cell Physiology, 2009. **50**(9): p. 1579-1586.

27. Rey, P., et al., *Over-expression of a pepper plastid lipid-associated protein in tobacco leads to changes in plastid ultrastructure and plant development upon stress.* The Plant Journal, 2000. **21**(5): p. 483-494.

28. Bantscheff, M., et al., *Quantitative mass spectrometry in proteomics: a critical review.* Anal Bioanal Chem, 2007. **389**(4): p. 1017-31.

29. Mann, M. and N.L. Kelleher, *Special Feature: Precision proteomics: The case for high resolution and high mass accuracy.* Proc Natl Acad Sci U S A, 2008. **105**: p. 18132-18138.

30. Domon, B. and R. Aebersold, *Options and considerations when selecting a quantitative proteomics strategy.* Nat Biotechnol, 2010. **28**(7): p. 710-21.

31. Liu, H., R.G. Sadygov, and J.R. Yates, 3rd, *A model for random sampling and estimation of relative protein abundance in shotgun proteomics.* Anal Chem, 2004. **76**(14): p. 4193-201.

32. Old, W.M., et al., *Comparison of label-free methods for quantifying human proteins by shotgun proteomics.* Mol Cell Proteomics, 2005. **4**(10): p. 1487-502.

33. Zybailov, B., et al., *Correlation of relative abundance ratios derived from peptide ion chromatograms and spectrum counting for quantitative proteomic analysis using stable isotope labeling.* Anal Chem, 2005. **77**(19): p. 6218-24.

34. Sandhu, C., et al., *Evaluation of data-dependent versus targeted shotgun proteomic approaches for monitoring transcription factor expression in breast cancer.* J Proteome Res, 2008. **7**(4): p. 1529-41.

35. Zybailov, B., et al., *Sorting signals, N-terminal modifications and abundance of the chloroplast proteome.* PLoS ONE, 2008. **3**(4): p. e1994.

36. Friso, G., et al., *Reconstruction of metabolic pathways, protein expression, and homeostasis machineries across maize bundle sheath and mesophyll chloroplasts: large-scale quantitative proteomics using the first maize genome assembly.* Plant Physiol, 2010. **152**(3): p. 1219-50.

37. Majeran, M., et al., *Structural and metabolic transitions of C4 leaf development and differentiation defined by microscopy and quantitative proteomics.* The Plant Cell, 2010. **22**(11): p. 3509-42.

38. Olinares, P.D., J. Kim, and K.J. van Wijk, *The Clp protease system; a central component of the chloroplast protease network.* Biochim Biophys Acta, 2011. **1807**(8): p. 999-1011.

39. Hu, Q., et al., *The Orbitrap: a new mass spectrometer.* J Mass Spectrom, 2005. **40**(4): p. 430-43.

40. Zybailov, B., et al., *Large scale comparative proteomics of a chloroplast Clp protease mutant reveals folding stress, altered protein homeostasis, and feedback regulation of metabolism.* Mol Cell Proteomics, 2009. **8**(8): p. 1789-1810.

41. Aubert, Y., et al., *RD20, a stress-inducible caleosin, participates in stomatal control, transpiration and drought tolerance in Arabidopsis thaliana.* Plant and Cell Physiology, 2010. **51**(12): p. 1975-1987.

42. Do, T.Q., et al., *A Defect in Coenzyme Q Biosynthesis Is Responsible for the Respiratory Deficiency in Saccharomyces cerevisiae abc1 Mutants.* J. Biol. Chem., 2001. **276**(21): p. 18161-18168.

43. Huang, F.-C., P. Molnar, and W. Schwab, *Cloning and functional characterization of carotenoid cleavage dioxygenase 4 genes.* J. Exp. Bot., 2009. **60**(11): p. 3011-3022.

44. Porfirova, S., et al., *Isolation of an Arabidopsis mutant lacking vitamin E and identification of a cyclase essential for all tocopherol biosynthesis.* Proc Natl Acad Sci U S A, 2002. **99**(19): p. 12495-500.

45. Eugeni-Piller, L., et al., *Chloroplast lipid droplet type II NAD(P)H quinone oxidoreductase is essential for prenylquinone metabolism and vitamin K1 accumulation.* Proc Natl Acad Sci U S A, 2011. **108**(34): p. 14354-9.

46. Vidi, P.A., F. Kessler, and C. Brehelin, *Plastoglobules: a new address for targeting recombinant proteins in the chloroplast.* BMC Biotechnol, 2007. **7**: p. 4.

47. Usadel, B., et al., *Co-expression tools for plant biology: opportunities for hypothesis generation and caveats.* Plant, Cell & Environment, 2009. **32**(12): p. 1633-1651.

48. Steinhauser, D., et al., *CSB.DB: a comprehensive systems-biology database.* Bioinformatics, 2004. **20**(18): p. 3647-3651.

49. Mutwil, M., et al., *GeneCAT--novel webtools that combine BLAST and co-expression analyses.* Nucl. Acids Res., 2008: p. W320-W326.

50. Wurtele, E., et al., *MetNet: Systems Biology Tools for Arabidopsis Concepts in Plant Metabolomics*, B.J. Nikolau and E.S. Wurtele, Editors. 2007, Springer Netherlands. p. 145-157.

51. Toufighi, K., et al., *The Botany Array Resource: e-Northerns, Expression Angling, and promoter analyses.* The Plant Journal, 2005. **43**(1): p. 153-163.

52. Manfield, I.W., et al., *Arabidopsis Co-expression Tool (ACT): web server tools for microarray-based gene expression analysis.* Nucleic Acids Research, 2006. **34**(suppl 2): p. W504-W509.

53. Fitter, D.W., et al., *GLK gene pairs regulate chloroplast development in diverse plant species.* Plant J, 2002. **31**(6): p. 713-27.

54. Rochaix, J.D., *Regulation of photosynthetic electron transport.* Biochim Biophys Acta, 2011. **1807**(3): p. 375-83.

55. Peng, L. and T. Shikanai, *Supercomplex formation with photosystem I is required for the stabilization of the chloroplast NADH dehydrogenase-like complex in Arabidopsis.* Plant Physiol, 2011. **155**(4): p. 1629-39.

56. Klimmek, F., et al., *Abundantly and rarely expressed Lhc protein genes exhibit distinct regulation patterns in plants.* Plant Physiol, 2006. **140**(3): p. 793-804.

57. Alboresi, A., et al., *Reactive oxygen species and transcript analysis upon excess light treatment in wild-type Arabidopsis thaliana vs a photosensitive mutant lacking zeaxanthin and lutein.* BMC Plant Biol, 2011. **11**: p. 62.

58. Sawchuk, M.G., et al., *Unique and overlapping expression patterns among members of photosynthesis-associated nuclear gene families in Arabidopsis.* Plant Physiol, 2008. **148**(4): p. 1908-24.

59. Kuznetsova, E., et al., *Genome-wide analysis of substrate specificities of the Escherichia coli haloacid dehalogenase-like phosphatase family.* J Biol Chem, 2006. **281**(47): p. 36149-61.

60. Simon-Plas, F., et al., *An update on plant membrane rafts.* Curr Opin Plant Biol, 2011.

61. Rey, P., et al., *Over-expression of a pepper plastid lipid-associated protein in tobacco leads to changes in plastid ultrastructure and plant development upon stress.* Plant J, 2000. **21**(5): p. 483-94.

62. Ducreux, L.J.M., et al., *Metabolic engineering of high carotenoid potato tubers containing enhanced levels of B-carotene and lutein.* Journal of Experimental Botany, 2005. **56**(409): p. 81-89.

63. Hortensteiner, S. and B. Krautler, *Chlorophyll breakdown in higher plants.* Biochim Biophys Acta, 2011. **1807**(8): p. 977-88.

64. Sakoh, M., K. Ito, and Y. Akiyama, *Proteolytic Activity of HtpX, a Membrane-bound and Stress-controlled Protease from Escherichia coli.* Journal of Biological Chemistry, 2005. **280**(39): p. 33305-33310.

65. Mokry, D.Z., et al., *Heterologous Expression Studies of Saccharomyces cerevisiae Reveal Two Distinct Trypanosomatid CaaX Protease Activities and Identify Their Potential Targets.* Eukaryotic Cell, 2009. **8**(12): p. 1891-1900.

66. Bracha, K., M. Lavy, and S. Yalovsky, *The Arabidopsis AtSTE24 Is a CAAX Protease with Broad Substrate Specificity.* Journal of Biological Chemistry, 2002. **277**(33): p. 29856-29864.

67. Greenwood, A.D., R.M. Leech, and J.P. Williams, *The osmiophilic globules of chloroplasts: I. Osmiophilic globules as a normal component of chloroplasts and their isolation and composition in Vicia faba L.* Biochimica et Biophysica Acta, 1963. **78**(1): p. 148-162.

68. Tevini, M. and D. Steinmuller, *Composition and Function of Plastoglobuli II. Lipid-Composition of Leaves and Plastoglobuli During Beech Leaf Senescence.* Planta, 1985. **163**(1): p. 91-96.

69. Bailey, J.L. and A.G. Whyborn, *The osmiophilic globules of chloroplasts II. Globules of the spinach-beet chloroplast.* Biochimica et Biophysica Acta, 1963. **78**(1): p. 163-174.

70. Beisel, K.G., et al., *Continuous turnover of carotenes and chlorophyll a in mature leaves of Arabidopsis revealed by 14CO2 pulse-chase labeling.* Plant Physiol, 2010. **152**(4): p. 2188-99.

71. Szymanska, R. and J. Kruk, *Plastochromanol, a "New" Lipophilic Antioxidant Is Synthesized by Tocopherol Cyclase in Arabidopsis Leaves: The Effect of High-Light Stress on the Level of Prenyllipid Antioxidants*, in *Photosynthesis. Energy from the Sun*, J.F. Allen, et al., Editors. 2008, Springer. p. 1581-1584.

72. Szymanska, R. and J. Kruk, *Plastoquinol is the Main Prenyllipid Synthesized During Acclimation to High Light Conditions in Arabidopsis and is Converted to Plastochromanol by Tocopherol Cyclase.* Plant Cell Physiol., 2010. **51**(4): p. 537-545.

73. Havaux, M., et al., *Vitamin E Protects against Photoinhibition and Photooxidative Stress in Arabidopsis thaliana.* Plant Cell, 2005. **17**(12): p. 3451-69.

74. Furt, F., et al., *A bimodular oxidoreductase mediates the specific reduction of phylloquinone (vitamin K1) in chloroplasts.* The Plant Journal, 2010. **64**(1): p. 38-46.

75. Allen, J.F., et al., *Chloroplast protein phosphorylation couples plastoquinone redox state to distribution of excitation energy between photosystems.* Nature, 1981. **291**(5810): p. 25-29.

76. Mullineaux, C.W. and J.F. Allen, *State 1-State 2 transitions in the cyanobacterium Synechococcus 6301 are controlled by the redox state of electron carriers between Photosystems I and II.* Photosynthesis Research, 1990. **23**(3): p. 297-311.

77. Allen, J.F., *Protein phosphorylation in regulation of photosynthesis.* Biochem Biophys Acta, 1992. **1098**: p. 275-335.

78. Norris, S.R., T.R. Barrette, and D. DellaPenna, *Genetic dissection of carotenoid synthesis in arabidopsis defines plastoquinone as an essential component of phytoene desaturation.* Plant Cell, 1995. **7**(12): p. 2139-49.

79. Livingston, A.K., et al., *Regulation of cyclic electron flow in C3 plants: differential effects of limiting photosynthesis at ribulose-1,5-bisphosphate carboxylase/oxygenase and glyceraldehyde-3-phosphate dehydrogenase.* Plant Cell Environ, 2010. **33**(11): p. 1779-88.

80. Livingston, A.K., et al., *An Arabidopsis mutant with high cyclic electron flow around photosystem I (hcef) involving the NADPH dehydrogenase complex.* Plant Cell, 2010. **22**(1): p. 221-33.

81. Puthiyaveetil, S., et al., *The ancestral symbiont sensor kinase CSK links photosynthesis with gene expression in chloroplasts.* Proc Natl Acad Sci U S A, 2008. **105**(29): p. 10061-6.

82. Reinhold, C., et al., *Short-term down-regulation of zeaxanthin epoxidation in Arabidopsis thaliana in response to photo-oxidative stress conditions.* Biochim Biophys Acta, 2008. **1777**(5): p. 462-9.

83. Xu, C.C., et al., *Suppression of zeaxanthin epoxidation by chloroplast phosphatase inhibitors in rice leaves.* Plant Science, 1999. **146**(1): p. 27-34.

84. Paramonova, N.V., N.I. Shevyakova, and V.V. Kuznetsov, *Ultrastructure of Chloroplasts and Their Storage Inclusions in the Primary Leaves of Mesembryanthemum crystallinum Affected by Putrescine and NaCl.* Russian Journal of Plant Physiology, 2004. **51**(1): p. 86-96.

85. Molas, J., *Changes of chloroplast ultrastructure and total chlorophyll concentration in cabbage leaves caused by excess of organic Ni(II) complexes.* Environmental and Experimental Botany, 2002. **47**(2): p. 115-126.

86. Britvec, M., et al., *Ultrastructure changes in grapevine chloroplasts caused by increased tropospheric ozone concentrations.* Biologia, 2001. **56**(4): p. 417-424.

87. Panou-Filotheou, H., A.M. Bosabalidis, and S. Karataglis, *Effects of Copper Toxicity on Leaves of Oregano (Origanum vulgare subsp. hirtum).* Ann Bot, 2001. **88**(2): p. 207-214.

88. Jones, A.M., et al., *Modifications to the Arabidopsis defense proteome occur prior to significant transcriptional change in response to inoculation with Pseudomonas syringae.* Plant Physiol, 2006. **142**(4): p. 1603-20.

89. Jasinski, M., et al., *AtOSA1, a member of the Abc1-like family, as a new factor in cadmium and oxidative stress response.* Plant Physiol, 2008. **147**(2): p. 719-31.

90. Youssef, A., et al., *Plant lipid-associated fibrillin proteins condition jasmonate production under photosynthetic stress.* The Plant Journal, 2010. **61**(3): p. 436-445.

91. Yang, Y., et al., *Fibrillin expression is regulated by abscisic acid response regulators and is involved in abscisic acid-mediated photoprotection.* PNAS, 2006. **103**(15): p. 6061-6066.

92. Galetskiy, D., et al., *Structure and dynamics of photosystem II light-harvesting complex revealed by high-resolution FTICR mass spectrometric proteome analysis.* Journal of The American Society for Mass Spectrometry, 2008. **19**(7): p. 1004-1013.

93. Monte, E., D. Ludevid, and S. Prat, *Leaf C40.4: a carotenoid-associated protein involved in the modulation of photosynthetic efficiency?* Plant J, 1999. **19**(4): p. 399-410.

94. Smith, P.K., et al., *Measurement of protein using bicinchoninic acid.* Anal Biochem, 1985. **150**(1): p. 76-85.

95. Friso, G., P.D. Olinares, and K.J. van Wijk, *The workflow for quantitative proteome analysis of chloroplast development and differentiation, chloroplast mutants, and protein interactions by spectral counting.* Methods Mol Biol, 2011. **775**: p. 265-82.

96. Olinares, P.D., L. Ponnola, and K.J. van Wijk, *Megadalton complexes in the chloroplast stroma of arabidopsis thaliana characterized by size exclusion chromatography, mass spectrometry and hierarchical clustering.* Mol Cell Proteomics, 2010. **9.7**: p. 1594-1615.

97. Shannon, P., et al., *Cytoscape: A Software Environment for Integrated Models of Biomolecular Interaction Networks.* Genome Research, 2003. **13**(11): p. 2498-2504.

98. Gasteiger, E., et al., *Protein Identification and Analysis Tools on the ExPASy Server*, in *The Proteomics Protocols Handbook*, J.M. Walker, Editor. 2005, Humana Press. p. 571-607.

CHAPTER THREE

ABC1K ATYPICAL KINASES IN PLANTS; FILLING THE ORGANELLAR KINASE VOID

3.1 ABSTRACT

Surprisingly few protein kinases have been demonstrated in chloroplasts or mitochondria. Here the "activity of bc_1 complex kinase" (ABC1K) protein family is discussed, which is suggested to locate in mitochondria and plastids, thus filling the kinase void. The ABC1Ks are atypical protein kinases and their ancestral function is the regulation of quinone synthesis. ABC1Ks have proliferated from 1-2 members in non-photosynthetic organisms to more than 16 members in algae and higher plants. The evolutionary history of the ABC1K family is reconstructed, and a functional domain analysis for angiosperms and a nomenclature for ABC1Ks in Arabidopsis, rice and maize is provided. Finally, it is hypothesized that targets of ABC1Ks include enzymes of prenyl-lipid metabolism and components of the organellar gene expression machineries.

3.2 DISCUSSION

3.2.1 The protein kinase-like superfamily The protein kinase-like (PKL) superfamily encompasses all protein kinases and a subset of small molecule/metabolite kinases (e.g. phosphatidyl-inositol phosphate kinases) [1, 2]. The PKL superfamily displays enormous sequence and structural variability to match the wide array of target substrates. PKLs can be subdivided between the eukaryotic protein kinases (ePKs) prevalent in the eukaryotes, and the

atypical protein kinases (aPKs), which predominate in the prokaryotes [2] (Figure 1). Two-component kinases (i.e. histidine-aspartate kinases) form a separate family and are important in prokaryotes [3], but have been adapted by eukaryotes [4]. Sequence alignment analyses of numerous, diverse ePKs have established an ~250 amino acid ePK catalytic domain containing twelve subdomains [5, 6], while x-ray crystal structures of ePKs provide functional context for these subdomains (see e.g. [7-11]). The aPKs share little or no homology with ePKs, although crystal structures indicate that most maintain a similar overall protein kinase-fold [12]. *In silico* sequence and structural studies of the entire PKL superfamily reveal only ~10 residues

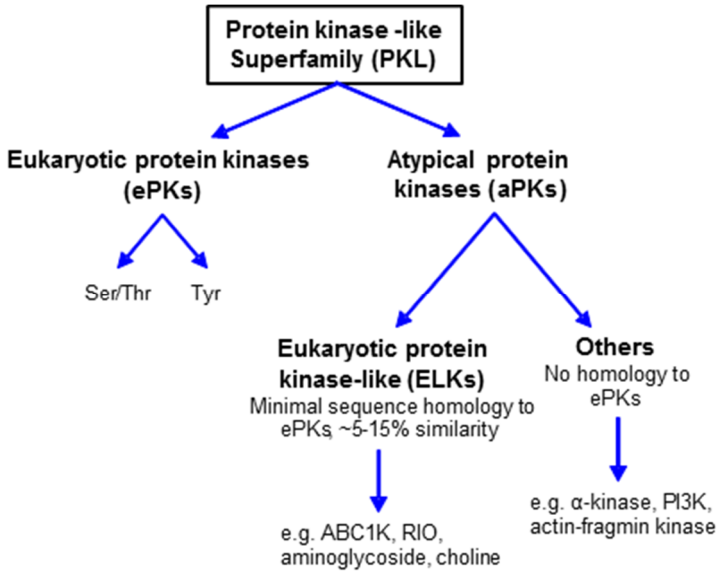

Figure 1. Categorical relationships of the ABC1K protein domain, compared with the ePK family of kinases. The diagram illustrates the categorization of the protein-kinase-like superfamily.

conserved across the ePKs and aPKs; and even these residues have been shown to be dispensable in certain PKLs [2, 12]. The ePK-like (ELK) group of aPKs, that share some sequence identity

with ePKs (usually < 15%), have emerged as important regulatory kinases of bacteria [13-16] and include the activity of bc_1 complex kinase" (ABC1K) family [17], RIO kinases [18, 19], aminoglycoside kinases [20], and others [2]. In this chapter the evolutionary history of ABC1Ks will be explored, and support for their significance in plant mitochondria and plastids will be provided.

3.2.2 A protein kinase void in plant plastids and mitochondria The complex orchestration of events in chloroplasts and mitochondria, such as photosynthetic processes and cellular respiration, and their need for rapid adjustment to alterations in environmental and developmental conditions, seemingly demands a level of control that could be provided by an assortment of kinases. So far nearly 200 Arabidopsis chloroplast phosphoproteins have been identified in Arabidopsis leaves [21, 22]. The true number of kinase targets in chloroplast and non-photosynthetic plastids is likely much larger, considering the technical challenges to identify phosphopeptides, and considering that samples from only a small number of developmental states and (a)biotic conditions have been analyzed [23-25]. Phosphoproteomic analysis of yeast mitochondria revealed a kinase network including 48 phosphoproteins involved in critical mitochondrial functions including carbohydrate metabolism, redox regulation, and apoptosis [26]. The phosphoproteome of plant mitochondria is poorly understood and fewer than 20 phosphoproteins have been detected in *Arabidopsis* [27].

So far, identified protein kinases are under-represented in plant plastids and mitochondria [28, 29], possibly because multiple kinases of plastids and mitochondria may be bacterial-derived kinases of the poorly annotated aPK family, rather than the better recognized ePKs [2]. Thus far in Arabidopsis, apart from ABC1Ks, 6-7 PKL kinases have been conclusively

demonstrated to localize to the plastid or mitochondria, despite significant and systematic efforts [28, 29]. In addition, one chloroplast and one mitochondrial two-component sensor kinase have been identified, and are the chloroplast sensor kinase (CSK) [30] and the pyruvate dehydrogenase kinase (PDK) [31], respectively. The experimentally identified ABC1Ks add seven kinases to Arabidopsis plastids and one to mitochondria (Table 1); because the ABC1Ks don't have many of the typical ePK features, they have often not been recognized as kinases (e.g. see [29]).

Characterization of plastid protein kinases has emphasized the role of phosphorylation in plastid gene expression and regulation of the photosynthetic thylakoid electron transport system. The state transition kinases, STN7 and STN8 localize to the thylakoid membrane system and phosphorylate subunits of the light-harvesting complex (LHC) and photosystem (PS), respectively, driving rapid alterations in light harvesting and electron transport in response to fluctuating environment [32-35]. Chloroplast stromal casein kinase IIα (cpCK2) appears to be a central regulator of various plastid functions [23]. cpCK2 was shown to interact with CSK providing a link between redox sensing and plastid transcriptional control [36]. The identification of two-component sensor kinases in plastids and mitochondria emphasizes the bacterial ancestry of the organelles and justifies the expectation that many of the organellar kinases are bacterial-derived aPKs.

3.2.3 ABC1Ks in plastids and mitochondria The ABC1Ks are an evolutionarily-ancient gene family, conserved throughout species of all three primary kingdoms (archaea, bacteria, and eukaryotes), but have greatly expanded in number in photosynthetic organisms. The gene family in *Arabidopsis thaliana* contains seventeen members (Table 1, Figure 2). Analyses of purified

plastoglobules (PGs) from *A. thaliana* chloroplasts identified six ABC1K proteins (AtABC1K1, 3-7) that localize predominantly (or exclusively) to this plastid location [37-39]. A seventh protein (AtABC1K8/OSA1) was shown to localize to the inner plastid envelope [40]. Furthermore, ABC1K13 is expected to be localized in mitochondria based on the localization of its functional homolog in yeast [17, 41]. Several others were observed in leaf or pollen samples (Table 1), but their subcellular localization was not determined. Proteome analysis of maize leaf fractions further supported plastid localization of eight ABC1K proteins; ZmABC1K1, 3 (2 homologues), 4, 5, 6, 8 and 9 were identified in maize proplastid and chloroplast fractions [42, 43], with ZmABC1K4 and 9 enriched in plastid nucleoids [44] (Table 1). Furthemore, seven rice ABC1K proteins were identified in chloroplasts (Table 1). Finally, TargetP, an *in silico* predictor of protein localization [45], predicts plastid or mitochondrial localization for most of the maize, rice and Arabidopsis ABC1K proteins (Table 1). Therefore, we suggest that most, if not all, ABC1K proteins in higher plants are located in plastids or mitochondria. Based on mass spectrometry analyses, ABC1Ks assigned to plastids are in general far more abundant in leaf samples than those assigned to mitochondria (Table 1); this is in agreement with the notion that the plastids contribute much more protein biomass to the leaf than mitochondria.

\

Table 1: The nomenclature and subcellular locatization of the ABC1K protein family in Arabidopsis, Rice and Maize

Sub-Family [a]	Name [b]	Sub-cellular location [c]	Arabidopsis homolog(s) [d]	TargetP [e]	Exp. local. [f]	Rice homolog(s) [g]	TargetP [e]	Exp. local. [h]	Maize homolog(s) [i]	TargetP [e]	Exp. local. [j]
1	ABC1K1	plastid (PG)	AT4G31390 [k]	P	PG	Os11g11000	P	plastid	GRMZM2G377115	P	PG
2	ABC1K2	plastid	AT5G24970	M	leaf	Os07g27480	M	n	GRMZM5G817551 [n]	M	n
3	ABC1K3	plastid (PG)	AT1G79600 [k]	P	PG	Os05g25840	P	plastid	GRMZM2G315125 GRMZM5G878070 [o]	P P	PG PG
4	ABC1K4	plastid (Nuc)	AT2G39190	P	leaf	Os02g56200	P	n	GRMZM5G855200 [p]	x	Nuc
5	ABC1K5	plastid (PG)	AT1G71810 [k]	P	PG	Os04g54790	P	plastid	GRMZM2G305007	M	PG
6	ABC1K6	plastid (PG)	AT3G24190	P	PG	Os02g57160	P	plastid	GRMZM2G157369	P	PG
7	ABC1K7	plastid (PG)	AT3G07700	x	PG	Os09g07660	P	plastid	GRMZM5G845129	P	n
8	ABC1K8	plastid (IE)	AT5G64940 [l]	P	IE	Os02g36570	P	plastid	GRMZM2G040511	P	Nuc
9	ABC1K9	plastid (PG)	AT5G05200	M	PG	Os07g12530	P	plastid	GRMZM2G031780	M	PG
10	ABC1K10	mitochondria	AT1G11390 AT1G61640	M M	leaf n	Os07g37180 Os04g56510	M M	n n	GRMZM2G067520 GRMZM2G087201 GRMZM2G368486	M M S	n n n
11	ABC1K11	mitochondria	AT5G24810	M	leaf	Os06g48770	M	leaf	GRMZM2G140917	M	n
12	ABC1K12	mitochondria	AT4G24810 AT5G50330	x x	n n	Os01g67720	x	n	GRMZM2G113264 GRMZM5G884972 [q]	M M	n n
13	ABC1K13	mitochondria (IM)	AT4G01660 [m]	x	pollen	Os01g21610	S	n	GRMZM2G003417 GRMZM2G124553	x M	n n
14	ABC1K14	mitochondria	AT1G65950	M	leaf	Os11g34750 Os11g34830	M M	n n	GRMZM2G040720	M	n
15	ABC1K15	mitochondria	AT2G40090	M	leaf	Os03g49140	x	n	GRMZM2G026180	x	n

(a) Subfamilies determined by phylogenetic analysis, as illustrated in figure 2. Subfamilies 1-8 belong to the photosynthetic-specific clade, subfamilies 9-10 to the ancestral clade and subfamilies 11-15 to the mitochondrial clade.

(b) Assigned name based on subfamilies

(c) Most likely subcellular location in Arabidopsis, rice or maize based on experimental data combined with predictions (see also PPDB - http://ppdb.tc.cornell.edu/). PG - plastoglobule; Nuc - nucleoid; IE - inner envelope; IM - inner membrane

(d) Gene/protein accession numbers are from Arabidopsis genome assembly TAIR10 (http://www.arabidopsis.org/)

(e) The predicted subcellular location by TargetP based on most likely gene model for each locus (P - plastid, M - mitochondria; S - secreted; x - cytosol)

(f) Subcellular localization reported in the literature (PG - plastoglobule - see Lundquist et al. 2012; IE - inner envelope - see Jasinski et al. 2008); Leaf - detected in Arabidopsis leaf samples; Pollen - this protein was reported in the pollen proteome (Grobei et al. 2009); n - not detected.

(g) Gene/protein accession numbers are from rice genome assembly v6 (http://rice.plantbiology.msu.edu/)

(h) Experimental location based on mass spectrometry analysis of rice chloroplasts and leaves. n - indicates that the protein was not detected in rice leaves or chloroplasts (Huang, Friso and van Wijk, unpublished).

(i) Gene/protein accession numbers are from maize genome assembly 5b.60 (http://www.maizesequence.org/)

(j) Experimental location based on mass spectrometry analysis of maize subfractions and leaves by the van Wijk lab. PG - plastoglobule; Nuc- nucleoid; n - not detected.

(k) Null mutant results in conditional stress phenotype. Unpublished data Lundquist, Giacomelli and van Wijk

(l) Mutant results in impaired cadmium tolerance (Jasinski et al 2009)

(m) Functionally complements ScCOQ8 mutant (Cardazzo et al 1997; Xie et al 2011)

(n) Gene/protein number in genome assemby 4a53 is GRMZM2G045183

(o) Gene/protein number in genome assemby 4a53 is GRMZM2G020627

(p) Gene/protein number in genome assemby 4a53 is GRMZM2G008643

(q) Gene/protein number in genome assemby 4a53 is GRMZM2G091267

Cladogram of diverse species containing ABC1Ks

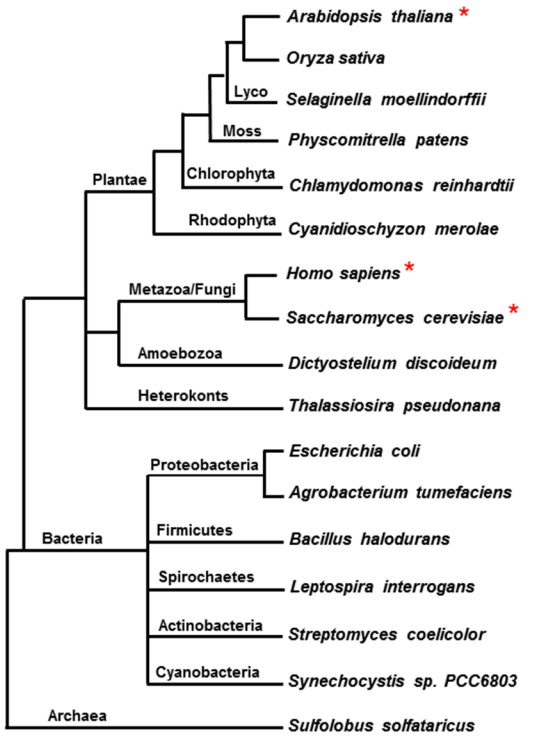

ABC1K gene family size in 42 representative species

Phylogenetic group	Species	# of loci
Dicots	Arabidopsis thaliana	17
	Medicago truncatula	17
	Populus trichocarpa	23
Monocots	Brachypodium distachyon	16
	Oryza sativa	17
	Sorghum bicolor	16
	Zea mays	20
Lycopod	Selaginella moellindorffii	20
Moss	Physcomitrella patens	27
Red algae	Cyanidioschyzon merolae D10	11
Green algae	Chlamydomonas reinhardtii	17
Cyanobacteria	Synechocystis sp. PCC6803	5
	Anabaena variabilis ATCC29413	4
	Prochlorococcus marinus subsp. Marinus str. CCMP	3
	Nostoc sp. PCC7120	4
	Acaryochloris marina str. MBIC11017	4
Metazoa	Drosophila melanogaster	3
	Homo sapiens	5
	Mus musculus	5
Fungi	Neurospora crassa	4
	Saccharomyces cerevisiae	3
Amoeba	Dictyostelium discoideum str. AX4	4
Oomycete	Phytophthora infestans	4
α-proteobacteria	Agrobacterium tumefaciens str. C58	1
	Brucella melitensis M28	1
β-proteobacteria	Ralstonia solancearum str. GMI1000	1
	Nitrosomonas europaea str. ATCC19718	2
γ-proteobacteria	Escherichia coli K12	1
	Yersinia pestis	1
	Providencia stuartii	1
ε-proteobacteria	Sulfuricurvum kujiense str. DSM 16994	1
Actinobacteria	Streptomyces coelicolor A3(2)	2
	Rhodococcus jostii st. RHA1	2
Firmicutes	Bacillus halodurans	1
Spirochaetes	Leptospira interrogans serovar Lai str. 56601	2
Crenarchaea	Sulfolobus solfataricus	1
	Metallosphaera sedula DSM 5348	1
Euryarchaea	Natrinema pellirubrum DSM 15624	2
	Haladaptatus paucihalophilus DX253	1
	Methanosarcina acetivorans	2
Thaumarchaea	Cenarchaeum symbiosum A	1
	Nitrosopumilus maritimus	1

Figure 2. A cladogram and table illustrating the diversity of species containing ABC1K proteins and their evolutionary relationships. A proliferation of homologs in photosynthetic species, especially eukaryotic species is seen in the table at right. The red asterisk indicates the three species with experimentally demonstrated functional homologs involved in UQ synthesis.

3.2.4 Identification of the ABC1K gene in yeast The founding member of the ABC1K protein family, *ABC1*/*COQ8* in yeast (hereafter, *ScCOQ8*), is a nuclear-encoded protein required for ubiquinone (UQ) synthesis in the mitochondria. This gene was found to be necessary for redox activity of the mitochondrial bc_1 complex involved in cellular respiration and was thus given the name abc1 (activity of bc_1 complex) [46]. Loss of the *ScCOQ8* gene causes a UQ deficiency and accumulation of the biosynthetic precursor 3-hexaprenyl-4-hydroxybenzoic acid, leading to instability of the bc_1 complex and the lack of bc_1 activity [47]. Missteps in the original analysis of *ScCOQ8* gene function have caused confusion. The *ScCOQ8* gene was initially believed to suppress a deleterious mutation in a cytochrome b translational activator (cbs2-223) leading to the incorrect conclusion that ScCOQ8p functions as a chaperone of cytochrome b [46, 48]. Not until a decade later was it found that *ABC1* is the *ScCOQ8* gene and that suppression of the translational activator mutant (cbs2-223) was due to a neighboring $tRNA^{Trp}$ gene [47, 49]. It is thus currently accepted that ScCOQ8p is required specifically for regulation of UQ synthesis, and is not involved in chaperone activity. Furthermore, it is important to emphasize that the ABC1K family has no relationship with the ATP-binding cassette (ABC) membrane transporter family.

3.2.5 Conservation of COQ8 function in UQ biosynthesis Analysis of homologs of yeast ScCOQ8p from diverse species has revealed remarkable functional conservation in UQ biosynthesis. Loss of UbiB or aarF, ScCOQ8p homologs in *Escherichia coli* and *Providencia stuartii*, respectively, causes UQ deficiency and concomitant accumulation of 2-octaprenylphenol, indicating a block in the first monoxygenation step in their UQ biosynthetic pathway [50]. The substrate enzyme catalyzing this monoxygenation step, the postulated target

of the UbiB/AarF, has not yet been identified in either *E. coli* or *P. stuartii* [50]. The functional homolog in *A. thaliana* was found by complementation of the yeast *ScCOQ8* deletion mutant with an *A. thaliana* cDNA library; the only complementing cDNA was *AtABC1K13* (At4g01660). This suggests that the *A. thaliana* genome only encodes a single functional homolog of *ScCOQ8*, which is supported by the phylogenetic analysis of the angiosperm *ABC1K* homologs (see below). Deleterious mutations in the human ABC1K homolog, ADCK3 (for aarF-domain containing kinase 3), also displays a UQ deficiency [51, 52]. Functional homology of this gene was confirmed by successful complementation of the *ScCOQ8* deletion mutant, when expressed along with a yeast mitochondrial transit peptide [17]. This heterologous expression of HsADCK3 in the *ScCOQ8* mutant restored both UQ biosynthetic complex stability and phosphorylation of several enzymes of the pathway (COQ3, COQ4 and COQ7), suggesting that the kinase activity of this ABC1K protein can target multiple enzymes in the UQ pathway.

3.2.6 Phylogeny of the ABC1K proteins Homologs of ScCOQ8p among the three branches of archaeal species (crenarchaea, euryarchaea, thaumarchaea) demonstrate strong BLAST hits (E-value < $3e^{-16}$). The presence of ABC1K homologs in all three branches of archaeal species, and throughout the bacterial kingdom, indicates their ancient origin prior to the archaea/bacterial split (Figure 2). Importantly, the archaea and many bacterial species do not synthesize UQ, but other types of prenylquinones, in particular menaquione [53], suggesting that the ancient function of ABC1Ks is regulation of menaquinone rather than UQ. A striking proliferation of the ABC1K family is found in algae and land plants (11-23 homologs per species), whereas non-photosynthetic prokaryotes and non-photosynthetic eukaryotes consistently contain respectively 1-2 and 3-5 homologs (Figure 2).

Construction of a phylogenetic tree from the ABC1K proteins of 42 diverse species of archaea, bacteria, and eukaryotes reveals a division into 15 subfamilies, which we name ABC1K1 to ABC1K15 (Figure 3). Immediately apparent is the fact that the archaeal homologs of multiple species all group in a clade evolutionarily distant from the homologs of bacteria and eukaryotes (except for one of two homologs of achaeal *Methanosarcina acetivorans*). This creates a natural outgroup incorporated into the phylogenetic tree, here assigned the archaeal clade (Figure 3). Within each subfamily, the seven angiosperm species (four monocots and three eudicots) all collapse into their own subclade (Figure 3). Immediately sister to each angiosperm clade are homologs from lycopod (*Selaginella moellendorfii*) and moss (*Physcomitrella patens*) with sequences from green and red algae also closely related, indicating that each of the 15 ABC1K families arose with the emergence of photosynthetic eukaryotes. Strikingly, the phylogenetic tree divides into three clear primary clades characterized by evolutionary origins and sub-cellular localization (Figure 3).

The first clade comprises eight subfamilies (1-8) and is specific for photosynthetic organisms. Cyanobacteria harbor three of the eight photosynthetic-specific subfamilies (1, 2, and 7) and it is likely that plastid endosymbiosis resulted in the introduction of these three proteins to a photosynthetic ancestor (see [54]) which subsequently expanded into the current eight members. The presence of algae in six of the eight subfamilies indicates that expansion of the plastid clade occurred very early in the development of the photosynthetic eukaryotic lineage. It is interesting that a majority of the plastid ABC1Ks (2-6) of algae and plants appear to be derived from the ancestral ABC1K2 of cyanobacteria, suggesting that they may have closely related or overlapping targets (Figure 3). Most of the higher plant proteins in this clade were identified in plastid fractions.

Figure 3. Phylogenetic tree of the ABC1K family among archaea, bacteria and eukaryotes. The full complement of 274 ABC1K proteins of 42 species, from diverse archaea, prokaryotes and eukaryotes were aligned using MUSCLE 3.5.1 (http://toolkit.tuebingen.mpg.de/muscle) and manually corrected in the case of truncated protein sequences. The tree was constructed using the RAxML software tool at CIPRES (http://www.phylo.org/sub_sections/portal/) using the General Time Reversal model with 1000 bootstrap iterations and has been illustrated as an unrooted tree (A) and a proportional polar tree layout (B) using FigTree v1.3.1 (http://tree.bio.ed.ac.uk/software/figtree/). A, unrooted tree illustrating the three primary clades, in addition to an archaeal group forming a natural root to the tree. The three clades can be categorized by their presumptive localizations and origins indicated by color; plastid endosymbiosis (green), mitochondrial endosymbiosis (blue), ancestral (purple), or outgroup (archaea specific clade) (orange). B, Expansion of the tree shown in (A) illustrating the distribution of species. Branch numbers indicate bootstrap support. Species names are colored to distinguish archaea, photosynthetic and non-photosynthetic bacteria and photosynthetic and non-photosynthetic eukaryotes. Angiosperm clades have been collapsed for legibility and are colored magenta. The 15 subfamilies are labeled around the perimeter of the wheel. Species are named as follows: Smoe, *Selaginella moelindorfii*; Ppat, *Physcomitrella patens*; Crei, *Chlamydomonas reinhardtii*; Cmer, *Cyanidioschyzon merolae*; Avar, *Anabaena variabilis*; Nsp, *Nostoc* sp.; Amar, *Acarychloris marina*; Ssp, *Synechocystis* sp.; Pmar, *Prochlorococcus marinus*; Ddis, *Dictyostelium discoideum*; Pinf, *Phytophthora infestans*; Hsap, *Homo sapiens*; Scer, *Saccharomyces cerevisiae*; Ncra, *Neurospora crassa*; Pstu, *Providencia stuartii*; Ypes, *Yersinia pestis*; Ecol, *Escherichia coli*; Neur, *Nitrosomonas europaea*; Rsol, *Ralstonia solancearum*; Bmel, *Brucella melitensis*; Atum, *Agrobacterium tumefaciens*; Lint, *Leptospira interrogans*; Scoe, *Streptomyces coelicolor*; Mace, *Methanosarcina acetivorans*; Bhal, *Bacillus halodurans*; Skuj, *Sulfuricurvum kujiense*; Mmus, *Mus musculus*; Dmel, *Drosophila melanogaster*; Rjos, *Rhodococcus jostii*; Nmar, *Nitrosopumilus maritimus*; Csym, *Cenarchaeum symbiosum*; Msed, *Metallosphaera sedula*; Ssol, *Sulfolobus solfataricus*; Hpau, *Haladaptatus paucihalophilus*; Npel, *Natrinema pellirubrum*.

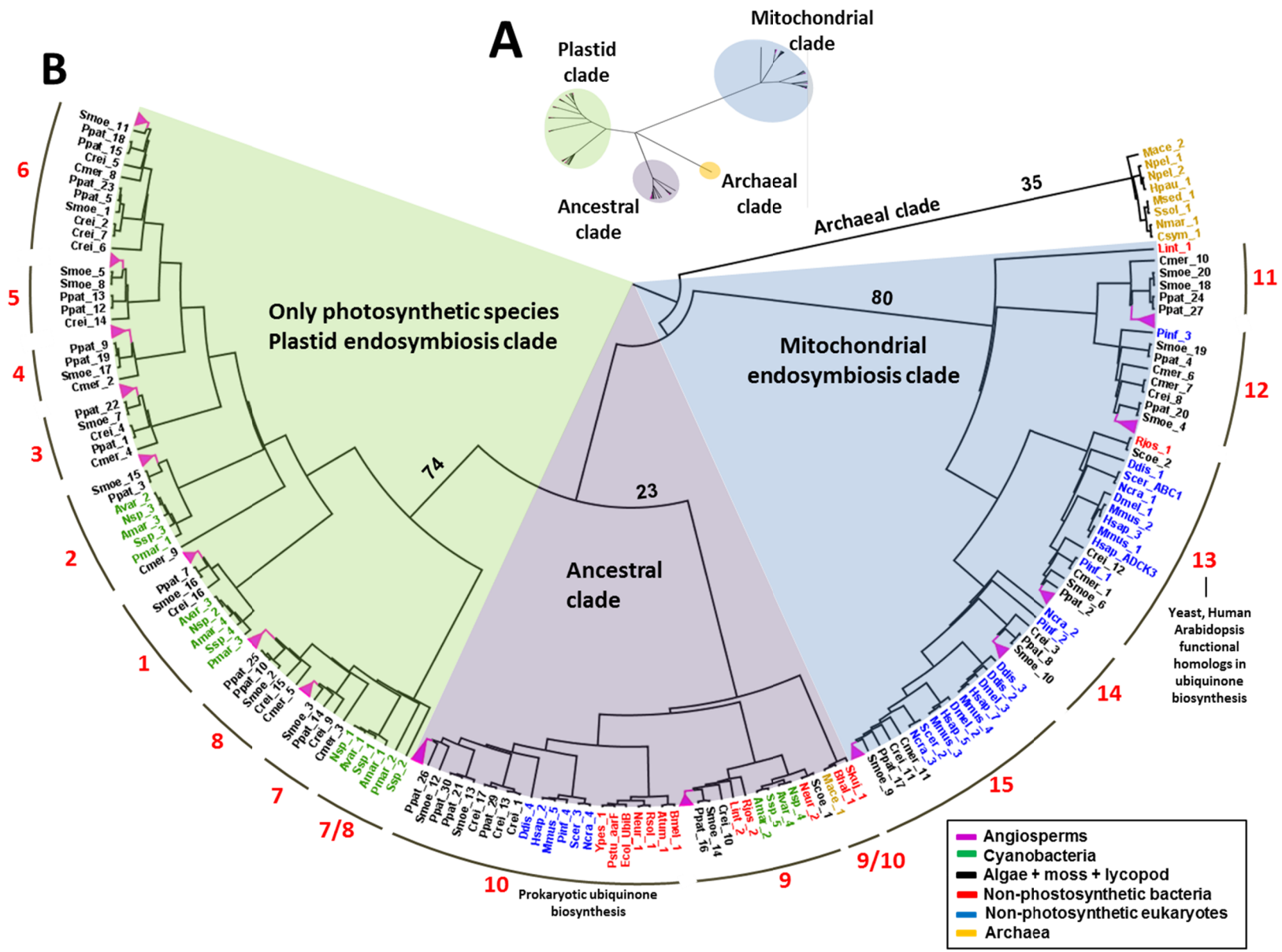
A
Plastid clade
Mitochondrial clade
Ancestral clade
Archaeal clade
B
Archaeal clade
35
80
74
23
Only photosynthetic species
Plastid endosymbiosis clade
Mitochondrial endosymbiosis clade
Ancestral clade
1
2
3
4
5
6
7
7/8
8
9
9/10
10
11
12
13
14
15
Prokaryotic ubiquinone biosynthesis
Yeast, Human Arabidopsis functional homologs in ubiquinone biosynthesis
Angiosperms
Cyanobacteria
Algae + moss + lycopod
Non-phostosynthetic bacteria
Non-photosynthetic eukaryotes
Archaea

The second clade consists of the subfamilies 11-15, which are likely predominantly targeted to the mitochondria. In the case of subfamily 13 (which corresponds with ScCOQ8p and its functional homologs in Arabidopsis and humans) experimental evidence supports the mitochondrial location assignment, since ScCOQ8p of subfamily 13 localizes to the inner mitochondrial envelope [17] and the UQ pathway localizes within the mitochondria [55]. Except for Arabidopsis mitochondrial ABC1K13, experimental localization data is lacking for plant proteins in this clade. However, *in silico* analysis of proteins by TargetP predicts mitochondrial targeting for most of the Arabidopsis, maize and rice members, and none of the plant proteins have been observed in plastids (Table 1). Furthermore, homologs of this clade are prevalent in both photosynthetic and non-photosynthetic species, as would be expected from genes of a mitochondrial origin derived from endosymbiosis prior to the divergence of the plants [56]. That homologs of actinobacteria (*Rhodococcus jostii* and *Streptomyces coelicolor*), and spirochaetes (*Leptospira interrogans*) are present in this clade rather than the α-proteobacteria, the presumed mitochondrial ancestors, may not be surprising considering the influence of a fluid evolutionary model of prokaryotic genomes, which posits that the ancestral mitochondrial donor genome did not contain the current set of α-proteobacterial genes because of genome evolution involving mutations, gene loss and horizontal gene transfer over > 1.5 billion years [57].

The third, central clade with subfamilies 9 and 10 contains the majority of the non-photosynthetic bacterial ABC1Ks, and their homologs in cyanobacteria, metazoa, and plants; this clade represents the ancestral group of ABC1Ks, derived not from organelle endosymbiosis but from the common ancestor of bacteria, archaea, and the nuclear genome of eukaryotes. However, subfamily 9 contains the photosynthetic prokaryotes (cyanobacteria) which lack in subfamily 10. Conversely, subfamily 10 contains non-photosynthetic eukaryotes, which lack in subfamily 9.

Cyanobacteria lack UQ, instead using plastoquinone 9 (PQ-9) for both photosynthetic and respiratory electron transport [58]. The ABC1Ks with demonstrated roles in UQ biosynthesis divide between subfamilies 10 and 13, consistent with the absence of cyanobacteria in these subfamilies. Furthermore, these ABC1Ks in non-photosynthetic prokaryotes (aarF in *P. stuartii* and UbiB in *E. coli*) fall into subfamily 10 (ancestral clade) while these ABC1Ks in eukaryotes (HsADCK3, ScCOQ8, and AtABC1K13) fall into subfamily 13 (mitochondrial clade). This may be a reflection of differences in biosynthetic pathways and requirements for regulation.

Remarkably, prokaryotic PQ-9 biosynthesis appears to have arisen from the UQ biosynthesis in ancestral proteobacteria [59]. This is supported by: i) the *Synechocystis* genome encodes for homologs of the *E. coli* UQ biosynthetic pathway (Ubi X, D, H, E), ii) the two pathways both derive their head group from 4-hydroxybenzoate, rather than homogentisate as in eukaryotic PQ-9 synthesis, and iii) the PQ-9 prenyl-transferase of *Synechocystis* functionally complements the *ubiA* deletion mutant in *E. coli* [59]. It can be expected that the regulatory ABC1K of UQ synthesis was similarly co-opted for PQ-9 synthesis in cyanobacteria. Thus it appears that plants, through endosymbiosis of plastid and mitochondrial ancestors, have inherited multiple pathways for quinone metabolism along with the corresponding regulatory ABC1Ks, resulting in the proliferation of the ABC1K family in photosynthetic eukaryotes.

Construction of an angiosperm-specific phylogenetic tree using the full complement of ABC1Ks from four monocots (*Z. mays*, *O. sativa*, *B. distachyon*, and *S. bicolor*) and three eudicots (*A. thaliana*, *M. truncatula*, *P. trichocarpa*) divides into 15 clearly distinguishable clades (sub-families) with strong bootstrap support (Figure 4). As with the larger phylogenetic tree in figure 3, the three primary clades with unique evolutionary origins and sub-cellular localizations are apparent.

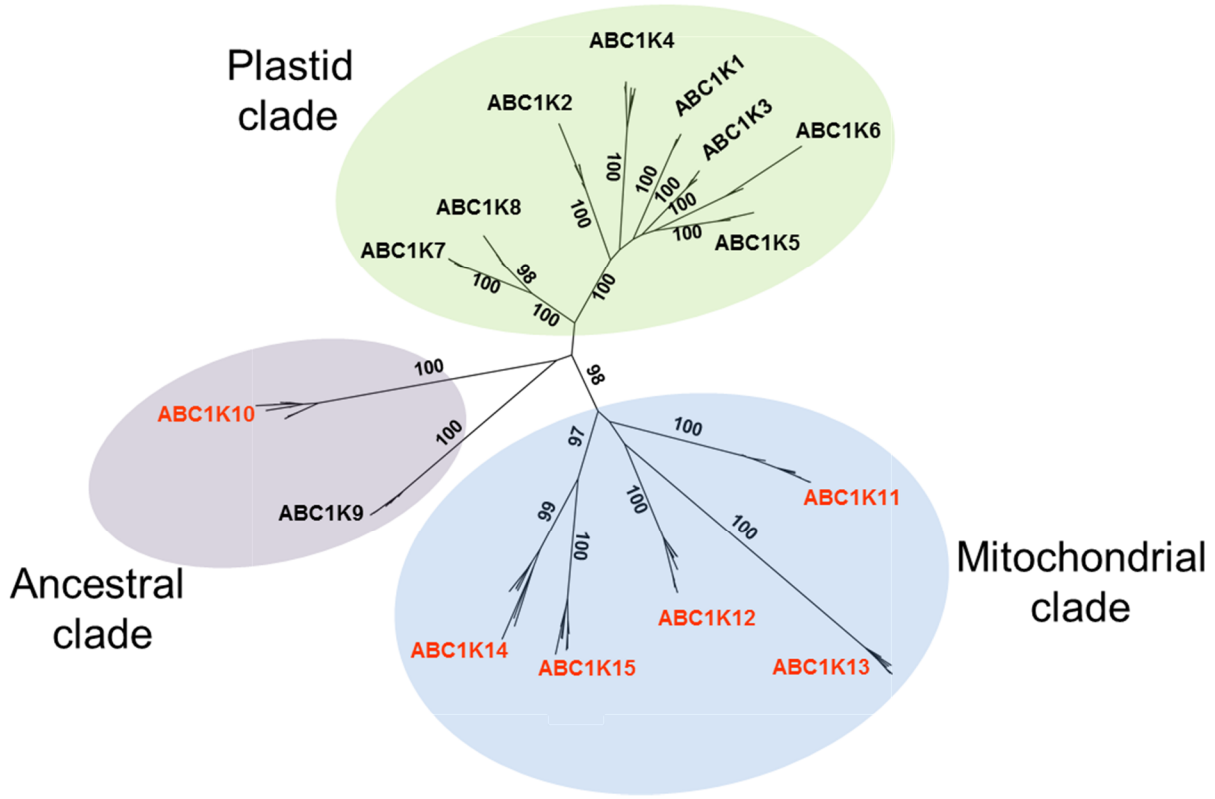

Figure 4. Phylogenetic tree of the angiosperm ABC1K proteins**.** The unrooted tree was based on the amino acid sequence alignment of the 126 ABC1K proteins from three eudicot species (*A. thaliana*, *M. truncatula*, and *P. trichocarpa*) and four monocot species (*Z. mays*, *O. sativa*, *B. distachyon*, *S. bicolor*) which was manually corrected in the case of the truncated protein products. The tree was generated as outlined in Figure 2. The three clades identified and illustrated in figure 2 are indicated here using the same color code and each of the 15 subfamilies are labeled. Subcellular localization of each subfamily (black – plastids, red – mitochondria) has been determined by experimental evidence or in the absence of experimental evidence by TargetP prediction of the *A. thaliana* homolog.

3.2.7 Defining the ABC1K protein domain Based on the alignment of 100 full length ABC1K protein sequences from the seven angiosperm species used in the phylogenetic tree (Figure 3), a common ABC1K domain is observed, spanning ~350 residues and containing twelve conserved motifs (Figure 5). Furthermore, eight of the ten key residues of the PKL superfamily identified in [2] are present in the ABC1K family and correspond to motifs III, IVa, IVb, VIIb, and VIII, involved in ATP binding and orientation (III, IVa and IVb), catalysis (VIIb), and Mg^{2+} chelation (VIII) [6, 8, 11, 60]. The other seven motifs of the ABC1K domain (I, II, V, VI, VIIa, IX, X) do not have homologous sequences in ePKs, but can be found in a number of proteins outside of the PKL superfamily with diverse enzyme activities. The significance of these ABC1K motifs is unknown and will likely require crystallization studies and mutational analysis.

Motifs conserved with ePKs The nucleotide-binding pocket (motif III) in the ABC1K family is unusual in that the first two characteristic Gly residues of nucleotide-binding pockets are both replaced with Ala. Between these two alanines is a single residue, either another Ala, or a serine or threonine. An invariant serine and glutamine, flanking 2 hydrophobic residues also appears in the ABC1K nucleotide-binding pocket. From the primary sequence alone it cannot be concluded which nucleotide (NTP) the ABC1Ks prefer as co-factor. The invariant lysine of PKLs (in motif II) lies in ABC1K motif IVa, fourteen residues downstream of motif III and is immediately downstream of two hydrophobic residues, as in the ePKs. The lysine helps to anchor the NTP by binding its α- and β- phosphates and positions the γ-phosphate for catalysis [6]. Motif IVb in ABC1Ks is characterized by an invariant (acidic) Asp residue, which we suggest is homologous

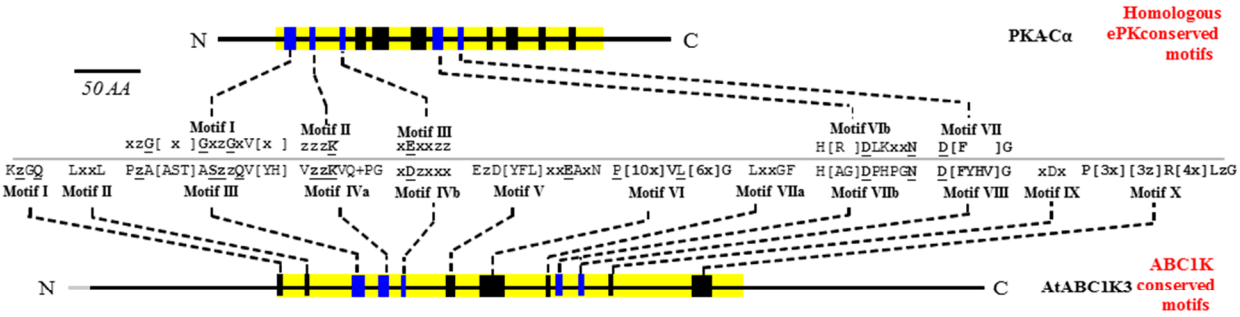

ABC1K motifs shared with the ePK motif

Motif III A part of the phosphate-binding loop of the NTP-binding pocket, this motif is responsible for anchoring the α- and β-phosphate groups and positioning the γ-phosphate for catalysis. The sequence in ABC1Ks is divergent from the "GxGxxG" sequence seen in ePKs and other NTP-binding pockets. However, the glycine-rich loop of ePKs forms a turn that is easily substituted with the small side-chains of Ala and Ser, as seen in the ABC1K family [60].

Motif IVa Contains the invariant lysine helping to anchor the NTP by binding the α- and β-phosphates and also forms a salt bridge with the carboxyl group of the Asp in motif IVb. As in ePKs, this invariant lysine lies 14 residues downstream of the NTP-binding pocket (12-21 residues in ePKs, ref. [60].

Motif IVb The aspartic acid residue is homologous to the conserved glutamic acid residue of ePK motif III, necessary for stabilization of the interaction between Lys of motif III and the α- and β-phosphate of NTP. As in casein kinase 2 and a number of other ePKs, the conserved acidic residue lies exactly 13 residues downstream of the invariant lysine [6], however the pair of hydrophobic residues downstream of glutamic acid (+3 from Glu), required in ePKs, is not maintained in ABC1Ks, but they rather conserve a hydrophobic residue at the next position (+1 from Asp), suggesting a different local protein fold.

Motif VIIb Referred to as the catalytic loop in ePKs, the conserved Asp serves as the catalytic base, activating the substrate hydroxyl group.

Motif VIII Anchors the Mg^{2+} necessary for positioning the α- and β-phosphate of the NTP. The Asp chelates the divalent cation through the assistance of a hydrophobic bond with the conserved Gly.

Figure 5. Conserved motifs of the ABC1K protein domain, compared with the ePK family of kinases. The twelve conserved motifs found in the ABC1K domain, from an alignment of 100 sequences of three eudicot species (*A. thaliana*, *M. truncatula*, and *P. trichocarpa*) and four monocot species (*Z. mays*, *O. sativa*, *B. distachyon*, *S. bicolor*), are illustrated using the prototypical ePK of *Mus musculus*, cAMP-dependent protein kinase Cα (PKACα), and AtABC1K3. Five motifs are shared between ABC1Ks and ePKs and are colored in blue in the cartoon and are aligned to each other for comparison. Conserved motifs are described using the single letter code of amino acid residues and residues conserved in >75% of sequences are shown. Bold, underlined residues are conserved in 100% of the aligned sequences, z indicates a hydrophobic residue, x indicates any residue, + indicates a positive-charged residue.

to the invariant (acidic) Glu of ePKs. An acidic residue is necessary for stabilization of the Lys-NTP interaction [6]. The catalytic motif (VIIb) contains a consensus HADPHPGN sequence in the ABC1K family. The Asp is 100% conserved among tested angiosperms and is likely homologous to the conserved Asp of ePK catalytic motifs, responsible for activating the substrate hydroxyl group via nucleophilic attack [6]. Mutation of this residue in ScCOQ8 resulted in the *abc1* deletion phenotype [17]. The histidines in the consensus sequence are conserved in all Arabidopsis ABC1Ks, except for ABC1K14 and ABC1K12 where the His positions are replaced with either Asn or Gln, indicating an absolute requirement for an amine-containing side chain at that position. Motif VIII comprises the D[FYHV]G motif which anchors the Mg^{2+} necessary for positioning NTP, using the invariant Asp to chelate this divalent cation [6]. The C-terminal motif of the ABC1K domain (motif X) deserves special mention because the motif in family 13 (PPEExxSLHRKxxG) is homologous with a motif in a number of proteins from diverse species including the RsbU phosphatase 2C of *Bacillus subtilis* [17]. X-ray crystallography studies of the RsbU protein have indicated that the sequence is critical for homodimerization by stabilizing the protein through helix-helix interaction [61]. Point mutations in motif X of HsABC1K13, (G549S, E551K) and ScCOQ8 (G475D) cause UQ deficiency, indicating a critical function for this motif in ABC1K function [17, 51, 52]. The homodimerization of the RsbU phosphatase facilitates binding with the RsbT serine kinase, creating a complex that mediates stress responses to environmental and nutritional signals in *B. subtilis* [62]. The other ABC1K families show divergent variants of this motif. Thus motif X in the ABC1Ks may similarly mediate protein-protein interactions necessary for mediating stress responses integral to ABC1K function (see below).

Domain architecture Land plant and red algae ABC1Ks in subfamily 11 (green algae has no observed homolog in this subfamily) contain a C-terminal β-lactamase domain, which in bacteria catalyzes hydrolysis of the β-lactam ring of penicillin. Identification of the intact catalytic motifs suggests that the lactamase domain is active [63]. Several β-lactamase domain proteins have been found in plants with other enzymatic activities such as glyoxylase proteins in rice and *A. thaliana* [64], and an *A. thaliana* DNA ligase [65]. The function of β-lactamase domains in plants and other eukaryotic species is unknown but it has been suggested that the fusion of the β-lactamase domain to ABC1K confers a unique mechanism of autoregulation of kinase activity [63].

Kinase activity among the ABC1Ks A direct demonstration of kinase activity in the ABC1K protein family has proven difficult. However, indirect results from point mutants in predicted kinase residues of the yeast and human abc1k genes [17, 51, 52, 66] and an *in-gelo* study of the *A. thaliana AtABC1K8/OSA1* gene have reinforced a protein kinase activity [40]. ScCOQ8p-dependent isoelectric point shifts of several subunits of the yeast UQ biosynthetic complex (COQ3, 5 and 7) have been detected in 2D IEF-SDS-PAGE gels, suggesting that ScCOQ8p either directly or in-directly phosphorylates several enzymes of the UQ biosynthesis complex in yeast [17, 66]. Biochemical phenotypes of point mutations in conserved kinase subdomains have further supported the participation of ScCOQ8p in UQ biosynthetic complex phosphorylation. Five of eight point mutants demonstrating the *abc1* deletion phenotype were mutated in residues of shared ePK-ABC1K motifs. In particular, mutation of the invariant lysine-216 (motif IVa) to an alanine caused dramatically reduced steady-state levels of the protein. Similarly, several

deleterious mutations in the human ADCK3, causing UQ deficiency, are point mutants in conserved kinase subdomains [51, 52].

3.2.8 Experimental studies of plant ABC1Ks and mRNA co-expression analysis In non-photosynthetic organisms, the ABC1K family has only been studied in relation to UQ biosynthesis. Yet, proliferation of the ABC1K family in photosynthetic eukaryotes implies an expansion of functions and targets.

Leaf proteome analysis showed that the six most abundant ABC1K proteins in Arabidopsis were located in thylakoid-associated lipoprotein particles, known as plastoglobules (PGs) (Table 1). Based on genome-wide co-expression analysis of these six ABC1Ks [39], we suggested that they have regulatory functions concerning formation, maintenance and optimization of photosynthetic performance through regulation of specific sets of enzymes involved in carotenoid biosynthesis, photoacclimation, senescence, and plastid gene expression. CrABC1K6 (EYE3) in the green algae *Chlamydomonas reinhardtii*, was located in carotenoid-rich lipophilic plastid particles (the pigment granule) in the eyespot of *Chlamydomonas.* Null mutants in *CrABC1K6* failed to develop pigment granules or eyespots. The Arabidopsis homolog of CrABC1K6 (AtABC1K6) is located in chloroplast PG [39] (Table 1), consistent with the belief that PGs serve as the precursors of the eyespot pigment granule [67]. Additionally, AtABC1K6 tightly co-expressed with zeaxanthin epoxidase (ZEP), suggesting a regulatory role in the xanthophyll cycle [39]. Based on various data (Table 1), we believe that higher plant ABC1K4 is located in the nucleoid, where it may help regulate plastid gene expression. The functions of mitochondrial ABC1K proteins include regulation of UQ biosynthesis but are

otherwise unclear, though we speculate that it includes regulation of mitochondrial gene expression.

Other experimental studies of plant ABC1K genes have emphasized a role in various types of abiotic stress tolerance, including the heavy metal cadmium. *AtABC1K8 (OSA1),* encoding for a chloroplast envelope protein, was transcriptionally upregulated in response to cadmium, and loss of *AtABC1K8* expression rendered plants more susceptible to cadmium toxicity, high-light, and H_2O_2 [40]. Even under optimal growth conditions, these *AtABC1K8* mutants displayed elevated biochemical markers of oxidative stress (e.g. SOD activity). Likewise, a homolog of the PG-localized AtABC1K7 from the heavy-metal over-accumulator species *Brassica juncea* was also up-regulated in response to 24 hours of treatment with cadmium [68]. The maize homolog ZmABC1K8 expressed primarily in green tissue, with highest expression levels in fully mature leaves, and its expression was enhanced in response to cadmium [69]. Conversely, *ZmABC1K8* mRNA accumulation was down-regulated by treatment with ABA, H_2O_2, and darkness, and did not respond to cold-treatment. It was suggested that heterologous expression of wheat ABC1K13 in *A. thaliana* conferred enhanced tolerance against a wide variety of stresses, but no evidence was presented for accumulation of the transgenic protein [70]. mRNA analysis of rice *ABC1K* genes suggested highest expression in leaf tissue and varying responses to abiotic stresses [71].

3.2.9 Conclusions and future directions Regulation of quinone synthesis is the ancient (archaeal) function of the ABC1K family. Plants, through endosymbiosis of plastid and mitochondrial ancestors, have inherited pathways for quinone metabolism along with the corresponding regulatory ABC1Ks. The requirement for additional quinolic and other prenyl-

lipid compounds likely further drove the expansion of the ABC1K family in algae and higher plants. These ABC1Ks localize in plastids and mitochondria in which they represent the majority of known kinases. The direct targets of ABC1Ks are not known, but likely include enzymes of prenyl-lipid metabolism (e.g. carotenoids) and components of the organellar gene expression machineries. Systematic analysis of ABC1K targets will be critical in defining the functional significance of the ABC1K family in photosynthetic organisms.

3.3 LITERATURE CITED

1. Cheek, S., H. Zhang, and N.V. Grishin, *Sequence and Structure Classification of Kinases.* Journal of Molecular Biology, 2002. 320(4): p. 855-881.

2. Kannan, N., et al., *Structural and Functional Diversity of the Microbial Kinome.* PLoS Biol, 2007. 5(3): p. e17.

3. Casino, P., V. Rubio, and A. Marina, *The mechanism of signal transduction by two-component systems.* Curr Opin Struct Biol, 2010. 20(6): p. 763-71.

4. Schaller, G.E., S.H. Shiu, and J.P. Armitage, *Two-component systems and their co-option for eukaryotic signal transduction.* Curr Biol, 2011. 21(9): p. R320-30.

5. Hanks, S.K., A.M. Quinn, and T. Hunter, *The protein kinase family: conserved features and deduced phylogeny of the catalytic domains.* Science, 1988. 241(4861): p. 42-52.

6. Hanks, S. and T. Hunter, *Protein kinases 6. The eukaryotic protein kinase superfamily: kinase (catalytic) domain structure and classification* The FASEB Journal 1995 9 (8): p. 576-596

7. Dirk, B., *Protein kinases - structure and function.* FEBS Letters, 1995. 369(1): p. 57-61.

8. Taylor, S.S. and E. Radzio-Andzelm, *Three protein kinase structures define a common motif.* Structure (London, England : 1993), 1994. 2(5): p. 345-355.

9. Bowyer, J.R., et al., *Carboxyl-terminal processing of the D1 protein and photoactivation of water-splitting in photosystem II. Partial purification and characterization of the processing enzyme from Scenedesmus obliquus and Pisum sativum.* J Biol Chem, 1992. 267(8): p. 5424-33.

10. Taylor, S.S., et al., *PKA: a portrait of protein kinase dynamics.* Biochimica et Biophysica Acta (BBA) - Proteins & Proteomics IPK'2003. Inhibitors of protein kinases and Workshop: Phosphoryl-transfer mechanisms, 2004. 1697(1-2): p. 259-269.

11. Dissmeyer, N. and A. Schnittger, *The age of protein kinases.* Methods in molecular biology (Clifton, N.J.), 2011. 779.

12. Scheeff, E.D. and P.E. Bourne, *Structural Evolution of the Protein Kinase-Like Superfamily.* PLoS Comput Biol, 2005. 1(5): p. e49.

13. Krupa, A. and N. Srinivasan, *Diversity in domain architectures of Ser/Thr kinases and their homologues in prokaryotes.* BMC Genomics, 2005. 6(1): p. 129.

14. Zhang, C.-C., *Bacterial signalling involving eukaryotic-type protein kinases.* Molecular Microbiology, 1996. 20(1): p. 9-15.

15. Shi, L., M. Potts, and P.J. Kennelly, *The serine, threonine, and/or tyrosine-specific protein kinases and protein phosphatases of prokaryotic organisms: a family portrait.* FEMS Microbiology Reviews, 1998. 22(4): p. 229-253.

16. Kennelly, P.J., *Protein kinases and protein phosphatases in prokaryotes: a genomic perspective.* FEMS Microbiology Letters, 2002. 206(1): p. 1-8.

17. Xie, L.X., et al., *Expression of the human atypical kinase ADCK3 rescues coenzyme Q biosynthesis and phosphorylation of Coq polypeptides in yeast coq8 mutants.* Biochimica et Biophysica Acta (BBA) - Molecular and Cell Biology of Lipids, 2011. 1811(5): p. 348-360.

18. LaRonde-LeBlanc, N. and A. Wlodawer, *A Family Portrait of the RIO Kinases.* Journal of Biological Chemistry, 2005. 280(45): p. 37297-37300.

19. LaRonde-LeBlanc, N. and A. Wlodawer, *The RIO kinases: An atypical protein kinase family required for ribosome biogenesis and cell cycle progression.* Biochimica et Biophysica Acta, 2005. 1754(12): p. 14-24.

20. Toth, M., et al., *Source of Phosphate in the Enzymic Reaction as a Point of Distinction among Aminoglycoside 2-Phosphotransferases.* Journal of Biological Chemistry, 2009. 284(11): p. 6690-6696.

21. Rokka, A., E.M. Aro, and A.V. Vener, *Thylakoid phosphoproteins: identification of phosphorylation sites.* Methods Mol Biol, 2011. 684: p. 171-86.

22. Baginsky, S. and W. Gruissem, *The Chloroplast Kinase Network: New Insights from Large-Scale Phosphoproteome Profiling.* Molecular Plant, 2009. 2(6): p. 1141-1153.

23. Reiland, S., et al., *Large-scale Arabidopsis phosphoproteome profiling reveals novel chloroplast kinase substrates and phosphorylation networks.* Plant Physiol, 2009. 150(2): p. 889-903.

24. Lohrig, K., et al., *Phosphorylation site mapping of soluble proteins: bioinformatical filtering reveals potential plastidic phosphoproteins in Arabidopsis thaliana.* Planta, 2009. 229(5): p. 1123-34.

25. Sugiyama, N., et al., *Large-scale phosphorylation mapping reveals the extent of tyrosine phosphorylation in Arabidopsis.* Mol Syst Biol, 2008. 4: p. 193.

26. Reinders, J.R., et al., *Profiling Phosphoproteins of Yeast Mitochondria Reveals a Role of Phosphorylation in Assembly of the ATP Synthase.* Molecular & Cellular Proteomics, 2007. 6(11): p. 1896-1906.

27. Ito, J., et al., *A survey of the Arabidopsis thaliana mitochondrial phosphoproteome.* Proteomics, 2009.

28. Schliebner, I., et al., *A Survey of Chloroplast Protein Kinases and Phosphatases in Arabidopsis thaliana.* Curr Genomics, 2008. 9(3): p. 184-90.

29. Bayer, R.G., et al., *Chloroplast-localized protein kinases: a step forward towards a complete inventory.* Journal of Experimental Botany, 2012. 63(4): p. 1713-1723.

30. Puthiyaveetil, S., et al., *The ancestral symbiont sensor kinase CSK links photosynthesis with gene expression in chloroplasts.* Proc Natl Acad Sci U S A, 2008. 105(29): p. 10061-6.

31. Thelen, J.J., J.A. Miernyk, and D.D. Randall, *Pyruvate dehydrogenase kinase from Arabidopsis thaliana: a protein histidine kinase that phosphorylates serine residues.* Biochemical Journal, 2000. 349(1): p. 195-201.

32. Pesaresi, P., et al., *Dynamics of reversible protein phosphorylation in thylakoids of flowering plants: The roles of STN7, STN8 and TAP38.* Biochim Biophys Acta, 2011. 1807(3): p. 887-896.

33. Tikkanen, M. and E.M. Aro, *Thylakoid protein phosphorylation in dynamic regulation of photosystem II in higher plants.* Biochim Biophys Acta, 2012. 1817(1): p. 232-238.

34. Turkina, M.V. and A.V. Vener, *Identification of phosphorylated proteins.* Methods Mol Biol, 2007. 355: p. 305-16.

35. Rochaix, J.D., *Regulation of photosynthetic electron transport.* Biochim Biophys Acta. 2011. 1807(3): p. 375-83.

36. Puthiyaveetil, S., et al., *Transcriptional control of photosynthesis genes: the evolutionarily conserved regulatory mechanism in plastid genome function.* Genome Biol Evol, 2010. 2: p. 888-96.

37. Vidi, P.A., et al., *Tocopherol cyclase (VTE1) localization and vitamin E accumulation in chloroplast plastoglobule lipoprotein particles.* J Biol Chem, 2006. 281(16): p. 11225-34.

38. Ytterberg, A.J., J.B. Peltier, and K.J. van Wijk, *Protein profiling of plastoglobules in chloroplasts and chromoplasts; a surprising site for differential accumulation of metabolic enzymes.* Plant Physiol, 2006. 140(3): p. 984-997.

39. Lundquist, P., et al., *The functional network of the Arabidopsis thaliana plastoglobule proteome based on quantitative proteomics and genome-wide co-expression analysis.* Plant Physiol, 2012.

40. Jasinski, M., et al., *AtOSA1, a member of the Abc1-like family, as a new factor in cadmium and oxidative stress response.* Plant Physiol, 2008. 147(2): p. 719-31.

41. Cardazzo, B., et al., *Isolation of an Arabidopsis thaliana cDNA by complementation of a yeast abc1 deletion mutant deficient in complex III respiratory activity.* Gene, 1998. 221(1): p. 117-25.

42. Friso, G., et al., *Reconstruction of metabolic pathways, protein expression, and homeostasis machineries across maize bundle sheath and mesophyll chloroplasts: large-scale quantitative proteomics using the first maize genome assembly.* Plant Physiol, 2010. 152(3): p. 1219-50.

43. Majeran, W., et al., *Structural and Metabolic Transitions of C4 Leaf Development and Differentiation Defined by Microscopy and Quantitative Proteomics in Maize.* The Plant Cell Online, 2010. 22(11): p. 3509-3542.

44. Majeran, W., et al., *Nucleoid-enriched proteomes in developing plastids and chloroplasts from maize leaves: a new conceptual framework for nucleoid functions.* Plant Physiol, 2012. 158(1): p. 156-89.

45. Emanuelsson, O., et al., *Locating proteins in the cell using TargetP, SignalP and related tools.* Nat Protoc, 2007. 2(4): p. 953-71.

46. Bousquet, I., G. Dujardin, and P.P. Slonimski, *ABC1, a novel yeast nuclear gene has a dual function in mitochondria: it suppresses a cytochrome b mRNA translation defect and is essential for the electron transfer in the bc 1 complex.* Embo J, 1991. 10(8): p. 2023-31.

47. Do, T.Q., et al., *A Defect in Coenzyme Q Biosynthesis Is Responsible for the Respiratory Deficiency in Saccharomyces cerevisiae abc1 Mutants.* J. Biol. Chem., 2001. 276(21): p. 18161-18168.

48. Brasseur, G., et al., *The nuclear ABC1 gene is essential for the correct conformation and functioning of the cytochrome bc1 complex and the neighbouring complexes II and IV in the mitochondrial respiratory chain.* Eur J Biochem, 1997. 246(1): p. 103-11.

49. Hsieh, E.J., J.B. Dinoso, and C.F. Clarke, *A tRNA(TRP) gene mediates the suppression of cbs2-223 previously attributed to ABC1/COQ8.* Biochem Biophys Res Commun, 2004. 317(2): p. 648-53.

50. Poon, W.W., et al., *Identification of Escherichia coli ubiB, a gene required for the first monooxygenase step in ubiquinone biosynthesis.* J Bacteriol, 2000. 182(18): p. 5139-46.

51. Mollet, J., et al., *CABC1 Gene Mutations Cause Ubiquinone Deficiency with Cerebellar Ataxia and Seizures.* The American Journal of Human Genetics, 2008. 82(3): p. 623-630.

52. Lagier-Tourenne, C., et al., *ADCK3, an Ancestral Kinase, Is Mutated in a Form of Recessive Ataxia Associated with Coenzyme Q10 Deficiency.* The American Journal of Human Genetics, 2008. 82(3): p. 661-672.

53. Nowicka, B. and J. Kruk, *Occurrence, biosynthesis and function of isoprenoid quinones.* Biochim Biophys Acta, 2010. 1797(9): p. 1587-605.

54. Price, D.C., et al., *Cyanophora paradoxa genome elucidates origin of photosynthesis in algae and plants.* Science, 2012. 335(6070): p. 843-7.

55. Tran, U.C. and C.F. Clarke, *Endogenous synthesis of coenzyme Q in eukaryotes.* Mitochondrion The Role of Coenzyme Q in Cellular Metabolism: Current Biological and Clinical Aspects, 2007. 7, Supplement(0): p. S62-S71.

56. Gray, M.W., G. Burger, and B.F. Lang, *Mitochondrial Evolution.* Science, 1999. 283(5407): p. 1476-1481.

57. Esser, C., W. Martin, and T. Dagan, *The origin of mitochondria in light of a fluid prokaryotic chromosome model.* Biology Letters, 2007. 3(2): p. 180-184.

58. Collins, M.D. and D. Jones, *Distribution of isoprenoid quinone structural types in bacteria and their taxonomic implication.* Microbiol Rev, 1981. 45(2): p. 316-54.

59. Sadre, R., C. Pfaff, and S. Buchkremer, *Plastoquinone-9 biosynthesis in cyanobacteria differs from that in plants and involves a novel 4-hydroxybenzoate solanesyltransferase.* Biochem J, 2012.

60. Leonard, C.J., L. Aravind, and E.V. Koonin, *Novel families of putative protein kinases in bacteria and archaea: evolution of the ℓukaryotic"protein kinase superfamily.* Genome Res, 1998. 8(10): p. 1038-47.

61. Delumeau, O., et al., *Functional and Structural Characterization of RsbU, a Stress Signaling Protein Phosphatase 2C.* Journal of Biological Chemistry, 2004. 279(39): p. 40927-40937.

62. Locke, J.C., et al., *Stochastic pulse regulation in bacterial stress response.* Science, 2011. 334(6054): p. 366-9.

63. Liobikas, J.B., et al., *Identification and analysis of a novel serine beta-lactamase-like plant protein by a bioinformatic approach.* Biologija, 2006(3): p. 126-129.

64. Mustafiz, A., et al., *Genome-wide analysis of rice and Arabidopsis identifies two glyoxalase genes that are highly expressed in abiotic stresses*, in *Functional & Integrative Genomics*. 2011, Springer Berlin / Heidelberg. p. 293-305.

65. Waterworth, W.M., et al., *A plant DNA ligase is an important determinant of seed longevity.* The Plant Journal, 2010. 63(5): p. 848-860.

66. Tauche, A., U. Krause-Buchholz, and G. Rodel, *Ubiquinone biosynthesis in Saccharomyces cerevisiae: the molecular organization of O-methylase Coq3p depends on Abc1p/Coq8p.* FEMS Yeast Research, 2008. 8(8): p. 1263-1275.

67. Merchant, S.S., et al., *The Chlamydomonas Genome Reveals the Evolution of Key Animal and Plant Functions.* Science, 2007. 318(5848): p. 245-250.

68. Fusco, N., et al., *Identification of cadmium-regulated genes by cDNA-AFLP in the heavy metal accumulator Brassica juncea L.* Journal of Experimental Botany, 2005. 56(421): p. 3017-3027.

69. Gao, Q.-S., et al., *Cloning of an ABC1-like Gene ZmABC1-10 and Its Responses to Cadmium and Other Abiotic Stresses in Maize (Zea mays L.).* Acta Agronomica Sinica, 2010. 36(12): p. 2073-2083.

70. Wang, C., et al., *TaABC1, a member of the activity of bc1 complex protein kinase family from common wheat, confers enhanced tolerance to abiotic stresses in Arabidopsis.* Journal of Experimental Botany, 2010.

71. Gao, Q.-S., et al., *Systematic Identification of Rice ABC1 Gene Family and Its Response to Abiotic Stress.* Rice Science, 2011. 18(3): p. 167-177.

CHAPTER FOUR

PLASTID-LOCALIZED ATYPICAL PROTEIN KINASES ABC1K1 AND ABC1K3 ARE NECESSARY FOR LIGHT STRESS ADAPTATION IN ARABIDOPSIS [1]

4.1 ABSTRACT

Despite the identification of nearly two hundred protein phosphorylation targets in plant plastids, less than a dozen protein kinases have been found to localize to this organelle to date. More than half of the protein kinases known to localize to the plastid are members of a large family of atypical protein kinases, the Activity of bc_1 complex kinases (ABC1Ks). ABC1K1 and ABC1K3 have been found in the *A. thaliana* chloroplast plastoglobule and are centrally-positioned as hubs in the plastoglobule transcriptional co-expression network, suggesting a significant regulatory role. Here, it is reported that *A. thaliana* T-DNA insertion mutants in A*BC1K1* and *ABC1K3* reveal a conditional bleaching phenotype upon a 10-fold increase in light intensity in mutants of both genes. The double mutant (*abc1k1* x *abc1k3*) demonstrated a senescent-like degreening under a 5-fold increase in light intensity that did not affect the single mutants, suggesting synergistic roles for each gene in the adaptation to excess excitation energy. Chloroplast ultrastructure of stressed *k1k3* leaves were altered under light stress, demonstrating granal hyperstacking, with smaller but more numerous plastoglobules compared to the wild-type. Quantitative proteomics revealed reduced accumulation of the plastoglobule-localized carotenoid cleavage dioxygenase 4 and altered expression of additional carotenoid metabolic enzymes under light stress in *k1k3* leaves. Quantitative prenyl-lipid profiling of the plastoglobule and thylakoid

[1] In-gel digestions and mass-spectrometry operation were performed by Dr. Anton Poliakov.

show accumulation of β-carotene and xanthophylls in plastoglobules of *k1k3* but not wild-type. Furthermore, increased accumulation of quinone compounds at the expense of tocopherols in *k1k3* PGs suggests a regulatory role for the ABC1Ks in the PG-localized tocopherol cyclase (VTE1) reaction. Collectively, the results suggest a role of ABC1K1 and ABC1K3 in the regulation of multiple prenyl-lipid metabolic pathways as an adaptation to excess excitation energy.

4.2 INTRODUCTION

Protein phosphorylation is known to regulate important plastid functions including photosynthetic activity and plastid gene transcription [1, 2]. Large-scale phosphoproteome analyses of Arabidopsis total leaf tissue or cell cultures have identified nearly two-hundred phosphoproteins in the plastid [3-6]. In addition to identification of the well-known phosphoproteins of photosystem and light harvesting complexes, targets of phosphorylation also include multiple enzymes of diverse plastidic processes such as gene transcription, carbohydrate metabolism, amino acid metabolism, lipid metabolism, and nucleotide metabolism, indicating extensive use of protein phosphorylation in plastid metabolism [3-6].

About a dozen protein kinases have been found to localize in the Arabidopsis plastid [7, 8], only four of which have an experimentally demonstrated function and known protein targets. The state transition kinase 7 (STN7) phosphorylates LHCII subunits, thereby regulating their distribution in the thylakoid membrane, the so-called state-transitions [2]. Its homolog, STN8, phosphorylates the photosystem II subunits, D1, D2, CP43, and PsbH, and potentially the thylakoid Ca^{2+}-sensitive receptor protein (CaS) [9, 10]. STN8-dependent phosphorylation of PSII has been implicated in control of thylakoid granal stacking and turnover of the D1 protein [11,

12]. Phosphorylation of several RNA-binding proteins and proteins of the plastid transcription machinery has been attributed to the chloroplast-localized casein kinase IIα homolog (cpCKIIα) of Arabidopsis [13-16]). Additionally, a bacteria-type two-component histidine kinase called chloroplast sensor kinase (CSK), is responsible for regulating gene transcription of plastid-encoded photosystem genes, psaA and psaB and physically interacts with cpCKIIα and the plastid transcription factor, sigma factor 1 (SIG-1), suggesting direct phosphorylation activity [1, 17]. More than half of the identified protein kinases of the plastid are members of the activity of bc_1 complex kinases (ABC1Ks), a family of atypical protein kinases that has proliferated from 1-2 members in non-photosynthetic species to more than 16 members in plants [18]. In Arabidopsis there are seventeen homologs, seven of which have been experimentally demonstrated to localize in the plastid [18-20]. The name for the family comes from the phenotype of a yeast deletion mutant which is unable to synthesize ubiquinone (UQ) and thus lacks activity of the mitochondrial bc_1 complex [21, 22]. A homolog in Arabidopsis, AtABC1K13, functionally complements the yeast deletion mutant indicating extensive conservation in UQ synthesis among eukaryotes [23].

Kinase activity of the ABC1Ks remains to be demonstrated, though indirect evidence from point mutants in the ABC1K domain supports the putative kinase assignment. Five of eight point mutants in the yeast *ABC1* demonstrating the *abc1* deletion phenotype were mutated in conserved residues shared with known protein kinases [24]. Similarly, several deleterious mutations in a human ABC1K homolog are point mutants in conserved kinase residues [25, 26]. Furthermore, yeast ABC1-dependent isoelectric point shifts of several subunits of the yeast UQ biosynthetic complex have been detected, indicating that ABC1 is either directly or in-directly responsible for phosphorylation of the UQ biosynthetic complex in yeast [24].

ABC1Ks have only been studied in relation to UQ synthesis in non-photosynthetic organisms. However the proliferation of the family in plants suggests an expansion of targets and functions. Six of the homologs in Arabidopsis have been found to localize to the chloroplast plastoglobule (PG), a lipoprotein particle attached to the thylakoid membrane that maintains a distinct population of lipids and about two dozen enzymes [19]. PGs are formed by the blebbing of the outer leaflet of the thylakoid membrane bilayer, resulting in a hydrophobic interior with a amphiphilic perimeter, permanently coupled to the thylakoid [27]. The permanent association of the PG and thylakoid membrane permits a conduit for metabolite exchange between the two structures. The nature of protein localization or protein association with the PG is unclear. However, metabolic enzymes acting on substrate deposited in the PG are likely peripherally associated with the PG through insertion of a hydrophobic face, permitting access to lipid substrate, as also proposed for allene oxide synthase (AOS) based on the elucidation of its three-dimensional structure [28]. Other PG proteins not acting directly on lipid substrate in the PG, such as the ABC1Ks, might also associate via a hydrophobic face, protein-protein interaction, or be tethered to the PG through covalent modifications.

Interestingly, PGs are rich stores of various quinones and contain multiple enzymes involved in their metabolism (e.g. tocopherol cyclase [VTE1] and NAD(P)H dehydrogenase C1 [NDC1]), suggesting ABC1Ks localized at the PG may be regulators of plastidic quinone metabolism. A genome-wide transcriptional coexpression network of the PG-localized genes finds ABC1Ks positioned as hubs of functional modules related to prenyl-lipid metabolism, protein turnover, redox signaling and senescence [19]. An *A. thaliana* insertion mutant of the inner envelope-localized AtABC1K8 revealed constitutively high accumulation of ROS and oxidative stress-associated genes, as well as sensitivity to cadmium stress [20]. Investigation of

the PG-localized AtABC1K1 using RNAi indicated an impairment in chlorophyll degradation, however the RNAi strategy unfortunately used the full length coding sequence of the gene likely causing many *ABC1K* genes to be affected [29].

Here we report evidence implicating the PG-localized AtABC1K1 and AtABC1K3 in adaptation to increased light intensities during growth. Null mutants of *ABC1K1* and *ABC1K3* result in rapid photobleaching and necrosis upon transition to a 10-fold increase in light intensity, while the corresponding double mutant (*abc1k1* x *abc1k3*) shows enhanced sensitivity, demonstrating senescent-like degreening when transferred to five-fold higher light intensity. Our molecular analyses support the proposed role of the PG and ABC1Ks in photoacclimation by regulating prenyl-lipid metabolic pathways of the plastid.

4.3 RESULTS

4.3.1 Isolation of PG-localized* ABC1K *mutants It has been reported previously that the *Arabidopsis thaliana* PG proteome contains at least six ABC1K putative kinase proteins, ABC1K1,3,5-7 and 9 [18]. Transcriptional coexpression analysis has placed the *ABC1K1* and *ABC1K3* genes centrally within the PG coexpression network, suggesting a central regulatory role in PG function [19]. To test the significance of ABC1K1 and ABC1K3 in plastoglobule function a reverse genetics approach was used. We obtained two SALK T-DNA insertion mutants in *ABC1K1* and one SALK T-DNA insertion mutant in *ABC1K3* and confirmed their insertion sites by sequencing genomic DNA (Figure 1A). RT-PCR from mature leaf tissue using primers specific to the 3'-end of the coding sequences indicated that no full-length transcripts of mutated genes were accumulating in the 3 insertion mutant lines (Figure 1B). However, the

insertion sites were downstream of the conserved kinase subdomains [30]. Thus, accumulation of truncated transcripts was tested using RT-PCR with primer pairs specific to the 5' and middle portions of the gene transcripts (Figure 1C), indicating that truncated transcript accumulates in the insertion mutants.

Antibodies raised against the C-termini of ABC1K1 and ABC1K3 were used for immunoblotting of total protein extract from mature leaf tissue of *abc1k1-1, abc1k1-2*, and *abc1k3*. Interestingly, a lesion in either *ABC1K* gene caused reduced accumulation of the other ABC1K protein, suggesting a common function and/or physical association for these two proteins (Figure 1D). Reduced levels of what appears to be truncated ABC1K1 accumulated in *abc1k1-1*, however no peptides of ABC1K1 or ABC1K3 were detected in leaf or PG proteomics experiments of *abc1k1-1* x *abc1k3* (*k1k3*), indicating that the insertion mutants fail to accumulate functional protein and are null mutants. In wild-type individuals ABC1K1 and ABC1K3 are expressed in mature wild-type leaf tissue, and accumulation was induced more than 4-fold and 19-fold, respectively, in response to a 5-fold increase in light intensity (Figure 1E).

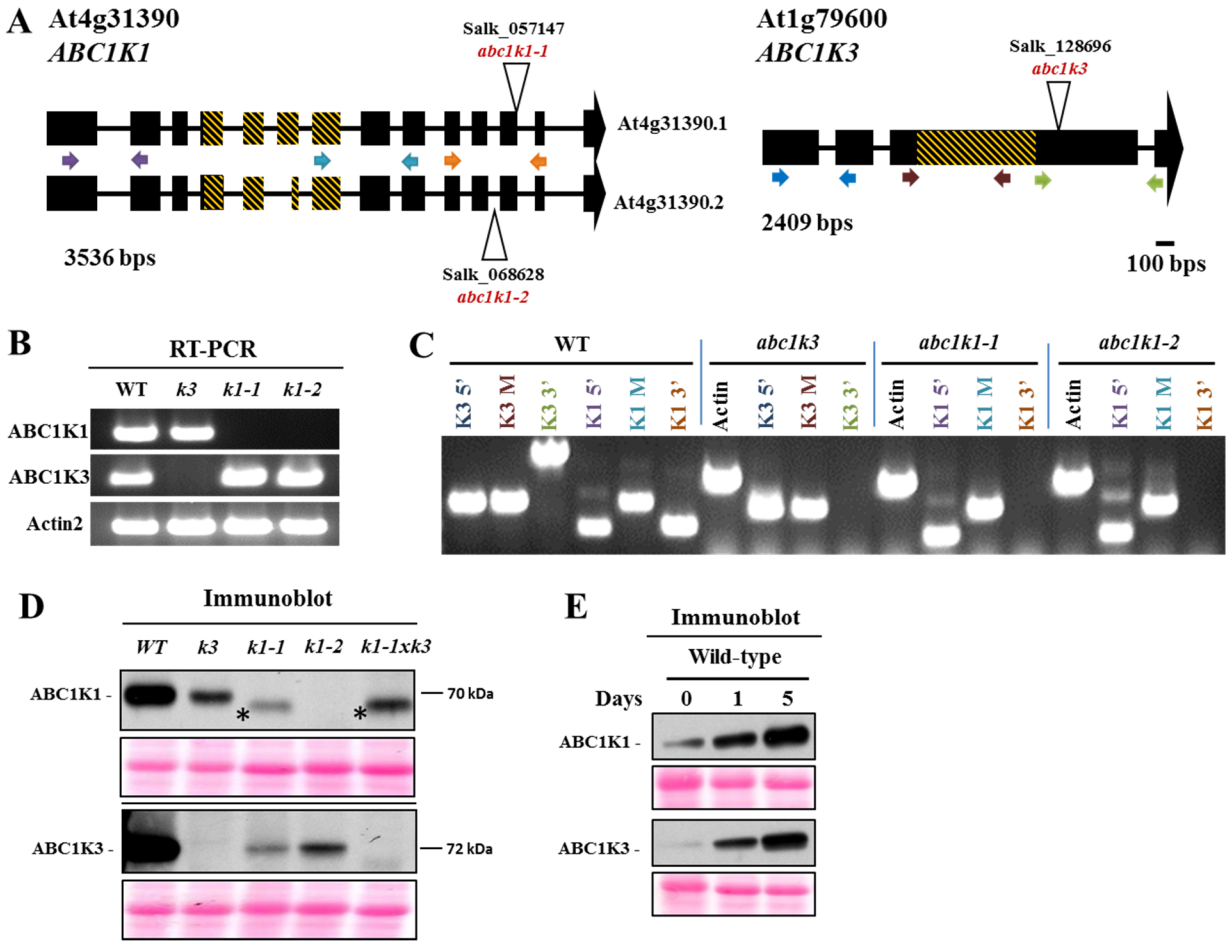

Figure 1. SALK insertions in *abc1k1-1*, *abc1k1-2*, and *abc1k3* are null mutants. A, the genetic structure of the *ABC1K1* and *ABC1K3* loci and the position of the T-DNA insertions are shown. Exons are indicated by black boxes, introns are indicated by lines. The orange hash marks indicate the location of the ABC1K domain [18]. Arrows below the genes indicate the positions of the forward and reverse primers used for the RT-PCR reactions shown in B and C. B, RT-PCR reactions (35 cycles) amplified the 3'-end of *ABC1K1*, *ABC1K3* or *ACTIN2* cDNA. C, RT-PCR reactions (30 cycles) of the 5'-end, middle (M), and 3'-end of *ABC1K1*, *ABC1K3* transcripts, *ACTIN2* was used as a loading control. B and C, total RNA was extracted from mature leaf tissue of Col-0 (WT), *abc1k1-1*, *abc1k1-2* and *abc1k3* single mutants. D and E, immunoblot of 30 µg of mature leaf tissue protein extracts. In C, tissue was unstressed; in D, wild-type tissue was treated with light stress for 0, 1, or 5 days. Asterisk indicates the presumed truncated protein of ABC1K1.

***4.3.2 A conditional light stress phenotype caused by loss of* ABC1K1 *and* ABC1K3** Mutant individuals could not be distinguished from wild-type when grown under permissive growth conditions (data not shown). However, when plants grown at ~100 μE m^{-2} s^{-1} were subsequently transferred to 1000 μE m^{-2} s^{-1}, a 10x light stress, late in the vegetative growth phase of development, it was found that null mutants displayed a unique phenotype, with widespread leaf photobleaching and necrosis appearing within 1 day (Figure 2A).

A cross of the *abc1k1-1* and *abc1k3* mutant lines was made to test for possible functional redundancy. As in the parental single mutants, the resulting double homozygous mutant (*k1k3*) was also found to grow and develop as the wild-type under permissive growth conditions and rapidly photobleached under the high-light stress treatment. However, *k1k3* displayed sensitivity to a milder light transition (to ~500 μE m^{-2} s^{-1}, 5x light stress) that was not found in the parental single mutants or the wild-type (Figure 2B). Under this moderate light stress, the mature *k1k3* leaves demonstrated a senescent-like phenotype, in which they began to visibly degreen only after about three days and failed to accumulate anthocyanins outside of the vasculature (Figure 2C). Younger leaf tissue appeared unaffected by the light stress treatment, as has been reported for other oxidative/light stress treatments [31]. This synergistic effect in *k1k3*, in combination with the compensation found in the single mutants under the moderate light stress regime, indicates non-redundant contributions of ABC1K1 and ABC1K3 to the light-stress response.

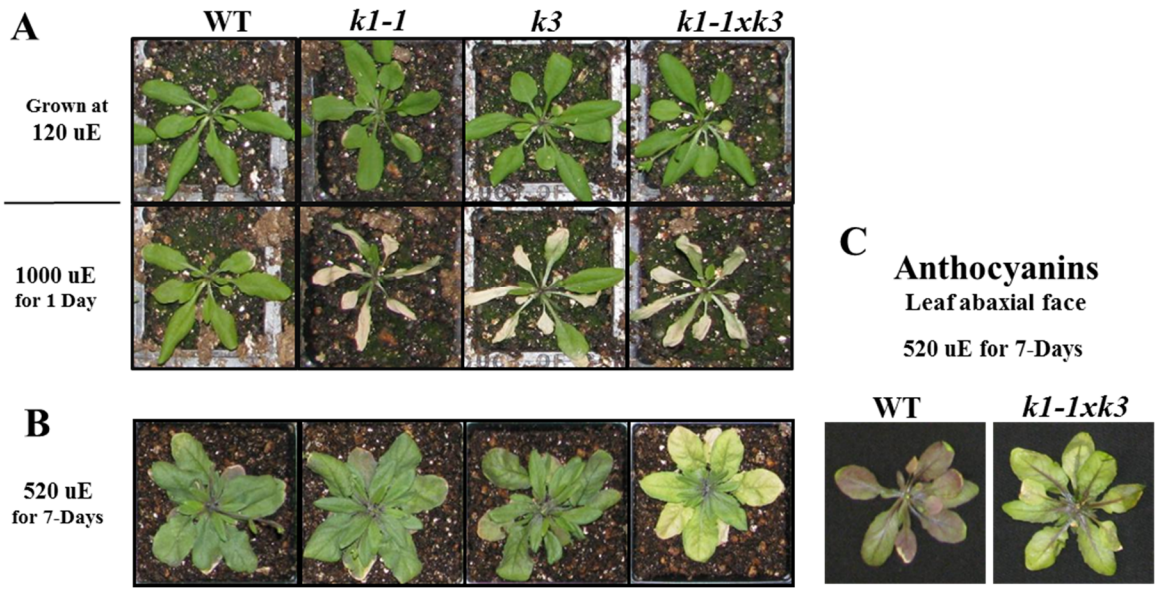

Figure 2. *abc1k1-1* and *abc1k3* demonstrate a conditional and synergistic light stress phenotype. A, mature, 3 week-old plants grown under a 120 µE light regime were transferred to 1000 µE and grown for 1 day. B, mature, 3 week-old plants grown under a 120 µE light regime, were transferred to 520 µE and grown for 7 days. C, the abaxial face of leaves of WT and *k1-1xk3* individuals treated with moderate-light stress treatment for 7 days demonstrate the lack of anthocyanin accumulation outside of the vasculature in *k1-1xk3* individuals.

Measurement of extracted chlorophylls and carotenoids revealed a steady depletion of the photosynthetic pigments in *k1k3* over the course of the light stress treatment, reaching levels 50% and 66% that of pre-stress tissue, respectively, after 7 days of light stress (Figure 3A). Quantification of xanthophyll pigments from leaf tissue indicated no impairment of xanthophyll cycle induction (i.e. conversion of violaxanthin into zeaxanthin) in *k1k3* although the total xanthophyll pool size did not shown an increase after the first day of stress as observed in the wild-type (Figure 3B). Immunoblotting of total leaf protein revealed near complete loss of the PSII core in *k1k3* after 3 days of light stress treatment (Figure 3C). Thus, it appears that degradation of photosystem II is concurrent with chlorophyll and carotenoid depletion in the

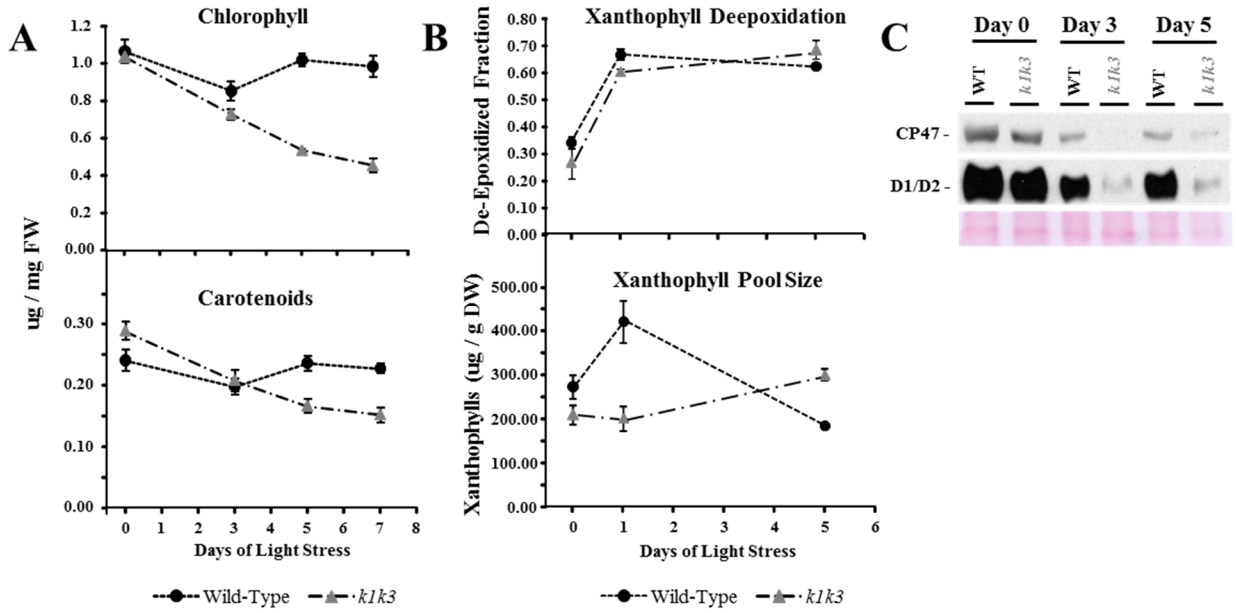

Figure 3. Moderate light stress causes depletion of chlorophyll, carotenoids and photosystem II core components in *k1k3*. A, Chlorophyll and carotenoid levels were measured in mature leaf tissue immediately prior to transferring to moderate light stress and after 3, 5 and 7 days of light stress. B, Measure of xanthophyll cycle induction and xanthophyll pool size in response to moderate light stress using HPLC. Xanthophyll de-epoxidation is measured as (Z+0.5A)/(Z+A+V) where Z is zeaxanthin, A is antheraxanthin and V is violaxanthin. The xanthophyll pool size is the total of Z, A, and V on dry weight basis. C, Immunoblots of mature leaf tissue in response to 5x light stress treatment. Total protein was extracted from mature leaf tissue immediately prior to transferring to 5x light stress and after 3 and 5 days of the light stress. 20 µg of protein from each sample was separated by SDS-PAGE and immunoblotted with indicated antibody. Ponceau stain of Rubisco large subunit is included as a loading control. Error bars measure one standard deviation of 3 biological replicates. Where error bars are not included, they are smaller than the data point symbol.

thylakoids of *k1k3* (also see *section 4.3.5* below).

A very similar senescent-like degreening with a lack of anthocyanins has been demonstrated in a PG-localized FBN1a,1b,4 RNAi knockdown line under an 8x high light stress (120 µE m^{-2} s^{-1} to 850 µE m^{-2} s^{-1}) combined with cold stress (23°C to 15°C) [32]. Surprisingly, this phenotype could be fully complemented by jasmonic acid (JA) treatment; however, a similar

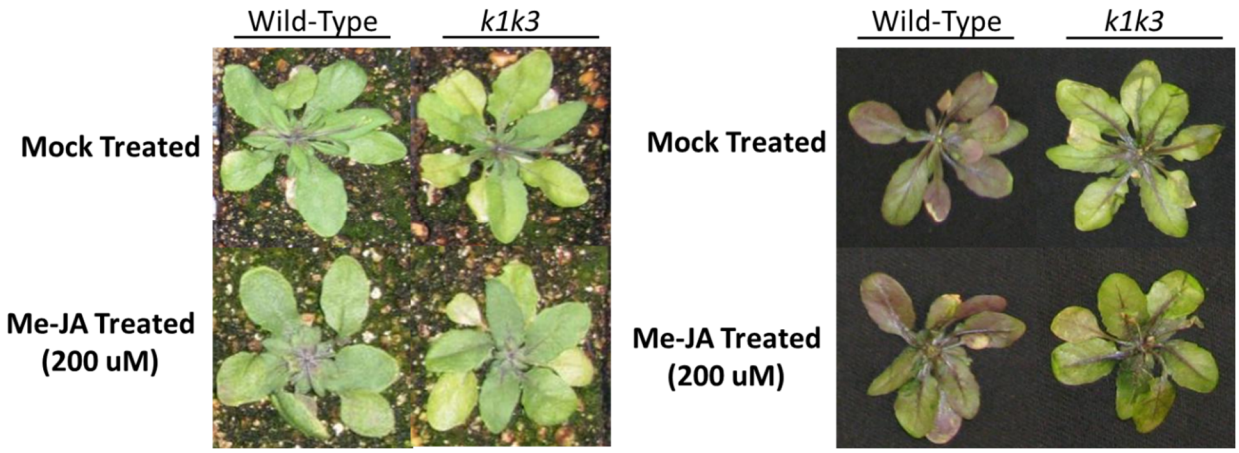

Figure 4. Treatment with methyl-jasmonate (Me-JA) fails to complement the 5x light stress phenotype found in *k1k3* individuals. Plants were treated with or without 200 μM Me-JA as a foliar spray once every 24 hours, beginning the day before the stress treatment. Individuals shown here have been under 5x light stress for seven days. A, adaxial face of the plants. B, abaxial face of the plants, illustrating lack of anthocyanins.

treatment on the *k1k3* individuals failed to prevent or delay the degreening (Figure 4).

The degreening observed in the *k1k3* leaves under moderate light stress may reflect induction of a senescence-like program, or an alternative programmed cell death (PCD) response. An easily discernible distinction between senescence and many other forms of PCD is the reversibility of senescence. Thus, plants were tested for their ability to regreen by subjecting them to the 5x light stress for either 3, 5 or 7 days and then returning them to low light levels (pre-stress intensity). Mature leaves which had initiated degreening failed to regreen, instead continuing to degreen and necrose albeit at a reduced rate than under the elevated light intensities (Figure 5). At the same time, young leaf tissue which did not initiate degreening while under the light stress treatment did not initiate 'delayed' degreening after returning to the original light intensity. This suggests that the light stress treatment initiates an irreversible PCD-like response in mature leaves within 3 days, the kinetics of which are dependent on the prevailing light

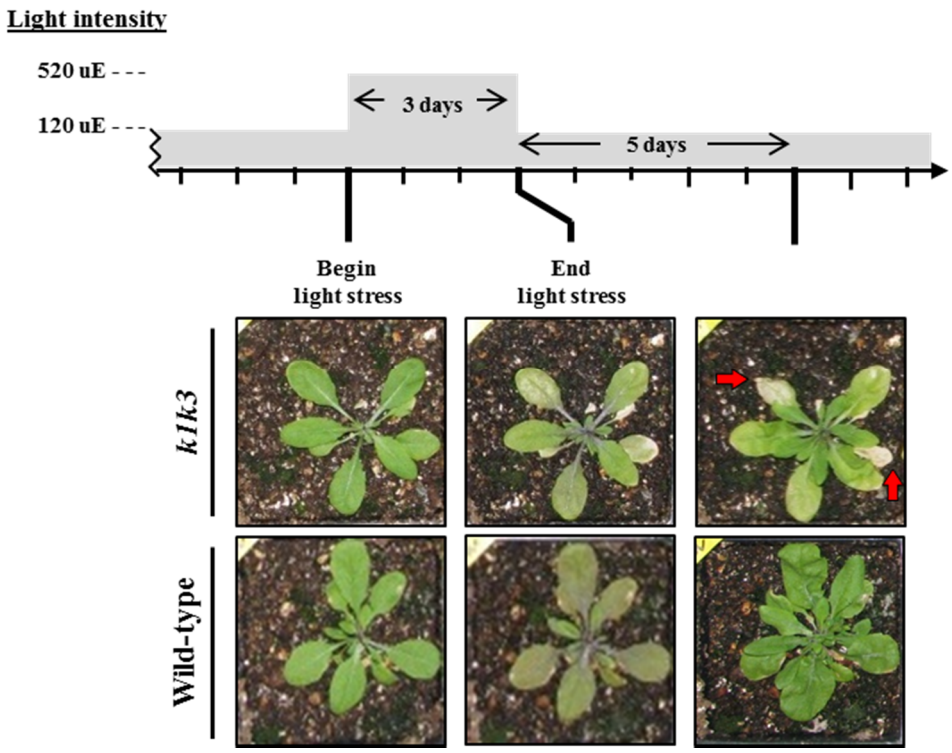

Figure 5. De-greening in *k1k3* continues to progress independent of stress once triggered. Plants were grown for 3 weeks under 120 µE m^{-2} s^{-1} before being transferred to 520 µE m^{-2} s^{-1}, to apply moderate light stress. After 3 days under the light stress, individuals were returned to 120 µE m^{-2} s^{-1} and monitored for an additional 5 days. Wild-type plants accelerated their growth rate and degraded anthocyanins that had accumulated during the stress, while *k1k3* plants continued to necrose and degreen. A representative individual from each genotype is illustrated. Red arrows point out leaf necrosis developing in the *k1k3* individual after removal from the moderate stress regime.

intensity. To study the role of the ABC1K1 and ABC1K3, *k1k3* offers a convenient tool as it provides viable tissue with a relatively mild light stress, minimizing pleiotropic effects. Thus, we sought to further characterize the response of *k1k3* to the 5x light stress treatment. The remainder of the experiments therefore concern comparison of wild-type and *k1k3* individuals.

***4.3.3 Oxidative stress in* k1k3** The degreening phenotype in *k1k3* may be due to elevated oxidative stress. Thus, ROS accumulation in the leaf was studied by tissue stains specific for

hydrogen peroxide (H_2O_2) and superoxide (O_2^-) immediately prior to the light transition, and at 2, 6, 16 hours and 2 days after light transition. Prior to light transition, strong H_2O_2 accumulation in the leaf vasculature and occasional small patches of accumulation along the leaf margins in both genotypes was found (Figure 6). The light transition did not lead to enhanced accumulation in either genotype, though H_2O_2 accumulation in the vasculature in both genotypes had decreased considerably at the 16 hour and 2 day time points. Staining for O_2^-, using nitroblue tetrazolium (NBT), revealed an intense burst of accumulation throughout the leaf tissue 2 hours after light transition in both genotypes (Figure 6), which tapered over the remainder of the time course.

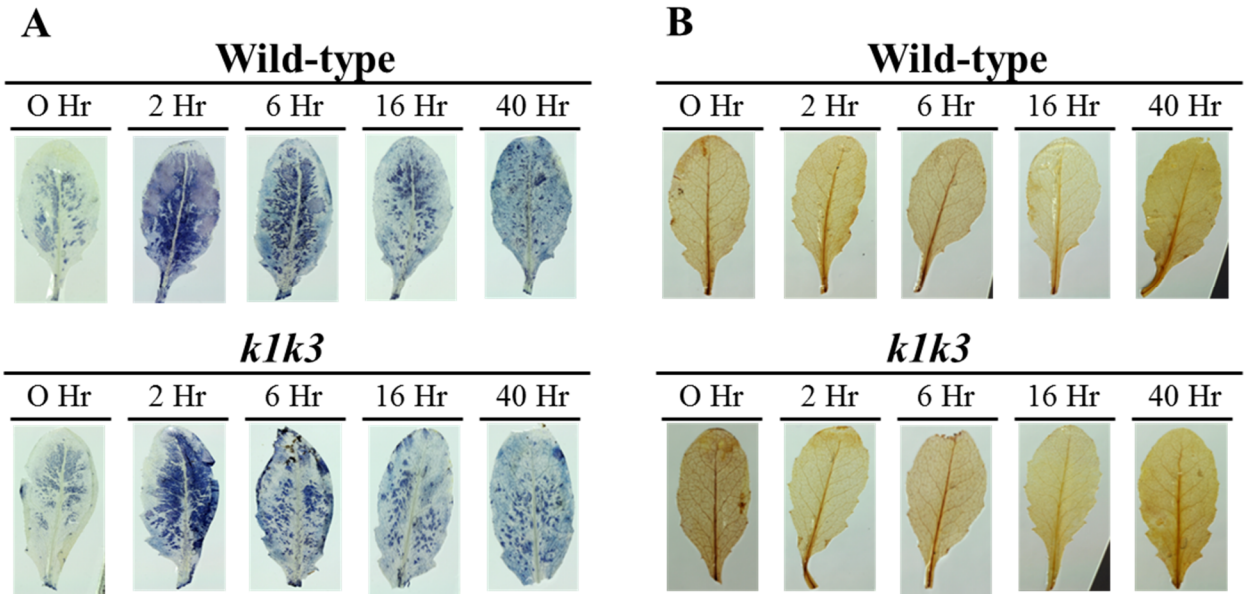

Figure 6. Cell stains for hydrogen peroxide and superoxide over moderate light stress time course. The number of hours under light stress before harvesting and staining are indicated. Photographs are representative of 3 biological replicates of each genotype and time point. A, nitroblue tetrazolium in the presence of superoxide develops a blue precipitate. B, diaminobenzidine in the presence of hydrogen peroxide develops a brown precipitate.

Singlet oxygen ($^1O_2$) is an additional ROS produced as a byproduct of normal photosynthetic activity, but is difficult to measure *in vivo*. Elevated levels of $^1O_2$ produced under excess excitation energy can activate an EXECUTER1- and EXECUTER2-dependent retrograde signaling pathway leading to programmed cell death [33]. Thus a dependence of light-stress sensitivity on $^1O_2$-dependent signaling was tested using the *EXECUTER1* and *EXECUTER2* genes (*EX1*, *EX2*). However, the phenotype of a quadruple mutant, deficient in the *EXECUTER* genes and the *ABC1K* genes, developed the same degreening phenotype at the same rate and magnitude under both light stress regimes (Figure 7). This contradicts the involvement of the EXECUTER-dependent $^1O_2$ signaling pathway in the 5x and 10x light stress phenotypes in *k1k3*.

The central role of the water-soluble ascorbate-glutathione cycle in ROS scavenging means changes in the ascorbate or glutathione levels may indicate changes in ROS levels in tissue [34]. Concentration and oxidation of the ascorbate and glutathione were measured from total leaf samples using absorbance spectrophotometry (Figure 8). Prior to light stress, ascrobate levels were identical between the two genotypes, though glutathione was about 20% higher in *k1k3*. In response to the 5x light stress, ascorbate levels increased in the wild-type tissue, whereas glutathione levels increased in *k1k3* tissue (Figure 8). The oxidation states of the ascorbate and glutathione were not significantly different between the genotypes.

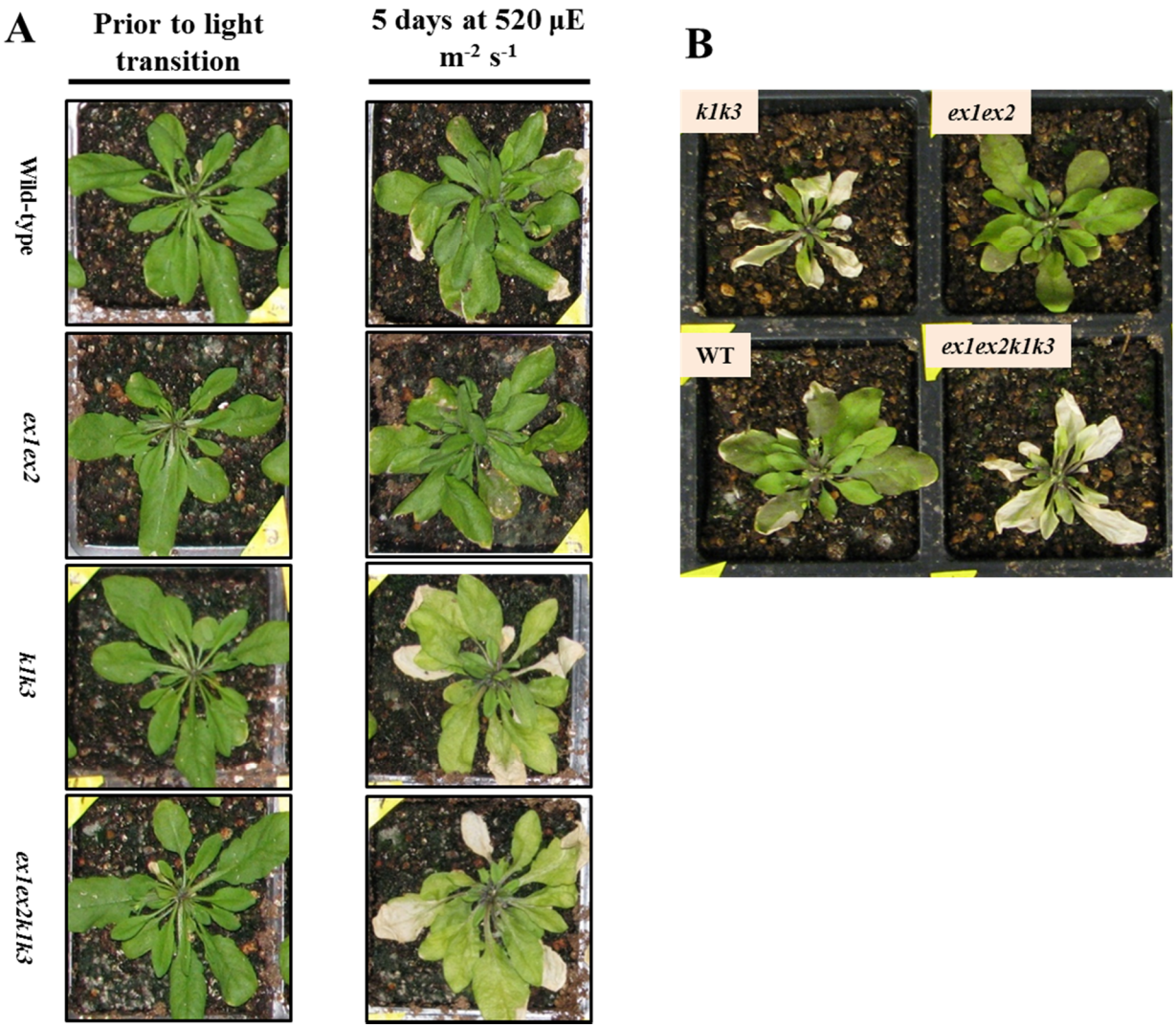

Figure 7. The conditional phenotype of *k1k3* is unaffected by lesions in the *EX1* and *EX2* loci involved in singlet oxygen retrograde signaling, leading to programmed cell death. Wild-type plants were grown up alongside *k1k3*, *ex1ex2*, and the corresponding quadruple mutant, *ex1ex2k1k3*. All four genotypes were found to grow and develop, at the same rate. When plants were transferred to 520 (A) or 1000 (B) µE m^{-2} s^{-1}, *ex1ex2* did not display a conditional light stress phenotype, while the quadruple mutant displayed the same degreening as *k1k3*.

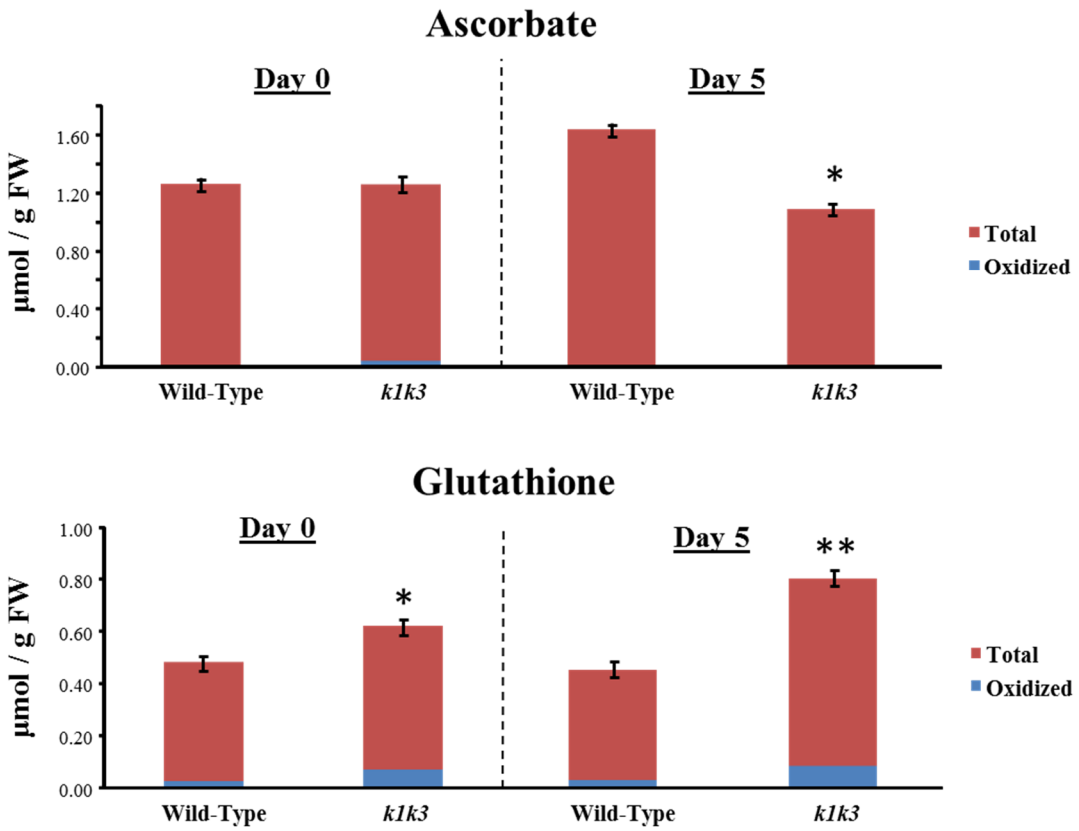

Figure 8. Ascorbate and glutathione levels in total leaf tissue. Ascorbate and glutathione were measured spectrophotometrically as described in [35]. Error bars indicate ± 1 standard error of four biological replicates. The standard error for amounts of oxidized compounds are too small for visualization in the image and have been excluded. Statistically significant differences of total levels of ascorbate or glutathione between genotypes are indicated by an asterisk, as follows: * p-value < 0.05; ** p-value < 0.01, n=4.

4.3.4 Electron microscopy The impact of loss of ABC1K1 and ABC1K3 on the ultrastructure of chloroplasts was tested under permissive growth and in response to 5x light stress. Prior to stress, ultrastructure of the PG and chloroplasts was indistinguishable between both genotypes (Figure 9A). Average chloroplast cross-sections in both genotypes were about 7.9 μm^2 and average PG cross-sections were about 6.3 nm^2. All PGs stained darkly in the presence of osmium tetroxide. An average of about 1.2 PGs could be found per μm^2 of chloroplast area in both genotypes.

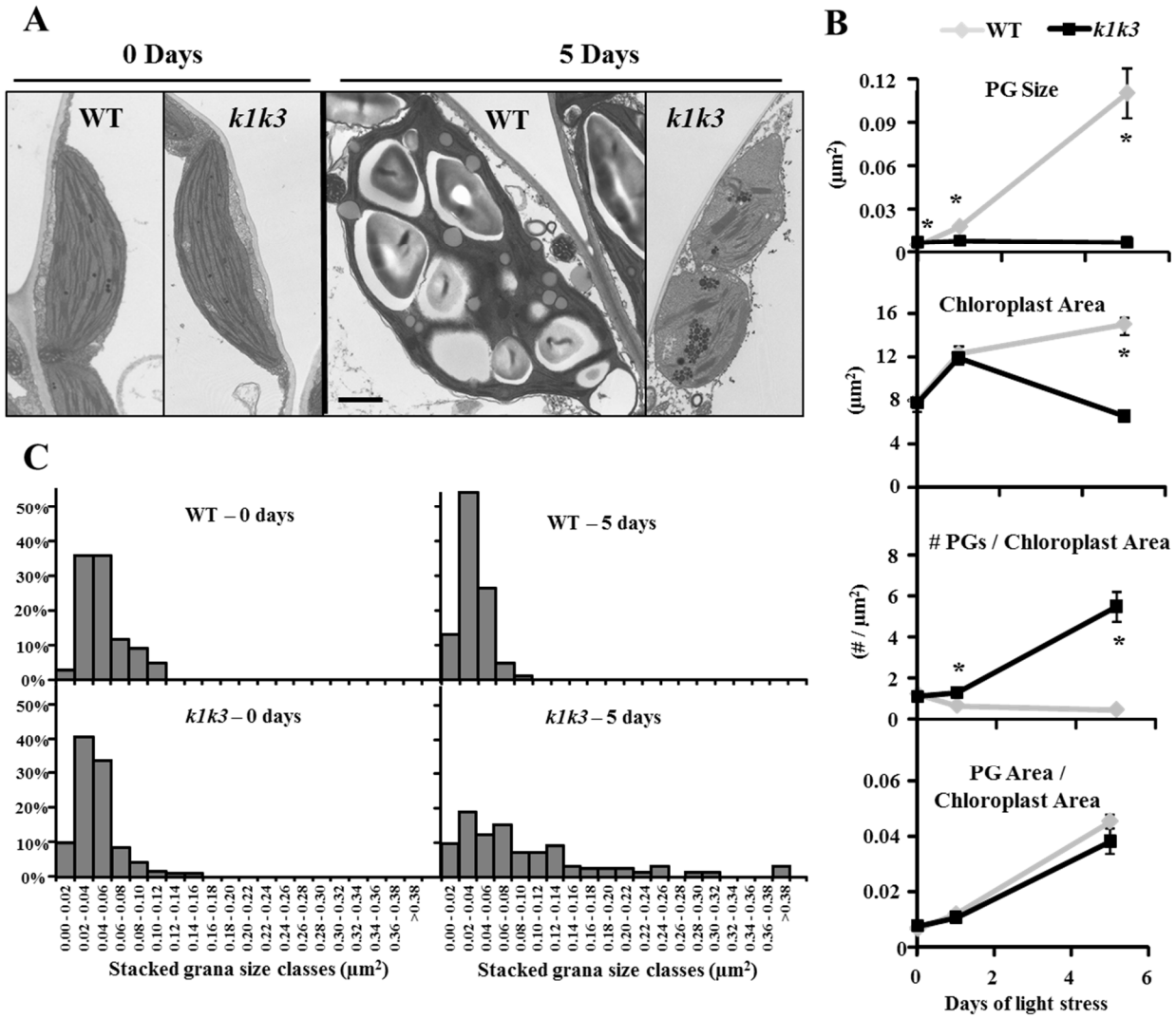

Figure 9. Plastid ultrastructure in wild-type and *k1k3* responds differently to moderate light stress. Mature leaf tissue was harvested 2 hours after the onset of the photoperiod after 0, 1, and 5 days of 5x light stress. A, representative micrographs after 0 and 5 days illustrate the genotype-specific responses to moderate light stress in the chloroplast ultrastructure. All micrographs are to the same scale. Black scale bar denotes 1 µm. B, graphs of four parameters measured from electron micrographs. Each data point represents the mean measurement from 24 micrographs of 3 individual plants. Error bars represent ± 1 standard error. * indicates $p \ll 0.001$ between the two genotypes at each time point. C, Histogram demonstrating the granal hyperstacking in *k1k3* after 0 and 5 days of moderate light stress. At least 80 granal stacks from 3 individuals were measured for each genotype at each time point.

In response to the 5x light stress, the plastid ultrastructure was altered in both genotypes, albeit in different ways. Wild-type PG size increased after 1 day of stress and increased further after 5 days under the stress treatment (Figure 9B), consistent with the well-documented dynamics of PG size in stressed tissue [36]. Concomitant with the increased size, the interior of many PGs stained lighter with a solid black periphery. In fact, the staining was reminiscent of oil bodies derived from the endoplasmic reticulum, see e.g. [37, 38]. The chloroplast area also increased after 1 and 5 days of light stress, causing a subtle decrease in the number of PGs per chloroplast area.

Under light stress, *k1k3* ultrastructure differed dramatically from the wild-type. However, the integrity of the chloroplasts and thylakoid membranes was maintained, indicating the degradation of photosynthetic pigments did not correspond to a dismantling of the photosynthetic organelles as a whole. The *k1k3* PG area remained remarkably consistent across the time-course, although, the number of PGs per chloroplast area increased almost 6-fold after 5 days of stress treatment, along with the induction of granal hyperstacking (Figure 9C). The size of the grana hyperstacking was on the order of that reported in the starch synthesis and sucrose export defective *adg1-1/tpt-1* double mutant [39]. The PGs, absent an increase in size, continued to stain solid black, lacking any light gray staining as seen in the wild-type light stressed PGs. The chloroplasts of *k1k3* also swelled transiently after 1 day of stress, in parallel with the wild-type, but had reverted back to near pre-stress levels by 5 days of stress. The two genotypes increase their ratio of PG area per chloroplast area in parallel, albeit using different methods; while the wild-type increases the size of its PGs, *k1k3* increases its number of PGs (Figure 9B). Thus, after light stress, *k1k3* PGs have a much higher surface area:volume ratio than wild-type, with

implications for the accumulation of amphiphilic versus hydrophobic lipids (see *section 4.4 Discussion*).

***4.3.5 Quantitative protein composition of the leaf tissue of wild-type and* k1k3** Understanding the protein abundance changes in *k1k3* leaf tissue can provide valuable information about the molecular nature of the degreening phenotype and the function of the *ABC1K1* and *ABC1K3* genes. Thus, a quantitative proteomics analysis using spectral counting was undertaken on total leaf protein samples collected from both genotypes after 0, 3, and 5 days of 5x light stress. A total of 2274 proteins (or groups of closely related proteins) were identified across the six genotype-time-points. ABC1K1 and ABC1K3 were identified in two and three of the three time points of wild-type, respectively, but no peptides were identified in *k1k3* individuals, supporting the null mutant assignment of the *abc1k1* and *abc1k3*. High correlation coefficients between the three replicates of each genotype-time point ($R^2 > 0.93$) indicate excellent reproducibility (data not shown).

At Day 0, prior to the light stress, only 15 of the 2274 proteins were differentially accumulating between the genotypes with a p-value < 0.01 as calculated by the GLEE software program [40]. Thus, very little protein phenotype was present in *k1k3* prior to light stress, consistent with the whole plant and molecular analyses presented above. One of the fifteen proteins showing differential accumulation at Day 0 was the PG-localized carotenid cleavage dioxygenase 4 (CCD4), which was persistently under-accumulating in *k1k3* leaves (~10-30% of WT) at all three time points.

Consistent with the pigment analyses and degreening phenotype, the PSI, PSII, Cytochrome b_6f, and NDH complexes, but not the coupling factor complex, were reduced in

k1k3 compared to wild-type under light stress (Figure 10A). This was especially pronounced for the PSII core complex. Proteins of the photorespiratory pathway and Calvin cycle accumulated to comparable levels in wild-type and *k1k3* at all three time points, and thus were not impacted by the loss of *ABC1K1* and *ABC1K3* as the photosystem complexes were (data not shown).

A regulatory role for ABC1K1 and ABC1K3 in plastid protein degradation and prenyl-lipid metabolism was suggested by the transcription coexpression patterns of *ABC1K1* and *ABC1K3*. In addition to the reduced levels of the PG-localized CCD4 in *k1k3* at all time-points, three prenyl-lipid coexpressers of *ABC1K1* and *ABC1K3* [19] were effected under light stress. Geranylgeranyl diphosphate reductase (GGDR) was not detected in *k1k3* after 3 days of stress, while zeaxanthin epoxidase (ZEP) and ζ–carotene desaturase (ZDS), were elevated in *k1k3* after 5 days of light stress (Figure 10B). Though the low abundance and large standard deviations of ZEP and ZDS made it difficult to determine the statistical significance of the genotypic effect, the GLEE software program considered the differences between wild-type and *k1k3* to be significant. Several subunits of the stromal Clp and thylakoid FtsH plastid protease complexes coexpressed with *ABC1K1* and *ABC1K3* as well. A slight but statistically significant elevation in the Clp complex was found in *k1k3* at 5 days of light stress (Figure 10C). Similarly, the FtsH complex and DegP protease subunits were elevated 3 days after light stress in *k1k3*, relative to wild-type.

Figure 10. Protein abundance of selected proteins and complexes in wild-type and *k1k3* total leaf tissue. Abundance was measured as the average of the sum of NadjSPC of all proteins from three biological replicates. Statistically significant differences between genotypes with p-value < 0.01 are indicated with a double asterisk above the time point.

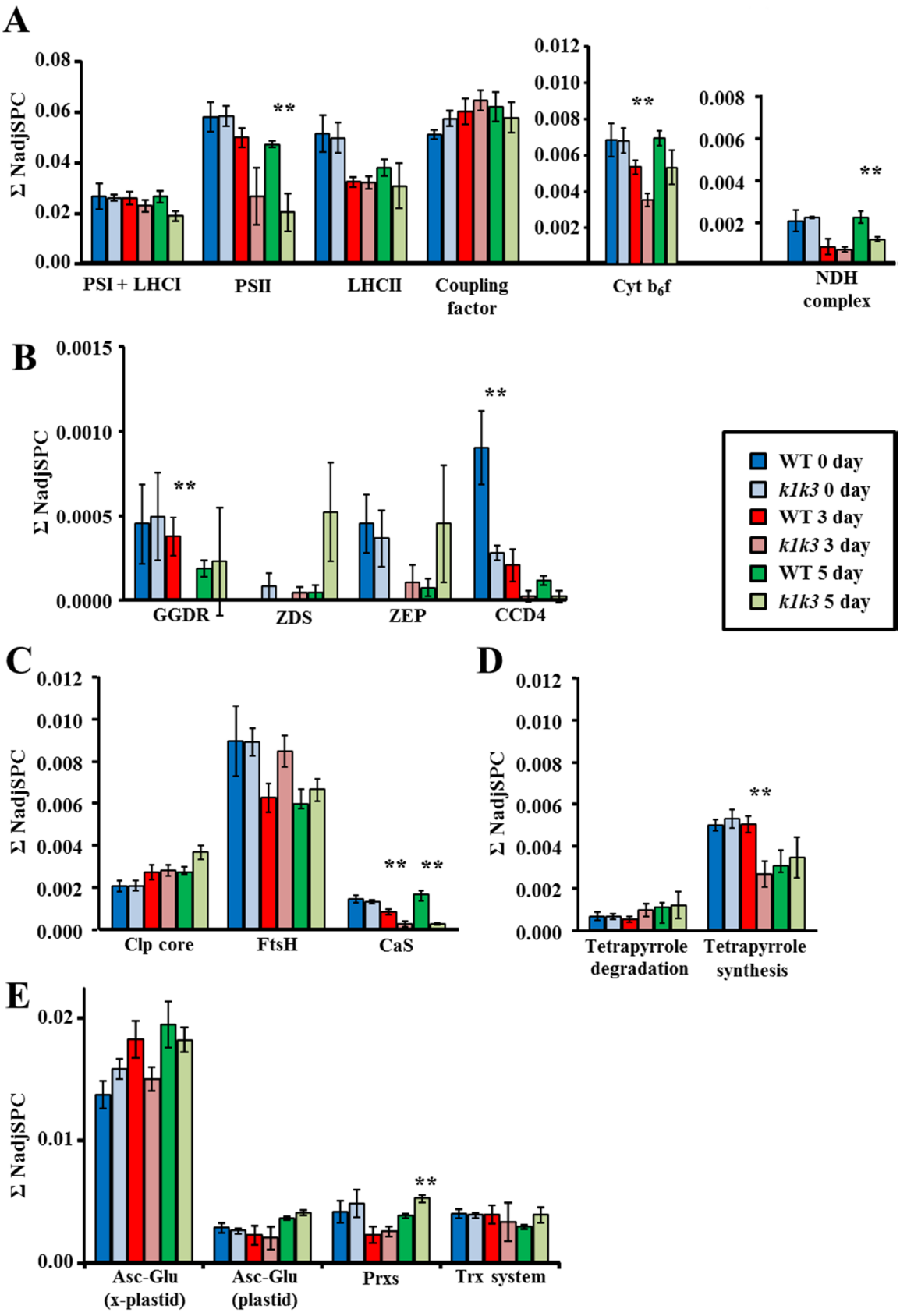
A
Σ NadjSPC
0.08
0.06
0.04
0.02
0.00
0.012
0.010
0.008
0.006
0.004
0.002
0.008
0.006
0.004
0.002
**
**
**
PSI + LHCI
PSII
LHCII
Coupling factor
Cyt b6f
NDH complex
B
Σ NadjSPC
0.0015
0.0010
0.0005
0.0000
**
**
GGDR
ZDS
ZEP
CCD4
WT 0 day
k1k3 0 day
WT 3 day
k1k3 3 day
WT 5 day
k1k3 5 day
C
Σ NadjSPC
0.012
0.010
0.008
0.006
0.004
0.002
0.000
** **
Clp core
FtsH
CaS
D
Σ NadjSPC
0.012
0.010
0.008
0.006
0.004
0.002
0.000
**
Tetrapyrrole degradation
Tetrapyrrole synthesis
E
Σ NadjSPC
0.02
0.01
0.00
**
Asc-Glu (x-plastid)
Asc-Glu (plastid)
Prxs
Trx system

It was reported previously that an RNAi line using the full length sequence of *ABC1K1* was impaired in chlorophyll degradation [29]. However, no altered levels of chlorophyll degradation enzymes (chlorophyllase, pheophorbide a oxygenase, and red chlorophyll catabolite reductase) were found in *k1k3* leaves either before or after light stress, which is surprising in light of the degreening phenotype (Figure 10D). On the other hand, proteins of tetrapyrrole synthesis were reduced in *k1k3* relative to wild-type at 3 days of light stress, suggesting reduced chlorophyll accumulation may be accomplished by reduced synthesis rather than elevated degradation in *k1k3*.

The light stress-dependent degreening in *k1k3* may be due to impaired induction of alternative electron flows which can serve to dissipate excess excitation energy. The PGR5 and PGRL1A and 1B proteins are implicated in regulation of cyclic electron flow around PSI [41, 42], and PGRL1A is a component of the PG coexpression network [19]. However, accumulation levels of the three proteins were indistinguishable between the genotypes. An alternative, PGR5-independent cyclic electron flow is created by the NAD(P)H dehydrogenase (NDH) complex, which catalyzes reduction of the photosynthetic PQ pool from stromal NAD(P)H [43-45]. Fifteen subunits in the NDH complex were identified and quantified in the proteomics. While protein investment of the NDH complex was comparable between genotypes prior to light stress and after 3 days of light stress, a significant depletion of the complex was apparent after 5 days of stress (Figure 10A).

Although the state transition kinases (STN7 and STN8) and phosphatase (TAP38) were not identified in the proteomics experiment, Calcium-sensing receptor protein (CaS), localized at the thylakoid membrane, accumulated at reduced levels in *k1k3* leaves (~15-30% of WT) under

stress. The function of CaS is unclear but is localized at the thylakoid membrane where it binds Ca^{2+} and is phosphorylated in an STN8-dependent manner [10].

Elevated levels of oxidative stress in leaf tissue could be expected to induce increased accumulation of ROS scavenging enzymes. Thus, the protein investment of the two genotypes in ROS scavenging was quantified (Figure 10E). Peroxiredoxins (Prxs) are thiol-dependent scavengers of a diverse set of peroxide substrates including H_2O_2 and peroxidized lipids [46]. Plastidic Prxs were found to accumulate at an elevated level 5 days after light stress. The increased investment at this time point was accounted for exclusively by the 2-Cys PrxB isoform which was 2-fold more abundant in *k1k3* than wild-type. Thioredoxins (Trxs) are redox-sensitive proteins that serve as important signaling components through redox regulation of various enzymes [47, 48], supply electrons to Prxs [49] and have been suggested to affect the LHCII state transition [50]. No differential accumulation of Trxs was found between genotypes either before or after stress. The ascorbate-glutathione ROS scavenging system relies on redox cycling of the antioxidant molecules ascorbate and glutathione, accomplishing the conversion of O_2^- and H_2O_2 to H_2O. Protein investment in the plastidic and extra-plastidic ascorbate-glutathione systems was comparable between genotypes both before and after light stress treatment (Figure 10E). Much of this ROS scavenging system was identified in the proteomics data including isoforms of (mono)dehydroascorbate reductase, ascorbate peroxidase, glutathione reductase, glutathione peroxidase, superoxide dismutase and catalase. In sum, evidence of elevated levels of ROS scavenging proteins in *k1k3* is confined to the plastidic 2-Cys PrxB, further suggesting that ROS accumulation is not substantially elevated in *k1k3*, consistent with ROS stains above.

Collectively, the leaf proteomics results reveal alterations in photosynthetic complexes, plastid protease machinery, and chlorophyll biosynthesis, consistent with the degreening

phenotype under light stress. Of particular interest, an altered accumulation was found in the carotenoid metabolic enzymes, CCD4, ZEP and ZDS, as well as the CaS signaling protein of the thylakoid membrane. The loss of ABC1K1 and ABC1K3 had very little impact on the leaf at the protein level prior to light stress, the CCD4 depletion being a notable exception.

***4.3.6 Quantitative protein composition of the PG of wild-Type and* k1k3** To more closely investigate how the plastoglobule proteome is affected by the loss of ABC1K1 and ABC1K3, the quantitative proteomics analysis was performed on PGs isolated 5 days after light stress from thylakoid membranes. Attempts using leaf tissue prior to light stress failed to extract PGs, likely because the PGs were smaller and lower abundant (Figure 9). Thylakoid membranes were sonicated to physically separate PGs from the thylakoid membrane system and were subsequently purified by density centrifugation. This methodology has been demonstrated to isolate more than 75% of the PG material from thylakoid membranes into highly enriched PG preparations [19]. To exclude potential low abundant contaminants, proteins were required to display an average NadjSPC of at least 0.001 in the PG preparations, representing 0.1% of the extracted protein mass. To identify PG-enriched proteins, at least 15-fold enriched protein abundance over the total leaf preparations was required (Figure 11). This identified a set of 37 and 39 PG-enriched proteins in WT and *k1k3*, respectively, twenty-three of which were enriched in both genotypes. In total fifty-three proteins were found enriched in at least one of the two genotypes and were compiled in Table 1.

The abundance of the fifty-three proteins was compared between the two genotypes to identify significant changes. A greater number of low-abundant contaminating proteins were extracted with the *k1k3* PG preparations, possibly as a result of the unique ultrastructure of the

chloroplast and PG. Thus, each protein's ratio between wild-type and *k1k3* differed depending on whether abundance was calculated from the whole PG preparations or was normalized to the set of fifty-three PG-enriched proteins. To identify the most significantly altered proteins a protein was required to be at least 2-fold up or down regulated by both calculations. Using this criterion it was found that most (~66%) of the wild-type core proteome of the PG was unchanged in *k1k3*.

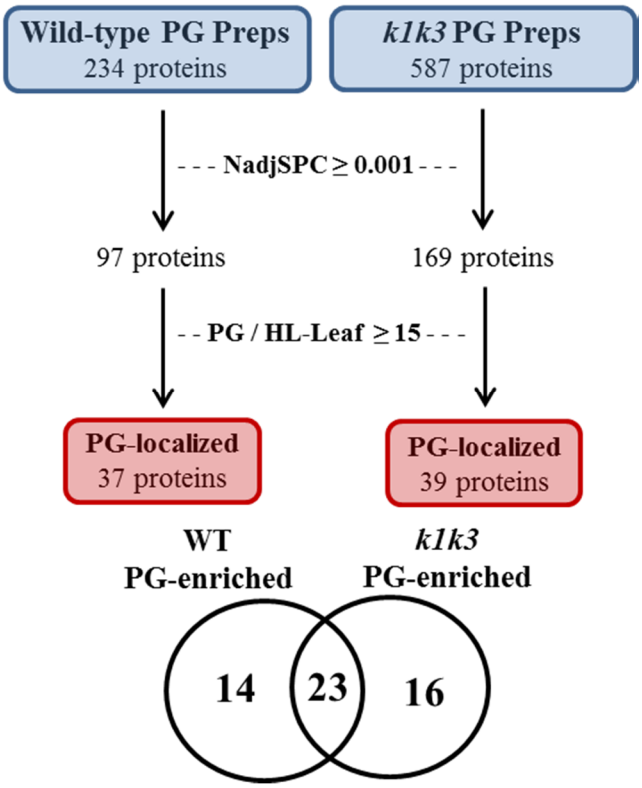

Figure 11. Workflow for identification of PG enriched proteins in wild-type and *k1k3* PG preparations. All proteins identified by more than one non-redundant peptide over three independent preparations of wild-type and *k1k3* PGs were filtered first by a minimal abundance corresponding to NadjSPC of 0.001, and second, to a minimal enrichment ratio of 15 over 5x light-stressed total leaf tissue of the same genotype. Twenty-three proteins were enriched in PG preparations of both genotypes by this method. Fourteen were exclusively enriched in the WT PG preparations and sixteen exclusively in the *k1k3* PG preparations.

Table 1. Abundances of WT and *k1k3* PG-enriched proteins under light stress

Accession	Name	WT core [a]	Module [a]	WT-enriched	*k1k3*-enriched	% of WT PG prep	% of *k1k3* PG prep	*k1k3* (% of WT)	*k1k3* (% of WT) [b]
AT1G73750	Unknown SAG	x	I	*x*		*0.2*	*0.0*	0% *	0%
AT3G07700	ABC1K7	x	I	*x*	*x*	*0.4*	*0.1*	*36%* *	*55%*
AT3G27110	M48 metalloprotease	x	I	*x*	*x*	*0.2*	*0.5*	254%	387%
AT1G54570	Diacylglycerol transferase 3 (DGAT 3)	x	I	*x*	*x*	*1.5*	*1.4*	*93%*	*142%*
AT5G13800	Pheophytinase (PPH)		I		*x*	*0.0*	*0.2*	∞ *	∞ *
AT1G79600	ABC1K3	x	II	*x*		*2.6*	*0.0*	0% *	0%
AT4G31390	ABC1K1	x	II	*x*		*2.6*	*0.0*	0% *	0%
AT3G24190	ABC1K6	x	II	*x*		*1.5*	*0.1*	5% *	8%
AT2G41040	UbiE methyltransferase related 2	x	II	*x*		*0.9*	*0.3*	28%	42%
AT4G19170	Carotenoid cleaveage dioxygenase (CCD4)	x	II	*x*	*x*	*1.8*	*0.3*	16% *	24%
AT2G34460	Flavin reductase-related 2	x	II	*x*	*x*	*0.9*	*0.6*	*73%*	*112%*
AT1G06690	Aldo/keto reductase	x	II	*x*		*0.9*	*0.6*	*73%*	*111%*
AT5G08740	NAD(P)H dehydrogenase C1 (NDC1)	x	II	*x*	*x*	*1.4*	*0.8*	*55%*	*84%*
AT5G20140	SOUL heme-binding 2		II		*x*	*0.0*	*0.1*	∞	∞
AT1G71480	Nuclear transport factor 2 (NTF2) family		II		*x*	*0.0*	*0.1*	∞ *	∞ *
AT4G18810	NAD(P)-binding UOS1		II	*x*		*0.3*	*0.4*	*119%*	*182%*
AT4G13200	Unknown protein 1	x	III	*x*	*x*	*1.2*	*1.0*	*79%*	*120%*
AT3G58010	Fibrillin 7a (FBN7a)	x	III	*x*	*x*	*2.3*	*1.8*	*75%*	*114%*
AT5G05200	ABC1K9	x	III	*x*	*x*	*3.0*	*1.9*	*64%* *	*98%*
AT2G35490	Fibrillin 2 (FBN2)	x	III	*x*	*x*	*3.6*	*3.9*	*108%*	*165%*
AT3G23400	Fibrillin 4 (FBN4)	x	III	*x*	*x*	*6.6*	*4.4*	*68%*	*103%*
AT4G03520	Thioredoxin M2		III	*x*		*0.2*	*0.0*	0%	0%
AT3G43540	Unknown protein 2	x	IV	*x*	*x*	*0.7*	*0.4*	*60%*	*92%*
AT2G42130	Fibrillin 7b (FBN7b)	x	IV	*x*	*x*	*1.4*	*0.5*	*35%* *	*53%*
AT3G26060	Peroxiredoxin Q (Prx Q)		IV		*x*	*0.0*	*0.2*	∞ *	∞ *
AT1G71810	ABC1K5	x		*x*		*1.0*	*0.0*	0% *	0%
AT5G41120	Esterase/lipase/thioesterase (Esterase 1)	x		*x*		*0.1*	*0.1*	*53%*	*81%*
AT3G26840	Diacylglycerol Acyltransferase 4 (DGAT 4)	x		*x*	*x*	*0.8*	*0.2*	21% *	32%
AT1G78140	UbiE methyltransferase related 1	x		*x*	*x*	*0.9*	*0.3*	30% *	46%
AT4G39730	PLAT/LH2 - 1	x		*x*	*x*	*1.0*	*0.3*	30%	46%
AT1G32220	Flavin reductase-related 1	x		*x*	*x*	*1.2*	*0.4*	*34%*	*52%*
AT2G46910	Fibrillin 8 (FBN8)	x		*x*	*x*	*1.1*	*0.5*	*50%*	*76%*
AT3G10130	SOUL heme-binding 1	x		*x*	*x*	*1.0*	*0.9*	*90%*	*137%*
AT4G32770	Tocopherol cyclase (VTE1)	x		*x*	*x*	*1.5*	*1.6*	*104%*	*158%*
AT4G22240	Fibrillin 1b (FBN1b)	x		*x*	*x*	*5.7*	*3.5*	*61%*	*93%*
AT4G04020	Fibrillin 1a (FBN1a)	x		*x*	*x*	*9.1*	*5.8*	*64%*	*97%*
ATCG01060	PsaC			*x*		*0.1*	*0.0*	0%	0%
AT5G62140	Unknown protein			*x*		*0.1*	*0.1*	*55%*	*84%*
AT1G74470	Geranylgeranyl-PP reductase (GGDR)			*x*		*0.3*	*0.1*	21% *	33%
AT3G01480	Cyclophilin 38 (CYP38)				*x*	*0.0*	*0.1*	2561%	3908%
AT3G11560	Unknown protein				*x*	*0.0*	*0.1*	∞ *	∞ *
AT2G22170	PLAT/LH2 - 2			*x*		*0.5*	*0.2*	30%	46%
AT5G16550	Unknown protein				*x*	*0.1*	*0.2*	296%	452%
AT4G05180	PsbQ OEC16-like				*x*	*0.0*	*0.2*	12545% *	19144%
AT5G16660	Unknown protein				*x*	*0.0*	*0.2*	∞ *	∞ *
AT3G56940	Mg-Protoporphyrin IX cyclase (CHL27)				*x*	*0.0*	*0.2*	977%	1491%
AT2G39330	Jacalin-related lectin 23			*x*	*x*	*0.1*	*0.3*	363%	555%
AT5G06220	Unknown protein				*x*	*0.0*	*0.3*	∞ *	∞ *
AT1G72520	LOX4				*x*	*0.0*	*0.4*	∞ *	∞ *
AT1G51110	Fibrillin 10 (FBN10)				*x*	*0.1*	*0.5*	793%	1210%
AT1G67360	Rubber elongation factor (REF) family				*x*	*0.2*	*0.5*	236%	360%
AT1G03630	Protoporphyrin IX reductase IX C(PORC)				*x*	*0.0*	*0.5*	8218% *	12541%
AT1G17420	LOX3				*x*	*0.0*	*1.5*	∞ *	∞ *
	All other proteins					*40.8*	*61.5*		

a) As determined in *Chapter Two*

b) Normalized to the set of 53 proteins listed in this table

Most of the core proteome that was altered in *k1k3* was down-regulated. Surprisingly, ABC1K5 and ABC1K6 were found at greatly reduced levels (~94% reduced) or not identified in the *k1k3* PG preparations. The strong depletion of ABC1K5 and ABC1K6 suggests their possible engagement in a complex with ABC1K1 and/or ABC1K3. Indeed, ABC1K6 is a member of the same co-expression module II as ABC1K1 and 3, associating with genes of isoprenoid metabolism and plastid proteolysis [19]. Consistent with the total leaf proteomics results, CCD4 was down-regulated about 80% in *k1k3* PG preparations. In addition to ABC1K6 and CCD4, other components of coexpression module II were also affected, including UbiE-like methyltransferase 2 and flavin reductase 2, which were depleted in *k1k3* PGs, and the SOUL heme-binding protein and nuclear transport factor 2 proteins, which accumulated specifically with *k1k3* PGs.

The fibrillin (FBN) proteins were unchanged in *k1k3* PG, with the exception of FBN10 which was only detected in *k1k3* PGs. Surprisingly, two proteins of the chloroplast biosynthesis pathway also accumulated in *k1k3* PGs, Mg-protoporphyrin IX monomethyl cyclase and protoporphyrin IX oxidoreductase C. The proteins reached levels of 0.2% and 0.5% of the total PG mass, which is comparable to the amount of core proteins such as Flavin reductase realated 1 and 2 and UbiE-like methyltransferase 1 and 2.

While DGAT3 levels remained constant, levels of DGAT4 decreased significantly in *k1k3* PGs. This is consistent with the apparent decrease of TAG accumulation in *k1k3* PGs (Figure 9), since the DGAT enzymes putatitively catalyze conversion of diacylglycerol to TAG.

A striking enrichment of JA biosynthetic enzymes at the *k1k3* PG was found (Figure 12). While lipoxygenase 2 (LOX2) did not change in abundance at the whole leaf level, it clearly associated with PGs to a greater degree in *k1k3* chloroplasts. Similarly, allene oxide synthase

(AOS) total leaf abundance was not altered, yet associated stronger with PGs in *k1k3*. Protein accumulation patterns of the other enzymes that were identified in leaf or PG preparations, including lower abundant LOX proteins and several isoforms of allene oxide cyclase (AOC), also showed preferential association with *k1k3* PGs. The PG is a logical localization for the initial steps of the JA biosynthetic pathway, which begins with enzymatic peroxidation of fatty acid molecules catalyzed by 13-LOX enzymes (e.g. LOX2, 3 and 4) (Figure 12B). The JA phytohormone has been implicated in induction of senescence in leaf tissue [51], leading to the suggestion that the degreening phenotype in *k1k3* is a JA-controlled response. This possibility can be tested with application of a JA inhibitor compound, or crossing *k1k3* with a JA insensitive mutant.

Note that while AOS is isolated with the PG preparations, it was not sufficiently enriched relative to total leaf samples in either the wild-type or *k1k3* preparations to justify characterization as PG-localized under the criteria used here. It is suggested that JA biosynthesis is carried out at both the thylakoid and PG, where physiologically relevant fractions of AOS are localizing.

Figure 12. Distribution of plastid-localized JA biosynthesis enzymes in WT and *k1k3* 5-day light stressed leaf or PG. A, NadjSPC are normalized within each protein, illustrating the protein's relative depletion/enrichment in each total leaf or plastoglobule (PG) preparation. A fourth allene oxide cyclase (AOC3) is putatively involved in JA biosynthesis but was not identified in leaf or PG preparations. B, The plastid-localized steps of the JA biosynthesis pathway begin with peroxidation of linolenic acid by 13-lipoxygenase (13-LOX), which may act on the free or esterified form of the fatty acid. The peroxidized fatty acid is subsequently epoxidized by allene oxide synthase (AOS) and cyclized by allene oxide cyclase (AOC) to form oxophytodienoic acid (OPDA), which is exported to the peroxisome for subsequent processing by OPDA Reductase (OPR) and three rounds of β-oxidation to produce the jasmonate phytohormone. The relative NadjSPC of LOX2 is set to 0.0129; of LOX3, 0.0147; of LOX4, 0.0040; of AOS, 0.0657; of AOC1, 0.0012; of AOC2, 0.0012, of AOC4, 0.0001; and of OPR, 0.0001.

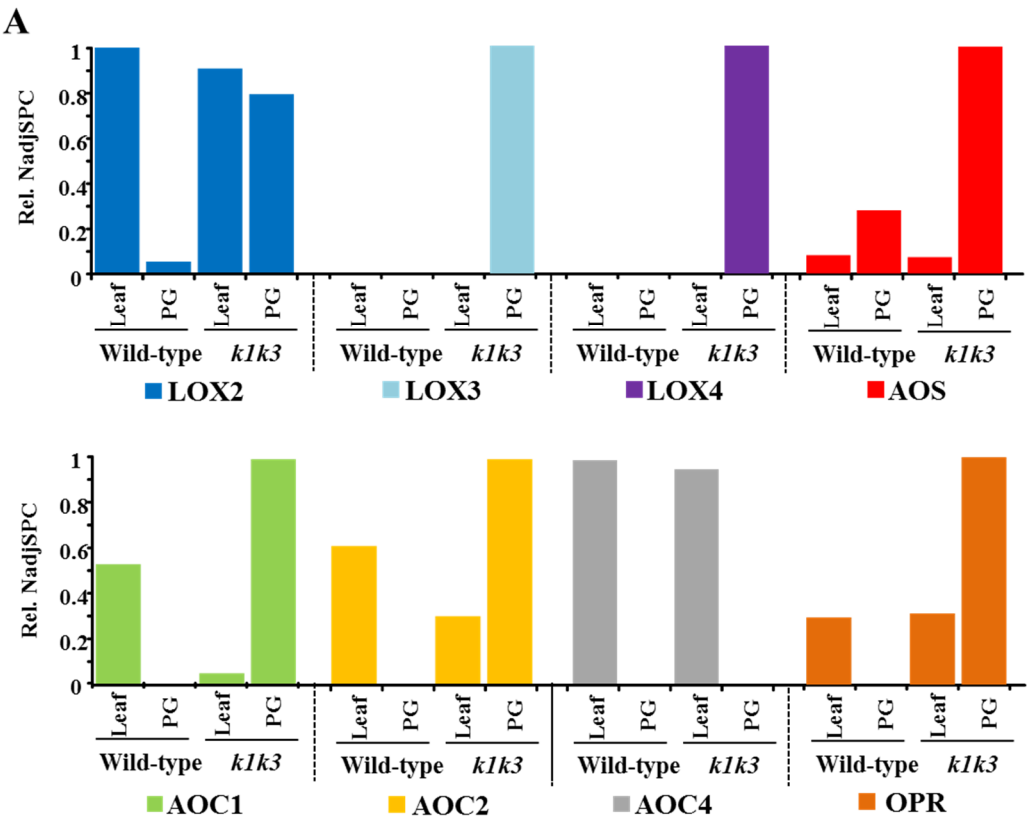
A
Rel. NadjSPC
1
0.8
0.6
0.4
0.2
0
Leaf
PG
Wild-type
k1k3
LOX2
LOX3
LOX4
AOS
AOC1
AOC2
AOC4
OPR

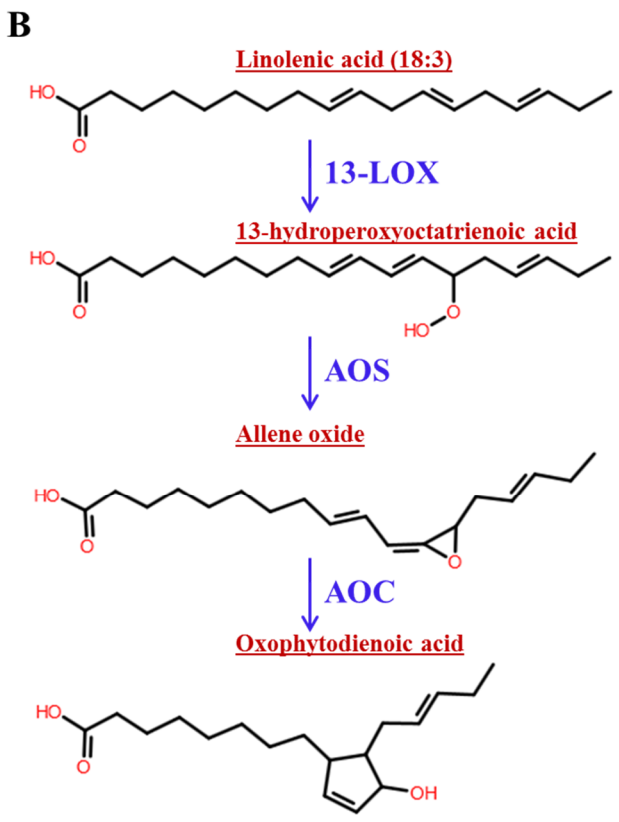
B
Linolenic acid (18:3)
13-LOX
13-hydroperoxyoctatrienoic acid
AOS
Allene oxide
AOC
Oxophytodienoic acid
HO
O
OH

***4.3.7 Quantitative prenyl-lipid metabolite profiling of the PG in wild-Type and* k1k3** Several clues have led us to hypothesize a function for ABC1K1 and ABC1K3 in prenyl-lipid metabolism: i) a yeast, bacterial, human and Arabidopsis ABC1K homolog is necessary for UQ synthesis in mitochondria [22-24, 52], ii) numerous prenyl-lipids, including several quinones, accumulate to high levels in the PG [53-56], iii) *ABC1K1* and *ABC1K3* coexpress strongly with a number of genes of prenyl-lipid metabolism [19], and iv) the PG ultrastructure in light-stressed *k1k3* chloroplasts favors a higher surface area:volume ratio and thus accumulation of amphiphilic metabolites such as prenyl-lipids (Figure 9A). Thus, we investigated the effect of loss of ABC1K1 and ABC1K3 on prenyl-lipid accumulation in light-stressed leaf tissue. A previously published method used C30 reverse-phase HPLC and a photodiode array detector to efficiently separate prenyl-lipid compounds and established expected retention times and absorption spectra of a number of carotenes, xanthophylls, quinones, tocopherols, and chlorophylls [57]. We used this HPLC method to characterize and quantify the prenyl-lipid profile of PGs and thylakoids from wild-type and *k1k3* individuals (Figure 13).

While most peaks of the chromatographic traces could be identified based on retention time and absorption spectrum, three metabolites (with retention times of 6.0, 19.6, and 24.5 minutes) were found at high abundance that were not identified in Ref. [57]. Absorption spectra of the peaks indicated that two were quinones and one a tocopherol. It was considered that the abundant quinone at 24.5 minutes was oxidized PQ-9 ($PQ\text{-}9_{ox}$). The only plastoquinone identified in Ref. [57], eluting at 5.6 minutes, is likely $PQ\text{-}9_{red}$ judging by its early elution on the C30 column and λ_{max} of 275 nm [58, 59].

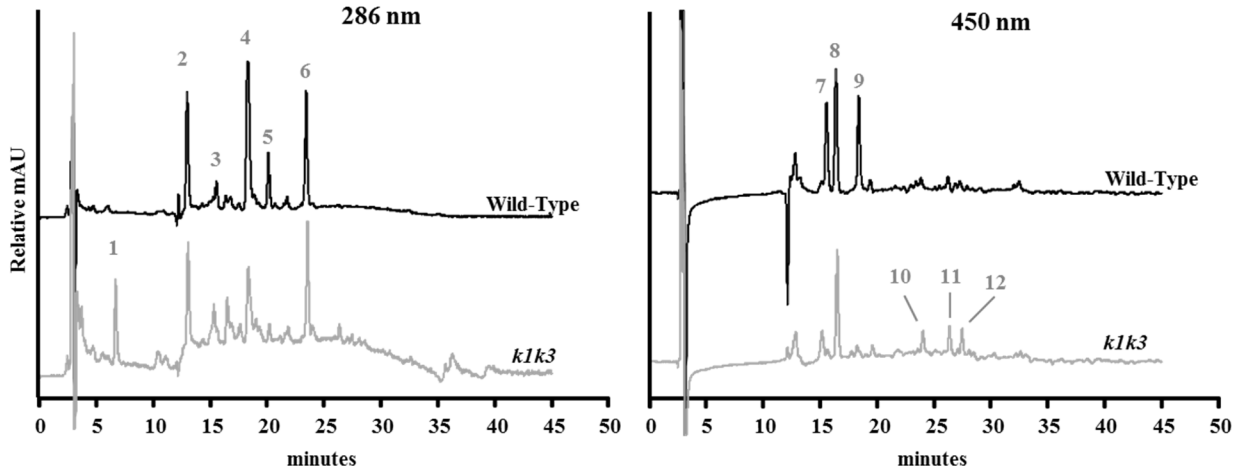

Figure 13. HPLC chromatographic traces of wild-type and *k1k3* PGs. Prenyl-lipids were extracted in chloroform, dried down, and resuspended in ethyl acetate prior to separation on a reverse-phase C30 column using a methyl t-butyl ether mobile phase. *k1k3* is offset from the wild-type along the y-axis. Identification of metabolite peaks was based on retention time and absorption spectrum, established in Ref. [57] with the exception of PC-8, and PQ-9, identified by HPLC-MS analysis (see text). Abundant peaks are indicated by number as follows: 1) Quinone 1 (MW = 746.6 Da), 2) α-tocopherol, 3) phylloquinone, 4) plastochromanol-8 (reduced), 5) 15-cis-phytoene, 6) plastoquinone-9 (oxidized), 7) chlorophyll b, 8) zeaxanthin, 9) chlorophyll a, 10) unidentified carotenoid, 11) β-carotene, 12) 9-cis-β-carotene.

HPLC-MS was used to confirm the identity of this quinone and the 2 other metabolites, using the same elution gradient and a single quadrupole mass spectrometer with ammonium acetate ($NH_4^+CH_3COO^-$) added post-column to induce ionization. The metabolite eluting at 24.5 minutes was confirmed as PQ-9_{ox} producing an absorption spectrum with the expected λ_{max} of 255 nm [58] and masses with m/z = 747.4 in (-) mode and 749.7, 766.7 and 771.6 in (+) mode, consistent with $M\text{-}H^-$, $M+H^+$, $M+NH_4^+$, and $M+Na^+$, respectively, where M is 748.6, the mass of PQ-9_{ox} (Figure 14A).

Figure 14. Absorption spectra and electrospray (ESI) mass spectra of plastoquinone-9, plastochromanol-8, and quinone 1. Major adducts are indicated in the mass spectra. A, The absorbance spectrum and ESI (+) and (-) mass spectra of reduced plastoquinone-9, eluting at 24.5 minutes, displays an absorbance peak of 255 nm and a mass of 748.6 Da, consistent with oxidized plastoquinone-9. B, Absorbance spectrum and ESI (+) and (-) mass spectra of reduced plastochromanol-8, eluting at 19.6 minutes displays an absorbance peak of 293 nm and a mass of 750.6 Da, consistent with reduced plastochromanol-8. Oxidized plastochromanol-8, eluting at 23.0 minutes, had an absorption peak at 298 nm (not shown). C, Mass chromatograms of the acetate adduct (809.4 m/z) and proton-less form (749.6 m/z) of plastochromanol-8 demonstrate that two distinct, separable redox forms are present in PGs. D, The absorbance spectrum and ESI (+) and (-) mass spectra of the unknown quinone detected only in *k1k3* PGs, eluting at 6.0 minutes displays a broad absorbance peak around 265 nm and a mass of 746.6 Da. This absorbance spectrum is indicative of a quinone, however no known plastid quinones or tocopherols (or their expected metabolic intermediates) have a mass of 746.6 Da.

A

Plastoquinone-9 (oxidized)
Retention Time: 24.4 mins

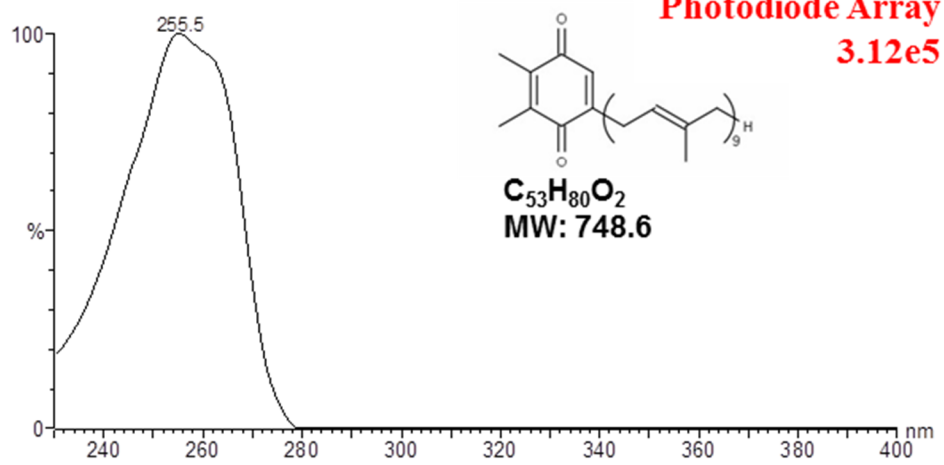

Plastoquinone-9 (oxidized)
Retention Time: 24.5 mins

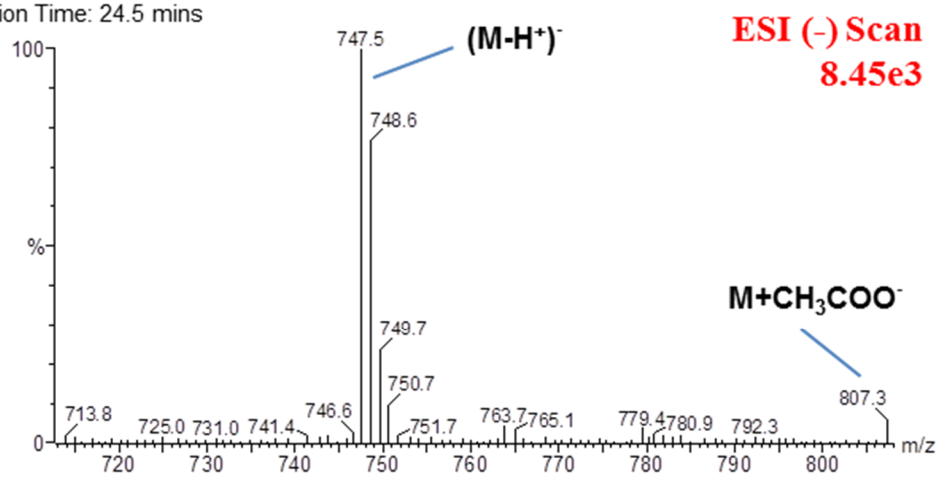

Plastoquinone-9 (oxidized)
Retention Time: 24.4 mins

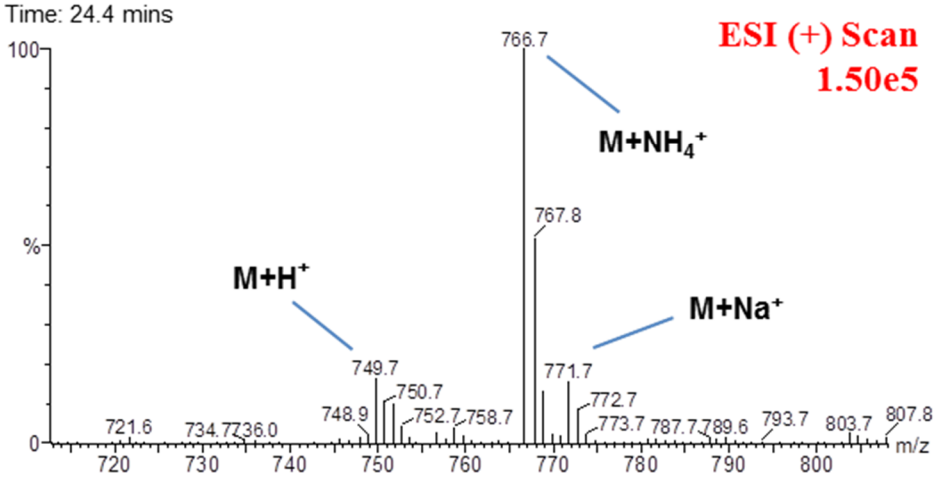

B

Plastochromanol-8 (reduced)
Retention Time: 19.6 mins

Photodiode Array
1.90e4

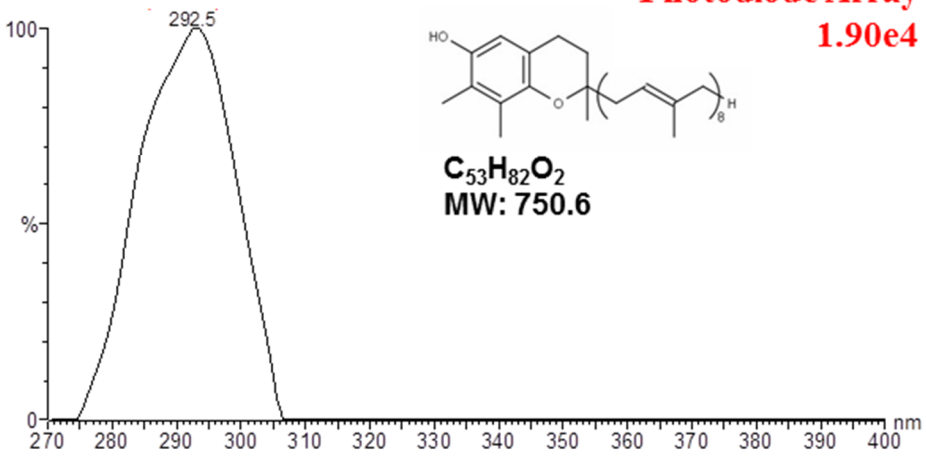

$C_{53}H_{82}O_2$
MW: 750.6

Plastochromanol-8 (reduced)
Retention Time: 19.6 mins

ESI (-) Scan
1.67e5

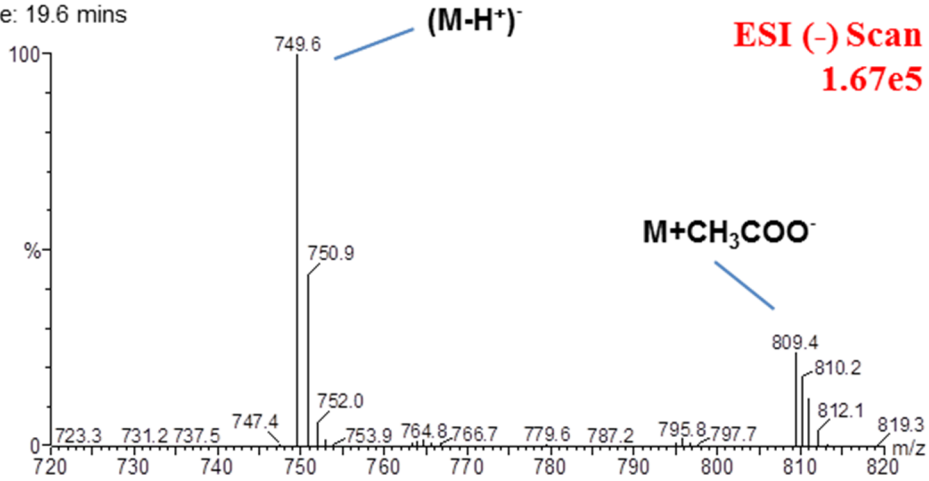

Plastochromanol-8 (reduced)
Retention Time: 19.7 mins

ESI (+) Scan
3.97e4

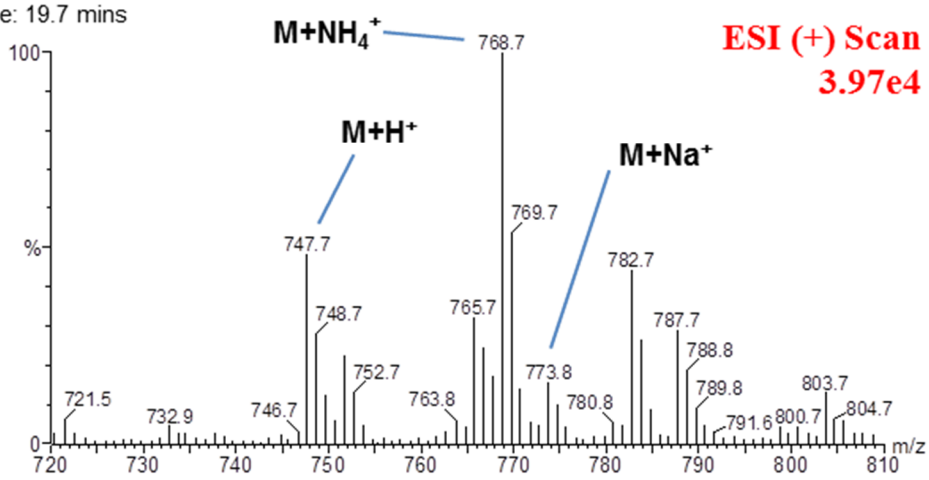

C

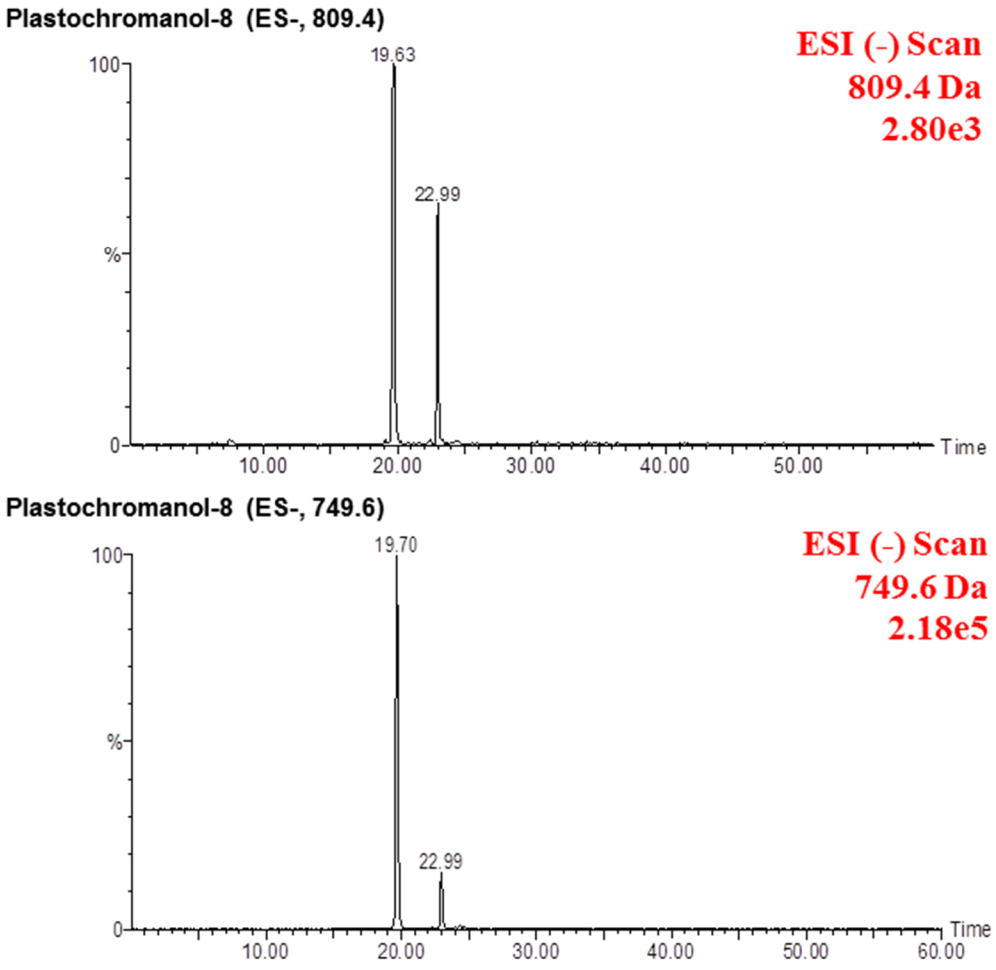
Plastochromanol-8 (ES-, 809.4)
ESI (-) Scan
809.4 Da
2.80e3
19.63
22.99
100
%
0
10.00
20.00
30.00
40.00
50.00
Time
Plastochromanol-8 (ES-, 749.6)
ESI (-) Scan
749.6 Da
2.18e5
19.70
22.99
100
%
0
10.00
20.00
30.00
40.00
50.00
60.00
Time

D

Quinone 1
Retention Time: 5.9 mins

Photodiode Array
1.33e4

MW: 746.6

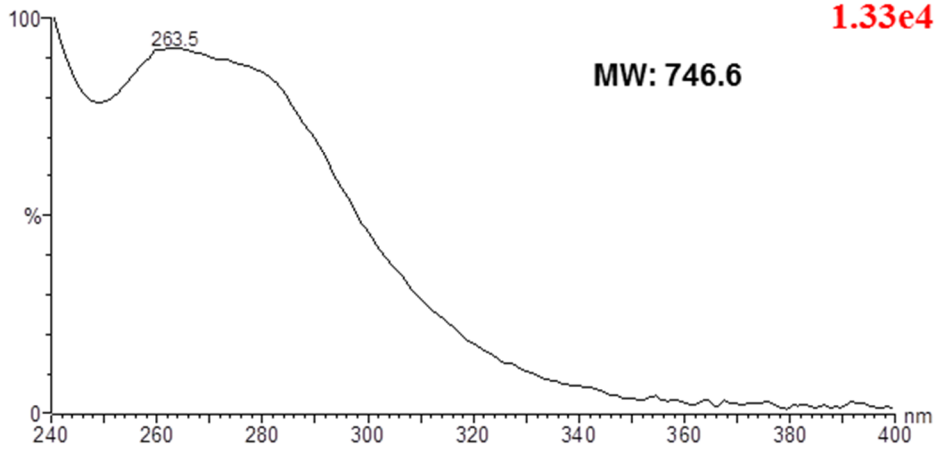

Quinone 1
Retention Time: 6.1 mins

ESI (-) Scan
2.80e3

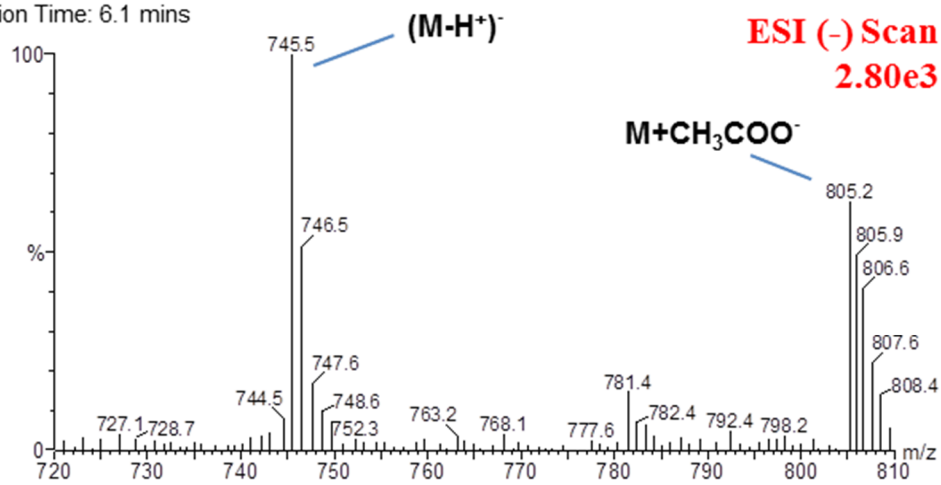

Quinone 1
Retention Time: 6.1 mins

ESI (+) Scan
2.69e4

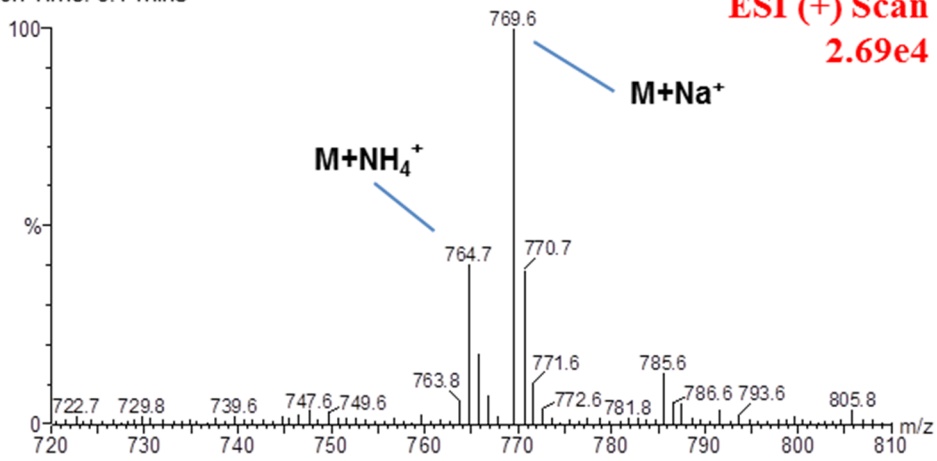

The abundant tocochromanol, with a retention time of 19.6 minutes, was found to be plastochromanol-8 (PC-8), with masses of m/z = 749.6 and 809.4 in (-) mode and 768.7 in (+) mode, consistent with $M\text{-}H^-$, $M+CH_3COO^-$, and $M+NH_4^+$, where M is 750.6, the mass of plastochromanol-8 (PC-8) (Figure 14B). Its reduction state could not be determined from the molecular weight alone, because the oxidized and reduced PC-8 have the same molecular weight. Chromatographic traces of the 749.6 deprotonated molecule and the 809.4 acetate adduct identified the other reduction state of PC-8 eluting 3.4 minutes later at 23.0 minutes, with much lower abundance (Figure 14C). Because reduction of PC-8 converts a carbonyl group to a more polar hydroxyl group it was concluded that the earlier eluting, more abundant form, was $PC\text{-}8_{red}$ (at 19.6 minutes), and the later eluting form was $PC\text{-}8_{ox}$ (at 23.0 minutes). The absorption spectra at 19.6 minutes, with a λ_{max} of 298 nm, matched the expected absorption spectrum of $PC\text{-}8_{red}$, which should be the same as γ–tocopherol since they share the same head group.

The final unknown quinone eluting at 6.0 minutes was identified only in PGs of *k1k3* but was absent in those from wild-type as well as both thylakoid preparations. Mass spectrometric analysis identified mass peaks with m/z = 745.5 and 805.8 in (-) mode and 769.6 in (+) mode co-eluting with this quinone at 6.0 minutes, consistent with a molecular weight of 746.6 (Figure 14D). While this molecule's absorption spectrum was found to be consistent with being a quinone molecule (i.e. a λ_{max} of ~264 nm), and its mass was conclusively measured, no known products or intermediates of tocochromanol/quinone metabolism fit this mass. Additional experimentation will be necessary to unambiquously identify this metabolite accumulating in *k1k3*.

The majority of the PG prenyl-lipid pool in both genotypes was composed of just three compounds: PQ-9, α-tocopherol, and PC-8; making up 90% (w/w) of the wild-type PG pool and

85% of the *k1k3* PG pool (Table 2). However, the ratio of these compounds was altered in *k1k3*; the relative amount of PQ-9 increased 1.9-fold and the amount of both tocochromanols decreased; PC-8, 1.8-fold and α-tocopherol, 1.3-fold. The unknown quinone with MW=746.6 Da accumulated to ~7% (w/w) of the pool size in the *k1k3* PG but was below the limit of detection in wild-type PGs. This compound may be a metabolic intermediate, indicating impairment in a tocochromanol/quinone metabolic pathway, or a prenyl-lipid oxidation product accumulating as a result of ROS scavenging.

Table 2. Quantitative metabolite profiles of thylakoid and PG prenyl lipids - (ng /µg prenyl lipid)

Prenyl Lipid Metabolite	Wild-type			*k1k3*		
	Pre-Thy[e]	Post-Thy[e]	PG	Pre-Thy[e]	Post-Thy[e]	PG
Plastoquinone-9[c]	104.1 ± 24.4	104.1 ± 16.8	193.8 ± 49.7	64.5 ± 28.6	46.7 ± 27.0	359.4 ± 53.7
Phylloquinone	11.1 ± 4.2	12.0 ± 6.6	4.9 ± 1.9	23.0 ± 2.5	24.1 ± 3.2	24.8 ± 7.9
Quinone 1[a,b]	n.d.	n.d.	n.d.	n.d.	n.d.	67.1 ± 70.5
Plastochromanol-8[c]	n.d.	n.d.	289.4 ± 48.1	n.d.	n.d.	160.4 ± 76.6
α-Tocopherol	162.6 ± 42.6	82.6 ± 24.4	421.6 ± 75.4	131.4 ± 15.0	119.2 ± 59.9	324.3 ± 117.5
γ-Tocopherol	n.d.	n.d.	n.d.	10.4 ± 7.1	19.7 ± 19.1	n.d.
Phytoene[d]	0.4 ± 0.1	0.2 ± 0.3	0.9 ± 0.1	n.d.	n.d.	0.2 ± 0.1
Lutein	138.2 ± 7.0	186.4 ± 29.0	0.3 ± 0.2	132.2 ± 15.8	135.4 ± 19.4	4.4 ± 01.5
Violaxanthin	28.6 ± 4.2	38.8 ± 5.5	1.1 ± 0.7	15.1 ± 2.4	16.4 ± 4.3	3.4 ± 2.4
Antheraxanthin	16.3 ± 1.9	21.8 ± 2.6	n.d.	15.5 ± 3.1	17.6 ± 2.5	n.d.
Zeaxanthin	80.6 ± 28.4	111.1 ± 37.9	3.7 ± 0.8	74.3 ± 28.1	94.4 ± 12.7	14.2 ± 5.3
Neoxanthin	0.4 ± 0.1	0.3 ± 0.3	n.d.	0.1 ± 0.3	0.4 ± 0.1	n.d.
α-carotene	4.0 ± 1.4	5.1 ± 1.7	n.d.	2.3 ± 0.3	2.4 ± 0.4	n.d.
β-Carotene	20.1 ± 7.0	24.4 ± 14.6	1.2 ± 0.6	16.0 ± 6.3	20.8 ± 8.5	10.5 ± 6.7
Other prenyl-lipids	421.8 ± 98.9	367.4 ± 23.9	83.2 ± 22.0	324.6 ± 15.3	330.0 ± 7.2	30.6 ± 16.1

a) unknown compounds were tentatively assigned to a compound class based upon their absorption spectrum
b) The molecular weight of Quinone 1 was determined by mass spectrometry to be 746.6 Da
c) oxidized and reduced forms
d) cis and trans forms
e) Lipids were extracted from thylakoid samples before and after sonication (pre- and post-thy, respectively)
n.d. = metabolite not detected

The carotenoid pool of the PG, although relatively small, changed in composition significantly in *k1k3*. It was found that carotenoid levels in the *k1k3* PGs were greater than what would be expected by thylakoid contamination alone. Because chlorophyll is believed to be present in thylakoid but not PGs, the level of thylakoid contamination in the PG preparations was estimated by comparing the amount of chlorophyll in the PGs to their levels in pre-sonicated thylakoid preparations. Chlorophyll levels in wild-type and *k1k3* PGs were 1-4% of that in thylakoid (Table 3). Carotenoid levels in the wild-type PG similarly ranged from 4-6% of thylakoid, with the exception of phytoene, the only carotenoid clearly present in the wild-type PG. However, additional carotenoids (β-carotene and the xanthophylls, zeaxanthin and violaxanthin) were found to accumulate in *k1k3* PGs, demonstrating PG/thylakoid ratios between 19-66%, which substantially exceeds what can be explained by thylakoid contamination.

Parallel metabolite analyses of the thylakoid preparations, pre and post-PG stripping, provided a comparison of metabolite distribution between thylakoids and plastoglobules (Table 2). Surprisingly, no PC-8 accumulates in the thylakoids despite its abundance in the PG. It can also be seen that more of the PQ-9 pool is deposited in the PG in *k1k3* individuals than in wild-type.

Table 3. Ratio of prenyl lipids in PGs vs. thylakoids (PG / pre-thy)

	Wild-type	*k1k3*
Chlorophyll a	4%	1%
Chlorophyll b	1%	1%
Lutein	0%	3%
β-carotene	6%	66%
Violaxanthin	4%	22%
Zeaxanthin	5%	19%
Phytoene	250%	∞

4.4 DISCUSSION

An analysis of T-DNA insertions in *ABC1K1* and *ABC1K3* which prevent accumulation of full-length transcripts and result in the absence of detectable peptides in total leaf or PG preparations has been presented. Germination, growth and development of *abc1k1-1, abc1k1-2* and *abc1k3* were indistinguishable from that of the wild-type under carefully controlled permissive environmental conditions. However, extreme sensitivity to a 10-fold increase in light intensity during vegetative growth was revealed, manifested as rapid photobleaching and necrosis (Figure 2A). The *k1k3* double mutant gradually degreened when exposed to a 5-fold increase in light intensity that failed to produce a phenotype in single mutants. This synergistic sensitivity in *k1k3* indicates non-redundant contributions of each gene product to the light stress response.

The sensitivity of the mutants indicates there may be accumulation of a photosensitizer that produces ROS. Yet, the similar accumulation patterns of H_2O_2 and O_2^- in the two genotypes as well as the EXECUTER-independent nature of degreening suggests that ROS accumulation does not account for the *k1k3* 5x light stress phenotype. It remains possible that uncontrolled oxidative damage due to higher levels of $^1O_2$ obscure any signaling pathway or that an alternative, unknown signalling pathway leads to the degreening. Knock down of *ABC1K1*, and likely other *ABC1K*s, by RNAi caused increased accumulation of the chlorophyll metabolic intermediates, chlorophyllide (Chlide) and protochlorophyllide (Pchlide) [29], which are known as potent photosensitizers via production of $^1O_2$ in the presence of light [60]. Pchlide is not thought to be an intermediate in chlorophyll degradation, thus its accumulation cannot be directly explained by impaired chlorophyll degradation (see *Chapter One, Figure 5*). However, both Pchlide and Chlide are intermediates in chlorophyll biosynthesis. Thus, impairments in the final steps of chlorophyll biosynthesis (chlorophyll synthetase and chlorophyll a oxygenase) or in the

assembly of chlorophyll into complexes could cause accumulation of both intermediates.

Curiously, despite the large-scale chlorophyll degradation occurring in *k1k3*, the light-stressed PG in *k1k3* accumulates significantly more protochlorophyllide oxidoreductase C (PORC), which catalyzes light-dependent reduction of Pchlide to Chlide as part of chlorophyll biosynthesis. The elevated levels of PORC may be a protection mechanism against oxidative stress, as has been reported in PORC-overexpressing Arabidopsis plants [61].

Results from the total leaf proteomics demonstrates significantly reduced accumulation of the PSI, PSII, and Cytochrome b_6f complexes under light stress, consistent with the degreening phenotype. A significant reduction in the NDH complex is also apparent after 5 days of light stress. The reduction of photosynthetic complexes may reduce the need for the NDH complex, meaning the reduction of NDH is likely an effect rather than a cause of the *k1k3* phenotype. It is likely that the elevated plastid protease machinery after light stress leads to the degradation of photosynthetic complexes.

It appears that the degreening in light-stressed *k1k3* is a genetically-controlled response rather than uncontrolled oxidative damage. This is supported by three observations. First, increased production of H_2O_2 or O_2^- could not be detected in *k1k3* (Figure 6). Second, the degreening was found to be irreversible after three days under the 5x light stress, indicating a committed genetically-controlled pathway had been initiated. And third, the persistent gradual decrease in chlorophyll and carotenoid is consistent with a systematic, controlled degradation of chlorophylls and carotenoids (Figure 3A). These observations cannot be taken as conclusive evidence that a genetic program is responsible for the degreening and photosynthetic degradation but favors this supposition.

The morphology of the PG has important implications for accumulation of lipophilic metabolites. The single monolayer periphery and hydrophobic interior require that amphiphilic compounds such as prenyl-lipids accumulate at the periphery of the PG, while hydrophobic compounds such as fatty acid phytyl esters (FAPEs) and triacylglycerol (TAG) deposit in the PG interior. Thus, the ratio of amphiphilic to hydrophobic metabolites at the PG must be matched by the ratio of surface area to volume of the PG. This can be controlled by the size (i.e. diameter) of the approximately spherical PGs. An increasing diameter achieves a lower surface area to volume ratio, which would be desirable when hydrophobic compounds such as FAPEs or TAGs are preferentially accumulating at the PG. Conversely, a decreasing diameter will achieve a higher surface area to volume ratio, preferred when amphiphilic compounds such as prenyl-lipids are in higher abundance.

While plastid ultrastructure under permissive growth conditions was indistinguishable between the wild-type and *k1k3*, striking differences in PGs were found under the 5x light stress. *k1k3* PGs remained small and stained dark but increased dramatically in number in response to the light stress. In contrast, wild-type PGs swelled and stained black around the periphery with a gray interior and the number of PGs remained small. It is speculated that this altered osmiophilicity of the PG interior reflects an altered lipid composition in the interior of the PG, e.g. a greater accumulation of TAGs. TAG has been reported to be one of the most abundant compounds of the PG where it must accumulate in the hydrophobic interior [56]. It would seem that the small PGs of *k1k3* accumulate very little TAG whereas the wild-type PGs, with their large hydrophobic interiors accumulate substantially more TAG. Indeed, the staining and appearance of PGs in the transmission electron micrographs is similar to that of TAG-rich oil bodies derived from the ER, see e.g. [37, 38]. In light of the substantially higher accumulation of

enzymes of jasmonic acid (JA) synthesis (e.g. lipoxygenase, AOS, AOC) it is proposed that increased competition for fatty acids by the JA biosynthesis pathway in *k1k3* plastids prevents accumulation of TAG in the PG.

An illustration of the apparent metabolic alterations at the *k1k3* PG is presented in Figure 15. Increased levels of 13-LOX and AOS indicate increased flux of fatty acids into JA synthesisis which, in combination with reduced levels of DGAT, would limit the accumulation of TAG at the PG. It is proposed that this reduction of TAG accounts for the smaller size of the PGs in *k1k3*. It is not clear whether fatty acids entering the JA biosynthetic pathway derive from turnover of galactolipids, *de novo* synthesis, di- or tri-acylglycerols, or an alternative source. The metabolite profiling measurements indicate that a larger portion of the PQ-9 pool is sequestered in the *k1k3* PG. This, and the apparent reduced activity of VTE1, increases the amount of PQ-9 in the PG where it may act as a ROS scavenger.

It is thought that the ancient function of the ABC1K family is the regulation of menaquinone metabolism [18]. Based on this and the observation that ABC1K1 and ABC1K3 localize to the PG, which is rich in quinones and contains several enzymes of their metabolism, it was hypothesized that ABC1K1 and ABC1K3 function in the regulation of plastidic quinone metabolism. Consistent with this hypothesis, it is shown here that loss of ABC1K1 and ABC1K3 causes altered accumulation of prenyl-lipids including quinones in the PG.

A reduction of the predominant tocochromanols, α-tocopherol and PC-8 were found with a concomitant increase in PQ-9 as well as an additional unknown quinone with a molecular weight of 746.6 Da. This observation indicates reduced activity of the PG-localized VTE1 enzyme, responsible for cyclization of the quinones, dimethylphytyl benzoquinone (DMPBQ) and PQ-9 to their tocochromanol products, α-tocopherol and PC-8, respectively (Figure 15).

Figure 15. A model of metabolic alterations in *k1k3* PGs. Upregulated pathways in *k1k3* are designated with red, thick lines and downregulated pathways are designated with blue, dashed lines. The model has been adapted from that presented in C*hapter Two*. For a detailed description of the model, pathways and abbreviations, see C*hapter Two, Figure 12*.

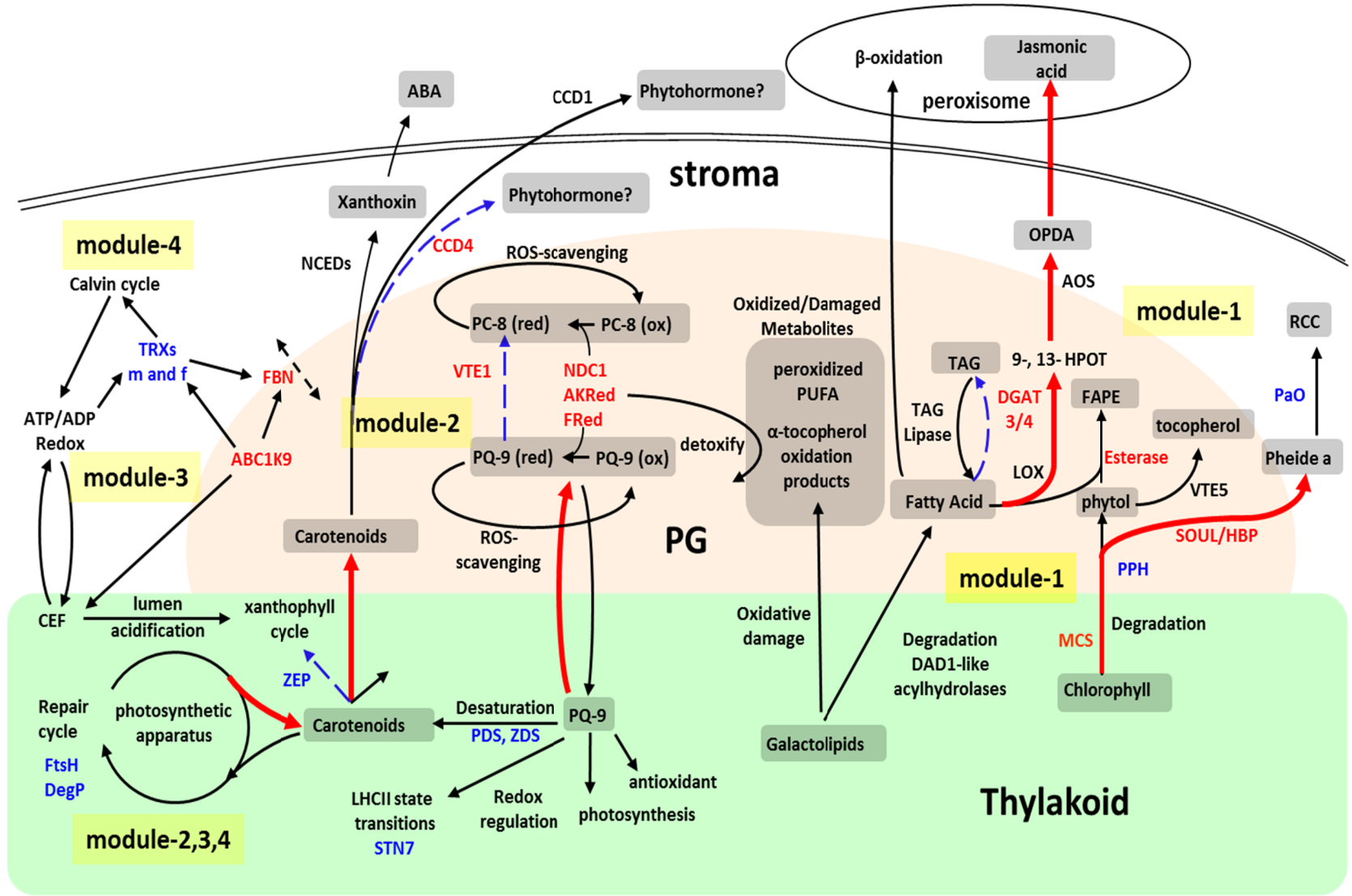
β-oxidation
Jasmonic acid
peroxisome
ABA
CCD1
Phytohormone?
stroma
Xanthoxin
Phytohormone?
module-4
Calvin cycle
NCEDs
CCD4
ROS-scavenging
OPDA
AOS
module-1
RCC
PC-8 (red)
PC-8 (ox)
Oxidized/Damaged Metabolites
TAG
9-, 13- HPOT
TRXs m and f
FBN
VTE1
NDC1 AKRed FRed
peroxidized PUFA
TAG Lipase
DGAT 3/4
FAPE
PaO
ATP/ADP Redox
module-2
tocopherol
module-3
ABC1K9
PQ-9 (red)
PQ-9 (ox)
detoxify
α-tocopherol oxidation products
LOX
Esterase
Pheide a
Carotenoids
ROS-scavenging
PG
Fatty Acid
phytol
VTE5
SOUL/HBP
module-1
PPH
CEF
lumen acidification
xanthophyll cycle
Oxidative damage
Degradation DAD1-like acylhydrolases
MCS
Degradation
ZEP
Repair cycle
photosynthetic apparatus
Carotenoids
Desaturation
PDS, ZDS
PQ-9
Chlorophyll
FtsH DegP
Galactolipids
LHCII state transitions STN7
Redox regulation
antioxidant photosynthesis
Thylakoid
module-2,3,4

The possibility that the unknown quinone was the VTE1 substrate, DMPBQ was considered; however, the molecular weight is inconsistent, and elution of the DMPBQ intermediate from *vte1* PGs did not match the elution time of the unknown quinone (data not shown). Importantly, the level of VTE1 enzyme was unchanged in *k1k3* PGs (Table 1), further indicating an impaired activity of the VTE1 enzyme. It is suggested that ABC1K1 and/or ABC1K3 is responsible for activation of VTE1 under excess excitation energy. This possibility awaits further testing.

Carotenoid compounds comprise a small fraction of the prenyl-lipid pool of wild-type light-stressed PGs, comprised almost exclusively of phytoene (Tables 2 and 3). However, it was found that loss of ABC1K1 and ABC1K3 dramatically changed the carotenoid composition in the PG. In addition to phytoene, accumulation of β-carotene, and to a lesser extent the xanthophylls lutein, zeaxanthin and violaxanthin was apparent (Table 3). The appearance of β-carotene and the xanthophylls in the *k1k3* PGs supports the hypothesis that PGs are the site of deposition and degradation of carotenoids released from photosystems and light harvesting complexes of the thylakoid (Figure 15). There is one PG-localized enzyme that is predicted to catalyze carotenoid degradation, CCD4, whose substrate(s) in *A. thaliana* have not been conclusively demonstrated. Interestingly, CCD4 levels in *k1k3* PGs were reduced by more than 3-fold (Table 1); whether accumulation of carotenoids and depletion of CCD4 at the *k1k3* PGs are directly related remains to be explored, but is an intriguing possibility.

This chapter has presented an investigation of *A. thaliana* T-DNA insertion mutants affected in two PG-localized atypical protein kinases, ABC1K1 and ABC1K3. Evidence is presented that ABC1K1 and ABC1K3 are regulators of plastidic metabolism, important for adaptation to excess excitation energy. Targets of ABC1K1 and ABC1K3 remain elusive but

likely are enzymes involved in prenyl-lipid metabolism, localized at the PG or thylakoid membrane.

4.5 MATERIALS AND METHODS

4.5.1 Plant Materials and Plant Growth Conditions The following SALK insertion mutants were acquired from the Arabidopsis Biological Resource Center: *abc1k1-1* (SALK 057147), *abc1k1-2* (SALK 068628), *abc1k3-1* (SALK 128696). Plants were grown on Cornell Mix soil with a 16-hour photoperiod of 120 μE m^{-2} s^{-1} actinic light at a constant 60% relative humidity and 22^{o} C ambient temperature. For light stress application, plants were moved late in the vegetative growth stage to 520 μE m^{-2} s^{-1} (5x light stress) or 1000 μE m^{-2} s^{-1} (10x light stress) actinic light during the dark period, while maintaining the same 16-hour photoperiod, 60% relative humidity, and 22^{o} C ambient temperature.

4.5.2 PG Isolation PG isolations were performed as in [19]. All PG preparations were made from 5 day moderate light-stressed leaf tissue, collected in the morning of the 6th day of stress. The resulting floating pad of PGs was removed with a hypodermic disposable syringe, flash frozen in liquid N_2, and stored at -80^{o} C.

4.5.3 Total Leaf Protein Extraction Protein was extracted from mature leaf tissue 3 hours into the photoperiod. While working in the dark at 4^{o} C, the mature leaf tissue was ground in liquid nitrogen and combined with 450 μl of protein extraction buffer (50 mM Tris pH 8.0, 2% sodium dodecyl sulfate, protease inhibitor cocktail). Samples were vortexed for 25 seconds and then

filtered through a 0.8 mL frit by centrifuging at 18,000 xg, for 1 minute. Protein concentrations of the supernatant were determined by the BCA assay kit (Pierce).

4.5.4 Transmission Electron Microscopy Leaf tissue from 3 individuals of each genotype at each time point was harvested 1 hour after the beginning of the photoperiod. Leaf margins and midribs were excluded and the remaining leaf tissue was divided into 1x2 mm sections with a fresh razor blade. Sections were processed as in [19], using 2% glutaraldehyde, 2 % paraformaldehyde, and subsequently 1% osmium tetroxide as fixative and 2% uranyl acetate as stain. Cured resin blocks were sectioned and imaged at Electron Microscopy Services; Colorado Springs, Colorado.

4.5.5 Leaf tissue stains for reactive oxygen species Two of the oldest leaves of three individuals from each genotype were harvested and submerged in 10 mL of diaminobenzidine (DAB) staining solution [10 mM Tris-Acetate pH 4.0, 0.05 % (w/v) DAB] or 10 mL of nitroblue tetrazolium (NBT) staining solution [50 mM potassium phosphate pH 7.8, 10 mM sodium azide, 0.5% (w/v) NBT]. Submerged tissue was vacuum-infiltrated in a desiccator for 10 minutes, two times, breaking the vacuum between each event. DAB-infiltrated tissue was subsequently incubated in the dark at room temperature for twenty-four hours. NBT-infiltrated tissue was incubated under a benchtop lamp for 15 minutes on each side of the leaf, before terminating the reaction by placing in warm 95% ethanol. Tissue from both treatments was destained in 95% ethanol at 45^{o} C, changing the ethanol solution several times as needed. Destained tissue was stored in 60% glycerol. Images were collected using a Nikon d90 digital SLR equipped with a

Tamron 90 mm f/2.8 macro lens. All images were white balanced and level-adjusted using Photoshop software (Adobe, v.11.0.2).

4.5.6 Ascorbate and glutathione measurements Ascorbate and glutathione measurements were made spectrophotometrically as adapted from Ref. [35]. Working under minimal light to protect ascorbate from oxidation, approximately 0.4 mg of mature leaf tissue was harvested and weighed before flash freezing in liquid nitrogen. Tissue was ground thoroughly and 1 mL of extraction buffer [2% (w/v) meta-phosphoric acid, 2 mM disodium-ethylenediaminetetraacetic acid] was added. Solution was centrifuged for 10 minutes at 18,000 xg at 4^{o} C, and aliquots of supernatant were taken for ascorbate and glutathione assay. For ascorbate determination, 100 µl of supernatant was mixed with 700 µl of phosphate buffer (100 mM sodium phosphate pH 6.8) and A_{265} was measured (Abs#1). To fully reduce ascorbate, 1 µl of dithiothreitol was added and sample incubated for 15 minutes at 37^{o} C. Following the incubation, A_{265} was measured again (Abs#2). To fully oxidize the ascorbate, 0.8 units of ascorbate oxidase (40 U/ml in 100 mM phosphate pH 5.6; Sigma-Aldrich, St. Louis, MO) was added to the sample and the A_{265} was measured (Abs#3). Total ascorbate was calculated as Abs#2 – Abs#3, reduced ascorbate was calculated as Abs#1 – Abs#3, and oxidized ascorbate was calculated as Abs#2 – Abs#1. A standard curve was created from stock solutions of ascorbate (0, 0.1, 0.25, 1.0 and 2.0 mM ascrobate in 2.5 mM dithiothreitol in extraction buffer) which were treated as the sample extracts above. Briefly, stock solution was centrifuged for 10 minutes at 18,000 xg at 4^{o} C. A 100 µl aliquot of supernatant was mixed with 700 µl of phosphate buffer, and A_{265} was measured. For determination of total glutathione, 20 µl of supernatant was neutralized in 130 µl of 280 mM sodium phosphate pH 7.5. Neutralized extract was then mixed with 700 µl of buffer B (125 mM

potassium phosphate pH 7.5, 6.3 mM disodium-ethylenediaminetetraacetic acid, 0.3 mM reduced nicotinamide adenine dinucleotide phosphate), 100 µl of buffer C (125 mM potassium phosphate pH 7.5, 6.3 mM disodium-ethylenediaminetetraacetic acid, 6 mM 5,5′-dithiobis(2-nitrobenzoic acid)) and 1.0 units of glutathione reductase (20 U/ml in 125 mM potassium phosphate pH 7.5, 6.3 mM disodium-ethylenediaminetetraacetic acid; Sigma-Aldrich, St. Louis, MO). The A_{412} of the solution was measured. To measure oxidized glutathione, 100 µl of extract was neutralized in 650 µl of 280 mM sodium phosphate pH 7.5 and 10 µl of vinylpyridine was added. The solution was incubated for 1 hour at 25^{o} C. Excess vinylpyridine was removed by adding 300 µl of diethyl ether, vortexing and centrifuging 3000 xg for 3 minutes. The upper phase was removed and the process was repeated once more. Vinlypyridine-depleted sample was then treated with 1.0 units of glutathione reductase and A_{412} was measured. A standard curve was created using stock solutions of glutathione (0, 10, 20, 30, 40, 50 µM in extraction buffer) which were treated as extract samples above. Briefly, stock solution was centrifuged for 10 minutes at 18,000 xg at 4^{o} C. A 20 µl aliquot of supernatant was neutralized in 130 µl of 280 mM sodium phosphate pH 7.5. Neutralized extract was then mixed with 700 µl of buffer B, 100 µl of buffer C, and 1.0 units of glutathione reductase, before measuring A_{412}.

4.5.7 PG sample preparation and in-gel digestion PG samples were normalized by OD 600nm and were lyophilized and solubilized in a modified Laemmli solubilization buffer (125 mM Tris-HCl pH 6.8, 6% sodium dodecyl sulfate, 10% β-mercaptoethanol, 20% glycerol). Samples were shaken gently at 30^{o} C for 15 minutes to ensure complete solubilization and subsequently heated at 80^{o} C for 10 minutes. Samples were centrifuged to remove insoluble material and proteins

were separated by SDS PAGE (6% acrylamide stacking, 12% separation). Each gel lane was cut in 5 slices and proteins were digested with trypsin, as described in [62].

4.5.8 Proteome analysis by nanoLC-LTQ-Orbitrap and data processing Peptides prepared from in-gel digestion and in-solution digestion were analyzed by data-dependent tandem mass spectrometry (MS/MS) using on-line LC-LTQ-Orbitrap (Thermo Electron) with dynamic exclusion, similar as described in [63]. Peak lists (.mgf format) were generated using DTA supercharge (v1.19) software (http://msquant.sourceforge.net/) and searched with Mascot v2.2 (Matrix Science) against a combined database containing the Arabidopsis genome with protein-coding gene models and 187 sequences for known contaminants (e.g. keratin, trypsin) (total 33,013 entries) and concatenated with a decoy database where all the sequences were randomized; in total this database contained 66,026 protein sequences. Off-line calibration for all precursors ions was done as described in [64]. Each of the peak lists were searched using Mascot v2.2 (maximum p-value of 0.01) for full tryptic peptides using a precursor ion tolerance set at ±6 ppm, fixed cysteine carbamido-methylation and variable methionine oxidation, protein N-terminal acetylation, glutamine deamidation and maximally one missed cleavage allowed. The maximum fragment ion tolerance (MS/MS) was 0.8 Da. For semi-tryptic peptides the search was performed with a precursor ion tolerance set at ±3 ppm, fixed cysteine carbamido-methylation and variable methionine oxidation, N-terminal acetylation, glutamine deamidation and maximally one missed cleavage allowed. Minimal ion score threshold was chosen such that a peptide false discovery rate (FDR) below 1% was achieved. Using an in-house written filter, the search results were further filtered as follows: For identification with two or more peptides, the minimum ion score threshold was set to 30. For protein identification based on a single peptide,

the minimum ion score threshold was set to 33, and the mass accuracy of the precursor ion was required to be within ±3 ppm. The peptide false discovery rate (FDR) was calculated as: 2 × (decoy hits) / (target + decoy hits) and below 1%. The FDR of proteins identified with two or more peptides was zero. Peptides with less than seven amino acids were discarded.

Several Arabidopsis genes have more than one gene model, and in such cases the protein form with the highest number of matched spectra was selected; if two gene models had the same number of matched spectra, the model with the lower digit was selected. For quantification, each protein accession was scored for total spectral counts (SPC), unique SPC (uniquely matching to an accession) and adjusted SPC. The latter assigns shared peptides to accessions in proportion to their relative abundance using unique spectral counts for each accession as a basis. The normalized adjSPC (NadjSPC) for each protein was calculated through division of adjSPC by the sum of all adjSPC values for the proteins from that gel lane. NadjSPC provides a relative protein abundance measure by mass, whereas NSAF estimates relative protein concentration within a particular sample.

4.5.9 Metabolite Extractions Working under minimal light and at 4^{o} C, PG preparations were normalized by OD 600nm and lyophilized. Prenyl lipids were extracted from normalized, lyophilized tissue essentially as in Ref. [57] except all solvent volumes were doubled. To lyophilized samples, 200 µl of methanol was added and was mixed for 10 minutes on a thermoshaker (Thermomixer R, Eppendorf) at 4^{o} C. 200ul of 50 mM Tris-HCl pH 7.5 + 1M NaCl was added and shaken for another 10 minutes. 800 µl of chloroform was added and the solution was incubated with gentle rocking for 15 minutes at 4^{o} C. Sample was centrifuged at 3000 xg for 5 minutes to achieve thorough phase separation and the hypophase was extracted by

glass Pasteur pipette. Extraction was repeated once by adding an additional 800 µl of chloroform and again incubating for 15 minutes at 4° C and centrifuging. Extracted prenyl lipids were dried down under a stream of nitrogen gas and stored at -20° C.

4.5.10 Metabolite Profiling by HPLC-PDA Separation of the metabolite extracts by HPLC was accomplished according to the method described in Fraser, et al. [57]. Chromatography was performed on a reverse-phase C30 column, 5 µm beads (250 x 4.6 mm) manufactured by YMC, Inc using an Agilent 1100 chromatography system with a flow rate of 1 mL/min, connected to a photodiode array detector, monitoring continuously from 260 – 700 nm. Extractions were resuspended in 250 µl of ethyl acetate and passed through a 0.45 µm syringe filter. Sample injections (25 µl) were separated with mobile phases of (A) 100% methanol, (B) 80% methanol in water + 0.2 % ammonium acetate, and (C) methyl *t*-butyl ether. A gradient elution was employed consisting of 95% A, 5% B isocratically for 12 minutes, a step to 80% A, 5% B, 15% C at 12 minutes, followed by a linear gradient to 30% A, 5% B, 65% C at 30 minutes and finally a return to the initial conditions (95% A, 5% B) by 60 minutes. Peak identities were established by comparison of retention times with those established by Fraser, et al [57] and the absorbance spectrum. Quantification was carried out using the Chromeleon software package v6.80 (Waters, Inc) by measuring the area under the curve at each compound's λ_{max}. Absorbance response factors for λ_{max} were calculated from calibration curves of a standard of each compound class; carotenoids (β-carotene), tocopherols (α-tocopherol), quinones (menadione), and chlorophyll (chlorophyll b).

4.5.11 Metabolite identification by HPLC-MS Metabolite extracts were separated as for the metabolite profiling described above. Post-column, flow was split 75:25, producing a flow of 250 μl/min. Using a syringe pump, ammonium acetate (0.5% w/v) was injected at a flow rate of 50 μl/min with a three-way adaptor. Electrospray mass spectra were acquired using a single quadrupole mass spectrometer scanning alternately in (+) and (-) modes.

Supplemental Table 1. Total leaf proteomics of wild-type and *k1k3*

Accession	GLEE - genotype effect (p<0.01)	Genotype (p<0.01)	lab annotation	subcellular location	BIN#	k1k3/wt average (days 0-3-	k1k3/wt 0day (NadjSPC)	k1k3/wt 3 day (NadjSPC)	k1k3/wt 5 day (NadjSPC)	wt 0 day. Average NadjSPC	wt 3 day Average NadjSPC	wt 5 day Average NadjSPC	k1k3 0day Average	k1k3 3day Average	k1k3 5dayAverag e NadjSPC
AT1G07890			L-ascorbate peroxidase 1, cytosolic (A	cytosol	21.2.1	0.78	1.01	0.69	0.73	0.00123	0.00193	0.00245	0.00124	0.00134	0.00180
AT1G75270			dehydroascorbate reductase (DHAR2	cytosol	21.2.1	0.84	0.87	0.87	0.81	0.00013	0.00038	0.00039	0.00012	0.00033	0.00031
AT5G03630			ATMDAR2; monodehydroascorbate	not plastid	21.2.1	0.95	1.08	0.84	0.96	0.00062	0.00081	0.00070	0.00067	0.00068	0.00068
AT1G19570			dehydroascorbate reductase-1 (DHAI	peroxisome	21.2.1	0.90	0.92	1.09	0.76	0.00114	0.00203	0.00305	0.00105	0.00222	0.00232
AT3G52880			monodehydroascorbate reductase, pu	peroxisome	21.2.1	0.88	1.08	0.82	0.85	0.00110	0.00164	0.00271	0.00118	0.00135	0.00229
AT4G35000			peroxisomal ascorbate peroxidase (A	peroxisome	21.2.1	0.80	0.84	0.51	1.25	0.00033	0.00049	0.00030	0.00027	0.00025	0.00038
AT5G28840			GDP-mannose 3,5-epimerase/ NAD b	not plastid	21.2.1.1	0.92	0.87	0.56	1.26	0.00011	0.00034	0.00039	0.00009	0.00019	0.00049
AT1G20620	yes		catalase 3 (CAT3)	peroxisome	21.6	0.88	1.22	0.64	0.60	0.00512	0.00341	0.00320	0.00623	0.00219	0.00193
AT4G35090			catalase 2 (CAT2)	peroxisome	21.6	1.10	1.35	0.88	1.19	0.00334	0.00654	0.00579	0.00451	0.00576	0.00690
AT1G63940			monodehydroascorbate reductase (M	plastid stroma	21.2.1	1.15	0.97	1.05	1.58	0.00102	0.00122	0.00069	0.00098	0.00129	0.00109
AT5G16710			dehydroascorbate reductase-2 (DHAI	plastid stroma	21.2.1	0.69	0.84	0.48	0.74	0.00048	0.00055	0.00080	0.00041	0.00027	0.00059
AT4G23100			gamma-glutamylcysteine synthetase (	plastid stroma	21.2.2	1.09	0.85	1.47	1.10	0.00017	0.00010	0.00046	0.00014	0.00015	0.00050
AT3G54660			gluthatione reductase,	plastid stroma	21.2.2	1.39	1.57	1.47	1.26	0.00021	0.00009	0.00032	0.00033	0.00013	0.00040
AT2G21170			triosephosphate isomerase-1 (TPI-1)	plastid stroma	1.3.5	0.94	1.08	0.95	0.80	0.00140	0.00207	0.00145	0.00151	0.00197	0.00116
AT2G21330			fructose-bisphosphate aldolase-1 (SF	plastid stroma	1.3.6	0.85	0.97	0.88	0.74	0.00406	0.00567	0.00586	0.00395	0.00496	0.00432
AT4G38970			fructose-bisphosphate aldolase-2 (SF	stroma	1.3.6	1.01	1.06	1.08	0.89	0.00704	0.00882	0.00780	0.00744	0.00954	0.00693
AT3G54050			fructose-bisphosphatase (FBPA), higl	plastid stroma	1.3.7	0.95	1.35	0.84	0.87	0.00152	0.00285	0.00356	0.00205	0.00239	0.00311
AT1G42970			glyceraldehyde-3-phosphate dehydro	plastid stroma	1.3.4	0.96	0.99	0.97	0.93	0.00697	0.01266	0.01074	0.00694	0.01234	0.01003
AT3G26650			glyceraldehyde 3-phosphate dehydro	plastid stroma	1.3.4	1.06	1.19	1.14	0.87	0.00920	0.00915	0.01019	0.01090	0.01046	0.00882
AT1G12900			glyceraldehyde-3-phosphate dehydro	plastid stroma	1.3.4	0.90	0.96	0.82	0.94	0.00447	0.00512	0.00527	0.00428	0.00418	0.00495
AT1G56190	yes		phosphoglycerate kinase-1 (PGK-2)	plastid stroma	1.3.3	1.16	1.78	1.00	0.99	0.00097	0.00164	0.00191	0.00172	0.00164	0.00189
AT3G12780			phosphoglycerate kinase-1 (PGK-1)	plastid stroma	1.3.3	1.03	1.19	1.09	0.86	0.01297	0.01320	0.01584	0.01537	0.01434	0.01364
AT1G32060			phosphoribulokinase-2 (PRK-2)	plastid stroma	1.3.12	1.19	1.14	1.18	1.24	0.00301	0.00367	0.00308	0.00344	0.00433	0.00381
AT3G04790			ribose 5-phosphate isomerase (PRI)	thylakoid-peripheral-st	1.3.10	0.89	0.91	0.93	0.86	0.00156	0.00097	0.00158	0.00141	0.00090	0.00135
AT5G61410			ribulose-5-phosphate-3-epimerase (R	plastid stroma	1.3.11	1.08	1.33	0.71	0.97	0.00142	0.00072	0.00082	0.00189	0.00051	0.00079
AT2G39730			Rubisco activase	plastid stroma	1.3.13	1.04	0.93	1.24	0.99	0.01144	0.01347	0.02526	0.01062	0.01666	0.02499
ATcG00490			Rubisco large subunit (RBCL)	plastid stroma	1.3.1	0.94	1.19	0.97	0.68	0.04704	0.09037	0.05461	0.05619	0.08732	0.03712
AT5G38410	yes		Rubisco small subunit 3b (RBCS-3B)	plastid stroma	1.3.2	0.86	1.20	0.64	0.85	0.00448	0.00665	0.00542	0.00539	0.00422	0.00459
AT1G67090			Rubisco small subunit-4 (RBCS-4)	plastid stroma	1.3.2	0.88	1.18	0.78	0.74	0.00487	0.00616	0.00603	0.00573	0.00484	0.00445
AT5G38430			Rubisco small subunit 1b (RBCS-1b)	plastid stroma	1.3.2	0.87	1.26	0.88	0.52	0.00242	0.00353	0.00290	0.00304	0.00311	0.00152
AT3G55800			sedoheptulose-bisphosphatase (SBPa	plastid stroma	1.3.9	0.95	0.96	0.95	0.95	0.00232	0.00331	0.00309	0.00223	0.00315	0.00294
AT3G60750			transketolase-1 (TKL-1)	plastid stroma	1.3.8	0.90	0.90	0.89	0.91	0.01799	0.01474	0.01241	0.01624	0.01308	0.01125
AT5G23060	2x yes	yes	Ca2+ sensing receptor - phosphopro	thylakoid-integral	1.1.30	0.46	0.91	0.29	0.15	0.00141	0.00082	0.00165	0.00129	0.00024	0.00024
AT3G63520			9,10 (9',10') 9-cis-epoxycarotenoid di	cytosol	16.1.4.1(	1.53	0.80	1.99	2.00	0.00056	0.00038	0.00049	0.00045	0.00076	0.00098
AT4G19170	yes	yes	carotenoid cleavage dioxygenase (CC	plastoglobules	16.1.4	0.26	0.31	0.10	0.17	0.00090	0.00020	0.00012	0.00028	0.00002	0.00002
ATcG00130			CFO-I - atpF	thylakoid-integral	1.1.4	1.26	1.18	1.49	1.09	0.00216	0.00225	0.00194	0.00254	0.00335	0.00211
AT4G32260			CFO-II - atpG	thylakoid-integral	1.1.4	0.92	0.92	0.89	1.00	0.00070	0.00119	0.00046	0.00064	0.00105	0.00046
ATcG00480			CF1b - atpB	thylakoid-peripheral-st	1.1.4	1.03	1.14	1.04	0.93	0.02326	0.03222	0.03047	0.02655	0.03359	0.02839
ATcG00120			CF1a - atpA	thylakoid-peripheral-st	1.1.4	1.04	1.15	1.05	0.94	0.01809	0.01748	0.02255	0.02075	0.01838	0.02118
AT4G04640			CF1y - atpC	thylakoid-peripheral-st	1.1.4	1.00	1.02	1.19	0.78	0.00360	0.00494	0.00434	0.00366	0.00586	0.00337
AT4G09650			CF1d - atpD	thylakoid-peripheral-st	1.1.4	1.13	0.96	1.30	1.24	0.00168	0.00104	0.00122	0.00161	0.00135	0.00151
ATcG00470			CF1e - atpE	thylakoid-peripheral-st	1.1.4	1.03	1.12	1.09	0.83	0.00128	0.00105	0.00096	0.00143	0.00114	0.00080
AT5G45390			ClpP4	plastid stroma	29.5.5	0.92	0.77	1.17	0.89	0.00042	0.00036	0.00093	0.00033	0.00043	0.00083
AT4G17040			ClpR4	plastid stroma	29.5.5	1.09	1.17	0.99	1.22	0.00033	0.00070	0.00037	0.00038	0.00070	0.00045
AT1G11750		yes	ClpP6	plastid stroma	29.5.5	1.42	0.97	1.50	1.78	0.00031	0.00041	0.00031	0.00030	0.00062	0.00056
AT1G02560		yes	ClpP5	plastid stroma	29.5.5	1.49	1.51	1.34	1.70	0.00016	0.00041	0.00029	0.00024	0.00056	0.00049
AT1G09130			ClpR3	plastid stroma	29.5.5	1.00	0.59	0.71	1.68	0.00024	0.00022	0.00024	0.00014	0.00016	0.00041
ATcG00540			petA - cytochrome f (cleavable ss of	thylakoid-integral	1.1.3	0.88	0.96	0.73	0.92	0.00333	0.00241	0.00281	0.00320	0.00175	0.00258
ATcG00720			petB - Cytochrome b6	thylakoid-integral	1.1.3	0.77	1.04	0.61	0.63	0.00274	0.00170	0.00320	0.00283	0.00104	0.00201
AT4G03280			petC - Rieske Fe-S protein	thylakoid-peripheral-lu	1.1.3	0.73	1.00	0.62	0.70	0.00054	0.00106	0.00081	0.00054	0.00066	0.00057
AT4G04020			fibrillin 1a (FBN1a)	plastoglobules	26.31*	0.95	1.12	0.85	0.94	0.00075	0.00116	0.00174	0.00084	0.00098	0.00162
AT3G23400			fibrillin 4 (FBN4)	plastoglobules	26.31*	0.89	0.94	0.85	0.88	0.00096	0.00100	0.00156	0.00091	0.00085	0.00138
AT4G22240			fibrillin 1b (FBN1b)	plastoglobules	26.31*	0.92	0.63	1.24	0.85	0.00056	0.00074	0.00113	0.00035	0.00091	0.00096
AT2G42130			fibrillin 7b (FBN7b) - model .4 score	plastoglobules	26.31*	0.72	0.69	0.59	0.89	0.00065	0.00055	0.00055	0.00045	0.00033	0.00049

Supplemental Table 1. (continued)

Accession	GLEE - genotype effect (p<0.01)	Genotype (p<0.01)	lab annotation	subcellular location	BIN#	klk3/wt average (days 0-3-	klk3/wt 0day (NadjSPC)	klk3/wt 3 day (NadjSPC)	klk3/wt 5 day (NadjSPC)	wt 0 day. Average NadjSPC	wt 3 day Average NadjSPC	wt 5 day Average NadjSPC	klk3 0day Average	klk3 3day Average	klk3 5dayAverage NadjSPC
AT2G35490		yes	fibrillin 2 (FBN2)	plastoglobules	26.31*	1.66	1.47	1.69	1.77	0.00025	0.00021	0.00040	0.00037	0.00035	0.00071
AT1G50250	yes	yes	FtsH1	thylakoid-integral	29.5.7	1.45	0.93	2.34	1.67	0.00137	0.00075	0.00026	0.00128	0.00175	0.00043
AT5G42270			FtsH5 (VAR1)	thylakoid-integral	29.5.7	1.16	1.07	1.24	1.17	0.00319	0.00303	0.00239	0.00343	0.00376	0.00280
AT2G30950			FtsH2 (VAR2 and Pftf)	thylakoid-integral	29.5.7	0.98	0.98	1.11	0.86	0.00367	0.00200	0.00224	0.00359	0.00223	0.00193
AT1G06430			FtsH8 TAT lTP	thylakoid-integral	29.5.7	1.26	0.83	1.63	1.40	0.00073	0.00046	0.00105	0.00061	0.00074	0.00147
AT1G74470	yes		geranylgeranyl reductase (GGDR)	thylakoid	16.1.1	0.71	1.10	0.00	1.23	0.00045	0.00038	0.00019	0.00049	0.00000	0.00023
ATcG01110			NDH H (NDH-7)	thylakoid	1.1.6	0.93	1.15	0.36	0.87	0.00058	0.00017	0.00046	0.00067	0.00006	0.00040
ATcG01100			NDH A (NDH-1)	thylakoid-integral	1.1.6	0.53	0.77	0.38	0.30	0.00061	0.00010	0.00060	0.00047	0.00004	0.00018
AT5G06290	yes		2-Cys Peroxiredoxin B (Prx B)	plastid stroma	21.5	1.58	1.02	1.41	2.21	0.00085	0.00054	0.00089	0.00087	0.00076	0.00197
AT3G52960			Peroxiredoxin IIE (PrxII E)	plastid stroma	21.5	1.18	0.96	1.34	1.26	0.00071	0.00067	0.00075	0.00068	0.00089	0.00094
AT3G11630			2-Cys Peroxiredoxin A (Prx A; forme	thylakoid-peripheral-st	21.5	1.15	1.33	0.99	1.01	0.00237	0.00085	0.00208	0.00314	0.00084	0.00209
AT4G22890		yes	PGRL1A	thylakoid-integral	1.1.40	0.69	0.74	0.58	0.80	0.00131	0.00128	0.00083	0.00097	0.00074	0.00067
AT1G80380			glycerate-kinase (GK) - Model .2 is b	plastid stroma	1.2.7	1.05	0.95	0.99	1.46	0.00095	0.00127	0.00041	0.00091	0.00125	0.00060
AT1G32470	yes		glycine cleavage system H protein	mitochondria	1.2.4.4	0.72	0.93	0.12	1.17	0.00017	0.00028	0.00028	0.00016	0.00003	0.00033
AT2G35370			Glycine decarboxylase (GDC) - subu	mitochondria	1.2.4.4	0.98	1.03	0.55	1.58	0.00038	0.00032	0.00019	0.00039	0.00018	0.00031
AT3G14415			glycolate oxidase-1 (GOX-1) - perox	peroxisome	1.2.2	1.00	1.34	0.87	0.99	0.00185	0.00456	0.00485	0.00247	0.00396	0.00481
AT3G14420			glycolate oxidase-1 (GOX-1) - perox	plastid	1.2.2	0.98	1.19	0.88	0.97	0.00517	0.01057	0.00942	0.00612	0.00932	0.00913
AT1G68010			hydroxypyruvate reductase 1 (HPR1)	peroxisome	1.2.6	1.07	1.09	0.96	1.19	0.00207	0.00489	0.00387	0.00227	0.00468	0.00460
AT5G36700			2-phosphoglycolate phosphatase-1 (P	plastid stroma	1.2.1	1.19	0.86	1.70	1.11	0.00120	0.00101	0.00184	0.00104	0.00172	0.00205
AT3G16140	yes		psaH-1 - subunit VI	thylakoid-integral	1.1.2.2	0.46	0.59	0.00	0.68	0.00038	0.00022	0.00024	0.00023	0.00000	0.00016
AT1G08380	yes		psaO	thylakoid-integral	1.1.2.2	0.41	1.12	0.06	0.26	0.00024	0.00002	0.00110	0.00027	0.00000	0.00029
AT2G46820			Photosystem I protein TMP14 - PSI-l	thylakoid	1.1.2.2	0.84	0.68	1.08	0.90	0.00037	0.00021	0.00013	0.00025	0.00022	0.00012
ATcG00340			psaB - subunit Ib	thylakoid-integral	1.1.2.2	0.98	1.04	0.98	0.91	0.00856	0.00790	0.00687	0.00895	0.00778	0.00622
ATcG00350			psaA - subunit Ia	thylakoid-integral	1.1.2.2	0.88	0.87	1.01	0.66	0.00588	0.00452	0.00252	0.00511	0.00458	0.00167
AT1G31330			psaF- subunit III - LTP - hydrophobi	thylakoid-integral	1.1.2.2	0.75	0.83	0.85	0.68	0.00111	0.00094	0.00289	0.00092	0.00080	0.00196
AT4G12800		yes	psaL - subunit XI (also named V)	thylakoid-integral	1.1.2.2	0.77	1.10	0.72	0.62	0.00105	0.00148	0.00189	0.00115	0.00106	0.00117
AT1G55670			psaG - subunit V- stromal side	thylakoid-integral	1.1.2.2	1.01	0.87	1.03	1.10	0.00038	0.00041	0.00046	0.00033	0.00043	0.00050
AT4G02770			psaD-2 subunit II - stromal side-tight	thylakoid-peripheral-st	1.1.2.2	0.76	1.08	0.71	0.57	0.00158	0.00237	0.00203	0.00171	0.00169	0.00116
AT1G61520			LHCI-3 - LHCI-680A CAB4	thylakoid-integral	1.1.2.1	0.85	0.92	0.88	0.78	0.00270	0.00289	0.00376	0.00250	0.00256	0.00293
AT3G47470			LHCI-4 - LHCI-730	thylakoid-integral	1.1.2.1	0.81	1.06	0.71	0.70	0.00210	0.00257	0.00231	0.00222	0.00182	0.00163
AT3G61470		yes	LHCI-2.1 - LHCI-680B	thylakoid-integral	1.1.2.1	0.65	1.03	0.47	0.43	0.00101	0.00091	0.00102	0.00104	0.00042	0.00044
AT3G54890			LHCI-1-1 - LHCI-730	thylakoid-integral	1.1.2.1	0.68	0.84	0.73	0.49	0.00076	0.00052	0.00073	0.00063	0.00038	0.00035
AT1G45474			LHCI-5 - new	thylakoid-integral	1.1.2.1	1.14	1.28	1.17	0.87	0.00022	0.00034	0.00016	0.00028	0.00040	0.00014
ATcG00680	2x yes	yes	psbB CP47	thylakoid-integral	1.1.1.2	0.71	1.07	0.56	0.42	0.01750	0.01384	0.01489	0.01871	0.00779	0.00620
ATcG00280	2x yes	yes	psbC CP43	thylakoid-integral	1.1.1.2	0.66	0.98	0.56	0.40	0.01157	0.01229	0.00991	0.01130	0.00692	0.00400
ATcG00270	2x yes	yes	psbD D2	thylakoid-integral	1.1.1.2	0.65	1.00	0.44	0.44	0.01045	0.00804	0.00953	0.01044	0.00353	0.00418
AT1G79040	2x yes	yes	psbR	thylakoid-integral	1.1.1.2	0.43	1.05	0.12	0.13	0.00039	0.00047	0.00032	0.00041	0.00006	0.00004
AT4G21280	2x yes	yes	psbQ OEC16 Tat ltp	thylakoid-peripheral-lu	1.1.1.2	0.55	1.15	0.32	0.37	0.00086	0.00136	0.00119	0.00099	0.00043	0.00044
AT4G05180	2x yes	yes	psbQ OEC16-like Tat lTP	thylakoid-peripheral-lu	1.1.1.2	0.46	0.82	0.20	0.11	0.00078	0.00060	0.00037	0.00064	0.00012	0.00004
ATcG00020	yes		psbA D1	thylakoid-integral	1.1.1.2	0.79	1.00	0.66	0.55	0.00470	0.00480	0.00159	0.00468	0.00316	0.00088
AT5G66570	yes	yes	psbO OEC33	thylakoid-peripheral-lu	1.1.1.2	0.59	0.96	0.35	0.51	0.00160	0.00205	0.00128	0.00153	0.00073	0.00066
AT3G50820	yes		psbO OEC33-like	thylakoid-peripheral-lu	1.1.1.2	0.60	0.93	0.24	0.52	0.00164	0.00112	0.00153	0.00152	0.00027	0.00080
ATcG00580	yes	yes	psbE cytb559a	thylakoid-integral	1.1.1.2	0.51	0.73	0.66	0.31	0.00065	0.00043	0.00103	0.00047	0.00028	0.00032
AT1G06680	yes		PsbP-1 OEC23 Tat lTP	thylakoid-peripheral-lu	1.1.1.2	0.76	0.95	0.75	0.52	0.00701	0.00411	0.00519	0.00663	0.00309	0.00268
AT2G05100	yes		LHCII-2.1	thylakoid-integral	1.1.1.1	1.61	2.09	1.04	1.58	0.00248	0.00206	0.00079	0.00517	0.00213	0.00125
AT2G05070	yes		LHCII-2.2	thylakoid-integral	1.1.1.1	0.52	0.33	0.80	0.69	0.00361	0.00102	0.00244	0.00121	0.00082	0.00168
AT1G29930	yes		LHCII-1.3 - 100% identical to lhcb-1	thylakoid-integral	1.1.1.1	1.12	0.98	1.78	1.00	0.00869	0.00263	0.00459	0.00850	0.00469	0.00456
AT2G40100	yes	yes	LHCII-4.3 -CP29	thylakoid-integral	1.1.1.1	0.56	0.91	0.46	0.45	0.00117	0.00087	0.00285	0.00106	0.00040	0.00129
AT4G10340			LHCII-5 - CP26	thylakoid-integral	1.1.1.1	0.90	1.09	0.78	0.83	0.00871	0.00924	0.00890	0.00948	0.00722	0.00739
AT5G01530			LHCII-4.1-CP29	thylakoid-integral	1.1.1.1	0.88	0.85	1.03	0.79	0.00798	0.00507	0.00506	0.00681	0.00524	0.00398
AT1G15820			LHCII-6 - CP24	thylakoid-integral	1.1.1.1	1.00	0.96	1.16	0.93	0.00599	0.00285	0.00303	0.00572	0.00330	0.00281
AT5G54270			LHCII-3	thylakoid-integral	1.1.1.1	0.78	0.79	0.85	0.74	0.00353	0.00196	0.00460	0.00280	0.00166	0.00339
AT3G08940			LHCII-4.2 - CP29 - model .2 is better	thylakoid-integral	1.1.1.1	0.84	0.95	0.88	0.61	0.00457	0.00219	0.00266	0.00436	0.00192	0.00164
AT2G34430			LHCII-1.4	thylakoid-integral	1.1.1.1	0.85	0.79	0.75	1.06	0.00260	0.00183	0.00146	0.00207	0.00137	0.00154

Supplemental Table 1. (continued)

Accession	GLEE - genotype effect (p<0.01)	Genotype (p<0.01)	lab annotation	subcellular location	BIN#	k1k3/wt average (days 0-3-	k1k3/wt 0day (NadjSPC)	k1k3/wt 3 day (NadjSPC)	k1k3/wt 5 day (NadjSPC)	wt 0 day. Average NadjSPC	wt 3 day Average NadjSPC	wt 5 day Average NadjSPC	k1k3 0day Average	k1k3 3day Average	k1k3 5dayAverag e NadjSPC
AT2G34420			LHCII-1.5	thylakoid-integral	1.1.1.1	1.21	1.23	1.39	0.69	0.00078	0.00225	0.00079	0.00096	0.00312	0.00055
AT3G27690			LHCII-2.3	thylakoid-integral	1.1.1.1	0.95	1.11	0.60	0.90	0.00157	0.00062	0.00101	0.00175	0.00037	0.00090
AT1G19670			chlorophyllase 1 (CLH1) (also ATH(	cytosol	19.50*	1.30	1.20	1.97	1.02	0.00030	0.00040	0.00083	0.00037	0.00078	0.00085
AT4G37000			red chlorophyll catabolite reductase (	plastid	19.50*	0.96	0.74	1.53	1.07	0.00032	0.00009	0.00021	0.00024	0.00013	0.00023
AT5G63570			glutamate-1-semialdehyde 2,1-amino	plastid stroma	19.3	0.97	1.13	0.96	0.88	0.00056	0.00065	0.00101	0.00063	0.00063	0.00089
AT3G48730			glutamate-1-semialdehyde 2,1-amino	plastid stroma	19.3	1.00	1.53	0.67	1.10	0.00035	0.00074	0.00066	0.00054	0.00050	0.00072
AT1G08520			Mg-protoporphyrin IX chelatase (CH	plastid	19.10	0.86	1.01	0.57	8.66	0.00076	0.00079	0.00001	0.00077	0.00045	0.00013
AT4G25080	yes	yes	magnesium-protoporphyrin IX methy	plastid	19.11	0.42	0.85	0.04	0.38	0.00049	0.00053	0.00023	0.00042	0.00002	0.00009
AT5G08280			hydroxymethylbilane synthase (HEM	plastid stroma	19.5	0.77	1.06	0.43	0.82	0.00035	0.00035	0.00028	0.00037	0.00015	0.00023
AT4G01690	yes		protoporphyrinogen oxidase (PPO) (I	plastid	19.9	1.96	1.31	1.08	16.20	0.00034	0.00022	0.00003	0.00045	0.00024	0.00047
AT2G40490			uroporphyrinogen decarboxylase (UI	plastid stroma	19.7	1.03	1.05	1.25	0.93	0.00026	0.00014	0.00037	0.00028	0.00017	0.00035
AT5G42980			thioredoxin h3 (Trx H3)	cytosol	21.1	1.09	1.09	0.92	1.51	0.00024	0.00055	0.00023	0.00026	0.00051	0.00035
AT1G21750			PDI Calsequestrin and thioredoxin dc	ER	21.1	1.16	1.25	0.83	1.39	0.00072	0.00064	0.00066	0.00090	0.00052	0.00091
AT5G60640			protein disulfide isomerase	ER	21.1	0.77	0.97	0.70	0.12	0.00058	0.00041	0.00013	0.00056	0.00028	0.00002
AT1G77510			thioredoxin	not plastid	21.1	1.03	0.88	0.85	1.51	0.00051	0.00026	0.00025	0.00045	0.00022	0.00037
AT2G47470		yes	thioredoxin family protein (ATPDIL2	peroxisome	21.1	0.61	0.86	0.36	0.72	0.00023	0.00032	0.00021	0.00020	0.00012	0.00015
AT1G76080			thioredoxin (CDSP32)	plastid stroma	21.1	1.32	0.94	1.22	1.82	0.00047	0.00058	0.00049	0.00045	0.00071	0.00088
AT1G03680			thioredoxin m1	thylakoid-peripheral-st	21.1	0.86	0.66	0.82	1.32	0.00030	0.00036	0.00017	0.00020	0.00030	0.00023
AT5G67030	yes		zeaxanthin epoxidase precursor (LOS	thylakoid	16.1.4	1.76	0.81	104.88	6.26	0.00045	0.00000	0.00007	0.00036	0.00010	0.00045
AT5G03880			glutaredoxin	thylakoid	21.4	0.99	0.69	1.15	1.21	0.00038	0.00026	0.00033	0.00026	0.00029	0.00040
AT4G13940			S-adenosyl-L-homocysteine hydrolas	not plastid	13.2.3.4	0.98	1.65	0.98	0.74	0.00059	0.00163	0.00166	0.00098	0.00159	0.00123
AT1G11840			glyoxalase I-2, putative (lactoylglutat	peroxisome	13.2.3.2	1.19	1.12	1.21	1.22	0.00060	0.00101	0.00078	0.00067	0.00122	0.00095
AT1G67280			glyoxalase I -1, putative (lactoylgluta	thylakoid-peripheral-st	13.2.3.2	0.98	0.94	0.98	1.02	0.00046	0.00048	0.00045	0.00044	0.00047	0.00046
AT4G08870	yes		arginase 2 (ARGAH2)	mitochondria	13.2.2.3	1.46	0.77	2.39	0.93	0.00101	0.00188	0.00198	0.00077	0.00450	0.00185
AT4G33010			glycine decarboxylase/glycine cleava	mitochondria	13.2.5.2	1.01	1.01	1.04	0.99	0.00490	0.00608	0.00604	0.00493	0.00634	0.00598
AT2G26080			glycine dehydrogenase [decarboxylat	mitochondria	13.2.5.2	0.97	1.09	0.93	0.90	0.00224	0.00321	0.00179	0.00244	0.00297	0.00161
AT1G11860			Glycine cleavage T-protein	not plastid	13.2.5.2	1.00	1.18	0.96	0.93	0.00226	0.00450	0.00430	0.00268	0.00434	0.00400
AT4G33680			aminotransferase, classes I and II - A	plastid stroma	13.1.3.5.	1.43	1.78	1.01	1.70	0.00024	0.00041	0.00033	0.00042	0.00042	0.00056
AT5G17920		yes	5-methyltetrahydropteroyltriglutamat	cytosol	13.1.3.4	0.81	1.01	0.76	0.63	0.00801	0.00961	0.00609	0.00811	0.00729	0.00386
AT5G49810			S-adenosylmethionine-dependent methyltransferase (MMT)		13.1.3.4.	1.02	0.74	1.27	1.70	0.00044	0.00003	0.00017	0.00033	0.00004	0.00029
AT3G03780	yes	yes	methionine synthase (AtMS2)	cytosol	13.1.3.4.	0.63	0.82	0.55	0.59	0.00215	0.00395	0.00216	0.00175	0.00216	0.00128
AT3G17390	yes	yes	S-adenosylmethionine synthetase 3 (M	not plastid	13.1.3.4.	0.38	0.92	0.16	0.01	0.00046	0.00080	0.00019	0.00042	0.00013	0.00000
AT1G14810			aspartate-semialdehyde dehydrogenas	plastid stroma	13.1.3.6.	1.17	1.49	0.80	1.26	0.00032	0.00044	0.00072	0.00047	0.00036	0.00091
AT3G19710	yes	yes	branched-chain amino acid aminotrar	cytosol	13.1.4.1.	0.39	1.09	0.37	0.17	0.00017	0.00057	0.00050	0.00018	0.00021	0.00008
AT3G58610			ketol-acid reductoisomerase	plastid stroma	13.1.4.1.	0.93	1.19	0.90	0.72	0.00080	0.00182	0.00080	0.00096	0.00163	0.00057
AT4G13430			isopropylmalate isomerase (IPMI) LS	plastid stroma	13.1.4.4	0.76	1.08	0.57	0.65	0.00024	0.00029	0.00017	0.00026	0.00017	0.00011
AT5G14200			3-isopropylmalate dehydrogenase-2,	plastid stroma	13.1.4.4.	0.78	1.21	0.82	0.60	0.00037	0.00119	0.00109	0.00045	0.00097	0.00065
AT1G17290			alanine aminotransferase (AlAAT1)	mitochondria	13.1.1.3.	0.97	1.13	0.61	1.42	0.00044	0.00079	0.00047	0.00050	0.00048	0.00067
AT5G19550			aspartate aminotransferase, cytoplasn	cytosol	13.1.1.2.	1.17	1.27	0.81	1.46	0.00021	0.00023	0.00022	0.00027	0.00019	0.00032
AT2G30970			putative aspartate aminotransferase A	mitochondria	13.1.1.2.	0.96	1.23	1.14	0.82	0.00011	0.00019	0.00043	0.00013	0.00022	0.00035
AT4G31990			aspartate aminotransferase, chloropla	plastid stroma	13.1.1.2.	1.12	1.07	1.20	1.08	0.00069	0.00097	0.00131	0.00074	0.00116	0.00142
AT3G22200			gamma-aminobutyrate transaminase s	mitochondria	13.1.1.1.	0.98	0.72	0.97	1.29	0.00029	0.00043	0.00026	0.00021	0.00041	0.00033
AT1G65960			glutamate decarboxylase 1 (GAD 1)	not plastid	13.1.1.1.	0.74	0.99	0.85	0.43	0.00121	0.00053	0.00115	0.00120	0.00045	0.00049
AT1G79440			succinate-semialdehyde dehydrogena	mitochondria	13.1.1.1.	1.04	0.86	1.48	0.75	0.00045	0.00042	0.00037	0.00039	0.00063	0.00028
AT2G19940			N-acetyl-gamma-glutamyl-phosphate	plastid stroma	13.1.2.3	1.32	1.07	1.60	1.31	0.00020	0.00019	0.00042	0.00021	0.00030	0.00054
AT1G80600			acetylornithine transaminase/AOTA/	plastid stroma	13.1.2.3.	0.90	1.30	0.55	1.45	0.00019	0.00055	0.00021	0.00025	0.00030	0.00031
AT4G24830			argininosuccinate synthase	plastid stroma	13.1.2.3.	1.13	0.91	0.57	1.73	0.00026	0.00016	0.00024	0.00024	0.00009	0.00042
AT5G63890			histidinol dehydrogenase (ATHDH) -	plastid stroma	13.1.7.8	0.94	1.20	0.88	0.81	0.00027	0.00046	0.00039	0.00033	0.00041	0.00031
AT4G14880			cysteine synthase / O-acetylserine (th	cytosol	13.1.5.3.	0.84	0.92	0.74	0.86	0.00152	0.00130	0.00136	0.00140	0.00095	0.00117
AT3G61440			cysteine synthase (O-acetylserine (thi	mitochondria	13.1.5.3.	0.91	1.54	0.58	1.03	0.00033	0.00081	0.00043	0.00051	0.00047	0.00044
AT2G43750			cysteine synthase	plastid stroma	13.1.5.3.	1.07	0.97	1.30	0.94	0.00136	0.00128	0.00121	0.00133	0.00166	0.00113
AT4G34200			D-3-phosphoglycerate dehydrogenas	plastid	13.1.5.1.	0.97	0.84	1.04	1.04	0.00093	0.00070	0.00085	0.00079	0.00073	0.00089
AT3G19480			D-3-phosphoglycerate dehydrogenas	plastid stroma	13.1.5.1.	1.35	1.19	1.27	1.49	0.00030	0.00016	0.00045	0.00036	0.00021	0.00067
AT5G14780			Formate dehydrogenase	mitochondria	25.10	0.99	0.73	1.55	0.93	0.00025	0.00019	0.00062	0.00018	0.00029	0.00057

Supplemental Table 1. (continued)

Accession	GLEE - genotype effect (p<0.01)	Genotype (p<0.01)	lab annotation	subcellular location	BIN#	k1k3/wt average (days 0-3-	k1k3/wt 0day (NadjSPC)	k1k3/wt 3 day (NadjSPC)	k1k3/wt 5 day (NadjSPC)	wt 0 day. Average NadjSPC	wt 3 day Average NadjSPC	wt 5 day Average NadjSPC	k1k3 0day Average	k1k3 3day Average	k1k3 5dayAverage NadjSPC
AT1G50480	yes		10-formyltetrahydrofolate synthetase	not plastid	25.2	1.69	1.03	9.87	1.64	0.00041	0.00003	0.00037	0.00042	0.00034	0.00061
AT4G37930			glycine/serine hydroxymethyltransfer	mitochondria	25.1	0.92	1.04	0.80	1.03	0.00460	0.01090	0.00662	0.00478	0.00874	0.00681
AT4G13930			glycine/serine hydroxymethyltransfer	not plastid	25.1	0.94	1.43	0.62	1.00	0.00018	0.00034	0.00036	0.00026	0.00021	0.00036
AT3G59970			methylenetetrahydrofolate reductase	not plastid	25.6	1.00	1.05	0.60	1.19	0.00119	0.00065	0.00104	0.00125	0.00039	0.00124
AT2G44160			methylenetetrahydrofolate reductase	not plastid	25.6	0.69	0.57	0.85	0.78	0.00041	0.00019	0.00020	0.00023	0.00016	0.00016
AT5G43940			alcohol dehydrogenase class III (AD	not plastid	25.11	1.05	0.91	0.88	1.22	0.00032	0.00040	0.00067	0.00029	0.00035	0.00082
AT2G45470	yes		fasciclin-like arabinogalactan-protein	plasma membrane	10.5.1	1.35	0.68	3.84	1.37	0.00105	0.00028	0.00115	0.00071	0.00106	0.00157
AT3G14310			pectinesterase and invertase/pectin n	not plastid	10.8.1	1.26	1.04	1.40	1.52	0.00059	0.00072	0.00012	0.00062	0.00101	0.00017
AT3G09840			cell division cycle protein 48 (CDC4	plasma membrane	31.2	1.18	0.90	0.76	1.84	0.00122	0.00037	0.00076	0.00109	0.00028	0.00140
AT1G04820	yes		tubulin alpha-2/alpha-4 chain (TUA4	not plastid	31.1	0.42	1.96	0.00	0.24	0.00019	0.00062	0.00021	0.00038	0.00000	0.00005
AT5G09810			actin 7 (ACT7) / actin 2	not plastid	31.1	1.00	1.37	0.84	0.98	0.00052	0.00107	0.00115	0.00071	0.00090	0.00113
AT1G20010			tubulin beta-5 chain (TUB5)	not plastid	31.1	0.98	1.12	0.48	1.98	0.00084	0.00067	0.00021	0.00094	0.00033	0.00041
AT5G19770			tubulin alpha-3/alpha-5 chain (TUA3	not plastid	31.1	1.03	1.39	0.49	1.05	0.00042	0.00032	0.00061	0.00059	0.00016	0.00065
AT5G44340			tubulin beta-4 chain (TUB4)	not plastid	31.1	0.76	0.91	0.39	0.77	0.00029	0.00014	0.00041	0.00026	0.00005	0.00032
AT4G20890			tubulin beta-9 chain (TUB9)	nucleus	31.1	0.71	0.99	0.53	0.60	0.00025	0.00022	0.00033	0.00025	0.00011	0.00020
AT5G10470			kinesin-related protein TH65 - dually	plasma membrane	31.1	1.76	1.78	2.07	1.69	0.00029	0.00005	0.00030	0.00052	0.00010	0.00051
AT3G18780			actin 2 (ACT2)	vacuole	31.1	1.14	1.18	0.95	1.40	0.00081	0.00174	0.00112	0.00095	0.00165	0.00156
AT3G11130			clathrin heavy chain	not plastid	31.4	0.98	1.04	1.01	0.89	0.00658	0.00446	0.00506	0.00685	0.00448	0.00451
AT4G34450			adaptin motif - putative coatomer gar	not plastid	31.4	0.78	0.88	0.58	0.96	0.00154	0.00119	0.00048	0.00135	0.00069	0.00046
AT2G21390			coatomer protein complex, subunit al	not plastid	31.4	0.74	0.86	0.40	0.58	0.00161	0.00031	0.00057	0.00139	0.00012	0.00033
AT5G54770	yes	yes	THI1 -involved in thiamine synthesis	plastid stroma	18.2	0.43	0.83	0.29	0.33	0.00058	0.00109	0.00077	0.00049	0.00032	0.00026
AT2G38230			PDX1.1 (Vitamine b6 synthesis)	cytosol	18.20*	1.12	0.74	1.09	1.44	0.00054	0.00079	0.00075	0.00040	0.00086	0.00108
AT5G01410			PDX1.3 (Vitamine b6 synthesis)	cytosol	18.20*	1.05	1.10	0.46	1.99	0.00025	0.00059	0.00035	0.00027	0.00027	0.00071
AT5G24770	yes	yes	vegetative storage protein 2 (VSP2)		33.1	1.68	1.76	3.28	1.05	0.00003	0.00021	0.00053	0.00006	0.00068	0.00055
AT5G24780	yes		acid phosphatase - vegetative storage	not plastid	33.1	1.45	0.50	2.47	1.01	0.00056	0.00097	0.00108	0.00028	0.00239	0.00110
AT3G16000			MFP1 - nucleoid binding	plastid nucleoid	28.3*	0.92	0.89	0.88	1.31	0.00056	0.00015	0.00006	0.00050	0.00013	0.00007
AT3G46780		yes	unknown protein (pTAC16)	thylakoid	28.3*	1.33	1.27	1.15	1.62	0.00194	0.00192	0.00156	0.00247	0.00220	0.00252
AT1G54100			aldehyde dehydrogenase, putative / a	cytosol	5.10	1.63	1.18	2.29	1.34	0.00010	0.00017	0.00023	0.00012	0.00039	0.00031
AT3G48000			aldehyde dehydrogenase (ALDH2)	mitochondria	5.10	1.36	0.96	1.61	1.39	0.00060	0.00084	0.00079	0.00058	0.00135	0.00110
AT5G17380			pyruvate decarboxylase family protei		5.2	1.12	0.41	86.54	1.44	0.00028	0.00000	0.00036	0.00012	0.00009	0.00052
AT5G54960			pyruvate decarboxylase - PDC2		5.2	1.50	0.73	3.50	1.69	0.00043	0.00012	0.00046	0.00032	0.00042	0.00078
AT5G09660			malate dehydrogenase, glyoxysomal/	peroxisome	6.3	0.91	1.04	0.73	0.94	0.00270	0.00272	0.00423	0.00280	0.00198	0.00398
AT3G52930	yes	yes	fructose-bisphosphate aldolase	cytosol	4.7	0.62	0.85	0.36	0.83	0.00069	0.00104	0.00053	0.00058	0.00038	0.00044
AT4G26530		yes	fructose-bisphosphate aldolase, cytop	cytosol	4.7	1.27	1.20	1.23	1.48	0.00206	0.00259	0.00129	0.00247	0.00318	0.00192
AT2G36460			Aldolase	cytosol	4.7	1.02	0.89	0.70	1.43	0.00036	0.00067	0.00065	0.00033	0.00047	0.00093
AT2G36530			Enolase (ENO2 also LOS2) dual targ	nucleus	4.12	0.79	1.08	0.75	0.68	0.00154	0.00222	0.00316	0.00165	0.00167	0.00215
AT5G42740			glucose-6-phosphate isomerase, cyto	not plastid	4.3	0.87	0.73	0.66	1.60	0.00042	0.00031	0.00017	0.00030	0.00020	0.00027
AT4G24620		yes	glucose-6-phosphate isomerase (PGI	plastid stroma	4.3	1.56	1.13	2.06	1.52	0.00042	0.00043	0.00080	0.00047	0.00089	0.00122
AT1G13440	2x yes	yes	glyceraldehyde-3-phosphate dehydro	nucleus	4.9	0.64	0.90	0.63	0.48	0.00357	0.00675	0.00560	0.00320	0.00428	0.00267
AT1G53310	yes		phosphoenolpyruvate carboxylase, pu		4.14	1.00	1.77	0.00	0.59	0.00035	0.00021	0.00015	0.00063	0.00000	0.00009
AT2G42600			phosphoenolpyruvate (PEP) carboxyl	not plastid	4.14	0.88	0.95	0.88	0.79	0.00610	0.00467	0.00467	0.00579	0.00412	0.00367
AT1G23190	yes	yes	phosphoglucomutase-3 (PGM-3)	cytosol	4.2	0.65	0.93	0.45	0.61	0.00091	0.00095	0.00137	0.00084	0.00043	0.00084
AT1G70730			phosphoglucomutase (PGM)	not plastid	4.2	0.93	1.00	0.90	0.89	0.00155	0.00181	0.00213	0.00155	0.00164	0.00190
AT5G51820			plastid phosphoglucomutase (PGM1)	plastid stroma	4.2	1.08	1.15	0.85	1.26	0.00148	0.00113	0.00094	0.00169	0.00097	0.00119
AT1G70820			phosphoglucomutase-2 (PGM-2)	plastid stroma	4.2	1.05	1.02	0.93	1.16	0.00068	0.00029	0.00045	0.00070	0.00027	0.00052
AT1G79550			phosphoglycerate kinase	not plastid	4.10	0.81	1.14	0.60	0.82	0.00071	0.00123	0.00214	0.00081	0.00074	0.00176
AT1G09780			Phosphoglycerate mutase	cytosol	4.11	0.63	0.70	0.88	0.28	0.00048	0.00056	0.00048	0.00033	0.00049	0.00013
AT3G08590			2,3-biphosphoglycerate-independent	not plastid	4.11	0.99	1.05	0.83	1.10	0.00054	0.00108	0.00141	0.00057	0.00090	0.00155
AT3G52990			pyruvate kinase, putative	not plastid	4.13	0.61	0.90	0.54	0.55	0.00034	0.00020	0.00154	0.00031	0.00011	0.00085
AT4G15530			pyruvate phosphate dikinase (PPDK)	plastid stroma	4.4	0.82	0.85	0.50	1.00	0.00104	0.00088	0.00142	0.00088	0.00044	0.00143
AT3G55440			triosephosphate isomerase-2 (TPI-2)	not plastid	4.8	1.01	1.26	1.05	0.81	0.00101	0.00158	0.00161	0.00127	0.00166	0.00130
AT3G03250		yes	UDP-glucose pyrophosphorylase	not plastid	4.1	0.66	0.97	0.67	0.55	0.00052	0.00112	0.00144	0.00050	0.00075	0.00079
AT5G17310			UDP-glucose pyrophosphorylase	not plastid	4.1	1.13	1.02	1.34	1.04	0.00041	0.00054	0.00075	0.00042	0.00072	0.00078
AT3G07390	yes	yes	auxin-responsive protein / auxin-indu	plasma membrane	17.2.3	1.76	1.01	2.76	1.81	0.00059	0.00043	0.00030	0.00059	0.00118	0.00055

Supplemental Table 1. (continued)

Accession	GLEE - genotype effect (p<0.01)	Genotype (p<0.01)	lab annotation	subcellular location	BIN#	klk3/wt average (days 0-3-	klk3/wt 0day (NadjSPC)	klk3/wt 3 day (NadjSPC)	klk3/wt 5 day (NadjSPC)	wt 0 day. Average NadjSPC	wt 3 day Average NadjSPC	wt 5 day Average NadjSPC	klk3 0day Average	klk3 3day Average	klk3 5dayAverage NadjSPC
AT3G02260			ubiquitin-protein ligase (BIG ; DARK OVER-EXPRESSION		17.2.2	0.63	0.75	0.06	0.29	0.00164	0.00002	0.00055	0.00122	0.00000	0.00016
AT3G44310		yes	nitrilase 1 (NIT1 or NITI) - dual loca	nucleus	17.2.1	0.64	0.97	0.56	0.55	0.00137	0.00158	0.00382	0.00133	0.00089	0.00210
AT3G25770			allene oxide cyclase 2 (OAC2;ERD1	thylakoid-peripheral-st	17.7.1.4	0.81	0.96	0.88	0.50	0.00105	0.00103	0.00075	0.00100	0.00090	0.00038
AT5G42650	yes		allene oxide synthase (AOS) (interact	thylakoid	17.7.1.3	1.27	1.00	2.47	0.90	0.00261	0.00221	0.00530	0.00261	0.00546	0.00476
AT3G25760	yes	yes	allene oxide cyclase 1 (OAC1;ERD1	plastid	17.7.1.3	0.65	0.95	1.11	0.10	0.00028	0.00026	0.00037	0.00027	0.00029	0.00004
AT3G45140			lipoxygenase AtLOX2, plastid	plastid stroma	17.7.1.2	1.02	1.03	1.11	0.91	0.01509	0.01351	0.01284	0.01551	0.01504	0.01166
AT3G44860	yes		S-adenosyl-L-methionine:carboxyl m		17.8.1	1.28	0.72	6.22	0.80	0.00042	0.00007	0.00020	0.00030	0.00042	0.00016
AT2G38040			carboxyltransferase (CT) alpha subur	envelope-inner-periphe	11.1.1	1.34	1.40	1.19	39.47	0.00057	0.00048	0.00000	0.00080	0.00058	0.00004
AT5G35360			biotin carboxylase (BC) - part of ACC	envelope-inner-periphe	11.1.1	1.18	1.10	0.90	1.99	0.00031	0.00034	0.00014	0.00034	0.00031	0.00029
AT1G36160			acetyl-CoA carboxylase - ACC1 (ACETYL-COENZYME A		11.1.1	0.79	0.88	absent in both	0.68	0.00043	0.00000	0.00033	0.00038	0.00000	0.00023
AT1G24360			Plastidial Ketoacyl-ACP Reductase	plastid stroma	11.1.4	0.98	0.90	1.10	0.98	0.00031	0.00019	0.00049	0.00028	0.00021	0.00048
AT3G16910	yes		acetyl-CoA synthetase (#7)	peroxisome	11.1.8	0.70	1.13	0.06	1.39	0.00021	0.00034	0.00019	0.00024	0.00002	0.00026
AT4G14070			Plastidial Long-Chain Acyl-CoA Syn	envelope	11.1.8	1.12	0.58	4.90	1.43	0.00045	0.00002	0.00059	0.00026	0.00008	0.00084
AT3G48990			OSB-CoA ligase (menE), At4CL8	not plastid	11.1.8	1.05	1.18	0.91	1.12	0.00048	0.00065	0.00044	0.00057	0.00059	0.00050
AT5G36880			acetyl-CoA synthetase (acetate-CoA	plastid stroma	11.1.8	0.84	0.91	0.80	0.80	0.00032	0.00045	0.00004	0.00029	0.00036	0.00003
AT5G46290			Ketoacyl-ACP Synthase I (Lipid Gen	plastid stroma	11.1.3	1.03	0.80	1.91	0.82	0.00021	0.00012	0.00027	0.00017	0.00023	0.00022
AT4G23850			long-chain-fatty-acid--CoA ligase / lc	not plastid	11.1.9	0.90	0.73	0.65	6.25	0.00056	0.00024	0.00003	0.00040	0.00016	0.00018
AT3G25860			E2 - dihydrolipoamide acetyltransfera	plastid	11.1.31	1.06	1.55	1.05	0.55	0.00026	0.00029	0.00024	0.00041	0.00030	0.00013
AT2G33150	yes		3-ketoacyl-CoA thiolase (KAT2)	peroxisome	11.9.4.5	3.16	1.46	2.69	3.39	0.00005	0.00003	0.00046	0.00008	0.00009	0.00155
AT4G16760	yes		acyl-CoA oxidase (ACX1)	peroxisome	11.9.4.2	1.73	0.89	1.66	3.21	0.00043	0.00064	0.00027	0.00038	0.00106	0.00088
AT4G29010			enoyl-CoA hydratase - AIM1 (ABN(	peroxisome	11.9.4.9	1.66	1.17	3.06	1.72	0.00046	0.00014	0.00054	0.00054	0.00042	0.00094
AT1G45201			lipase class 3 family protein		11.9.2	1.05	0.88	1.15	1.11	0.00059	0.00024	0.00143	0.00052	0.00028	0.00158
AT1G66970			glycerophosphoryl diester phosphodi	plasma membrane	11.9.3.3	1.20	1.08	1.35	1.31	0.00133	0.00056	0.00071	0.00143	0.00075	0.00092
AT4G26690			MRH5/SHV3 (morphogenesis of roo	plasma membrane	11.9.3.3	1.30	0.96	1.69	1.50	0.00071	0.00044	0.00034	0.00068	0.00074	0.00052
AT3G15730			phospholipase D alpha 1 (PLD {alpha	not plastid	11.9.3.1	0.96	1.05	0.77	1.02	0.00136	0.00079	0.00076	0.00142	0.00061	0.00077
AT4G17470			palmitoyl protein thioesterase family		11.9.1	1.65	0.04	4.13	1.56	0.00002	0.00003	0.00048	0.00000	0.00014	0.00074
AT1G48600			phosphoethanolamine N-methyltransf	not plastid	11.3	0.68	0.89	0.58	0.67	0.00056	0.00100	0.00135	0.00050	0.00058	0.00091
AT2G24270			NON-phosphorylating NADP glycera	cytosol	2	0.93	1.22	0.77	0.91	0.00106	0.00175	0.00286	0.00129	0.00135	0.00261
AT1G10760	2x yes	yes	WaterDikinase (Sex1; R1 protein)	plastid stroma	2.2.2.3	0.63	1.12	0.43	0.43	0.00188	0.00123	0.00337	0.00210	0.00053	0.00143
AT5G26570	yes		phosphoglucan water dikinase (PWD	plastid stroma	2.2.2.3	0.71	1.14	0.35	0.48	0.00139	0.00066	0.00164	0.00158	0.00023	0.00078
AT1G69830	2x yes	yes	alpha-amylase - AtAMY3	plastid stroma	2.2.2.1	0.47	1.22	0.00	0.00	0.00039	0.00034	0.00029	0.00047	0.00000	0.00000
AT4G17090	yes		beta-amylase 3 (BAM3 or BMY8 or	plastid stroma	2.2.2.1	0.87	0.87	0.51	1.72	0.00066	0.00117	0.00050	0.00058	0.00059	0.00086
AT4G15210	yes		beta-amylase 5 (BAM5 or BMY1 or RAM1) - not plastid		2.2.2.1	0.63	1.13	0.92	0.41	0.00082	0.00591	0.00949	0.00093	0.00542	0.00386
AT3G46970	yes	yes	heteroglycan phosphorylase-2 (PHS2	cytosol	2.2.2.2	0.62	1.11	0.13	0.57	0.00224	0.00182	0.00372	0.00248	0.00024	0.00214
AT3G29320			starch phosphorylase-1	plastid stroma	2.2.2.2	0.98	1.08	0.85	0.91	0.00089	0.00050	0.00038	0.00095	0.00042	0.00034
AT4G29130			hexokinase 1 (HXK1	mitochondria	2.2.1.4	1.07	1.68	absent in both	0.93	0.00014	0.00000	0.00062	0.00024	0.00000	0.00058
AT1G12240	yes	yes	beta-fructosidase (BFRUCT4) / beta-	vacuole	2.2.1.3.3	1.88	0.75	1.71	4.47	0.00053	0.00108	0.00030	0.00039	0.00184	0.00134
AT2G40840	yes		transglucosidase (disproportionating	cytosol	2.3	0.52	0.90	0.24	0.34	0.00071	0.00050	0.00069	0.00064	0.00012	0.00023
AT5G48300	yes		ADP-glucose pyrophosphorylase - sn	plastid stroma	2.1.2.1	1.40	0.83	2.11	1.79	0.00125	0.00054	0.00085	0.00105	0.00115	0.00152
AT5G19220			ADP-glucose pyrophosphorylase (AI	plastid stroma	2.1.2.1	1.51	1.37	1.73	1.43	0.00079	0.00084	0.00095	0.00109	0.00145	0.00135
AT5G03650			starch branching enzyme class II (SB	plastid stroma	2.1.2.3	0.80	1.06	0.02	0.63	0.00036	0.00005	0.00032	0.00038	0.00000	0.00020
AT1G43670			D-fructose-1,6-bisphosphate 1-phosp	not plastid	2.1.1.3	1.19	1.14	0.95	1.45	0.00039	0.00043	0.00046	0.00045	0.00041	0.00067
AT5G20280			ATSPS1F (SUCROSE PHOSPHATE SYNTHASE 1F); suc		2.1.1.1	0.92	1.36	102.37	0.67	0.00052	0.00000	0.00128	0.00070	0.00010	0.00085
AT4G14040	2x yes	yes	selenium-binding protein	not plastid	15	0.34	1.07	0.18	0.30	0.00019	0.00064	0.00093	0.00020	0.00011	0.00028
AT5G19140			auxin/aluminum-responsive protein, p	not plastid	15	0.97	0.87	0.99	1.06	0.00036	0.00024	0.00034	0.00032	0.00024	0.00037
AT4G23600	2x yes		nicotianamine aminotransferase	not plastid	15.2	1.00	0.62	2.04	0.71	0.00376	0.00397	0.00922	0.00233	0.00810	0.00656
AT5G14910			unknown protein - heavy metal bindi	plastid stroma	15.2	1.09	1.08	1.16	0.96	0.00027	0.00022	0.00013	0.00029	0.00026	0.00012
AT1G16880			uridylyltransferase-related	thylakoid-peripheral-st	3.8.3	1.09	0.87	1.23	1.25	0.00083	0.00057	0.00073	0.00072	0.00070	0.00091
AT2G27680			aldo/keto reductase family protein	plastid stroma	3.5	1.19	1.52	1.33	0.97	0.00015	0.00019	0.00036	0.00022	0.00025	0.00035
AT1G04420			aldo/keto reductase family protein	plastid stroma	3.5	1.23	0.81	1.53	1.29	0.00048	0.00051	0.00070	0.00039	0.00078	0.00091
AT5G51970			NAD-dependent sorbitol (L-iditol) de		3.3	1.13	0.80	1.40	1.16	0.00033	0.00035	0.00046	0.00026	0.00048	0.00053
AT4G30310			ribitol kinase, putative	not plastid	3.3	1.38	0.65	1.49	1.79	0.00016	0.00024	0.00023	0.00011	0.00036	0.00041
AT5G49650			xylulose kinase (DXK1)	cytosol	3.7	1.45	0.83	1.82	1.99	0.00024	0.00017	0.00016	0.00020	0.00031	0.00031
AT1G56500	yes	yes	haloacid dehalogenase-like hydrolase	plastid stroma	3.2	1.83	1.29	1.76	5.95	0.00060	0.00045	0.00009	0.00077	0.00079	0.00051

Supplemental Table 1. (continued)

Accession	GLEE - genotype effect (p<0.01)	Genotype (p<0.01)	lab annotation	subcellular location	BIN#	k1k3/wt average (days 0-3-	k1k3/wt 0day (NadjSPC)	k1k3/wt 3 day (NadjSPC)	k1k3/wt 5 day (NadjSPC)	wt 0 day. Average NadjSPC	wt 3 day Average NadjSPC	wt 5 day Average NadjSPC	k1k3 0day Average	k1k3 3day Average	k1k3 5dayAverage NadjSPC
AT1G79600	2x yes	yes	ABC1 kinase 3 (ABC1K3)	plastoglobules	26.56*	0.00	0.00	0.02	0.00	0.00055	0.00005	0.00075	0.00000	0.00000	0.00000
AT5G05200			ABC1 kinase 9 (ABC1K9)	plastoglobules	26.56*	1.47	2.84	1.78	1.14	0.00006	0.00015	0.00037	0.00016	0.00028	0.00043
AT5G44020	yes		acid phosphatase class B family prote	not plastid	26.13	1.75	0.52	5.80	2.65	0.00056	0.00013	0.00016	0.00029	0.00078	0.00042
AT3G57260			glucan endo-1,3-beta-glucosidase		26.4	0.89	0.70	2.17	absent in both	0.00056	0.00009	0.00000	0.00040	0.00019	0.00000
AT1G08640			weak J-domain protein CJD1 (ARC6	envelope-inner-integra	26.29*	1.32	0.88	1.26	2.41	0.00012	0.00039	0.00007	0.00011	0.00049	0.00017
AT3G14210			myrosinase (TGG2)-associated protein	(very abundant)	26.28	1.18	0.90	1.21	1.33	0.00147	0.00197	0.00249	0.00133	0.00239	0.00332
AT1G52400	3x yes		6-phospho-beta-galactosidase (BGLU	ER	26.3	1.61	0.59	3.21	3.13	0.00301	0.00132	0.00062	0.00178	0.00425	0.00193
AT4G02520	yes		glutathione transferase Phi (ATGSTF	plastid	26.9	0.75	0.87	0.49	1.00	0.00138	0.00160	0.00091	0.00120	0.00079	0.00091
AT1G78380			glutathione transferase 8 (AtGSTU19	cytosol	26.9	0.97	0.72	0.98	1.16	0.00113	0.00120	0.00132	0.00082	0.00118	0.00153
AT2G30870			glutathione transferase -Phi class (AT	cytosol	26.9	0.81	0.70	0.89	0.86	0.00107	0.00105	0.00116	0.00075	0.00093	0.00099
AT5G02790		yes	gluthatione Transferase Lamda -1B (	cytosol	26.9	0.54	0.95	0.29	0.45	0.00038	0.00036	0.00074	0.00037	0.00011	0.00033
AT2G30860			glutathione S-transferase class phi (A	not plastid	26.9	0.86	0.97	0.64	0.97	0.00110	0.00144	0.00189	0.00107	0.00092	0.00183
AT1G78370		yes	glutathione transferase (Tau class) - A	not plastid	26.9	0.74	1.05	0.62	0.71	0.00092	0.00209	0.00137	0.00097	0.00129	0.00098
AT2G29450			glutathione S-transferase (103-1A) (	not plastid	26.9	1.07	1.00	1.20	1.01	0.00062	0.00093	0.00121	0.00063	0.00112	0.00122
AT1G02930		yes	glutathione S-transferase	not plastid	26.9	0.44	0.71	0.32	0.43	0.00019	0.00033	0.00072	0.00014	0.00011	0.00031
AT1G27130			glutathione S-transferase, putative	not plastid	26.9	1.00	0.68	1.36	1.02	0.00027	0.00024	0.00024	0.00018	0.00032	0.00025
AT2G47730		yes	glutathione transferase GSTF8 (GST(	plastid	26.9	1.34	1.15	1.04	1.71	0.00048	0.00083	0.00094	0.00055	0.00086	0.00161
AT3G55040			gluthatione Transferase Lamda -2 (GI	plastid stroma	26.9	1.13	0.91	0.97	1.37	0.00029	0.00004	0.00029	0.00026	0.00003	0.00039
AT2G26740			epoxide hydrolase, soluble (sEH)		26.1	1.30	0.95	1.59	1.50	0.00029	0.00029	0.00010	0.00027	0.00046	0.00015
AT3G23600			dienelactone hydrolase family protein	nucleus	26.1	0.97	1.14	1.17	0.66	0.00043	0.00052	0.00059	0.00049	0.00060	0.00039
AT3G16400	2x yes		jacalin lectin family protein		26.16	5.13	0.01	5.26	517.23	0.00010	0.00016	0.00000	0.00000	0.00084	0.00052
AT1G52000			jacalin lectin family/myrosinase-bind	not plastid	26.16	1.33	0.60	1.96	185.73	0.00070	0.00052	0.00000	0.00042	0.00101	0.00019
AT3G16470			JR1 (Jacalin lectin family protein)	plastid or cytosolic?	26.16	1.15	0.59	1.63	2.25	0.00111	0.00071	0.00026	0.00065	0.00115	0.00058
AT1G71500			Rieske [2Fe-2S] domain	thylakoid	26.30	1.11	0.91	1.22	1.24	0.00149	0.00129	0.00131	0.00135	0.00157	0.00162
AT1G23740			NADPH dependent ketone reductase	plastid stroma	26.7	1.01	0.92	0.94	1.16	0.00091	0.00191	0.00163	0.00084	0.00179	0.00188
AT1G15140			oxidoreductase NAD-binding domair	plastid stroma	26.7	0.86	1.18	0.62	0.76	0.00029	0.00024	0.00040	0.00034	0.00015	0.00031
AT5G53490			peptapetide repeat TL17.4 (PPR)	thylakoid-peripheral-lu	26.54*	0.69	0.69	0.76	0.59	0.00028	0.00048	0.00030	0.00020	0.00037	0.00018
AT3G49120			peroxidase, Atpx34	cell wall	26.12	0.85	0.42	1.18	0.86	0.00022	0.00029	0.00092	0.00009	0.00035	0.00079
AT1G71695			peroxidase 12 (PER12) (P12) (PRXR	cell wall	26.12	1.07	0.81	34.62	1.10	0.00021	0.00000	0.00063	0.00017	0.00003	0.00069
AT4G27520		yes	plastocyanin-like domain-containing	not plastid	26.19	1.62	1.22	1.72	2.19	0.00049	0.00081	0.00020	0.00060	0.00139	0.00044
AT4G01050		yes	thylakoid Rhodanese-like domain (TI	thylakoid	26.23	1.57	2.19	1.85	1.14	0.00019	0.00036	0.00050	0.00042	0.00066	0.00057
AT3G12800			short-chain dehydrogenase/reductase	peroxisome	26.22	1.45	0.77	2.41	1.32	0.00019	0.00017	0.00027	0.00014	0.00041	0.00036
AT1G01320			tetratricopeptide repeat (TPR)-contai	not plastid	26.33*	1.14	1.32	1.04	1.02	0.00099	0.00032	0.00110	0.00130	0.00034	0.00113
AT4G28080			tetratricopeptide repeat (TPR)-containing	protein	26.33*	0.85	0.95	0.01	25.66	0.00082	0.00014	0.00000	0.00078	0.00000	0.00003
AT5G13430			ubiquinol-cytochrome C reductase ir(	mitochondria	9.5	0.98	1.62	0.90	0.35	0.00021	0.00036	0.00017	0.00034	0.00033	0.00006
AT2G07698	yes		ATP synthase alpha chain, mitochonc	not plastid	9.9	1.26	1.08	1.74	0.97	0.00166	0.00188	0.00211	0.00179	0.00328	0.00204
AT5G08690			H+-transporting ATP synthase beta c	mitochondria	9.9	1.06	1.25	1.13	0.91	0.00382	0.00528	0.00743	0.00478	0.00597	0.00679
AT2G33040			ATP synthase gamma chain, mitocho	mitochondria	9.9	0.84	0.81	1.09	0.76	0.00060	0.00043	0.00121	0.00048	0.00047	0.00092
ATMG01190			atp1 ATPase subunit 1	mitochondria	9.9	1.14	1.02	0.50	1.49	0.00018	0.00059	0.00114	0.00018	0.00029	0.00169
AT5G13450			ATP synthase delta chain, mitochond	mitochondria	9.9	1.15	1.35	1.16	1.04	0.00027	0.00046	0.00057	0.00037	0.00054	0.00060
AT5G63510			NADH-DH subunit -CA	mitochondria	9.1.1.5	1.10	0.67	1.06	1.51	0.00020	0.00024	0.00023	0.00013	0.00025	0.00035
AT5G37510	yes		NADH-DH 76kDa subunit - Comple:	mitochondria	9.1.1	1.54	0.81	11.56	3.23	0.00076	0.00002	0.00022	0.00061	0.00021	0.00070
AT5G04140		yes	ferredoxin-dependent glutamate synth	plastid stroma	12.2.1.1	1.17	1.10	1.17	1.25	0.01473	0.01443	0.01369	0.01619	0.01691	0.01716
AT5G53460			NADH-GOGAT or NADH- glutamat	plastid	12.2.1.2	0.82	0.88	0.46	1.13	0.00242	0.00060	0.00020	0.00214	0.00028	0.00023
AT1G66200			ATGSR2 (Arabidopsis thaliana gluta	not plastid	12.2.2	0.68	1.13	0.46	0.54	0.00070	0.00054	0.00142	0.00079	0.00025	0.00076
AT5G35630			glutamate-ammonia ligase (GS2), chl	plastid stroma	12.2.2	0.92	1.07	0.90	0.80	0.00468	0.00517	0.00461	0.00500	0.00464	0.00368
AT2G15620			nitrite reductase (ferredoxin)	plastid stroma	12.1.2	0.85	1.02	0.81	0.74	0.00174	0.00176	0.00200	0.00177	0.00142	0.00149
AT1G37130			NIA2 (NITRATE REDUCTASE 2)		12.1.1	0.69	0.93	0.43	0.22	0.00065	0.00010	0.00027	0.00060	0.00004	0.00006
AT5G64570	yes		XYL4 (beta-xylosidase 4); hydrolase,	hydrolyzing O-glycos	35.1	1.87	0.35	3.25	1.85	0.00015	0.00017	0.00027	0.00005	0.00057	0.00051
AT1G76160			multi-copper oxidase type I family pr	cell wall	35.1	1.09	1.08	0.96	1.45	0.00034	0.00032	0.00013	0.00037	0.00031	0.00019
AT1G03220			homologous to xylanase inhibitor I (E	cell wall	35.1	2.03	4.33	3.85	1.31	0.00003	0.00010	0.00036	0.00013	0.00040	0.00047
AT1G64790			unknown protein HEAT domains	not plastid	35.1	0.86	0.90	3.29	0.74	0.00153	0.00003	0.00106	0.00137	0.00011	0.00079
AT5G40770			ATPHB3 (PROHIBITIN 3)	not plastid	35.1	1.00	0.52	1.25	1.20	0.00051	0.00041	0.00075	0.00026	0.00051	0.00089
AT5G19820			PBS lyase HEAT-like repeat-contain	not plastid	35.1	1.07	1.04	0.74	1.14	0.00059	0.00009	0.00072	0.00062	0.00006	0.00082

Supplemental Table 1. (continued)

Accession	GLEE - genotype effect (p<0.01)	Genotype (p<0.01)	lab annotation	subcellular location	BIN#	klk3/wt average (days 0-3-	klk3/wt 0day (NadjSPC)	klk3/wt 3 day (NadjSPC)	klk3/wt 5 day (NadjSPC)	wt 0 day. Average NadjSPC	wt 3 day Average NadjSPC	wt 5 day Average NadjSPC	klk3 0day Average	klk3 3day Average	klk3 5dayAverage NadjSPC
AT4G21150			ribophorin II (RPN2) family protein	not plastid	35.1	1.30	0.93	1.73	1.70	0.00065	0.00036	0.00021	0.00060	0.00062	0.00036
AT3G63460			WD-40 repeat family protein, similar	not plastid	35.1	0.93	0.66	1.63	1.76	0.00090	0.00020	0.00013	0.00059	0.00033	0.00023
AT2G41530			ATSFGH (ARABIDOPSIS THALIA	not plastid	35.1	0.88	0.73	0.92	0.95	0.00031	0.00047	0.00033	0.00022	0.00043	0.00031
AT1G17100			SOUL heme-binding protein cHBP1	not plastid	35.1	1.09	0.87	0.92	1.34	0.00029	0.00017	0.00036	0.00025	0.00016	0.00048
AT2G23600			ACL (ACETONE-CYANOHYDRIN	not plastid	35.1	0.71	0.76	0.28	0.93	0.00036	0.00019	0.00030	0.00027	0.00005	0.00028
AT3G14990			4-methyl-5(b-hydroxyethyl)-thiazole	not plastid	35.1	1.34	0.95	1.05	2.57	0.00026	0.00021	0.00013	0.00025	0.00022	0.00033
AT1G49750			leucine-rich repeat family protein	not plastid	35.1	1.12	0.74	absent in both	2.65	0.00052	0.00000	0.00013	0.00038	0.00000	0.00034
AT2G45740			peroxisomal biogenesis factor 11 fam	peroxisome	35.1	1.69	0.62	1.47	2.80	0.00015	0.00027	0.00020	0.00009	0.00040	0.00056
AT4G12420			multi-copper oxidase (SKU5)-dual lo	plasma membrane	35.1	1.57	0.85	1.93	2.46	0.00042	0.00022	0.00024	0.00036	0.00043	0.00060
AT3G48420			haloacid dehalogenase-like hydrolase	plastid stroma	35.1	1.12	1.07	0.93	1.32	0.00052	0.00074	0.00080	0.00056	0.00069	0.00106
AT3G23940			dihydroxyacid dehydratase	plastid stroma	35.1	0.86	0.85	0.82	0.93	0.00030	0.00019	0.00021	0.00025	0.00015	0.00020
AT2G34460			flavin reductase-related 2	plastoglobules	35.1	1.16	0.81	3.62	0.86	0.00037	0.00011	0.00043	0.00030	0.00038	0.00037
AT4G35250			vestitone reductase-related	thylakoid	35.1	1.03	1.23	0.49	1.65	0.00035	0.00060	0.00042	0.00043	0.00030	0.00068
AT1G21680			unknown protein Dipeptidyl peptidase	IV (DPP IV) N-termi	35.1	1.16	1.14	1.23	1.08	0.00021	0.00063	0.00041	0.00024	0.00078	0.00045
AT5G37830			OXP1 (OXOPROLINASE 1); hydrolase		35.1	0.70	0.81	0.29	2.56	0.00107	0.00041	0.00003	0.00087	0.00012	0.00007
AT3G27890		yes	NADPH-dependent FMN reductase - very abundant?		35.1	1.79	0.95	3.43	1.14	0.00012	0.00014	0.00019	0.00012	0.00047	0.00021
AT4G17140			pleckstrin homology (PH) domain-co	ntaining protein	35.1.19	0.73	0.66	19.47	1.00	0.00129	0.00000	0.00025	0.00085	0.00002	0.00025
AT5G07020			proline-rich protein family	thylakoid	35.1.42	1.55	0.77	1.11	2.29	0.00014	0.00012	0.00022	0.00010	0.00013	0.00049
AT5G02940	2x yes	yes	unknown protein	envelope	35.2	3.08	0.83	33.17	4.72	0.00057	0.00004	0.00013	0.00047	0.00118	0.00061
AT2G32240	yes		unknown protein DUF869 domain		35.2	0.56	0.66	0.10	0.96	0.00136	0.00041	0.00013	0.00090	0.00004	0.00012
AT3G16640			TCTP homolog - tumor protein homo	not plastid	35.2	0.78	1.06	0.56	0.85	0.00048	0.00076	0.00049	0.00051	0.00042	0.00042
AT5G02240			unknown protein - NAD dependent e	not plastid	35.2	1.07	0.65	0.20	1.86	0.00020	0.00017	0.00030	0.00013	0.00003	0.00056
AT3G61870			unknown protein	plastid	35.2	1.08	1.16	1.30	0.85	0.00034	0.00022	0.00034	0.00039	0.00029	0.00029
AT2G37660			3-beta-hydroxy-delta5-steroid dehydr	plastid stroma	35.2	1.10	1.07	0.77	1.23	0.00060	0.00019	0.00057	0.00064	0.00014	0.00071
AT1G62780			unknown protein (NIPSNAP domain)	plastid stroma	35.2	0.83	1.33	0.50	0.99	0.00025	0.00055	0.00037	0.00033	0.00028	0.00037
AT1G21440			carboxyvinyl-carboxyphosphonate ph	plastid stroma	35.2	1.04	1.05	0.64	1.32	0.00010	0.00037	0.00052	0.00010	0.00024	0.00069
AT2G31670			unknown protein	plastid stroma	35.2	0.96	1.04	1.07	0.80	0.00019	0.00039	0.00033	0.00020	0.00042	0.00026
AT1G16080			unknown protein	plastid stroma	35.2	0.95	0.88	0.73	1.39	0.00067	0.00090	0.00058	0.00059	0.00065	0.00080
AT1G32220			Flavin-reductase related 1	plastoglobules	35.2	0.68	0.36	3.47	0.37	0.00029	0.00009	0.00047	0.00010	0.00030	0.00017
AT3G59780			unknown protein	thylakoid	35.2	0.88	0.90	0.88	0.83	0.00130	0.00077	0.00032	0.00116	0.00068	0.00026
AT5G38660			APE1- (ACCLIMATION OF PHOT	thylakoid	35.2	1.14	1.05	1.04	1.55	0.00033	0.00045	0.00017	0.00034	0.00046	0.00027
AT5G08050			unknown protein	thylakoid	35.2	0.85	0.74	0.79	1.14	0.00032	0.00034	0.00020	0.00024	0.00027	0.00023
AT4G01150			unknown protein	thylakoid-integral	35.2	0.87	0.69	1.00	0.96	0.00098	0.00063	0.00097	0.00068	0.00064	0.00094
AT4G09010			TL29	thylakoid-peripheral-lu	35.2	0.95	0.98	1.07	0.84	0.00115	0.00074	0.00112	0.00113	0.00079	0.00094
AT1G54780			thylakoid lumen 18.3 kDa	thylakoid-peripheral-lu	35.2	1.30	1.18	1.68	0.99	0.00075	0.00079	0.00066	0.00088	0.00133	0.00065
AT4G02530			thylakoid lumen protein TL16.5	thylakoid-peripheral-lu	35.2	1.19	1.13	1.07	1.39	0.00023	0.00023	0.00022	0.00026	0.00024	0.00030
AT1G73060			LPA3 - PSII assembly factor associat	thylakoid-peripheral-st	35.2	0.80	0.78	0.14	1.04	0.00038	0.00014	0.00043	0.00030	0.00002	0.00045
AT5G40450			unknown protein		35.2	0.94	0.91	2.59	1.81	0.00404	0.00002	0.00009	0.00367	0.00004	0.00016
AT5G47690			unknown protein		35.2	1.52	1.27	63.43	1.62	0.00032	0.00000	0.00016	0.00041	0.00006	0.00026
AT5G35170			adenylate kinase	plastid	23.4.1	0.59	0.60	0.63	0.56	0.00053	0.00032	0.00067	0.00032	0.00021	0.00038
AT1G15690	yes		AVP1 (vacuolar-type H+-pumping p	vacuole-tonoplast	23.4.99	1.24	0.80	1.97	1.10	0.00227	0.00188	0.00261	0.00181	0.00370	0.00287
AT5G09650			Inorganic phosphatase like	thylakoid-peripheral-st	23.4.99	0.85	0.96	0.70	0.95	0.00082	0.00085	0.00036	0.00079	0.00059	0.00034
AT4G09320			NDPK1 - very abundant & multiple l	peroxisome	23.4.10	0.72	0.88	0.62	0.90	0.00037	0.00089	0.00019	0.00033	0.00055	0.00017
AT5G63310			NDPK2-stromal	plastid stroma	23.4.10	1.12	0.97	1.25	1.04	0.00030	0.00050	0.00027	0.00029	0.00062	0.00028
AT3G09820		yes	adenosine kinase 1 (ADK1)	not plastid	23.3.2.1	0.54	0.68	0.32	0.57	0.00036	0.00031	0.00052	0.00025	0.00010	0.00029
AT1G27450	yes		Adenine phosphoribosyltransferase-1	cytosol	23.3.1.1	0.73	1.12	0.30	0.96	0.00036	0.00062	0.00053	0.00040	0.00018	0.00051
AT1G74260			formyl-glycinamidine ribonucleotide	plastid stroma	23.1.2.4	0.88	0.93	0.78	0.84	0.00095	0.00019	0.00066	0.00088	0.00015	0.00055
AT4G18440	2x yes		adenylosuccinate lyase	plastid stroma	23.1.2.8	2.40	1.20	2.53	3.19	0.00069	0.00129	0.00083	0.00083	0.00327	0.00266
AT1G29900	yes		carbamoylphosphate synthetase	plastid stroma	23.1.1.1	0.95	1.03	0.34	2.32	0.00102	0.00067	0.00024	0.00105	0.00023	0.00056
AT4G30530		yes	Glutamine amidotransferase class-I r	not plastid	23.1.99	0.54	0.70	0.42	0.50	0.00049	0.00041	0.00073	0.00034	0.00017	0.00036
AT3G25530			glyoxylate reductase 1 (GR1) (AtGH	cytosol	7.1.3	0.89	0.86	0.85	0.95	0.00086	0.00093	0.00108	0.00074	0.00079	0.00102
AT3G02360			6-phosphogluconate dehydrogenase	cytosol	7.1.3	1.38	1.12	1.46	1.50	0.00019	0.00026	0.00022	0.00021	0.00037	0.00034
AT1G17650			glyoxylate reductase 2 (GR2)	plastid stroma	7.1.3	1.03	0.88	1.00	1.13	0.00031	0.00003	0.00044	0.00028	0.00003	0.00050
AT3G26710			CCB1 Protein ; cytochrome b6 heme	thylakoid	29.8	0.64	1.10	0.51	0.49	0.00020	0.00022	0.00044	0.00022	0.00011	0.00022

Supplemental Table 1. (continued)

Accession	GLEE - genotype effect (p<0.01)	Genotype (p<0.01)	lab annotation	subcellular location	BIN#	klk3/wt average (days 0-3-	klk3/wt 0day (NadjSPC)	klk3/wt 3 day (NadjSPC)	klk3/wt 5 day (NadjSPC)	wt 0 day. Average NadjSPC	wt 3 day Average NadjSPC	wt 5 day Average NadjSPC	klk3 0day Average	klk3 3day Average	klk3 5dayAverage NadjSPC
AT5G17170			unknown protein Rubredoxin and PD	thylakoid	29.8	0.73	0.68	1.02	0.60	0.00029	0.00019	0.00030	0.00020	0.00019	0.00018
ATcG01130			YCF1.2	thylakoid-integral	29.8	1.04	1.05	38.95	0.99	0.00115	0.00000	0.00084	0.00121	0.00004	0.00082
AT5G23120			HCF136 Tat ltp	thylakoid-peripheral-lu	29.8	1.25	1.22	1.29	1.23	0.00102	0.00089	0.00095	0.00125	0.00115	0.00117
AT5G22800	yes		Ala-tRNA synthetases (Ala-RS2) (du	plastid stroma	29.1.7	1.47	1.08	1.46	35.28	0.00127	0.00062	0.00001	0.00138	0.00090	0.00051
AT1G50200			Ala tRNA synthetases class II (A) (A	plastid stroma	29.1.7	1.02	1.04	0.40	1.46	0.00043	0.00031	0.00040	0.00044	0.00012	0.00059
AT4G26300			Arg-tRNA synthetase	plastid stroma	29.1.19	1.20	0.74	2.17	1.58	0.00042	0.00009	0.00029	0.00031	0.00019	0.00045
AT1G29880			Gly-tRNA synthetase (GlyRS-1). Als	mitochondria	29.1.14	1.22	1.18	0.85	1.59	0.00067	0.00067	0.00075	0.00079	0.00057	0.00119
AT3G48110			Gly t-RNA synthetase (GlyRS-2) (EI	plastid stroma	29.1.14	1.14	0.66	0.92	1.73	0.00050	0.00019	0.00047	0.00033	0.00017	0.00082
AT4G10320			isoleucyl-tRNA synthetase, putative		29.1.5	0.97	0.99	0.06	0.98	0.00054	0.00002	0.00032	0.00054	0.00000	0.00031
AT1G09620			Leu-tRNA synthetase	cytosol	29.1.4	0.89	0.88	0.82	0.98	0.00109	0.00097	0.00086	0.00096	0.00079	0.00085
AT4G33090	yes		M1 aminopeptidase - PM1 (Aberrant	plasma membrane	29.5	1.58	0.77	1.91	3.51	0.00116	0.00064	0.00038	0.00089	0.00122	0.00132
AT3G02090			mitochondrial processing peptidase (I	mitochondria	29.5	1.07	0.92	1.55	0.95	0.00093	0.00070	0.00171	0.00086	0.00109	0.00163
AT1G51980			mitochondrial processing peptidase a	mitochondria	29.5	1.90	1.04	3.35	1.68	0.00014	0.00012	0.00026	0.00014	0.00040	0.00043
AT2G24200			eucyl aminopeptidase (LAP1)	not plastid	29.5	1.16	1.23	1.29	0.88	0.00131	0.00232	0.00140	0.00162	0.00299	0.00123
AT4G38220			aminoacylase	not plastid	29.5	1.89	1.42	1.49	5.65	0.00009	0.00031	0.00004	0.00013	0.00046	0.00025
AT5G36210			serine-type acylpeptidase (AARE2)	not plastid	29.5	1.17	1.28	0.96	1.85	0.00027	0.00026	0.00004	0.00034	0.00025	0.00008
AT1G63770	yes		glycyl aminopeptidase (M1) (model .	plastid stroma	29.5	1.41	0.88	1.40	2.07	0.00139	0.00067	0.00112	0.00122	0.00093	0.00232
AT3G05350			aminopeptidase (M24) (APP2)	plastid stroma	29.5	1.13	0.98	1.80	0.98	0.00028	0.00015	0.00039	0.00028	0.00028	0.00038
AT1G11910			aspartyl protease family protein	vacuole	29.5.4	0.99	0.82	1.45	0.91	0.00046	0.00048	0.00193	0.00038	0.00070	0.00177
AT1G47128			cysteine proteinase (RD21A) / thiol p	vacuole	29.5.3	1.17	0.64	2.27	1.09	0.00025	0.00017	0.00082	0.00016	0.00040	0.00089
AT4G36760			aminopeptidase P1 (ATAPP1)	plasma membrane	29.5.7	1.64	0.79	2.07	2.75	0.00025	0.00012	0.00014	0.00020	0.00025	0.00040
AT3G19170	2x yes	yes	AtPrep1 - (AtZnMP) metalloprotease	plastid stroma	29.5.7	1.60	1.13	1.88	1.99	0.00328	0.00232	0.00231	0.00372	0.00436	0.00460
AT5G65620			Zn oligopeptidase A (M3 family)	plastid stroma	29.5.7	1.19	1.02	1.06	1.79	0.00099	0.00083	0.00048	0.00100	0.00087	0.00087
AT5G51070	2x yes		ClpD (Erd1)	plastid stroma	29.5.5	3.42	0.80	5.18	5.61	0.00019	0.00017	0.00009	0.00015	0.00088	0.00053
AT5G50920	yes	yes	ClpC1 (also named HSP93-V) - high	plastid stroma	29.5.5	1.36	1.08	1.32	1.86	0.00720	0.00822	0.00466	0.00779	0.01088	0.00867
AT2G47390			thylakoid associated glutamyl endope	plastid stroma	29.5.5	1.29	1.09	1.65	1.44	0.00098	0.00043	0.00036	0.00106	0.00071	0.00052
AT4G12060			ClpT2 (formerly ClpS2)	plastid stroma	29.5.5	1.26	0.80	1.47	1.60	0.00022	0.00033	0.00009	0.00017	0.00048	0.00014
AT3G14067		yes	subtilase family protein	not plastid	29.5.1	1.41	0.89	1.84	1.52	0.00095	0.00074	0.00162	0.00084	0.00136	0.00246
AT4G20850			subtilase family protein, Tripeptidyl-p	plastid stroma	29.5.1	1.26	1.07	1.61	1.38	0.00312	0.00109	0.00194	0.00332	0.00176	0.00268
AT3G62250	yes		UBQ5 (UBIQUITIN 5); protein binding		29.5.11	1.78	0.33	2.22	6.85	0.00034	0.00005	0.00009	0.00011	0.00011	0.00064
AT2G30110			ubiquitin activating enzyme 1 (UBA1	not plastid	29.5.11.2	1.10	0.60	1.31	1.55	0.00039	0.00003	0.00041	0.00024	0.00004	0.00064
AT1G70320			UPL2 (UBIQUITIN-PROTEIN LIG/		29.5.11.4	0.79	0.91	21.98	0.29	0.00157	0.00000	0.00043	0.00144	0.00002	0.00012
AT2G32730	yes		26S proteasome regulatory subunit (F	cytosol	29.5.11.2	1.39	0.69	2.65	27.71	0.00070	0.00009	0.00001	0.00048	0.00023	0.00040
AT2G20580			26S proteasome regulatory subunit (F	cytosol	29.5.11.2	1.09	0.81	0.90	1.52	0.00099	0.00015	0.00070	0.00080	0.00014	0.00106
AT1G56450			20S proteasome beta subunit G1); pe	cytosol	29.5.11.2	1.15	0.96	1.35	1.04	0.00026	0.00046	0.00033	0.00025	0.00062	0.00034
AT3G60820			20S proteasome beta subunit F1 (PBI	cytosol	29.5.11.2	1.15	0.77	1.20	1.46	0.00032	0.00033	0.00033	0.00025	0.00039	0.00048
AT4G31300			20S proteasome beta subunit A (PBA	cytosol	29.5.11.2	1.17	0.34	1.59	3.08	0.00030	0.00034	0.00006	0.00010	0.00055	0.00018
AT3G22110			20S proteasome alpha subunit C (PA	cytosol	29.5.11.2	0.89	0.68	1.19	0.87	0.00029	0.00022	0.00024	0.00020	0.00027	0.00021
AT4G24820			26S proteasome regulatory subunit (F	cytosol	29.5.11.2	1.27	1.12	1.41	1.24	0.00012	0.00021	0.00026	0.00013	0.00029	0.00032
AT5G42020	yes		luminal binding protein 2 precursor (I	ER	29.6	0.64	0.39	0.58	1.33	0.00108	0.00115	0.00049	0.00042	0.00066	0.00065
AT3G12580	2x yes	yes	Hsc70-4	cytosol	29.6	1.68	0.38	1.57	2.09	0.00045	0.00517	0.00287	0.00017	0.00811	0.00601
AT5G28540	yes		luminal binding protein 1 precursor (I	ER	29.6	0.79	1.13	0.38	0.83	0.00186	0.00162	0.00128	0.00209	0.00061	0.00106
AT4G37910	yes		mtHsc70-1	mitochondria	29.6	0.84	1.00	0.35	1.33	0.00076	0.00088	0.00062	0.00076	0.00031	0.00083
AT3G13860	yes		Cpn60/HSP60 - mito's	mitochondria	29.6	2.07	0.87	1.80	4.25	0.00024	0.00010	0.00015	0.00021	0.00019	0.00062
AT5G15450	yes		ClpB3 -HSP100 family	plastid stroma	29.6	1.42	0.87	1.12	3.07	0.00087	0.00188	0.00063	0.00076	0.00209	0.00194
AT3G01480	yes	yes	Tlp-40 (or CYCLOPHILIN 38 - CYF	thylakoid-peripheral-lu	29.6	0.65	1.10	0.57	0.09	0.00097	0.00050	0.00072	0.00106	0.00028	0.00007
AT5G02490	yes		Hsc70-2 (not plastid)		29.6	1.48	0.95	0.48	538.33	0.00032	0.00037	0.00000	0.00030	0.00018	0.00054
AT4G24190			HSP90 or GRP94 - similar to Sheper	ER	29.6	1.07	0.88	1.15	1.56	0.00217	0.00178	0.00057	0.00191	0.00205	0.00089
AT3G23990		yes	Cpn60/HSP60 - mito's	mitochondria	29.6	1.42	1.02	1.40	1.74	0.00087	0.00098	0.00119	0.00089	0.00137	0.00207
AT5G09590			heat shock protein mtHsc70-2 (Hsc70	mitochondria	29.6	0.93	0.98	0.91	0.92	0.00059	0.00133	0.00113	0.00058	0.00121	0.00103
AT2G33210			Cpn60/HSP60 - mito's	mitochondria	29.6	1.28	1.19	1.26	1.34	0.00047	0.00072	0.00073	0.00055	0.00092	0.00098
AT3G07770			Hsp90-6	mitochondria	29.6	1.14	1.04	0.92	2.76	0.00034	0.00061	0.00011	0.00035	0.00056	0.00030
AT3G03960			TCP-1/cpn60 chaperonin family	not plastid	29.6	1.14	0.98	0.56	2.52	0.00035	0.00034	0.00019	0.00034	0.00019	0.00047
AT2G16600			peptidyl-prolyl cis-trans isomerase, c	not plastid	29.6	1.33	0.73	1.40	2.11	0.00022	0.00038	0.00013	0.00016	0.00053	0.00027

Supplemental Table 1. (continued)

Accession	GLEE - genotype effect (p<0.01)	Genotype (p<0.01)	lab annotation	subcellular location	BIN#	klk3/wt average (days 0-3-	klk3/wt 0day (NadjSPC)	klk3/wt 3 day (NadjSPC)	klk3/wt 5 day (NadjSPC)	wt 0 day. Average NadjSPC	wt 3 day Average NadjSPC	wt 5 day Average NadjSPC	klk3 0day Average	klk3 3day Average	klk3 5dayAverage NadjSPC
AT3G11830			TCP-1/cpn60 chaperonin family	not plastid	29.6	1.17	0.74	0.35	2.48	0.00028	0.00022	0.00023	0.00021	0.00008	0.00057
AT3G20050			TCP-1-alpha / chaperonin (CCT1)	not plastid	29.6	1.10	0.77	1.39	1.69	0.00049	0.00019	0.00019	0.00038	0.00026	0.00032
AT5G02500			HSP70-1 (HSC70-1) (not plastid) - v	nucleus	29.6	1.00	1.08	1.02	0.81	0.00487	0.00421	0.00231	0.00526	0.00430	0.00188
AT2G28000		yes	Cpn60-alpha-1	plastid stroma	29.6	1.25	1.07	1.32	1.29	0.00440	0.00778	0.00638	0.00469	0.01025	0.00822
AT1G55490		yes	Cpn60-beta-2	plastid stroma	29.6	1.26	1.14	1.26	1.38	0.00350	0.00576	0.00345	0.00401	0.00723	0.00476
AT2G04030			cpHSP90 (Hsp90-5)	plastid stroma	29.6	1.11	1.15	0.98	1.25	0.00263	0.00501	0.00400	0.00303	0.00490	0.00498
AT4G24280		yes	cpHSP70-1 (DnaK homologue)	plastid stroma	29.6	1.28	0.97	1.29	1.53	0.00239	0.00311	0.00285	0.00231	0.00402	0.00436
AT3G62030			peptidylprolyl isomerase ROC4 (CYI	plastid stroma	29.6	0.84	0.69	1.16	0.68	0.00315	0.00288	0.00259	0.00217	0.00333	0.00176
AT5G49910			cpHSP70-2 (Dnak homologue)	plastid stroma	29.6	1.32	0.88	1.32	1.87	0.00223	0.00165	0.00173	0.00195	0.00219	0.00325
AT3G13470			Cpn60-beta-1	plastid stroma	29.6	1.12	1.09	0.87	1.34	0.00123	0.00209	0.00254	0.00134	0.00182	0.00341
AT5G20720			Cpn21 (also Cpn20)	plastid stroma	29.6	1.04	0.95	0.75	1.38	0.00104	0.00155	0.00162	0.00098	0.00116	0.00224
AT5G55220			Trigger Factor	plastid stroma	29.6	1.09	1.45	1.07	0.71	0.00050	0.00081	0.00043	0.00072	0.00087	0.00030
AT5G56500			Cpn60-beta-3 - model .2 has higher s	plastid stroma	29.6	1.07	1.42	1.11	0.95	0.00015	0.00029	0.00055	0.00022	0.00032	0.00052
AT5G17710			GrpE-1 (EMB1241 - EMBRYO DEF	plastid stroma	29.6	0.83	0.56	0.76	2.14	0.00026	0.00057	0.00009	0.00015	0.00043	0.00018
AT4G25130			methionine sulfoxide reductase type A	plastid stroma	29.11*	1.22	0.92	1.26	2.01	0.00030	0.00026	0.00010	0.00027	0.00033	0.00020
AT5G42390			stromal processing peptidase (SPP)	plastid stroma	29.9*	0.84	1.00	0.81	0.72	0.00020	0.00028	0.00020	0.00020	0.00022	0.00014
AT1G56070	yes		elongation factor 2, EF-2	not plastid	29.2.4	0.84	0.99	0.66	0.84	0.00645	0.00533	0.00461	0.00638	0.00351	0.00389
AT1G09640			elongation factor 1B-gamma, putative	cytosol	29.2.4	1.09	0.69	0.58	1.49	0.00017	0.00020	0.00043	0.00012	0.00012	0.00064
AT1G07930			elongation factor 1-alpha (E-Tu)	not plastid	29.2.4	0.89	1.01	0.82	0.88	0.00262	0.00444	0.00405	0.00263	0.00365	0.00356
AT1G57720			elongation factor 1B-gamma, putative	not plastid	29.2.4	0.87	1.45	0.38	1.07	0.00037	0.00058	0.00038	0.00054	0.00022	0.00041
AT1G30230			elongation factor 1-beta / EF-1-beta	not plastid	29.2.4	1.13	1.23	0.57	1.74	0.00022	0.00028	0.00021	0.00028	0.00016	0.00037
AT4G29060		yes	PSRP-7 - (110 kDa fusion of 65kDa	plastid ribosome	29.2.4	1.24	1.05	1.20	2.32	0.00212	0.00203	0.00046	0.00222	0.00243	0.00106
AT4G20360			elongation factor Tu (EF-Tu-1), plast	plastid stroma	29.2.4	0.94	1.09	0.82	0.93	0.00623	0.00743	0.00927	0.00679	0.00609	0.00865
AT1G62750			elongation factor Tu-G (EF-G) (sco1	plastid stroma	29.2.4	0.94	1.11	0.90	0.76	0.00293	0.00299	0.00234	0.00325	0.00269	0.00179
AT5G13650			elongation factor protein, typeA/bipA	plastid stroma	29.2.4	0.80	0.97	0.42	0.96	0.00074	0.00064	0.00073	0.00072	0.00027	0.00070
AT3G08740			elongation factor P (EF-P)	plastid stroma	29.2.4	1.39	1.86	1.31	0.02	0.00018	0.00038	0.00004	0.00034	0.00050	0.00000
AT3G13920	yes		initiation factor 4A-1 (eIF-4A-1), DE	not plastid	29.2.3	0.93	1.07	0.55	1.52	0.00080	0.00206	0.00115	0.00086	0.00113	0.00176
AT1G54270	yes		initiation factor 4A-2 (eIF-4A-2), DE	not plastid	29.2.3	0.50	1.03	0.51	0.13	0.00031	0.00041	0.00046	0.00032	0.00021	0.00006
AT4G11420			EIF3A (eukaryotic translation initiati	not plastid	29.2.3	1.53	1.10	0.43	2.72	0.00034	0.00005	0.00017	0.00038	0.00002	0.00047
AT3G56150			eukaryotic translation initiation factor	not plastid	29.2.3	0.61	0.57	absent in both	0.74	0.00062	0.00000	0.00016	0.00035	0.00000	0.00012
AT5G57870			eukaryotic translation initiation factor	nucleus	29.2.3	0.97	0.90	0.85	2.48	0.00076	0.00026	0.00006	0.00068	0.00022	0.00014
AT1G22780	yes		40S ribosomal protein S18 (RPS18A	cytosol	29.2.1.2.	0.62	1.29	0.25	1.17	0.00033	0.00088	0.00020	0.00042	0.00022	0.00024
AT2G31610	2x yes	yes	40S ribosomal protein S3 (RPS3A)	cytosol	29.2.1.2.	0.35	0.16	0.29	0.67	0.00034	0.00052	0.00031	0.00005	0.00015	0.00021
AT5G07090			40S ribosomal protein S4 (RPS4B)	cytosol	29.2.1.2.	0.95	0.89	0.52	2.30	0.00073	0.00031	0.00013	0.00064	0.00016	0.00030
AT3G11940			40S ribosomal protein 5A (ATRPS5/	cytosol	29.2.1.2.	0.90	1.86	0.31	0.95	0.00020	0.00034	0.00027	0.00036	0.00010	0.00026
AT5G20290			40S ribosomal protein S8 (RPS8A)	cytosol	29.2.1.2.	0.69	0.86	0.33	0.83	0.00054	0.00038	0.00033	0.00046	0.00013	0.00027
AT5G15200			40S ribosomal protein S9 (RPS9B)	cytosol	29.2.1.2.	1.00	1.06	0.23	1.45	0.00026	0.00017	0.00026	0.00027	0.00004	0.00037
AT1G72370			40S ribosomal protein SA (RPSaA)	cytosol	29.2.1.2.	0.93	0.97	0.89	1.03	0.00074	0.00238	0.00072	0.00072	0.00212	0.00073
AT3G53430		yes	60S ribosomal protein L12 (RPL12B	cytosol	29.2.1.2.	0.63	0.73	0.39	0.87	0.00034	0.00052	0.00040	0.00025	0.00020	0.00035
AT1G43170			60S ribosomal protein L3 (RPL3A)	cytosol	29.2.1.2.	0.88	2.01	0.36	1.03	0.00015	0.00050	0.00053	0.00031	0.00018	0.00055
AT3G25520	yes	yes	60S ribosomal protein L5 (RPL5)	cytosol	29.2.1.2.	0.49	1.01	0.18	0.43	0.00024	0.00033	0.00040	0.00024	0.00006	0.00017
AT1G74050			60S ribosomal protein L6 (RPL6C)	cytosol	29.2.1.2.	0.61	0.41	0.19	1.38	0.00025	0.00030	0.00023	0.00010	0.00006	0.00032
AT2G01250			60S ribosomal protein L7 (RPL7B)	cytosol	29.2.1.2.	0.92	1.11	0.61	0.99	0.00029	0.00027	0.00040	0.00032	0.00017	0.00040
AT1G33120			60S ribosomal protein L9 (RPL90B)	cytosol	29.2.1.2.	0.79	0.84	0.54	1.08	0.00062	0.00056	0.00036	0.00053	0.00030	0.00039
AT3G09200			60S acidic ribosomal protein P0 (RPI	cytosol	29.2.1.2.	0.70	0.51	0.61	1.02	0.00055	0.00082	0.00057	0.00028	0.00050	0.00058
ATcG00800	yes		30S ribosomal protein S3	plastid ribosome	29.2.1.1.	0.83	0.98	0.10	1.08	0.00067	0.00039	0.00072	0.00066	0.00004	0.00078
AT3G52150			PSRP-2 associates with 30S (substitu	plastid ribosome	29.2.1.1.	0.93	0.78	1.09	1.04	0.00041	0.00018	0.00026	0.00031	0.00020	0.00027
AT2G33800			30S ribosomal protein S5	plastid ribosome	29.2.1.1.	1.15	1.35	0.59	2.68	0.00024	0.00036	0.00010	0.00033	0.00021	0.00027
ATcG00780			50S ribosomal protein L14	plastid ribosome	29.2.1.1.	1.00	1.31	0.33	2.66	0.00024	0.00033	0.00009	0.00032	0.00011	0.00023
ATcG00830			50S ribosomal protein L2A (identical	plastid ribosome	29.2.1.1.	0.70	1.09	0.37	0.81	0.00023	0.00034	0.00020	0.00025	0.00013	0.00016
AT3G63490			50S ribosomal protein L1	plastid ribosome	29.2.1.1.	0.77	0.91	0.55	0.79	0.00052	0.00041	0.00066	0.00047	0.00023	0.00052
AT1G32990			50S ribosomal protein L11	plastid ribosome	29.2.1.1.	1.45	1.87	0.55	2.34	0.00025	0.00027	0.00016	0.00046	0.00015	0.00037
AT3G27830			50S ribosomal protein L12-A (homol	plastid ribosome	29.2.1.1.	0.90	0.60	0.86	1.32	0.00024	0.00027	0.00020	0.00015	0.00024	0.00026
AT3G25920			50S ribosomal protein L15	plastid ribosome	29.2.1.1.	0.72	0.88	0.56	28.68	0.00053	0.00071	0.00000	0.00047	0.00040	0.00003

Supplemental Table 1. (continued)

Accession	GLEE - genotype effect (p<0.01)	Genotype (p<0.01)	lab annotation	subcellular location	BIN#	klk3/wt average (days 0-3-	klk3/wt 0day (NadjSPC)	klk3/wt 3 day (NadjSPC)	klk3/wt 5 day (NadjSPC)	wt 0 day. Average NadjSPC	wt 3 day Average NadjSPC	wt 5 day Average NadjSPC	klk3 0day Average	klk3 3day Average	klk3 5dayAverage NadjSPC
AT1G35680			50S ribosomal protein L21	plastid ribosome	29.2.1.1.	1.19	1.46	0.96	1.65	0.00030	0.00041	0.00004	0.00043	0.00039	0.00007
AT2G43030			50S ribosomal protein L3	plastid ribosome	29.2.1.1.	0.76	1.10	0.44	0.67	0.00080	0.00070	0.00047	0.00088	0.00031	0.00032
AT1G07320			50S ribosomal protein L4	plastid ribosome	29.2.1.1.	1.70	1.15	2.11	3.25	0.00032	0.00010	0.00009	0.00037	0.00022	0.00028
AT4G01310			50S ribosomal protein L5	plastid ribosome	29.2.1.1.	0.93	1.15	0.17	1.02	0.00055	0.00024	0.00066	0.00063	0.00004	0.00067
AT1G05190	yes	yes	50S ribosomal protein L6	plastid ribosome	29.2.1.1.	2.27	1.66	2.48	3.04	0.00029	0.00038	0.00013	0.00049	0.00094	0.00039
AT3G44890	yes		50S ribosomal protein L9	plastid ribosome	29.2.1.1.	0.88	1.20	0.08	1.40	0.00025	0.00023	0.00019	0.00030	0.00002	0.00026
AT5G30510			30S ribosomal protein S1	plastid ribosome	29.2.1.1.	1.02	1.13	1.17	0.79	0.00043	0.00052	0.00051	0.00049	0.00060	0.00040
AT3G63190			Putative ribosome recycling factor	plastid stroma	29.2.9*	0.83	0.73	0.58	1.18	0.00034	0.00026	0.00029	0.00025	0.00015	0.00034
AT4G01800	yes		cpSecA	thylakoid-peripheral-st	29.3.3	1.64	1.14	1.77	3.54	0.00120	0.00055	0.00027	0.00137	0.00097	0.00097
AT1G06950		yes	Tic110	envelope-inner-integra	29.3.3	1.26	1.01	1.34	1.89	0.00282	0.00238	0.00085	0.00285	0.00321	0.00160
AT2G24820			Tic55 (putative Rieske iron-sulfur pr	envelope-inner-integra	29.3.3	0.90	1.33	1.24	0.74	0.00023	0.00019	0.00107	0.00030	0.00024	0.00080
AT2G47840			Tic20-II (group 2)	envelope-inner-integra	29.3.3	1.54	1.53	0.79	4.50	0.00034	0.00039	0.00010	0.00052	0.00031	0.00046
AT4G02510			OEP86 (TOC159) (putative chloropl	envelope-outer	29.3.3	1.31	1.23	2.15	1.31	0.00154	0.00014	0.00077	0.00189	0.00029	0.00101
AT3G46740			OEP75 (TOC75-III) = Chloroplast in	envelope-outer	29.3.3	1.22	0.70	1.35	5.27	0.00064	0.00034	0.00007	0.00044	0.00046	0.00038
AT3G18890			Tic62 -interacts with FNR (dual local	thylakoid	29.3.3	1.29	1.23	0.95	2.02	0.00136	0.00096	0.00058	0.00168	0.00090	0.00117
AT2G20890			TF1 - thylakoid formation1	thylakoid-peripheral-st	29.3.3	0.95	0.97	0.90	0.98	0.00087	0.00072	0.00095	0.00084	0.00065	0.00093
AT5G53480			Importin-beta N-terminal domain	not plastid	29.3.1	0.88	0.74	2.07	0.79	0.00140	0.00024	0.00111	0.00104	0.00049	0.00087
AT5G40480			Nucleoporin gp210	nucleus	29.3.1	0.95	0.81	43.95	1.19	0.00060	0.00000	0.00017	0.00048	0.00004	0.00021
AT2G16950			protein transporter		29.3.1	0.79	0.53	1.42	0.82	0.00059	0.00022	0.00037	0.00031	0.00031	0.00030
AT2G47170			ADP-ribosylation factor 1 (ARF1) (g	golgi	29.3.4.9	1.10	0.92	1.25	1.10	0.00076	0.00095	0.00069	0.00070	0.00118	0.00075
AT1G23310			alanine 2-oxoglutarate amino transfer	peroxisome	1.2.3	1.03	1.15	0.87	1.16	0.00381	0.00605	0.00434	0.00439	0.00525	0.00504
AT2G13360			alanine-glyoxylate aminotransferase (	peroxisome	1.2.3	1.12	1.06	1.23	1.07	0.00236	0.00283	0.00386	0.00250	0.00349	0.00413
AT5G66190			FNR-1	thylakoid-peripheral-st	1.1.7	0.98	1.04	0.97	0.93	0.00284	0.00355	0.00325	0.00295	0.00343	0.00304
AT1G20020			FNR-2 (interaction with Cytf, maybe	thylakoid-peripheral-st	1.1.7	1.00	0.98	1.20	0.75	0.00106	0.00096	0.00074	0.00104	0.00115	0.00055
AT1G20340	yes		plastocyanin-1 (PC-1)	thylakoid-peripheral-lu	1.1.5.1	0.57	0.91	0.22	0.56	0.00086	0.00087	0.00112	0.00079	0.00019	0.00063
AT1G44575			psbS (NPQ4 - null mutant)	thylakoid-integral	1.1.1.2	1.32	0.89	1.38	1.73	0.00274	0.00185	0.00264	0.00242	0.00256	0.00457
AT1G09340			HIP1.3 (cytosol - heteroglycan-intera	plastid stroma	27	0.96	1.05	0.66	1.11	0.00313	0.00382	0.00550	0.00329	0.00253	0.00608
AT5G26742			DEAD box RNA helicase (RH3) (EM	plastid nucleoid	27.6*	1.37	1.25	0.98	1.65	0.00078	0.00045	0.00092	0.00098	0.00044	0.00152
AT4G24770			chloroplast ribonucleoprotein CP31A	plastid stroma	27.1.5*	0.93	1.09	0.25	1.23	0.00059	0.00038	0.00055	0.00064	0.00010	0.00068
AT4G34110			polyadenylate-binding protein 2 (PAI	not plastid	27.1	1.11	0.81	1.05	1.62	0.00037	0.00030	0.00026	0.00030	0.00032	0.00042
AT3G20390			Endoribonuclease L-PSP	thylakoid-peripheral-st	27.1	1.07	0.93	1.16	1.11	0.00056	0.00066	0.00054	0.00053	0.00076	0.00060
AT1G80070			SUS2 (ABNORMAL SUSPENSOR 2)		27.1.1	0.88	0.87	absent in both	0.90	0.00075	0.00000	0.00039	0.00065	0.00000	0.00035
AT1G18080			ATARCA (Homolog of the Tobacco	not plastid	27.3.99	1.10	1.03	0.81	2.07	0.00046	0.00048	0.00017	0.00047	0.00039	0.00036
AT3G63140			Rap41 or CSP41A	plastid stroma	27.3.99	0.76	1.12	0.65	0.67	0.00021	0.00033	0.00053	0.00024	0.00021	0.00036
AT5G07350			tudor domain-containing protein / nu	not plastid	27.3.73	1.18	1.08	0.42	3.36	0.00039	0.00020	0.00009	0.00042	0.00008	0.00029
AT2G37220			RNA binding protein CP29 B'	plastid stroma	27.4	0.80	0.68	0.77	0.94	0.00062	0.00034	0.00062	0.00042	0.00026	0.00058
AT2G35410			putative RNA binding protein	plastid stroma	27.4	1.70	1.57	1.80	1.86	0.00024	0.00019	0.00007	0.00038	0.00034	0.00013
AT3G52380			RNA-binding protein cp33	plastid stroma	27.4	0.93	1.02	1.01	0.61	0.00026	0.00026	0.00014	0.00026	0.00026	0.00009
AT5G04590			sulphite reductase	plastid stroma	14.3	1.21	1.12	1.11	1.42	0.00081	0.00072	0.00067	0.00091	0.00079	0.00096
AT5G60600			4-hydroxy-3-methylbutyl diphosphat	thylakoid-peripheral-st	16.1.1.6	0.97	0.98	0.85	1.16	0.00127	0.00228	0.00144	0.00124	0.00195	0.00167
AT3G63410			vte3 - MPBQ/MSBQ methyl transfe	envelope-inner	16.1.3.3	1.07	1.32	0.54	1.18	0.00067	0.00047	0.00069	0.00088	0.00025	0.00081
AT1G74920			betaine-aldehyde dehydrogenase, put	not plastid	16.4.2.1	1.22	0.88	1.25	1.48	0.00025	0.00035	0.00027	0.00022	0.00044	0.00040
AT5G26000			thioglucoside glucohydrolase 1 (TGC	not plastid	16.5.1	1.05	0.93	1.02	1.27	0.00853	0.00478	0.00559	0.00797	0.00488	0.00710
AT5G25980			myrosinase or thioglucoside glucohyc	not plastid	16.5.1	1.12	0.88	1.21	1.31	0.00643	0.00359	0.00646	0.00568	0.00435	0.00848
AT4G09000			14-3-3 protein GF14 chi (grf1)	not plastid	30.7	1.10	0.88	0.86	1.74	0.00083	0.00054	0.00047	0.00074	0.00046	0.00082
AT2G42590			14-3-3 protein GF14 mu (grf9) - plas	not plastid	30.7	0.67	0.68	0.42	1.14	0.00060	0.00060	0.00031	0.00041	0.00025	0.00036
AT5G16050			14-3-3 protein GF14 upsilon (grf5)	not plastid	30.7	1.05	1.13	1.12	0.53	0.00043	0.00031	0.00011	0.00049	0.00035	0.00006
AT1G22300			14-3-3 protein GF14 epsilon (grf10)	not plastid	30.7	1.25	1.09	1.60	0.79	0.00028	0.00022	0.00008	0.00030	0.00036	0.00006
AT3G02520			14-3-3 protein GF14 nu (grf7)	not plastid	30.7	0.86	0.43	1.33	0.80	0.00015	0.00019	0.00035	0.00006	0.00025	0.00028
AT5G10450			14-3-3 protein GF14 lambda (grf6/Al	nucleus	30.7	0.92	1.02	0.66	1.11	0.00064	0.00063	0.00055	0.00065	0.00042	0.00061
AT5G65430			14-3-3 protein GF14 kappa (grf8)	nucleus	30.7	1.39	0.64	1.64	7.64	0.00030	0.00020	0.00003	0.00019	0.00033	0.00021
AT5G38480			14-3-3 protein GF14 psi (grf3/RCI1)	plasma membrane	30.7	0.87	1.13	0.85	0.64	0.00037	0.00027	0.00042	0.00042	0.00023	0.00027
AT1G52410	3x yes		myosin-related, Poly-adenylate bindi	nucleus	30.3	1.04	0.52	12.60	365.14	0.00262	0.00009	0.00000	0.00136	0.00108	0.00037
AT5G61790			calnexin 1 (CNX1)	ER	30.3	1.15	0.83	1.43	1.28	0.00046	0.00043	0.00020	0.00038	0.00062	0.00026

Supplemental Table 1. (continued)

Accession	GLEE - genotype effect (p<0.01)	Genotype (p<0.01)	lab annotation	subcellular location	BIN#	klk3/wt average (days 0-3-	klk3/wt 0day (NadjSPC)	klk3/wt 3 day (NadjSPC)	klk3/wt 5 day (NadjSPC)	wt 0 day. Average NadjSPC	wt 3 day Average NadjSPC	wt 5 day Average NadjSPC	klk3 0day Average	klk3 3day Average	klk3 5dayAverage NadjSPC
AT2G33380			RD20 protein induced by ABA during dehydration, EF-han		30.3	1.45	1.01	1.82	1.40	0.00017	0.00033	0.00086	0.00017	0.00060	0.00121
AT4G17170	yes	yes	Rab2-like GTP-binding protein (RAI		30.5	2.01	1.25	2.23	2.54	0.00025	0.00046	0.00016	0.00031	0.00103	0.00040
AT3G46060	yes		Ras-related protein (ARA-3) / small (	plasma membrane	30.5	2.09	0.67	2.18	249.59	0.00019	0.00021	0.00000	0.00013	0.00046	0.00025
AT1G06400			Ras-related GTP-binding protein (AI		30.5	1.70	1.28	1.64	74.23	0.00012	0.00038	0.00000	0.00015	0.00062	0.00007
AT5G59840			Ras-related GTP-binding family prot		30.5	0.45	0.78	0.36	0.37	0.00018	0.00043	0.00026	0.00014	0.00016	0.00009
AT3G18820			Ras-related GTP-binding protein, put	not plastid	30.5	1.05	1.72	0.79	0.89	0.00016	0.00021	0.00031	0.00028	0.00016	0.00028
AT5G20010			GTP-binding nuclear protein (RAN-1	nucleus	30.5	0.75	0.66	0.73	0.79	0.00026	0.00143	0.00097	0.00017	0.00105	0.00076
AT4G17530			Ras-related GTP-binding protein, put	nucleus	30.5	1.25	1.44	0.66	2.32	0.00008	0.00044	0.00023	0.00012	0.00029	0.00053
AT3G43300			guanyl-nucleotide exchange factor/	protein binding (MIN7; I	30.5	0.92	1.10	1.11	0.54	0.00144	0.00019	0.00082	0.00159	0.00021	0.00045
AT3G45780			PHOT1 (phototropin 1); kinase, som	plasma membrane	30.11	1.03	0.98	43.95	0.93	0.00085	0.00000	0.00004	0.00083	0.00004	0.00003
AT5G41790			CIP1 (COP1-INTERACTIVE PROTEIN 1)		30.11.1	0.79	0.69	63.43	1.02	0.00192	0.00000	0.00057	0.00132	0.00006	0.00058
AT1G30360	2x yes	yes	ERD4 protein	not plastid	20.2.3	2.33	0.73	10.05	4.01	0.00075	0.00007	0.00040	0.00055	0.00068	0.00162
AT5G52640	2x yes	yes	heat shock protein 81-1 (HSP81-1) /	not plastid	20.2.1	2.20	0.94	2.77	2.52	0.00082	0.00107	0.00130	0.00077	0.00296	0.00328
AT3G09440	yes	yes	HSP70 (HSC70-3) (not plastid)	not plastid	20.2.1	1.65	1.06	2.75	1.73	0.00154	0.00070	0.00149	0.00164	0.00192	0.00258
AT1G79920			heat shock protein 70, putative / HSP		20.2.1	1.24	1.11	0.99	2.00	0.00135	0.00115	0.00061	0.00150	0.00114	0.00123
AT4G16660		yes	heat shock protein 70, putative / HSP		20.2.1	0.59	0.59	0.58	0.65	0.00044	0.00075	0.00007	0.00026	0.00043	0.00005
AT5G56030			Hsp90.2	cytosol	20.2.1	0.98	0.97	1.02	0.96	0.00265	0.00209	0.00312	0.00258	0.00213	0.00299
AT5G56010			Hsp90-3	cytosol	20.2.1	1.11	1.08	1.12	1.34	0.00159	0.00112	0.00023	0.00172	0.00125	0.00031
AT5G56000			Hsp90-4	cytosol	20.2.1	1.15	1.02	0.77	1.64	0.00020	0.00017	0.00019	0.00021	0.00013	0.00031
AT1G79930			Heat shock hsp70 protein	not plastid	20.2.1	0.92	0.69	0.87	1.44	0.00017	0.00066	0.00014	0.00012	0.00057	0.00020
AT4G23670	yes		Pathogenesis-related protein Bet v I f	not plastid	20.2.99	0.59	1.10	0.53	0.49	0.00067	0.00289	0.00169	0.00074	0.00152	0.00082
AT5G20630	yes		germin-like protein (GER3)	extracellular	20.2.99	2.09	0.91	0.33	2.78	0.00014	0.00007	0.00042	0.00013	0.00002	0.00116
AT4G18810	yes	yes	UV-B and ozone similarly regulated	plastid stroma	20.2.99	1.94	1.19	1.35	3.83	0.00024	0.00021	0.00016	0.00029	0.00028	0.00061
AT3G26450			major latex protein-related / MLP-rel	not plastid	20.2.99	0.69	1.18	0.25	0.91	0.00016	0.00035	0.00034	0.00019	0.00009	0.00031
AT1G33590			disease resistance protein-related / LI	not plastid	20.1.7	1.60	1.63	2.26	1.31	0.00005	0.00015	0.00036	0.00008	0.00035	0.00047
AT3G61220			NADPH short-chain dehydrogenase/r	cytosol	*20.3	0.84	0.67	1.66	0.47	0.00021	0.00019	0.00033	0.00014	0.00031	0.00016
AT1G70410			beta carbonic anhydrase 4 (CA4)	plasmamembrane	8.3	0.93	0.88	0.96	0.95	0.00043	0.00036	0.00035	0.00038	0.00035	0.00033
AT3G01500			beta-carbonic anhydrase-1 (beta CA1	plastid stroma	8.3	1.16	1.05	1.42	0.98	0.00695	0.01114	0.01161	0.00727	0.01578	0.01140
AT5G14740			beta carbonic anhydrase 2 (CA2)- N-	plastid stroma	8.3	1.00	1.09	0.94	1.02	0.00337	0.00599	0.00240	0.00367	0.00560	0.00245
AT2G05710	yes	yes	Aconitase 3 (ACO3)- likely dually ta	mitochondria	8.2.3	1.71	1.00	3.92	1.67	0.00144	0.00048	0.00159	0.00145	0.00190	0.00265
AT1G04410	yes	yes	malate dehydrogenase, cytosolic,	cytosol	8.2.9	0.74	1.26	0.62	0.59	0.00142	0.00355	0.00206	0.00180	0.00221	0.00122
AT5G11670			NADP-malic enzyme 2 (NADP-ME2	cytosol	8.2.10	1.02	0.95	1.15	1.04	0.00186	0.00068	0.00135	0.00177	0.00079	0.00141
AT4G00570			malate oxidoreductase, NAD-ME2	mitochondria	8.2.10	0.78	0.77	2.66	0.58	0.00041	0.00005	0.00043	0.00031	0.00013	0.00025
AT3G47520			malate dehydrogenase [NAD], plastic	plastid stroma	8.2.99	1.09	0.70	1.55	1.19	0.00073	0.00039	0.00091	0.00051	0.00061	0.00108
AT5G58330			malate dehydrogenase [NADP]	plastid stroma	8.2.99	1.08	1.02	1.10	1.08	0.00028	0.00036	0.00098	0.00029	0.00040	0.00106
AT3G55410			2-oxoglutarate dehydrogenase, E1 su	mitochondria	8.1.5	1.19	0.91	2.55	1.42	0.00112	0.00019	0.00021	0.00102	0.00048	0.00030
AT4G26970			Aconitase 2 (ACO2)	mitochondria	8.1.3	1.09	0.88	1.42	1.15	0.00199	0.00103	0.00103	0.00175	0.00146	0.00118
AT4G35830			Aconitase 1 (ACO1) - likely dually ta	mitochondria	8.1.3	1.02	1.21	0.65	2.41	0.00108	0.00145	0.00023	0.00131	0.00094	0.00056
AT2G44350			citrate synthase	mitochondria	8.1.2	0.87	0.76	0.78	0.94	0.00017	0.00017	0.00046	0.00013	0.00013	0.00043
AT5G50950			fumarate hydratase 2 (FUM2)	cytosol	8.1.8	0.97	0.74	0.53	7.87	0.00052	0.00017	0.00003	0.00039	0.00009	0.00022
AT1G65930			NADP+ isocitrate dehydrogenase (IC	cytosol	8.1.4	0.71	0.77	0.70	0.68	0.00102	0.00130	0.00096	0.00079	0.00091	0.00065
AT1G53240			malate dehydrogenase [NAD]	mitochondria	8.1.9	0.86	0.94	0.76	0.86	0.00137	0.00117	0.00215	0.00129	0.00089	0.00185
AT5G50850			pyruvate dehydrogenase E1 compone	mitochondria	8.1.1.1	0.99	1.02	1.15	0.88	0.00042	0.00047	0.00083	0.00043	0.00054	0.00073
AT3G13930			Dihydrolipoamide Acetyltransferase,	mitochondria	8.1.1.2	1.42	1.13	1.67	1.52	0.00023	0.00021	0.00014	0.00026	0.00034	0.00022
AT1G48030			E3-1 dihydrolipoamide dehydrogena	mitochondria	8.1.1.3	1.05	1.03	1.19	0.96	0.00139	0.00200	0.00267	0.00143	0.00238	0.00257
AT5G66760			succinate dehydrogenase (ubiquinone	mitochondria	8.1.7	1.67	1.40	2.03	1.43	0.00020	0.00034	0.00032	0.00028	0.00070	0.00045
AT2G20420			succinyl-CoA ligase beta subunit	mitochondria	8.1.6	0.98	0.83	1.02	1.09	0.00044	0.00036	0.00047	0.00037	0.00037	0.00052
AT1G59870	yes		PDR8/PEN3 (PLEIOTROPIC DRUG	plasma membrane	34.16	1.20	1.05	4.84	1.25	0.00425	0.00015	0.00138	0.00445	0.00074	0.00173
AT4G35100	yes		PIP3 (PLASMA MEMBRANE INTF	plasma membrane	34.19.1	1.50	1.02	1.42	4.70	0.00110	0.00039	0.00017	0.00112	0.00056	0.00082
AT2G45960			aquaporin (PIP1.2) - plasma membra	plasma membrane	34.19.1	1.11	0.91	1.04	1.26	0.00097	0.00093	0.00176	0.00087	0.00096	0.00221
AT3G53420			aquaporin (PIP2.1) - plasma membra	plasma membrane	34.19.1	1.17	1.04	0.92	1.60	0.00116	0.00115	0.00104	0.00120	0.00105	0.00167
AT4G23400		yes	PIP1;5/PIP1D (plasma membrane intrinsic protein 1;5); wat		34.19.1	1.79	1.61	0.07	2.38	0.00034	0.00001	0.00015	0.00054	0.00000	0.00035
AT3G16240			delta tonoplast integral protein (delta	vacuole-tonoplast	34.19.2	0.97	1.03	1.15	0.84	0.00182	0.00084	0.00205	0.00187	0.00097	0.00172
AT3G26520			gamma tonoplast intrinsic protein1;2	vacuole-tonoplast	34.19.2	1.16	1.14	1.12	1.22	0.00036	0.00065	0.00068	0.00041	0.00073	0.00082

Supplemental Table 1. (continued)

Accession	GLEE - genotype effect (p<0.01)	Genotype (p<0.01)	lab annotation	subcellular location	BIN#	k1k3/wt average (days 0-3-	k1k3/wt 0day (NadjSPC)	k1k3/wt 3 day (NadjSPC)	k1k3/wt 5 day (NadjSPC)	wt 0 day. Average NadjSPC	wt 3 day Average NadjSPC	wt 5 day Average NadjSPC	k1k3 0day Average	k1k3 3day Average	k1k3 5dayAverage NadjSPC
AT5G12470			envelope protein MEP3 - putative inr	envelope	34.8	1.43	1.20	1.84	1.35	0.00040	0.00036	0.00073	0.00048	0.00066	0.00098
AT5G46110			TPT - IEP30 = Phosphate/triose-phos	envelope-inner-integra	34.8	1.02	0.97	1.14	0.91	0.00227	0.00233	0.00151	0.00221	0.00266	0.00137
AT1G32080			envelope protein (MEP1) or LrgB	envelope-inner-integra	34.8	0.81	0.78	0.32	1.11	0.00169	0.00037	0.00080	0.00132	0.00012	0.00089
AT5G12860			2-oxoglutarate/malate translocator (D	envelope-inner-integra	34.8	0.92	1.05	0.74	0.98	0.00031	0.00051	0.00086	0.00033	0.00038	0.00084
AT1G01790			K+ efflux antiporter, putitive (KEA1)	envelope-inner-integra	34.8	1.40	0.80	2.18	2.85	0.00087	0.00020	0.00025	0.00070	0.00045	0.00072
AT4G25450			ABC transporter family (NAP8)	envelope-inner-integra	34.8	1.23	0.84	3.30	1.20	0.00042	0.00009	0.00038	0.00035	0.00029	0.00045
AT1G80300			ATP/ADP translocator (AATP1 ort A	envelope-inner-integra	34.8	1.12	25.66	1.21	1.07	0.00000	0.00005	0.00057	0.00003	0.00006	0.00061
AT2G28900			Amino acid transporter (OEP16:HP1	envelope-outer	34.8	0.89	0.76	0.80	1.14	0.00033	0.00036	0.00030	0.00025	0.00029	0.00034
AT5G14040			phosphate transporter (PHT3-1 or PH	mitochondria	34.8	0.99	1.19	1.02	0.84	0.00075	0.00115	0.00124	0.00089	0.00117	0.00105
AT3G08580			mitochondrial ADP,ATP carrier prot	mitochondria	34.9	0.94	1.00	1.12	0.63	0.00561	0.00626	0.00498	0.00562	0.00704	0.00312
AT5G19760			oxoglutarate/malate translocator (DT	mitochondria	34.9	1.44	1.00	1.51	2.00	0.00066	0.00078	0.00042	0.00066	0.00118	0.00084
AT5G46800			mitochondrial carnitine/acyl (CAC) c	not plastid	34.9	0.88	0.63	1.26	0.95	0.00060	0.00028	0.00059	0.00038	0.00035	0.00056
AT1G72150	2x yes	yes	PATELLIN 1 cell plate fraffick ing (F	not plastid	34.99	1.68	0.94	2.83	3.32	0.00203	0.00073	0.00042	0.00190	0.00207	0.00138
AT1G22530	2x yes		SEC14 cytosolic factor family protei	not plastid	34.99	1.59	0.79	3.83	4.97	0.00109	0.00019	0.00013	0.00086	0.00073	0.00065
AT1G78900			ATPase 70 kDa	vacuole	34.1	1.14	1.02	1.35	0.97	0.00644	0.00790	0.00569	0.00659	0.01063	0.00551
AT1G12840			V-ATPase subunit C (VATC) (DET3	vacuole	34.1	1.09	1.29	1.73	0.69	0.00033	0.00061	0.00114	0.00043	0.00106	0.00079
AT4G39080			VHA-A3 (VACUOLAR PROTON A	vacuole-tonoplast	34.1	1.24	0.95	1.57	1.25	0.00155	0.00127	0.00146	0.00148	0.00199	0.00183
AT2G18960	yes		ATPase 1, plasma membrane-type	plasma membrane	34.1.2	1.06	1.09	1.92	0.80	0.00367	0.00093	0.00361	0.00401	0.00178	0.00289
AT1G20260			vacuolar H+-ATPase subunit B	not plastid	34.1.1	1.20	1.01	1.21	1.43	0.00188	0.00214	0.00152	0.00189	0.00257	0.00217
AT4G38510			probable H+-transporting ATPase	not plastid	34.1.1	1.21	0.97	1.08	1.95	0.00088	0.00096	0.00046	0.00085	0.00104	0.00089
AT3G58730			v-ATPase subunit D (vATPD)	not plastid	34.1.1	0.83	0.62	0.62	1.59	0.00047	0.00024	0.00020	0.00029	0.00015	0.00032
AT4G11150			V-ATPase subunit E (VATE)	vacuole	34.1.1	0.98	1.30	0.77	0.80	0.00037	0.00046	0.00012	0.00049	0.00036	0.00009
AT5G67500			Voltage dependent ion channel VDA	mitochondria	34.20	1.15	0.80	2.37	1.06	0.00034	0.00014	0.00052	0.00027	0.00032	0.00055
AT3G01280			Voltage dependent ion channel VDA	mitochondria	34.20	1.02	0.58	1.49	1.12	0.00030	0.00018	0.00045	0.00017	0.00026	0.00050
AT5G15090			Voltage dependent ion channel VDA	mitochondria	34.18	1.17	1.04	1.80	0.97	0.00036	0.00032	0.00078	0.00038	0.00058	0.00076

Supplemental Table 2. Plastoglobule protein abundance in wild-type and *k1k3*

Accession	Lab Annotation	Curated Loc.	MapMan Bin #	MapMan Bin Name	WT Rep 1 NadjSPC	WT Rep 2 NadjSPC	WT Rep 3 NadjSPC	*k1k3* Rep 1 NadjSPC	*k1k3* Rep 2 NadjSPC	*k1k3* Rep 3 NadjSPC	p-value
AT5G19940	fibrillin (FIB6)	plastid	26.31*	misc.fibrillins	0.00000	0.00000	0.00000	0.00138	0.00126	0.00125	0.000
AT3G24190	ABC1 kinase - ABC1K6	plastid	26.56*	misc.ABC1k family	0.01841	0.01743	0.01681	0.00000	0.00194	0.00028	0.000
AT3G27830	50S ribosomal protein L12-A (I	plastid ribosome	29.2.1.1.1.2	protein.synthesis.ribosom	0.00000	0.00000	0.00000	0.00020	0.00017	0.00017	0.000
AT3G27850	50S ribosomal protein L12-C (I	plastid ribosome	29.2.1.1.1.2	protein.synthesis.ribosom	0.00000	0.00000	0.00000	0.00020	0.00017	0.00017	0.000
ATCG00680	psbB CP47	thylakoid-integra	1.1.1.2	PS.lightreaction.photosys	0.01841	0.01878	0.02053	0.00099	0.00457	0.00104	0.000
AT3G61870	unknown protein		35.2	not assigned.unknown	0.00057	0.00060	0.00044	0.00000	0.00000	0.00000	0.000
AT4G31390	ABC1 kinase - ABC1K3	plastoglobules	26.56*	misc.ABC1k family	0.02224	0.02854	0.02118	0.00000	0.00000	0.00000	0.000
AT1G71810	ABC1 kinase - ABC1K1	plastoglobules	26.56*	misc.ABC1k family	0.00921	0.01307	0.01288	0.00000	0.00000	0.00000	0.001
AT5G05200	ABC1 kinase - AB1K4 (DUF77	plastoglobules	26.56*	misc.ABC1k family	0.03173	0.03530	0.03625	0.01777	0.02113	0.01756	0.001
AT3G25760	allene oxide cyclase 1 (OAC1;I	plastid	17.7.1.3	hormone metabolism.jasn	0.00000	0.00000	0.00000	0.00082	0.00069	0.00053	0.001
ATCG00480	CF1b - atpB	thylakoid-periphe	1.1.4	PS.lightreaction.ATP syn	0.04737	0.04273	0.05405	0.01746	0.02161	0.01833	0.001
AT2G04030	cpHSP90	plastid stroma	29.6	protein.folding	0.00042	0.00099	0.00044	0.00363	0.00405	0.00296	0.001
AT1G79600	ABC1 kinase - ABC1K2	plastoglobules	26.56*	misc.ABC1k family	0.01700	0.02374	0.02708	0.00000	0.00000	0.00000	0.002
ATCG00280	psbC CP43	thylakoid-integra	1.1.1.2	PS.lightreaction.photosys	0.00779	0.00916	0.01026	0.00109	0.00320	0.00153	0.002
AT3G02900			35.2	not assigned.unknown	0.00000	0.00000	0.00000	0.00020	0.00023	0.00014	0.002
AT1G64770	NDF2- associates with the NDI	thylakoid	1.1.6	PS.lightreaction.NADH I	0.00028	0.00030	0.00044	0.00000	0.00000	0.00000	0.002
AT5G08740	pyridine nucleotide-disulphide	plastoglobules; m	35; 9.2.3	not assigned; mitochondr	0.01346	0.01292	0.01463	0.00740	0.00902	0.00666	0.002
AT3G04870	zeta-carotene desaturase (ZDS)	plastid	16.1.4.3	secondary metabolism.isc	0.00000	0.00000	0.00000	0.00217	0.00308	0.00194	0.002
ATCG00540	petA - cytochrome f (cleavable	thylakoid-integra	1.1.3	PS.lightreaction.cytochro	0.00411	0.00376	0.00524	0.00069	0.00137	0.00076	0.002
AT4G19170	9-cis-epoxycarotenoid dioxyger	plastoglobules	16.1.4	secondary metabolism.isc	0.01544	0.02329	0.02402	0.00286	0.00228	0.00326	0.003
AT2G38040	carboxyltransferase (CT) alpha	envelope-inner-p	11.1.1	lipid metabolism.FA synt	0.00000	0.00000	0.00000	0.00089	0.00126	0.00076	0.003
AT1G76180	dehydrin -ERD14		20.2.99	stress.abiotic.unspecified	0.00000	0.00000	0.00000	0.00079	0.00046	0.00062	0.003
AT5G16660	unknown protein - C/M - envel	envelope	35.2	not assigned.unknown	0.00000	0.00000	0.00000	0.00276	0.00171	0.00187	0.003
AT2G42130	fibrillin (FIB7b) - model .4 sco	thylakoid-periphe	26.31*	misc.fibrillins	0.01332	0.01037	0.01354	0.00385	0.00605	0.00451	0.003
AT3G26840	Diacyl glycerol transferase (DA	plastoglobules	11.1	lipid metabolism.glycolip	0.01048	0.00916	0.01398	0.00059	0.00263	0.00146	0.003
ATCG00800	30S ribosomal protein S3	plastid ribosome	29.2.1.1.1.1	protein.synthesis.ribosom	0.00014	0.00000	0.00000	0.00158	0.00194	0.00111	0.004
AT2G47400	CP12 protein		1.3.14*	PS.calvin cycle regulatior	0.00000	0.00000	0.00000	0.00020	0.00011	0.00021	0.004
AT1G15820	LHCII-6 - CP24	thylakoid-integra	1.1.1.1	PS.lightreaction.photosys	0.00411	0.00331	0.00437	0.00069	0.00183	0.00076	0.004
AT3G07700	ABC1 kinase family		26.56*	misc.ABC1k family	0.00680	0.00661	0.00917	0.00030	0.00263	0.00125	0.005
AT1G20340	plastocyanin-1 (PC-1)	thylakoid-periphe	1.1.5.1	PS.lightreaction.other ele	0.00028	0.00000	0.00000	0.00079	0.00126	0.00125	0.005
AT5G49910	cpHSP70-2 (Dnak homologue)	plastid stroma	29.6	protein.folding	0.00000	0.00000	0.00000	0.00200	0.00223	0.00350	0.005
AT4G21280	psbQ OEC16 Tat ltp	thylakoid-periphe	1.1.1.2	PS.lightreaction.photosys	0.00000	0.00000	0.00000	0.00485	0.00262	0.00484	0.005
AT1G71480	nuclear transport factor 2 (NTF	plastid	29.3.1	protein.targeting.nucleus	0.00000	0.00000	0.00000	0.00118	0.00148	0.00076	0.005
ATCG00340	psaB - subunit Ib	thylakoid-integra	1.1.2.2	PS.lightreaction.photosys	0.00482	0.00766	0.00677	0.00059	0.00206	0.00042	0.005
AT4G22890	PGRL1A	thylakoid-integra	1.1.40	PS.lightreaction.cyclic el	0.00085	0.00075	0.00044	0.00000	0.00000	0.00000	0.005
AT1G06430	FtsH8 TAT lTP	thylakoid-integra	29.5.7	protein.degradation.metal	0.00409	0.00287	0.00312	0.00000	0.00123	0.00021	0.006
AT5G23060	Ca2+ sensing receptor - phosph	thylakoid-integra	1.1.30	PS.lightreaction.state trar	0.00354	0.00646	0.00677	0.00000	0.00011	0.00000	0.006
AT1G61520	LHCI-3 - LHCI-680A CAB4	thylakoid-integra	1.1.2.1	PS.lightreaction.photosys	0.00609	0.00826	0.00830	0.00138	0.00354	0.00174	0.006

Supplemental Table 2. (continued)

Accession	Lab Annotation	Curated Loc.	MapMan Bin #	MapMan Bin Name	WT Rep 1 NadjSPC	WT Rep 2 NadjSPC	WT Rep 3 NadjSPC	*k1k3* Rep 1 NadjSPC	*k1k3* Rep 2 NadjSPC	*k1k3* Rep 3 NadjSPC	p-value
AT4G25130	methionine sulfoxide reductase	plastid stroma	29.11*	protein.methione sulfoxic	0.00000	0.00000	0.00000	0.00059	0.00114	0.00083	0.006
AT2G37660	3-beta-hydroxy-delta5-steroid d	plastid stroma	35.2	not assigned.unknown	0.00000	0.00000	0.00000	0.00112	0.00057	0.00103	0.006
ATCG00020	psbA D1	thylakoid-integra	1.1.1.2	PS.lightreaction.photosys	0.00269	0.00165	0.00284	0.00049	0.00034	0.00028	0.006
AT1G78140	Ubie_methyltransferase-related	plastoglobules	35.1	not assigned.no ontology	0.00864	0.01217	0.00852	0.00306	0.00377	0.00167	0.007
ATCG00470	CF1e - atpE	thylakoid-periphe	1.1.4	PS.lightreaction.ATP syn	0.00085	0.00090	0.00087	0.00030	0.00057	0.00049	0.007
AT5G02500	HSP70-1 (HSC70-1) (not plasti	cytosol	29.6	protein.folding	0.00028	0.00000	0.00000	0.00153	0.00176	0.00271	0.007
AT1G31330	psaF- subunit III - LTP - hydrop	thylakoid-integra	1.1.2.2	PS.lightreaction.photosys	0.00156	0.00195	0.00262	0.00059	0.00023	0.00035	0.007
AT3G47470	LHCI-4 - LHCI-730	thylakoid-integra	1.1.2.1	PS.lightreaction.photosys	0.00552	0.00346	0.00393	0.00079	0.00137	0.00097	0.007
AT5G42270	FtsH5 (VAR1)	thylakoid-integra	29.5.7	protein.degradation.metal	0.00589	0.00649	0.00830	0.00039	0.00297	0.00028	0.008
AT3G26060	Peroxiredoxin Q (Prx Q) (monc	plastid	21.5	redox.peroxiredoxins	0.00000	0.00000	0.00000	0.00296	0.00206	0.00146	0.008
ATCG00120	CF1a - atpA	thylakoid-periphe	1.1.4	PS.lightreaction.ATP syn	0.03323	0.02898	0.04049	0.01195	0.01897	0.01056	0.009
AT5G06220	unknown protein		35.2	not assigned.unknown	0.00000	0.00000	0.00000	0.00248	0.00480	0.00293	0.009
ATCG00350	psaA - subunit Ia	thylakoid-integra	1.1.2.2	PS.lightreaction.photosys	0.00269	0.00240	0.00415	0.00000	0.00080	0.00000	0.009
AT1G76080	thioredoxin (CDSP32)	plastid stroma	21.1	redox.thioredoxin	0.00000	0.00000	0.00000	0.00109	0.00057	0.00062	0.010
AT4G12800	psaL - subunit XI (also named '	thylakoid-integra	1.1.2.2	PS.lightreaction.photosys	0.00184	0.00135	0.00175	0.00059	0.00091	0.00035	0.010
AT5G09660	malate dehydrogenase, glyoxys	peroxisome	6.3	gluconeogenesis.Malate I	0.00241	0.00300	0.00306	0.00128	0.00000	0.00104	0.010
AT5G41120			35.1	not assigned.no ontology	0.00326	0.00361	0.00240	0.00010	0.00069	0.00139	0.010
AT1G32220	flavin reductase-related (3Beta_	plastid stroma; pl	35.2	not assigned.unknown	0.00708	0.00706	0.00917	0.00415	0.00491	0.00361	0.011
AT4G31530	unknown protein - dehydrogena	plastid stroma	35.2	not assigned.unknown	0.00000	0.00000	0.00000	0.00030	0.00034	0.00014	0.014
AT5G50100	unknown protein, contains Pfam domain PF0413		35.2	not assigned.unknown	0.00000	0.00000	0.00000	0.00059	0.00069	0.00028	0.014
AT2G44060	late embryogenesis abundant family protein (LEA		33.2	development.late embryo	0.00000	0.00000	0.00000	0.00020	0.00011	0.00028	0.014
AT1G80380	phosphoribulokinase-1 (PRK-1)	plastid stroma	1.3.12	PS.calvin cyle.PRK	0.00000	0.00000	0.00000	0.00059	0.00034	0.00083	0.014
AT5G56030	heat shock protein 81-2 (HSP81-2)		20.2.1	stress.abiotic.heat	0.00000	0.00000	0.00000	0.00208	0.00132	0.00090	0.014
AT4G24280	cpHSP70-1 (DnaK homologue)	plastid stroma	29.6	protein.folding	0.00000	0.00000	0.00000	0.00550	0.00223	0.00525	0.015
AT3G27110			29.5	protein.degradation	0.00212	0.00240	0.00175	0.00563	0.00502	0.00354	0.015
AT1G18060	unknown protein (fibrillin?)	thylakoid	35.2	not assigned.unknown	0.00000	0.00015	0.00000	0.00069	0.00114	0.00056	0.015
AT3G45140	lipoxygenase AtLOX2, plastid	plastid stroma	17.7.1.2	hormone metabolism.jasn	0.00142	0.00150	0.00153	0.01056	0.00622	0.01367	0.016
AT4G32260	CFO-II - atpG	thylakoid-integra	1.1.4	PS.lightreaction.ATP syn	0.00156	0.00180	0.00131	0.00099	0.00103	0.00090	0.016
AT4G01800	cpSecA	plastid stroma; th	29.3.3	protein.targeting.chloropl	0.00000	0.00015	0.00000	0.00030	0.00046	0.00028	0.018
AT1G06690	aldo/keto reductase family prot	plastoglobules	35.1	not assigned.no ontology	0.01147	0.01052	0.00983	0.00711	0.00765	0.00451	0.018
AT2G41040	Ubie_methyl transferase - SAM	plastoglobules	35.1	not assigned.no ontology	0.00567	0.00751	0.00852	0.00168	0.00434	0.00160	0.019
AT2G30950	FtsH2 (VAR2 and Pftf)	thylakoid-integra	29.5.7	protein.degradation.metal	0.00483	0.00479	0.00430	0.00069	0.00299	0.00021	0.019
AT2G34460	flavin reductase-related (3Beta_	plastoglobules	35.1	not assigned.no ontology	0.00892	0.01052	0.01114	0.00464	0.00719	0.00687	0.019
AT2G46910	fibrillin (FIB8)	plastoglobules	26.31*	misc.fibrillins	0.01020	0.00781	0.01048	0.00415	0.00662	0.00500	0.019
AT1G17420			17.7.1.2	hormone metabolism.jasn	0.00000	0.00000	0.00000	0.01367	0.02184	0.00826	0.021
AT1G12900	glyceraldehyde-3-phosphate del	plastid stroma	1.3.4	PS.calvin cyle.GAP	0.00021	0.00000	0.00000	0.00095	0.00206	0.00261	0.022
AT5G42650	allene oxide synthase (AOS)	plastoglobules; th	17.7.1.3	hormone metabolism.jasn	0.02111	0.02193	0.02642	0.07612	0.07743	0.04228	0.022
AT3G62030	peptidylprolyl isomerase ROC4	plastid stroma	29.6	protein.folding	0.00000	0.00000	0.00000	0.00346	0.00114	0.00271	0.023

Supplemental Table 2. (continued)

Accession	Lab Annotation	Curated Loc.	MapMan Bin #	MapMan Bin Name	WT Rep 1 NadjSPC	WT Rep 2 NadjSPC	WT Rep 3 NadjSPC	*k1k3* Rep 1 NadjSPC	*k1k3* Rep 2 NadjSPC	*k1k3* Rep 3 NadjSPC	p-value
AT4G20360	elongation factor Tu (EF-Tu-1)	plastid stroma	29.2.4	protein.synthesis.elongati	0.00071	0.00240	0.00349	0.00764	0.00537	0.00539	0.024
ATCG00270	psbD D2	thylakoid-integra	1.1.1.2	PS.lightreaction.photosys	0.00382	0.00225	0.00480	0.00030	0.00148	0.00028	0.025
AT1G06680	PsbP-1 OEC23 Tat lTP	thylakoid-periphe	1.1.1.2	PS.lightreaction.photosys	0.00212	0.00060	0.00087	0.01659	0.00640	0.01125	0.027
AT3G12780	phosphoglycerate kinase-1 (PG	plastid stroma	1.3.3	PS.calvin cyle.phosphogl	0.00042	0.00000	0.00000	0.02460	0.00767	0.01949	0.027
AT5G27290	unknown protein		35.2	not assigned.unknown	0.00000	0.00000	0.00000	0.00020	0.00023	0.00007	0.027
AT1G08550	Violaxanthin Deepoxidase (VD	thylakoid-periphe	16.1.4.21	secondary metabolism.isc	0.00000	0.00000	0.00000	0.00030	0.00057	0.00090	0.028
AT1G42960	Hp17	thylakoid	35.2	not assigned.unknown	0.00000	0.00000	0.00000	0.00020	0.00023	0.00049	0.029
AT5G35170	adenylate kinase	plastid	23.4.1	nucleotide metabolism.ph	0.00014	0.00000	0.00000	0.00020	0.00046	0.00035	0.032
AT2G23670	unknown protein	thylakoid	35.1	not assigned.no ontology	0.00000	0.00000	0.00000	0.00020	0.00011	0.00035	0.032
AT1G79550	phosphoglycerate kinase		4.1	glycolysis.phosphoglycer	0.00000	0.00000	0.00000	0.00166	0.00046	0.00146	0.033
AT4G35250	vestitone reductase-related	thylakoid	35.1	not assigned.no ontology	0.00042	0.00120	0.00109	0.00010	0.00023	0.00000	0.034
AT4G01690	protoporphyrinogen oxidase (Pl	plastid	19.9	tetrapyrrole synthesis.pro	0.00057	0.00075	0.00131	0.00385	0.00582	0.00243	0.035
AT2G21170	triosephosphate isomerase-1 (T	plastid stroma	1.3.5	PS.calvin cycle.TPI	0.00000	0.00000	0.00000	0.00099	0.00046	0.00160	0.037
ATCG00730	petD - subIV	thylakoid-integra	1.1.3	PS.lightreaction.cytochro	0.00028	0.00060	0.00044	0.00000	0.00023	0.00000	0.038
AT2G21330	fructose-bisphosphate aldolase-	plastid stroma; pl	1.3.6	PS.calvin cyle.aldolase	0.01657	0.01402	0.01743	0.00775	0.00652	0.01308	0.038
AT1G74470	geranylgeranyl reductase (GGD	thylakoid	16.1.1	secondary metabolism.isc	0.00751	0.00315	0.00393	0.00000	0.00148	0.00035	0.040
AT4G29060	PSRP-7 - (110 kDa fusion of 65	plastid ribosome	29.2.4	protein.synthesis.elongati	0.00000	0.00000	0.00000	0.00188	0.00046	0.00146	0.040
AT5G56000	heat shock protein 81.4 (hsp81.4)/	Hsp90 protein	20.2.1	stress.abiotic.heat	0.00071	0.00090	0.00022	0.00000	0.00000	0.00000	0.040
AT1G16880	uridylyltransferase-related	plastid stroma; th	3.8.3	minor CHO metabolism.g	0.00000	0.00015	0.00000	0.00109	0.00034	0.00125	0.041
AT2G46820	Photosystem I protein TMP14 -	thylakoid	1.1.2.2	PS.lightreaction.photosys	0.00057	0.00075	0.00109	0.00000	0.00046	0.00014	0.042
AT3G11630	2-Cys Peroxiredoxin A (Prx A;	plastid stroma; th	21.5	redox.periredoxins	0.00000	0.00000	0.00000	0.00366	0.00091	0.00245	0.042
AT4G28025	unknown protein		35.2	not assigned.unknown	0.00057	0.00015	0.00066	0.00000	0.00000	0.00000	0.042
AT1G03630	PORC- ~constitutive expressio	thylakoid-periphe	19.14	tetrapyrrole synthesis.pro	0.00028	0.00030	0.00000	0.00375	0.00898	0.00353	0.043
AT4G02770	psaD-2 subunit II - stromal side	thylakoid-periphe	1.1.2.2	PS.lightreaction.photosys	0.00496	0.00300	0.00328	0.00000	0.00240	0.00042	0.043
AT3G56940	CHL27 or Crd1	envelope-inner-p	19.12	tetrapyrrole synthesis.ma	0.00057	0.00120	0.00022	0.00158	0.00297	0.00187	0.044
AT3G52960	Peroxiredoxin IIE (PrxII E)	plastid stroma	21.5	redox.periredoxins	0.00000	0.00000	0.00000	0.00276	0.00069	0.00174	0.045
AT4G03280	petC - Rieske Fe-S protein	thylakoid-periphe	1.1.3	PS.lightreaction.cytochro	0.00028	0.00060	0.00066	0.00000	0.00000	0.00028	0.047
AT3G26070	fibrillin (FIB3a)	thylakoid-periphe	26.31*	misc.fibrillins	0.00014	0.00030	0.00000	0.00188	0.00260	0.00069	0.049
AT2G35490	fibrillin (FIB2)	plastoglobules; th	26.31*	misc.fibrillins	0.05779	0.06099	0.05372	0.03693	0.05093	0.02971	0.050
AT5G06290	2-Cys Peroxiredoxin B (Prx B)	plastid stroma	21.5	redox.periredoxins	0.00000	0.00000	0.00000	0.00226	0.00046	0.00227	0.051
AT1G56190	phosphoglycerate kinase-1 (PG	plastid stroma	1.3.3	PS.calvin cyle.phosphogl	0.00042	0.00000	0.00000	0.00354	0.00089	0.00389	0.051
AT4G04020	fibrillin (FIB1a)	plastoglobules; th	26.31*	misc.fibrillins	0.09653	0.07413	0.08322	0.05799	0.07023	0.04484	0.051
AT3G11560	unknown protein		35.2	not assigned.unknown	0.00000	0.00000	0.00000	0.00147	0.00240	0.00054	0.052
AT3G43540	unknown protein slr1699 - PIR	thylakoid	35.2	not assigned.unknown	0.01289	0.00781	0.00808	0.00247	0.00571	0.00493	0.053
AT3G04890			35.2	not assigned.unknown	0.00000	0.00000	0.00000	0.00020	0.00046	0.00014	0.054
AT5G19850			35.1	not assigned.no ontology	0.00000	0.00000	0.00000	0.00010	0.00023	0.00007	0.054
AT3G54890	LHCI-1-1 - LHCI-730	thylakoid-integra	1.1.2.1	PS.lightreaction.photosys	0.00071	0.00015	0.00044	0.00000	0.00000	0.00000	0.055
AT1G72150	PATELLIN 1 cell plate frafficking (PATL1)		34.99	transport.misc	0.00000	0.00000	0.00000	0.00039	0.00034	0.00007	0.056

Supplemental Table 2. (continued)

Accession	Lab Annotation	Curated Loc.	MapMan Bin #	MapMan Bin Name	WT Rep 1 NadjSPC	WT Rep 2 NadjSPC	WT Rep 3 NadjSPC	*k1k3* Rep 1 NadjSPC	*k1k3* Rep 2 NadjSPC	*k1k3* Rep 3 NadjSPC	p-value
AT3G54050	fructose-bisphosphatase (FBPA	plastid stroma	1.3.7	PS.calvin cyle.FBPase	0.00014	0.00000	0.00000	0.00227	0.00057	0.00305	0.059
AT1G23740	oxidoreductase, zinc-binding de	plastid stroma	26.7	misc.oxidases - copper, fl	0.00000	0.00000	0.00000	0.00425	0.00069	0.00389	0.060
AT1G73750			35.2	not assigned.unknown	0.00524	0.00300	0.00109	0.00000	0.00000	0.00000	0.060
AT1G55480	unknown protein	thylakoid-periphe	35.2	not assigned.unknown	0.00000	0.00000	0.00000	0.00039	0.00069	0.00014	0.062
AT1G16080	unknown protein	plastid stroma	35.2	not assigned.unknown	0.00000	0.00000	0.00000	0.00089	0.00023	0.00132	0.063
AT5G30510	30S ribosomal protein S1	plastid ribosome	29.2.1.1.3.1	protein.synthesis.ribosom	0.00000	0.00000	0.00000	0.00079	0.00023	0.00125	0.063
AT1G53240	malate dehydrogenase [NAD],	mitochondria	8.1.9	TCA / org.transformation	0.00000	0.00000	0.00000	0.00390	0.00069	0.00448	0.063
AT5G28540	luminal binding protein 1 precu	ER	29.6	protein.folding	0.00000	0.00000	0.00000	0.00286	0.00147	0.00062	0.064
AT5G46110	TPT - IEP30 = Phosphate/triose	envelope-inner-in	34.8	transport.metabolite trans	0.00071	0.00090	0.00044	0.00000	0.00046	0.00014	0.064
AT1G11860	aminomethyltransferase-related	precursor protein	13.2.5.2	amino acid metabolism.d	0.00000	0.00000	0.00000	0.00918	0.00137	0.00736	0.065
AT3G63410	vte3 - MPBQ/MSBQ methyl tr	envelope-inner	16.1.3.3	secondary metabolism.isc	0.00085	0.00165	0.00131	0.00000	0.00091	0.00000	0.065
AT4G04640	CF1y - atpC	thylakoid-periphe	1.1.4	PS.lightreaction.ATP syn	0.00680	0.00541	0.00983	0.00079	0.00502	0.00278	0.066
AT1G51110	fibrillin (FIB10)	thylakoid-periphe	26.31*	misc.fibrillins	0.00297	0.00180	0.00109	0.00454	0.00742	0.00347	0.070
AT5G58330	malate dehydrogenase [NADP]	plastid stroma	8.2.99	TCA / org.transformation	0.00000	0.00000	0.00000	0.00069	0.00023	0.00125	0.071
AT1G32060	phosphoribulokinase-2 (PRK-2)	plastid stroma	1.3.12	PS.calvin cyle.PRK	0.00000	0.00015	0.00000	0.00168	0.00091	0.00375	0.072
AT5G58070	lipocalin, putative		11	lipid metabolism	0.00000	0.00000	0.00000	0.00059	0.00057	0.00007	0.074
AT4G09000	14-3-3 protein GF14 chi (grf1)		30.7	signalling.14-3-3 proteins	0.00000	0.00000	0.00000	0.00100	0.00011	0.00099	0.075
AT5G12860	2-oxoglutarate/malate transloca	envelope-inner-in	34.8	transport.metabolite trans	0.00028	0.00030	0.00022	0.00000	0.00023	0.00000	0.075
AT4G34240	aldehyde dehydrogenase (ALDH3); 3-chloroallyl		5.1	fermentation.aldehyde de	0.00000	0.00000	0.00000	0.00030	0.00080	0.00021	0.078
AT1G56070	elongation factor 2, EF-2	not plastid	29.2.4	protein.synthesis.elongati	0.00000	0.00045	0.00109	0.00118	0.00308	0.00181	0.078
AT1G71500	Rieske [2Fe-2S] domain	thylakoid	26.3	misc.other Ferredoxins ar	0.00071	0.00030	0.00044	0.00030	0.00011	0.00000	0.080
AT5G58250	unknown protein	plastid	35.2	not assigned.unknown	0.00000	0.00000	0.00000	0.00059	0.00023	0.00125	0.082
AT1G52400	6-phospho-beta-galactosidase (BG1)		26.3	misc.gluco-, galacto- and	0.00000	0.00240	0.00087	0.00711	0.00582	0.00194	0.086
AT4G23600	nicotianamine aminotransferase		15.2	metal handling.binding, c	0.00000	0.00000	0.00000	0.00395	0.00034	0.00305	0.087
AT4G10340	LHCII-5 - CP26	thylakoid-integra	1.1.1.1	PS.lightreaction.photosys	0.00609	0.00331	0.00742	0.00267	0.00343	0.00222	0.088
AT1G23310	alanine 2-oxoglutarate amino tr	peroxisome	1.2.3	PS.aminotransferases per	0.00000	0.00000	0.00000	0.00444	0.00046	0.00576	0.090
AT4G05180	psbQ OEC16-like Tat lTP	thylakoid-periphe	1.1.1.2	PS.lightreaction.photosys	0.00000	0.00015	0.00000	0.00345	0.00035	0.00238	0.091
AT5G52640	heat shock protein 81-1 (HSP81-1) / heat shock p		20.2.1	stress.abiotic.heat	0.00000	0.00000	0.00000	0.00187	0.00085	0.00030	0.094
AT5G67030	zeaxanthin epoxidase precursor	thylakoid	16.1.4	secondary metabolism.isc	0.00000	0.00000	0.00022	0.00089	0.00308	0.00097	0.095
AT3G60750	transketolase-1 (TKL-1)	plastid stroma	1.3.8	PS.calvin cyle.transketola	0.00000	0.00000	0.00000	0.00346	0.00228	0.01014	0.096
AT1G68010	hydroxypyruvate reductase (HP	peroxisome	1.2.6	PS.photorespiration.hydr	0.00000	0.00000	0.00000	0.00395	0.00046	0.00604	0.099
AT5G25980	myrosinase or thioglucoside glu	not plastid	16.5.1	secondary metabolism.su	0.00000	0.00090	0.00153	0.00449	0.00130	0.00609	0.100

4.6 LITERATURE CITED

1. Puthiyaveetil, S., et al., *The ancestral symbiont sensor kinase CSK links photosynthesis with gene expression in chloroplasts.* Proceedings of the National Academy of Sciences, 2008. **105**(29): p. 10061-10066.

2. Bellafiore, S., et al., *State transitions and light adaptation require chloroplast thylakoid protein kinase STN7.* Nature, 2005. **433**(7028): p. 892-895.

3. Lohrig, K., et al., *Phosphorylation site mapping of soluble proteins: bioinformatical filtering reveals potential plastidic phosphoproteins in Arabidopsis thaliana*, in *Planta*. 2009, Springer Berlin / Heidelberg. p. 1123-1134.

4. Baginsky, S. and W. Gruissem, *The Chloroplast Kinase Network: New Insights from Large-Scale Phosphoproteome Profiling.* Molecular Plant, 2009. **2**(6): p. 1141-1153.

5. Reiland, S., et al., *Large-Scale Arabidopsis Phosphoproteome Profiling Reveals Novel Chloroplast Kinase Substrates and Phosphorylation Networks.* Plant Physiology, 2009. **150**(2): p. 889-903.

6. Sugiyama, N., et al., *Large-scale phosphorylation mapping reveals the extent of tyrosine phosphorylation in Arabidopsis.* 2008. **4**.

7. Bayer, R.G., et al., *Chloroplast-localized protein kinases: a step forward towards a complete inventory.* Journal of Experimental Botany, 2012. **63**(4): p. 1713-1723.

8. Schliebner, I.P., M; Zuhlke, J.; Dietzmann, A; Leister, D., *A Survey of Chloroplast Protein Kinases and Phophatases in Arabidopsis thaliana.* Current Genomics, 2008. **9**(3): p. 184-190.

9. Bonardi, V., et al., *Photosystem II core phosphorylation and photosynthetic acclimation require two different protein kinases.* Nature, 2005. **437**(7062): p. 1179-1182.

10. Vainonen, J.P., et al., *Light regulation of CaS, a novel phosphoprotein in the thylakoid membrane of Arabidopsis thaliana.* FEBS Journal, 2008. **275**(8): p. 1767-1777.

11. Fristedt, R., P. Granath, and A.V. Vener, *A Protein Phosphorylation Threshold for Functional Stacking of Plant Photosynthetic Membranes.* PLoS ONE, 2010. **5**(6): p. e10963.

12. Fristedt, R., et al., *Phosphorylation of Photosystem II Controls Functional Macroscopic Folding of Photosynthetic Membranes in Arabidopsis.* Plant Cell, 2009. **21**(12): p. 3950-3964.

13. Kanekatsu, M., et al., *Biochemical characterization of a 34 kDa ribonucleoprotein (p34) purified from the spinach chloroplast fraction as an effective phosphate acceptor for casein kinase II.* FEBS Lett, 1993. **335**(2): p. 176-80.

14. Lisitsky, I. and G. Schuster, *Phosphorylation of a chloroplast RNA-binding protein changes its affinity to RNA.* Nucleic Acids Res, 1995. **23**(13): p. 2506-11.

15. Baginsky, S., K. Tiller, and G. Link, *Transcription factor phosphorylation by a protein kinase associated with chloroplast RNA polymerase from mustard (Sinapis alba).* Plant Molecular Biology, 1997. **34**(2): p. 181-9.

16. Ogrzewalla, K., et al., *The plastid transcription kinase from mustard (Sinapis alba L.). A nuclear-encoded CK2-type chloroplast enzyme with redox-sensitive function.* European Journal of Biochemistry, 2002. **269**(13): p. 3329-37.

17. Puthiyaveetil, S., I.M. Ibrahim, and J.F. Allen, *Redox signalling components and regulatory pathways of state transitions and photosystem stoichiometry adjustment in chloroplasts.* Plant, Cell & Environment, 2011. **35**(2): p. 347-359.

18. Lundquist, P.K., J.I. Davis, and K.J. van Wijk, *ABC1K atypical kinases in plants; filling the organellar kinase void.* Trends in Plant Science, 2012. manuscript in review.

19. Lundquist, P.K., et al., *The Functional Network of the Arabidopsis Plastoglobule Proteome Based on Quantitative Proteomics and Genome-Wide Coexpression Analysis.* Plant Physiology, 2012. **158**(3): p. 1172-1192.

20. Jasinski, M., et al., *AtOSA1, a Member of the Abc1-Like Family, as a New Factor in Cadmium and Oxidative Stress Response.* Plant Physiol., 2008. **147**(2): p. 719-731.

21. Bousquet, I., G. Dujardin, and P.P. Slonimski, *ABC1, a novel yeast nuclear gene has a dual function in mitochondria: it suppresses a cytochrome b mRNA translation defect and is essential for the electron transfer in the bc 1 complex.* Embo J, 1991. **10**(8): p. 2023-31.

22. Do, T.Q., et al., *A Defect in Coenzyme Q Biosynthesis Is Responsible for the Respiratory Deficiency in Saccharomyces cerevisiae abc1 Mutants.* J. Biol. Chem., 2001. **276**(21): p. 18161-18168.

23. Cardazzo, B., et al., *Isolation of an Arabidopsis thaliana cDNA by complementation of a yeast abc1 deletion mutant deficient in complex III respiratory activity.* Gene, 1998. **221**(1): p. 117-125.

24. Xie, L.X., et al., *Expression of the human atypical kinase ADCK3 rescues coenzyme Q biosynthesis and phosphorylation of Coq polypeptides in yeast coq8 mutants.* Biochimica et Biophysica Acta (BBA) - Molecular and Cell Biology of Lipids, 2011. **1811**(5): p. 348-360.

25. Mollet, J., et al., *CABC1 Gene Mutations Cause Ubiquinone Deficiency with Cerebellar Ataxia and Seizures.* The American Journal of Human Genetics, 2008. **82**(3): p. 623-630.

26. Lagier-Tourenne, C., et al., *ADCK3, an Ancestral Kinase, Is Mutated in a Form of Recessive Ataxia Associated with Coenzyme Q10 Deficiency.* The American Journal of Human Genetics, 2008. **82**(3): p. 661-672.

27. Austin, J.R., 2nd, et al., *Plastoglobules are lipoprotein subcompartments of the chloroplast that are permanently coupled to thylakoid membranes and contain biosynthetic enzymes.* Plant Cell, 2006. **18**(7): p. 1693-703.

28. Lee, D.-S., et al., *Structural insights into the evolutionary paths of oxylipin biosynthetic enzymes.* Nature, 2008. **455**(7211): p. 363-368.

29. Yang, S., et al., *AtACDO1, an ABC1-like kinase gene, is involved in chlorophyll degradation and the response to photooxidative stress in Arabidopsis.* Journal of Experimental Botany, 2012.

30. Leonard, C.J., L. Aravind, and E.V. Koonin, *Novel Families of Putative Protein Kinases in Bacteria and Archaea: Evolution of the "Eukaryotic" Protein Kinase Superfamily.* Genome Res., 1998. **8**(10): p. 1038-1047.

31. Havaux, M., et al., *Photodamage of the Photosynthetic Apparatus and Its Dependence on the Leaf Developmental Stage in the npq1 Arabidopsis Mutant Deficient in the Xanthophyll Cycle Enzyme Violaxanthin De-epoxidase.* Plant Physiology, 2000. **124**(1): p. 273-284.

32. Youssef, A., et al., *Plant lipid-associated fibrillin proteins condition jasmonate production under photosynthetic stress.* The Plant Journal, 2010. **61**(3): p. 436-445.

33. op den Camp, R.G.L., et al., *Rapid Induction of Distinct Stress Responses after the Release of Singlet Oxygen in Arabidopsis.* Plant Cell, 2003. **15**(10): p. 2320-2332.

34. Foyer, C.H. and G. Noctor, *Ascorbate and Glutathione: The Heart of the Redox Hub.* Plant Physiology, 2011. **155**(1): p. 2-18.

35. Luwe, M., U. Takahama, and U. Heber, *Role of Ascorbate in Detoxifying Ozone in the Apoplast of Spinach (Spinacia oleracea L.) Leaves.* Plant Physiology, 1993. **101**(3): p. 969-976.

36. Brehelin, C., F. Kessler, and K.J. van Wijk, *Plastoglobules: versatile lipoprotein particles in plastids.* Trends in Plant Science, 2007. **12**(6): p. 260-6.

37. Huang, C.-Y., et al., *Oil Bodies and Oleosins in Physcomitrella Possess Characteristics Representative of Early Trends in Evolution.* Plant Physiology, 2009. **150**(3): p. 1192-1203.

38. White, D.A., I.D. Fisk, and D.A. Gray, *Characterisation of oat (Avena sativa L.) oil bodies and intrinsically associated E-vitamers.* Journal of Cereal Science, 2006. **43**(2): p. 244-249.

39. Hausler, R.E., et al., *Chlororespiration and Grana Hyperstacking: How an Arabidopsis Double Mutant Can Survive Despite Defects in Starch Biosynthesis and Daily Carbon Export from Chloroplasts.* Plant Physiology, 2009. **149**(1): p. 515-533.

40. Poliakov, A., et al., *A statistical solution for pair-wise comparative proteome analysis using large scale label-free spectral counting*. 2012. Manuscript in preparation.

41. Munekage, Y., et al., *PGR5 Is Involved in Cyclic Electron Flow around Photosystem I and Is Essential for Photoprotection in Arabidopsis.* Cell, 2002. **110**(3): p. 361-371.

42. DalCorso, G., et al., *A Complex Containing PGRL1 and PGR5 Is Involved in the Switch between Linear and Cyclic Electron Flow in Arabidopsis.* Cell, 2008. **132**(2): p. 273-285.

43. Rumeau, D., G. Peltier, and L. Cournac, *Chlororespiration and cyclic electron flow around PSI during photosynthesis and plant stress response.* Plant, Cell & Environment, 2007. **30**(9): p. 1041-1051.

44. Sazanov, L.A., P.A. Burrows, and P.J. Nixon, *The plastid ndh genes code for an NADH-specific dehydrogenase: Isolation of a complex I analogue from pea thylakoid membranes.* Proceedings of the National Academy of Sciences, 1998. **95**(3): p. 1319-1324.

45. Burrows, P.A., et al., *Identification of a functional respiratory complex in chloroplasts through analysis of tobacco mutants containing disrupted plastid ndh genes.* 1998. **17**(4): p. 868-876.

46. Apel, K. and H. Hirt, *Reactive Oxygen Species: Metabolism, Oxidative Stress, and Signal Transduction.* Annual Review of Plant Biology, 2004. **55**(1): p. 373-399.

47. Vieira Dos Santos, C. and P. Rey, *Plant thioredoxins are key actors in the oxidative stress response.* Trends in Plant Science, 2006. **11**(7): p. 329-334.

48. Lemaire, S., et al., *Thioredoxins in chloroplasts.* Current Genetics, 2007. **51**(6): p. 343-365.

49. Dietz, K.-J., *Peroxiredoxins in Plants and Cyanobacteria.* Antioxidants & Redox Signaling, 2011. **15**(4): p. 1129-1159.

50. Puthiyaveetil, S., *A mechanism for regulation of chloroplast LHC II kinase by plastoquinol and thioredoxin.* FEBS Lett, 2011. **585**(12): p. 1717-21.

51. He, Y., et al., *Evidence Supporting a Role of Jasmonic Acid in Arabidopsis Leaf Senescence.* Plant Physiology, 2002. **128**(3): p. 876-884.

52. Poon, W.W., et al., *Identification of Escherichia coli ubiB, a gene required for the first monooxygenase step in ubiquinone biosynthesis.* J Bacteriol, 2000. **182**(18): p. 5139-46.

53. Lohmann, A., et al., *Deficiency in Phylloquinone (Vitamin K1) Methylation Affects Prenyl Quinone Distribution, Photosystem I Abundance, and Anthocyanin Accumulation in the Arabidopsis AtmenG Mutant.* J. Biol. Chem., 2006. **281**(52): p. 40461-40472.

54. Zbierzak, A.M., et al., *Intersection of the tocopherol and plastoquinol metabolic pathways at the plastoglobule.* Biochemical Journal, 2009. **425**(2): p. 389-399.

55. Szymanska, R. and J. Kruk, *Plastoquinol is the Main Prenyllipid Synthesized During Acclimation to High Light Conditions in Arabidopsis and is Converted to Plastochromanol by Tocopherol Cyclase.* Plant Cell Physiol., 2010. **51**(4): p. 537-545.

56. Steinmuller, D. and M. Tevini, *Composition and Function of Plastoglobuli .1. Isolation and Purification from Chloroplasts and Chromoplasts.* Planta, 1985. **163**(2): p. 201-207.

57. Fraser, P.D., et al., *Application of high-performance liquid chromatography with photodiode array detection to the metabolic profiling of plant isoprenoids.* The Plant Journal, 2000. **24**(4): p. 551-558.

58. Redfearn, E.R. and J. Friend, *Studies on plastoquinone--1. Determination of the concentration and oxidation-reduction state of plastoquinone in isolated chloroplasts.* Phytochemistry, 1962. **1**(3): p. 147-151.

59. Martinis, J., F. Kessler, and G. Glauser, *A novel method for prenylquinone profiling in plant tissues by ultra-high pressure liquid chromatography-mass spectrometry.* Plant Methods, 2011. **7**(1): p. 23.

60. Meskauskiene, R., et al., *FLU: A negative regulator of chlorophyll biosynthesis in Arabidopsis thaliana.* Proceedings of the National Academy of Sciences, 2001. **98**(22): p. 12826-12831.

61. Pattanayak, G.K. and B.C. Tripathy, *Overexpression of Protochlorophyllide Oxidoreductase C Regulates Oxidative Stress in Arabidopsis.* PLoS ONE, 2011. **6**(10): p. e26532 EP -.

62. Friso, G., P.D.B. Olinares, and K.J. van Wijk, *The Workflow for Quantitative Proteome Analysis of Chloroplast Development and Differentiation, Chloroplast Mutants, and Protein Interactions by Spectral Counting*, in *Chloroplast Research in Arabidopsis*, R.P. Jarvis, Editor. 2011, Humana Press: New York. p. 265-282.

63. Zybailov, B., et al., *Sorting Signals, N-Terminal Modifications and Abundance of the Chloroplast Proteome.* PLoS ONE, 2008. **3**(4): p. e1994 EP -.

64. Olinares, P.D.B., L. Ponnala, and K.J. van Wijk, *Megadalton Complexes in the Chloroplast Stroma of Arabidopsis thaliana Characterized by Size Exclusion Chromatography, Mass Spectrometry, and Hierarchical Clustering.* Molecular & Cellular Proteomics, 2010. **9**(7): p. 1594-1615.

CHAPTER FIVE

IDENTIFYING TARGETS OF THE ABC1K1 AND ABC1K3 ATYPICAL KINASES

5.1 INTRODUCTION

The question remains, what are the phosphorylation target(s) of the ABC1K1 and ABC1K3 proteins? The results favor a hypothesis in which each kinase targets one or more proteins, pathways or processes for phosphorylation, thereby altering protein activity, localization or protein interactions. The synergistic light-stress phenotype demonstrated in *k1k3* in *Chapter 4* indicates non-redundant contributions of ABC1K1 and ABC1K3 to the adaptation to increased light intensity. This suggests distinct targets by the two kinases, but does not rule out one or more common phosphorylation targets. Potential ABC1K1,3 targets affecting the photoacclimation/light-stress response are numerous (see *section 1.2.3)* and include xanthophyll cycle enzymes, proteins involved in prenyl-lipid metabolism, and regulators of thylakoid linear and cyclic electron flows. It is likely that the targets need to be (at least transiently) localized to PGs to undergo phosphorylation, thereby limiting the potential target list.

Target candidates of ABC1K1 and ABC1K3 The transcription co-expression network of the plastoglobule (PG), described in *Chapter 2*, suggests that ABC1K1 and ABC1K3 function in the regulation of prenyl-lipid metabolism and protein turnover. Such functions are supported by the proteomics and metabolite profiling analyses of the *k1k3* double mutant; i) significant alterations were found in tocochromanol, quinone and carotenoid accumulation in *k1k3* leaf tissue and PGs, ii) accumulation of carotenoid cleavage dioxygenase 4 (CCD4), zeaxanthin epoxidase (ZEP),

geranylgeranyl diphosphate reductase (GGDR), and ζ-carotene desaturase (ZDS) were affected by loss of *ABC1K1* and *ABC1K3*. Evidence supporting the most promising targets of ABC1K1 or ABC1K3 is described below.

Zeaxanthin epoxidase (ZEP) – ABC1K3 was found by multiple software programs to coexpress very tightly with *ZEP* (see *Chapter 2*). Indeed, several avenues of evidence suggest that ZEP activity is regulated post-transcriptionally, possibly by phosphorylation. First, mRNA levels of *ZEP* are constant during the diurnal induction/reduction of the xanthophyll cycle [1]. Second, an investigation of zeaxanthin epoxidation under photo-oxidative stress indicated that ZEP activity can be down-regulated very rapidly in a stress-dependent manner and requires a thylakoid-associated factor that is not STN7 or STN8 [2]. Furthermore, the inactivation of ZEP by phosphatase inhibitors suggests that phosphorylation of ZEP reduces its activity [3]. Additional circumstantial evidence further supports a regulatory role for ABC1K1 or ABC1K3 in ZEP activity. The elevated expression of ZEP in *k1k3* leaf tissue could represent a compensatory response for reduced enzyme activity (see *Chapter 4*). In addition, much higher levels of ZEP in *k1k3* PGs suggest it may be recruited to PGs in the *k1k3* mutant. It is suggested that ZEP migrates in and out of PGs and requires PG location for phosphorylation by ABC1Ks. Finally, ZEP is a monoxygenase, similar as the few known direct targets of mitochondrial *ABC1K*s involved in ubiquinone biosynthesis.

Tocopherol cyclase – VTE1 is a PG-localized enzyme converting dimethylphytyl benzoquinone and plastoquinone-9 to the antioxidants α-tocopherol and plastochromanol-8, respectively [4]. The *VTE1* gene does not coexpress with other enzymes of the tocopherol biosynthesis pathway

or with other genes of the PG, which is indicative of post-transcriptional control. Accumulation of the metabolites downstream of VTE in *k1k3* PGs was significantly reduced relative to wild-type, and a greater number of VTE1 substrate (PQ-9) was found in the mutant PGs, both consistent with a reduced activity of VTE1 in the absence of ABC1K1 and ABC1K3. Additionally, it was found that VTE1 protein accumulated to similar levels in *k1k3* and wild-type PGs, despite the increased accumulation of VTE1 substrate in these PGs, further supporting a reduced activity of VTE1 (see *Chapter 4*).

Chlorophyll metabolism – The light stress sensitivity in the *k1k3* double mutant is indicative of accumulation of photosensitizer(s) leading to damage and turnover, or induction of a retrograde signalling pathway to the nucleus resulting in proteome remodeling. An intriguing possibility is that the loss of ABC1K1 and ABC1K3 leads to impaired chlorophyll metabolism and accumulation of one or more chlorophyll intermediates which are photosensitizers. A recent investigation of an RNAi line targeting *ABC1K1* caused a constitutive yellow leaf phenotype and accumulation of protochlorophyllide and chlorophyllide in leaf tissue [5]. However, the investigators used a full cDNA sequence of *ABC1K1* which would target other genes with homology to *ABC1K1* as well. Unfortunately, the investigators did not report the expression levels of the other members of the *ABC1K* family. It is highly likely that several members of the *ABC1K* family were knocked down and thus the phenotype of the RNAi line cannot be attributed to a specific loss of ABC1K1. The induction of the 2-Cys peroxiredoxin B protein (2-Cys PrxB) in *k1k3* under stress does however implicate *ABC1K1* and *ABC1K3* in chlorophyll biosynthesis. Elevated protein levels of 2-Cys PrxB were reported in a tobacco mutant of Mg-protoporphyrin monomethylester cyclase, disrupted in chlorophyll biosynthesis [6]. Indeed, 2-Cys PrxB is

localized at the thylakoid membrane and is required for protochlorophyllide synthesis *in vitro* [7]. PGs are known to play a role in chlorophyll metabolism, as phytol released from degraded chlorophyll is deposited in the PG. Additionally, several proteins of the chlorophyll degradation pathway are included in the PG coexpression network in the senescence module 1 (see *Chapter 2*).

Carotenoid cleavage dioxygenase 4 (CCD4) and state transition kinase 7 (STN7) – A striking result from the total leaf proteomics work on *k1k3* was the strong reduction of CCD4 levels in the mutant (see *Chapter 4*). The observation of reduced levels prior to light stress is important in that it indicates the reduction is not a pleiotropic response to the light stress treatment. The results suggest a role for ABC1K1 or ABC1K3 in regulation of CCD4. As phosphorylation of state transition kinase 7 (STN7) has been shown to protect it from degradation [8], phosphorylation may similarly confer protein stability to CCD4 which is dependent on ABC1K1 or ABC1K3. ABC1K3 was found to coexpress strongly with STN7, thus it is possible that ABC1K3 may be responsible for maintaining the phosphorylation and stability of STN7 as well. Consistent with this notion, STN7 was identified by mass-spectrometry in one of the wild-type total leaf biological replicates prior to light stress but not in *k1k3*.

5.2 YEAST 2-HYBRID ANALYSIS OF PROTEIN-PROTEIN INTERACTIONS

The hypothesized targets of ABC1K1 and ABC1K3 outlined above, as well as many of the PG-localized proteins, will be tested for protein-protein interaction using the yeast 2-hybrid (Y2H) technology. The Y2H system expresses two exogenous proteins of interest in yeast which

have been fused with the N- and C-terminal halves of a reporter enzyme, such that protein interaction between the proteins of interest reconstitutes reporter enzyme activity.

Yeast 2-hybrid systems There are several different Y2H systems available which reconstitute various reporter enzymes and are outlined below.

Classical yeast 2-hybrid systems - The original Y2H system reconstituted the activation and DNA-binding domains of the GAL4 transcription factor which promotes expression of a reporter gene in the yeast strain. A number of different reporter genes have been introduced permitting multiple assays for protein-protein interaction. This system requires the targeting of the tested proteins to the yeast nucleus, which excludes transcription factors or largely hydrophobic proteins from being tested.

The split-ubiquitin system - The split-ubiquitin Y2H assay is another popular Y2H system which uses the ubiquitin protein as reporter assay. Split-ubiquitin Y2H was originally designed for testing of soluble proteins but has been adapted for membrane-based assays which are more appropriate for integral membrane proteins, as well as proteins that require post-translational modifications introduced at the endoplasmic reticulum or golgi apparatus [9-11]. In both variations the ubiquitin protein is reconstituted and protein degradation by the yeast proteasome is triggered, leading to the release of a reporter protein. Conveniently, the split-ubiquitin assay does not require localization of the proteins in the nucleus, allowing proteins with strong localization signals or hydrophobic proteins to be tested.

hSos/Ras recruitment systems - A third Y2H system utilizes induction of the Ras signaling pathway at the yeast plasma membrane to rescue a temperature-sensitive yeast mutant lacking the Ras protein. One protein of interest is targeted to the plasma membrane by a myristoylation site and the other protein of interest is fused with human Ras or human hSos, such that interaction at the plasma membrane reconstitutes the Ras function in yeast, complementing the growth phenotype. Unfortunately, spontaneous reversion of the yeast mutant has been reported, meaning tests of the growth-sensitive phenotype must be tested before and after transformation of the yeast [12].

The Invitrogen ProQuest Y2H system for ABC1K1 and ABC1K3 To test for protein-protein interactions between ABC1K1 or ABC1K3 with potential substrates, a targeted Y2H assay using the Invitrogen ProQuest technology will be used. The ProQuest technology relies on a classical Y2H system accomplishing the reconstitution of the GAL4 transcription factor in the yeast nucleus. An approach relying on nuclear targeting of proteins is favored because the PG-localized proteins contain relatively little hydrophobicity and are presumed to be only peripherally associated with the PG membrane perimeter.

The ProQuest system uses the MaV203 yeast strain which has been engineered to encode three different reporter genes for the use of multiple assays for positive protein-protein interaction confirmation. The reporter genes include the auxotrophic markers, HIS3 and URA3 genes, which encode enzymes in biosynthesis of the essential amino acids histidine and uracil, for selection on drop-out media plates, and the lacZ gene for blue-white colony formation and quantitative assay using colorimetry. Vectors are included that harbor the Krev1 protein and the RalGDS protein in wild-type and mutated forms to produce control interactions of varying

strengths. The wild-type form of RalGDS interacts strongly with the Krev1. A mutated form, RalGDSm1 demonstrates a weakened interaction, while another mutated form, RalGDSm2, abolishes all interaction and serves as a negative control.

The occurrence of false positives (the detection of protein-protein interaction by the assay where interaction does not occur or is biologically irrelevant) can be a problem in Y2H assays. This concern has been addressed in two ways in the ProQuest system. First, because many false positives are context-dependent [13], each of the reporter genes (HIS3, URA3, and lacZ) use a different promoter sequence which can be recognized by the GAL4 transcription factor. Second, the expression plasmids encoding the protein fusions use an ARS/CEN3 origin of replication, which maintains the plasmid at low-copy number in the yeast cells.

Current state The initial priority is to test interactions between the ABC1K1 and ABC1K3 and the most promising target candidates: ZEP, CCD4, and VTE1. Genes will be cloned and proteins expressed in the absence of chloroplast transit peptide as this more accurately represents the plastid-localized in vivo form of the proteins. Currently, ABC1K1 and ABC1K3 have been successfully cloned into the pCR8 entry vector and ABC1K1 has been subcloned into the ProQuest bait plasmid. Confirmation of successful subcloning of ABC1K1 in the prey plasmid is underway. Cloning of ZEP, VTE1, CCD4, and pheophytinase (PPH) into pCR8 is also underway.

5.3 LITERATURE CITED

1. North, H.M., et al., *Analysis of xanthophyll cycle gene expression during the adaptation of Arabidopsis to excess light and drought stress: Changes in RNA steady-state levels do not contribute to short-term responses.* Plant Science, 2005. **169**(1): p. 115-124.

2. Reinhold, C., et al., *Short-term down-regulation of zeaxanthin epoxidation in Arabidopsis thaliana in response to photo-oxidative stress conditions.* Biochimica et Biophysica Acta (BBA) - Bioenergetics, 2008. **1777**(5): p. 462-469.

3. Xu, C.C., et al., *Suppression of zeaxanthin epoxidation by chloroplast phosphatase inhibitors in rice leaves.* Plant Science, 1999. **146**(1): p. 27-34.

4. Zbierzak, A.M., et al., *Intersection of the tocopherol and plastoquinol metabolic pathways at the plastoglobule.* Biochemical Journal, 2009. **425**(2): p. 389-399.

5. Yang, S., et al., *AtACDO1, an ABC1-like kinase gene, is involved in chlorophyll degradation and the response to photooxidative stress in Arabidopsis.* Journal of Experimental Botany, 2012.

6. Peter, E., et al., *Mg Protoporphyrin Monomethylester Cyclase Deficiency and Effects on Tetrapyrrole Metabolism in Different Light Conditions.* Plant and Cell Physiology, 2010. **51**(7): p. 1229-1241.

7. Stenbaek, A., et al., *NADPH-dependent thioredoxin reductase and 2-Cys peroxiredoxins are needed for the protection of Mg-protoporphyrin monomethyl ester cyclase.* FEBS Letters, 2008. **582**(18): p. 2773-2778.

8. Willig, A., et al., *The Phosphorylation Status of the Chloroplast Protein Kinase STN7 of Arabidopsis Affects Its Turnover.* Plant Physiology, 2011. **157**(4): p. 2102-2107.

9. Johnsson, N. and A. Varshavsky, *Split ubiquitin as a sensor of protein interactions in vivo* Proceedings of the National Academy of Sciences 1994 **91** (22): p. 10340-10344

10. Thaminy, S., J. Miller, and I. Stagljar, *The Split-Ubiquitin Membrane-Based Yeast Two-Hybrid System*, in *Protein-Protein Interactions Methods and Applications*, H. Fu, Editor. 2004, Humana Press: Totawa, NJ.

11. Stagljar, I., et al., *A genetic system based on split-ubiquitin for the analysis of interactions between membrane proteins in vivo* Proceedings of the National Academy of Sciences 1998 **95** (9): p. 5187-5192

12. Causier, B. and B. Davies, *Analysing protein-protein interactions with the yeast two-hybrid system*, in *Plant Molecular Biology*. 2002, Springer Netherlands. p. 855-870.

13. Bartel, P., et al., *Elimination of false positives that arise in using the two-hybrid system.* Biotechniques, 1993. **14**(6): p. 920-924.